

University of Southampton Research Repository

Copyright © and Moral Rights for this thesis and, where applicable, any accompanying data are retained by the author and/or other copyright owners. A copy can be downloaded for personal non-commercial research or study, without prior permission or charge. This thesis and the accompanying data cannot be reproduced or quoted extensively from without first obtaining permission in writing from the copyright holder/s. The content of the thesis and accompanying research data (where applicable) must not be changed in any way or sold commercially in any format or medium without the formal permission of the copyright holder/s.

When referring to this thesis and any accompanying data, full bibliographic details must be given, e.g.

Thesis: Author (Year of Submission) "Full thesis title", University of Southampton, name of the University Faculty or School or Department, PhD Thesis, pagination.

Data: Author (Year) Title. URI [dataset]

UNIVERSITY OF SOUTHAMPTON

Faculty of Social Sciences
School of Mathematics

**Exact Methods for Defects in Conformal
Field Theory**

by

Adam Chalabi

ORCID: [0000-0002-6596-1772](https://orcid.org/0000-0002-6596-1772)

*A thesis for the degree of
Doctor of Philosophy*

January 2023

University of Southampton

Abstract

Faculty of Social Sciences
School of Mathematics

Doctor of Philosophy

Exact Methods for Defects in Conformal Field Theory

by Adam Chalabi

The defect operators admitted by a given quantum field theory (QFT) contain crucial information. E.g in 4d gauge theories some defects play the role of order parameters, classifying phases of the theory. Defects are also omnipresent in real-world laboratories. E.g. real systems typically have impurities and defects, which may change their properties. Since QFT can be used to describe such systems in the continuum limit, it is essential to systematically understand defects in QFT.

This thesis explores defects in d -dimensional conformal field theories (CFT). CFTs arise naturally at fixed points of renormalisation group (RG) flows and describe real physical systems at criticality. We focus on p -dimensional defects, with $p \leq d - 1$, that preserve some of the system's conformal invariance. Conformal defects give rise to defect-localised contributions to the CFT's Weyl anomaly. Their coefficients are often called defect central charges. They control many physical observables, and obey interesting bounds, constraints, and relations, partially characterising the defect.

We report novel and original results about conformal defects and their central charges across dimensions. Our results are exact and apply to large classes of defects. Firstly, we determine the form of the defect Weyl anomaly of a $p = 4$ conformal defect in a CFT of arbitrary co-dimension $q = d - 4$. We show how some of the new defect central charges appear in physical observables, and discuss bounds that they need to obey.

We then illustrate these results with a set of simple, yet non-trivial, examples of defects in free CFTs. Using existing methods available in free field theories, we compute various correlation functions exactly for arbitrary p , and demonstrate how to extract defect central charges when $p = 2$ and $p = 4$. Moreover, we study novel defect RG flows which are found to obey monotonicity theorems.

Finally, we develop novel techniques to compute central charges for superconformal defects in a large class of interacting superconformal field theories. Our methods rely on supersymmetric localisation, and thus are non-perturbative in the coupling constants. We illustrate our techniques in numerous examples.

Contents

List of Figures	ix
List of Tables	xi
List of Acronyms	xiii
Declaration of Authorship	xv
I Introduction	1
1 Motivation	3
2 Conformal Field Theory in $d > 2$	11
2.1 Conformal symmetry	11
2.2 States and operators	13
2.3 Correlation functions and CFT data	17
2.4 Curved background	20
2.5 Weyl anomaly	23
3 Conformal Defects	35
3.1 Correlation functions and DCFT data	35
3.2 Examples of conformal defects	42
3.3 Submanifold geometry	44
3.4 Defect Weyl anomaly	46
4 Entanglement Entropy	53
4.1 Entanglement in finite quantum systems	53
4.2 Entanglement in QFT	55
4.3 Entanglement in free QFTs and the heat kernel	56
4.4 Entanglement in CFT	59
4.5 Entanglement in DCFT	62
5 Supersymmetry	67
5.1 Flat space supersymmetry	67
5.2 Supersymmetric localisation	70
5.3 Superconformal symmetry	72
5.4 Weyl anomaly in SCFTs	76
5.5 Superconformal defects	79

II	Research	83
6	Weyl Anomaly of 4d Conformal Defects	85
6.1	Defect Weyl anomaly	85
6.1.1	Defect Weyl anomaly for $d \geq 6$	86
6.1.2	Boundary Weyl anomaly for $d = 5$	90
6.2	Defect central charges from observables	91
6.2.1	Displacement operator two-point function	91
6.2.2	Stress-tensor one-point function	95
6.3	Discussion	102
7	Monodromy Defects in Free Field Theories	105
7.1	Background	105
7.2	Free scalar	108
7.2.1	Mode expansion and propagator	109
7.2.2	Correlation functions and central charges	113
7.2.3	Entanglement entropy	121
7.3	Free fermion	124
7.3.1	Mode expansion and propagator	125
7.3.2	Correlation functions and central charges	127
7.3.3	Entanglement entropy	133
7.4	Defect RG flows	135
7.4.1	Scalar monodromy flows	135
7.4.2	Fermion monodromy flows	140
7.5	Discussion	144
8	Central Charges of 2d Superconformal Defects	147
8.1	Review: 2d superconformal defects	148
8.2	Partition function on S^4	156
8.3	SUSY partition function on $S^1 \times S^{d-1}$	167
8.4	Discussion	175
9	Concluding Remarks	177
III	Appendices	185
Appendix A	Chapter 3	187
Appendix A.1	Isolating the anomaly: $p = 2$ conformal defect in a $d = 4$ CFT	187
Appendix B	Chapter 6	193
Appendix B.1	4d defect Weyl anomaly basis	193
Appendix C	Chapter 7	199
Appendix C.1	Spherical defects	199
Appendix C.2	Scalar propagator	201
Appendix C.3	Fermion propagator	204
Appendix C.4	Useful formulae	207

Appendix D Chapter 8	209
Appendix D.1 Special functions and zeta-function regularisation	209
References	213

List of Figures

- 2.1 *Left:* Illustration of quantisation on spatial slices. The Euclidean time coordinate $\tau \in [-\infty, +\infty]$ extends along the vertical axis. Dashed lines are hypersurfaces of constant τ . *Right:* Illustration of radial quantisation. The radial coordinate $r = |x|$ plays the role of time. Dashed lines are hypersurfaces of constant $r \in [0, +\infty]$. Note that the Hilbert spaces associated with the spatial slices in the two quantisation schemes are different, however, there exists an isomorphism between them. In particular, the two Hilbert spaces have the same dimension. 15
- 3.1 Configuration for the null geodesic v^μ described in eq. (3.4.43). The null geodesic (blue) passes by the defect (red, labelled Σ) at an angle ψ in the $x^1 - x^2$ plane and at a distance ℓ away in the x^3 direction. 50
- 4.1 *Left:* Illustration of the path integral representation of the matrix elements of the reduced density matrix ρ_A . The path integral is evaluated over the blue region with boundary conditions $\phi_s(\vec{x}_A)$ and $\phi_r(\vec{x}_A)$ at $\tau = 0^-$ and $\tau = 0^+$, respectively, which are only supported on the spatial region A . *Right:* Illustration of the replica trick. The Rényi entropy $S_n(A)$ is mapped to the path integral over the n -sheeted cover of space-time, with sheets glued together along the cuts as indicated by dashed lines. Repeated subscripts on ϕ on adjacent cuts indicate that the boundary conditions are identified and integrated over in the path integral, thus effecting matrix multiplication of ρ_A 57
- 4.2 A spherical entangling surface in $d = 4$ centred on the $p = 2$ defect at time $\tau = 0$. The defect's contribution to the universal EE of the region enclosed is given by eq. (4.5.45). 65
- 7.1 Sketch of the configuration we employ to compute the defect contribution to the EE in $d = 4$. The figure is an instance in time at $\tau = 0$. The defect (red) extends along the x^1 direction, while the entangling surface (green) extends along the remaining orthogonal directions and intersects the defect at $x^1 = 0$. The defect's contribution to the universal EE of the region to either side of the entangling surface is given by eq. (7.2.69). . . 122
- 7.2 The quantity $\rho^2 \langle |\varphi|^2 \rangle_\zeta - \rho^2 \langle |\varphi|^2 \rangle_{\zeta=0}$ as a function of the dimensionless quantity $\rho \lambda^{\frac{1}{2\alpha}}$ for $d = 4$, $\alpha = 0.75$, and different values of ζ . While in the UV the quantity depends on ζ , in the IR limit all the curves go to zero. . . 139
- 7.3 The quantity $\rho^4 \langle J^\theta \rangle_\zeta - \rho^4 \langle J^\theta \rangle_{\zeta=1}$ as a function of $\rho \lambda^{\frac{1}{2\alpha-1}}$ for $d = 4$, $\alpha = 0.75$, and different values of ζ . While in the UV the quantity depends on ζ , in the IR limit all the curves go to zero. 144

- 8.1 Linear quiver diagram corresponding to a 2d $\mathcal{N} = (2, 2)$ GLSM. Its field content consists of $U(K_i)$ 2d vector multiplets for $i = 1, \dots, n$, N fundamental ϕ_n^{fund} and N anti-fundamental $\tilde{\phi}_n^{\text{anti-fund}}$ chiral multiplets coupled to the $U(K_n)$ vector, one chiral multiplet $\phi_{i(i+1)}^{\text{bif}}$ in the bifundamental representation of $(\mathbf{K}_i, \bar{\mathbf{K}}_{i+1})$, and one chiral multiplet $\phi_{(i+1)i}^{\text{bif}}$ in the bifundamental representation $(\bar{\mathbf{K}}_i, \mathbf{K}_{i+1})$ for each $1 \leq i \leq n - 1$. Additionally, depending on the particular details of the 2d $\mathcal{N} = (2, 2)$ gauge theory, there can be one adjoint chiral X_i of $U(K_i)$ for each node. This quiver diagram can be used to construct a surface operator whenever the 4d $\mathcal{N} = 2$ gauge theory has at least an $S[U(N) \times U(N)]$ flavour or gauge symmetry group. 150

List of Tables

- 5.1 Minimal spinors of $SO(d-1,1)$ and SUSY for $2 \leq d \leq 6$. The spinors obey Majorana (M), Majorana-Weyl (MW), symplectic Majorana (SM), and symplectic Majorana-Weyl (SMW) conditions depending on d as summarised in the second column. The number of real components of each minimal spinor is reported in the third column. $\mathcal{N} \in \mathbb{Z}$ counts the number of minimal spinors-worth of SUSY generators. When $d = 2, 6$, minimal spinors are chiral. We write $\mathcal{N} = (p, q)$ for $p, q \in \mathbb{Z}$ to keep track of chiralities. The number of real supercharges for given \mathcal{N} is reported in the last column. 68

List of Acronyms

ABJM	Aharony-Bergman-Jafferis-Maldacena	QED	quantum electrodynamics
AdS	anti-de Sitter	QFT	quantum field theory
AGT	Alday-Gaiotto-Tachikawa	QM	quantum mechanics
ANEC	average null energy condition	RG	renormalisation group
BCFT	boundary conformal field theory	SCA	superconformal algebra
BPS	Bogomol'nyi-Prasad-Sommerfield	SCE	supersymmetric Casimir energy
BRST	Becchi-Rouet-Stora-Tyutin	SCFT	superconformal field theory
CFT	conformal field theory	SCI	superconformal index
CS	Chern-Simons	SQCD	supersymmetric quantum chromodynamics
DCFT	defect conformal field theory	SQM	supersymmetric quantum mechanics
DOF	degree(s) of freedom	SUSY	supersymmetry/supersymmetric
EE	entanglement entropy	SW	Seiberg-Witten
EOM	equation(s) of motion	SYM	super-Yang-Mills
FI	Fayet-Iliopoulos	UV	ultra-violet
GLSM	gauged linear sigma model	VEV	vacuum expectation value
IR	infra-red	VOA	vertex operator algebra
NLSM	non-linear sigma model	WZ	Wess-Zumino
OPE	operator product expansion	WZNW	Wess-Zumino-Novikov-Witten
QCD	quantum chromodynamics	YM	Yang-Mills

Declaration of Authorship

I declare that this thesis and the work presented in it is my own and has been generated by me as the result of my own original research.

I confirm that:

1. This work was done wholly or mainly while in candidature for a research degree at this University;
2. Where any part of this thesis has previously been submitted for a degree or any other qualification at this University or any other institution, this has been clearly stated;
3. Where I have consulted the published work of others, this is always clearly attributed;
4. Where I have quoted from the work of others, the source is always given. With the exception of such quotations, this thesis is entirely my own work;
5. I have acknowledged all main sources of help;
6. Where the thesis is based on work done by myself jointly with others, I have made clear exactly what was done by others and what I have contributed myself;
7. Parts of this work have been published as: refs. [1–3]. I have also collaborated on [4, 5], the contents of which are not covered in this thesis.

Signed:.....

Date:.....

Acknowledgements

I would like to express my deepest gratitude to my supervisor Andy O'Bannon. His guidance was paramount for navigating my PhD, and his continuous support throughout the last four years has been indispensable. He knew when to push me and when to step in while treating me as an equal collaborator. His help has been invaluable in my journey towards finding my place in the scientific community and forging new collaborations. My approach to research has been shaped by his wide-angle view of physics which taught me to not lose sight of observation and experiment.

I am deeply indebted to my collaborators Lorenzo Bianchi, Chris Herzog, Prem Kumar, Vladímír Procházka, Anton Pribytok, Brandon Robinson, Ronnie Rodgers, and Jacopo Sisti who have taught me so much over the last few years. I am particularly grateful to Brandon and Jacopo who have been a constant source of support since the early days of my PhD research. They remained patient when faced with my numerous and sometimes annoying questions. Undoubtedly, it was through our countless discussions about physics that I learnt the most over the last few years. I would also like to highlight Chris, Lorenzo, and Prem. Their invaluable support in the second half of my PhD has helped to prepare me for the next stage of my research career. I am also very grateful to Kristan Jensen; although we didn't formally collaborate, his help was indispensable in setting up one of my research projects. I would also like to thank my thesis examiners Madalena Lemos and Kostas Skenderis for carefully reading the present manuscript and for their valuable feedback. Their thoughtful comments during the viva and in their report have helped me to improve my thesis.

I would further like to thank the members of my research group for creating such a welcoming and stimulating environment. I am particularly grateful to Marika Taylor for inspiring me to stay open to other fields of research beyond my own, and her invaluable help in navigating the jungle of university regulations and administrative matters. I am also grateful to David Turton for his advice at various points during my PhD. Throughout my years in Southampton, I was lucky enough to share an office with Ernesto Bianchi, Elliot Bridges, Davide Bufalini, Federico Capone, Joan Garcia i Tormo, Zezhuang Hao, Callum Hunter, George Katsianis, Iván Muñoz, and Sami

Rawash. I will miss having my almonds shamelessly stolen and chatting about obscure maths questions. In addition to my office mates, I would like to thank Thomas Celora, Bidisha Chakrabarty, Alex Davey, Dani Hasenbichler, Filip Landgren, Tristan Madeleine, Enrico Parisini, Hynek Paul, Aaron Poole, Kostas Rigatos, Luis Rocha, Matt Russell, Michele Santagata, Arvind Shekar, Linus Too, and Mritunjay Verma, who have made my time in Southampton all the more enjoyable. I will miss our numerous reading groups and conversations about physics and maths as well as the times we shared outside the university.

Over the many past years spent thinking about physics and maths, I met numerous people and many of them have become my dearest friends. There are far too many to name but I'd like to point out a few of the ones who have stayed in physics and maths. I'm very grateful for having met Tanuj Gomez and Neil Talwar during my undergraduate days. I miss our shared flat which was the backdrop to many of Tanuj's attempts to explain formal aspects of geometry and topology to me. I'm very grateful for having met Weijie Chee, Nicky Li, Atul Sharma, Diandian Wang, Dan Zhang, and Ziruo Zhang during our shared time in the catacombs of the CMS. It was through countless discussions with them that I learnt the very basic tools of our trade. Even though we are scattered across the globe now, we have found ways to keep talking about physics, life, and the universe. I would also like to thank Volodia Schaub, Joe Smith, and Jake Stedman, with whom I've had the pleasure to talk about various bits of physics during my time as a visitor at KCL.

I could not have undertaken this journey without the unwavering support of my family, and in particular my parents Rima and Talik, and my sister Laura. Their unconditional love encouraged me to pursue my interests, no matter how obscure or abstract they seemed to them. Finally, this thesis would not have been possible without Lucille Calmon, who has accompanied me on this journey since the very start and been a monumental pillar of support in the last few years.

To my friend Michael Zhao, a gifted mathematician and one of the kindest people I met. I wish he was here today.

Part I

Introduction

Chapter 1

Motivation

Since its inception, quantum field theory (QFT) has proven to be an incredibly powerful tool. Arguably the most celebrated QFT is the Standard Model of particle physics, which provides the best description of all fundamental forces except gravity. However, QFT is more than just a tool to compute cross sections of particle decays. It has found numerous applications. E.g. QFT describes many-body systems in the continuum limit. It is thus of immense importance in condensed matter physics, and can be used to describe superconductivity, Luttinger liquids, quantum Hall physics, and many more systems, see e.g. [6]. In the context of cosmology, QFT is used to describe primordial fluctuations which give rise to the large-scale structures we see in the sky via inflation. QFT also underpins string theory, a consistent theory of quantum gravity. Moreover, certain QFTs are intricately related to beautiful pieces of mathematics, including knot theory [7], Morse theory [8], and category theory [9,10], to name a few. Together with string theory, it has also spurred new advances in mathematics, sometimes proving long-standing conjectures, e.g. in the context of the geometry and topology of various types of manifolds [11–14], quantum groups [15], moonshine theory [16], and the geometric Langlands programme [17].

Famously, QFT is plagued by pesky infinities which arise from very high and very low energy modes. The latter, so-called infra-red (IR) divergences can be avoided if the theory is put on a compact space as the wavelength of a particle can no longer become infinitely large. High energy, or ultra-violet (UV) divergences are more persistent. To deal with them, one may e.g. impose a hard cut-off, i.e. only keeping modes up to a certain energy scale. From a Wilsonian point of view, a QFT is an effective theory with an associated Lagrangian, valid up to some cut-off scale associated with the emergence of new physics. As one lowers the cut-off scale by performing the path integral over modes with energies between the old and new cut-offs, the coupling constants in the QFT change, or ‘run’. Equivalently, this can be thought of as a coarse-graining of the description as one lowers the energy scale. This running of

couplings is called a renormalisation group (RG) flow. Depending on the type of interactions, some coupling constants will become large as the cut-off is lowered.

This poses a challenge for theorists. Despite its vast applicability, there is a limited set of techniques to compute physical observables of a given QFT. For weakly-interacting QFTs one can work with the Lagrangian and use perturbation theory in the coupling constants. However, at strong coupling the Lagrangian is less useful, and QFT becomes difficult. This lack of tools is problematic as many fundamental theories of nature are strongly coupled in certain regimes. One such theory is quantum chromodynamics (QCD), which describes the constituents of subatomic particles as part of the Standard Model, and is an example of a gauge theory. QCD is asymptotically free, i.e. it is strongly coupled at low energies. Arguably the best one can do is to put the theory on a lattice. Numerical methods can then be used to make theoretical predictions, e.g. for the masses of light hadrons [18]. However, lattice methods come with their own set of limitations, e.g. they cannot simulate any dynamical real-time processes. A building block of QCD is Yang-Mills (YM) theory, which shares its asymptotic freedom. It is unknown whether this simple theory has a mass gap, i.e. whether the lightest particles are massive. Lattice simulations suggest it does, however, no formal proof exists. Establishing such a proof and showing that YM theory can be made mathematically rigorous is one of the unsolved Millennium Prize Problems in mathematics.

In the absence of generic analytic tools at strong coupling, one may wonder whether general principles may guide us towards a better understanding of QFT, including in the strong coupling regime. The uselessness of a Lagrangian description at strong coupling suggests that the information that uniquely characterises a QFT may be encoded differently. In some sense, this information should play the role of coordinates in an abstract space of QFTs. General principles may then impose constraints on this information, carving out regions of consistent theories in this larger space of QFTs, and may even lead to a classification scheme for QFTs.

Symmetries are essential tools for characterising and classifying QFTs. In particular, in any local, unitary QFT in d dimensions, Noether's theorem for the Lorentz group requires the existence of a symmetric, conserved stress tensor, $T^{\mu\nu} = T^{\nu\mu}$ and $\partial_\mu T^{\mu\nu} = 0$, with $\mu, \nu = 1, 2, \dots, d$. In this sense, $T^{\mu\nu}$ is *universal*: we can *always* characterise a local Lorentz-invariant QFT, in part, via correlations of $T^{\mu\nu}$ with itself and other operators.

A particularly powerful symmetry is supersymmetry (SUSY), an extension of the usual Poincaré algebra to include fermionic generators. Currently, there are no experimental indications that SUSY is realised in our universe. If it exists, it must be broken at energy scales accessible to current experiments. Nonetheless, it is of immense use to theorists. SUSY provides a remarkable abundance of tools for certain

toy models of the QFTs describing nature. E.g. SUSY allows for determination of the IR dynamics of some asymptotically free QFTs [19,20], and for exact computation of certain quantities [21–24]. This makes supersymmetric QFTs (SQFTs) excellent laboratories for theorists.

Conformal symmetry is yet another extension of the Poincaré group. Conformal symmetry includes invariance under scale transformations. In nature, scale and conformal invariance arise naturally at phase transitions and critical phenomena. QFTs that enjoy invariance under the conformal group are called conformal field theories (CFTs). Famously, the Ising model of ferromagnetism at criticality is described by a CFT in $d = 2, 3$. In string theory, a 2d CFT provides the underlying description of a string propagating in spacetime.

More abstractly in QFT, scale invariance appears at the fixed points of RG flows. In unitary QFTs, this typically enhances to invariance under the full conformal group. This makes CFTs natural starting points for characterising and classifying QFTs. Moreover, in a local, unitary CFT, conformal symmetry fixes the correlation functions of all local operators in terms of the two- and three-point functions of a subset of local operators, called conformal primaries. Specifically, conformal symmetry fixes the form of correlation functions of primaries, which in turn determine correlation functions involving their conformal descendants. This dramatically simplifies the problems of characterisation and classification for CFTs, and the QFTs connected to them via RG flows.

Classically, conformal invariance ensures that the stress tensor of a CFT has vanishing trace, $T^\mu{}_\mu = 0$. In the quantum theory, this translates to a Ward identity whereby $T^\mu{}_\mu = 0$ inside correlation functions away from other operator insertions. On a curved background, $T^\mu{}_\mu = 0$ classically but not necessarily in the quantum theory. Indeed, it is an important property of CFTs in even dimensions that scale invariance is broken by quantum effects when the theory is placed on a curved metric background. This breaking is captured by the Weyl anomaly. It states that the trace of the stress tensor must be given by scalar invariants of the background fields, including curvature invariants of the metric, multiplying the identity operator.

The coefficients of these invariants are often called central charges. They are important pieces of information about the CFT and control various physical quantities, including the thermodynamic entropy in $d = 2$ [25,26] and the entanglement entropy (EE) [27–30]. Moreover, the 2- and 3-point functions of $T^{\mu\nu}$ are fixed (in part) by Weyl anomaly coefficients when $d \in 2\mathbb{Z}$. Importantly, some central charges obey positivity constraints and/or must decrease along RG flows from an UV to an IR fixed point [31–34,34–40]. These co-called c-theorems rely only on generic principles, like locality, Lorentz invariance, and unitarity, making them powerful non-perturbative constraints on QFTs. The decreasing quantities provide a measure of the number of

degrees of freedom (DOF) of a QFT, which we expect to decrease along an RG flow, as massive modes decouple. Most importantly for characterisation and classification, c-theorems impose irreversibility along RG flows, providing a hierarchical order among QFTs, with CFTs occupying privileged places in the space of QFTs.

QFTs allow for deformations by extended operators, called defects, which enrich the dynamics and extend the algebra of local operators. It is common to also include boundaries in the discussion of defects as a boundary of a QFT can be considered as a special case of an interface between a QFT and a trivial or topological QFT. Boundaries and defects are ubiquitous in physics. E.g. in string theory, strings can end on defects in spacetime, called branes. Heuristically, strings may tug and pull on these branes giving rise to local excitations of this defect. The dynamics of these branes in the IR are naturally described by QFT. Branes in string theory may end on other branes, or intersect with one another, naturally giving rise to boundaries or defects in the low-energy QFT description of each brane's excitations. This suggests that defects are a fundamental ingredient of QFT.

Defects also play a fundamental role in more traditional fields of physics. E.g. any experiment is necessarily performed on a system of finite size. In the presence of a boundary, a physical system can have interesting dynamics confined to its surface. E.g. topological insulators are insulating in their interior but can support electric currents on their surface. Impurities in materials can be thought of as higher co-dimension defects. E.g. the Kondo effect describes the change of electrical resistivity with temperature of a metal in the presence of magnetic impurities. In fact, the Kondo problem and the study of impurities were instrumental in the development of the RG, see e.g. the review [41]. Since QFT can be used to describe various condensed matter systems in the continuum limit, it is crucial to gain a better understanding of boundaries and defects in QFT. This includes the development of tools as well as a more formal exploration of defects.

Indeed, defects are essential for understanding the complete spectra of QFTs, and it has been suggested recently that defects may provide a basis for a more robust classification scheme of QFTs and phases of matter [42–45]. E.g. in gauge theories, line operators are crucial for classifying the QFT's vacua, and for distinguishing gauge theories with the same gauge *algebras* but different gauge *groups* [43]. Similarly, higher-dimensional defects can be crucial for classifying vacua, for example by providing order parameters that can detect whether higher-dimensional objects, such as strings, have condensed. Co-dimension one defects, also known as interfaces or domain walls, can provide natural maps between QFTs related by dualities, RG flows, and other transformations.

A defect in QFT necessarily breaks translational symmetry in directions normal to the submanifold on which it is supported, so that $T^{\mu\nu}$ is no longer conserved. Indeed, now

$\partial_\mu T^{\mu i} = \delta^{(q)} \mathcal{D}^i$, where $\delta^{(q)}$ is a delta function that localises to the defect in the q directions normal to the defect, and \mathcal{D}^i is the displacement operator. The displacement operator is a defect-localised scalar, and is a vector in the normal directions, labelled by the index $i = p + 1, \dots, d$. In correlation functions, the insertion of \mathcal{D}^i acts as a local geometric deformation of the defect, which “displaces” a point on the defect in a normal direction, hence its name. Since it descends from the stress tensor of the ambient theory, the displacement operator is itself *universal* in the defect spectrum: we can always characterise a local QFT with a defect, in part, via correlations of \mathcal{D}^i with itself and other operators.

In generic QFTs, defects remain poorly characterised. However, much progress can be made by imposing restrictive symmetries. In this thesis we will be interested in conformal symmetry. A standalone CFT is invariant under the conformal group of d dimensions. If a p -dimensional defect insertion or boundary preserves the conformal group in p dimensions as a sub-group, the combined system is called a defect CFT (DCFT) or boundary CFT (BCFT), respectively. As is the case with ordinary CFTs, DCFTs and BCFTs are natural starting points for characterising and classifying defects. In particular, they sit at the endpoints of RG flows, including those localised to the defect or boundary, and those of the ambient QFT. Local correlators in a BCFT or DCFT are completely determined by (1) the ambient CFT data, i.e. the spectrum of primaries and their 3-point functions, (2) the spectrum of defect or boundary primaries, whose 2- and 3-point correlators with one another are fixed by the defect or boundary conformal symmetry up to a set of dimensionless coefficients, and (3), the mixed 2-point functions of ambient and defect/boundary primaries. The study of BCFT and DCFT has seen tremendous progress in recent years in a wide range of contexts. See e.g. [46] for a survey.

In a DCFT or BCFT, the conformal symmetry preserved by the defect or boundary requires $T^\mu_\mu = 0$. Much like CFTs, a DCFT or BCFT can exhibit a Weyl anomaly in curved space and/or when the defect or boundary is curved. In contrast to the Weyl anomaly in CFTs, now $T^\mu_\mu \neq 0$ generically consists of contributions from both the ambient CFT, when d is even, and from defect or boundary localised terms, which can potentially be non-vanishing for both even and odd p . The coefficients of defect/boundary Weyl anomalies define defect/boundary central charges that are crucial for characterisation and classification. E.g. some defect central charges determine the defect’s contribution to the EE [47–50]. However, relatively little is known about defect central charges compared to their CFT counterparts. For instance, they should determine many correlation functions involving $T^{\mu\nu}$ and \mathcal{D}^i , but exactly how has been determined only for a subset of them [51–54]. These results subsequently imply positivity constraints for some defect central charges [50, 52]. A defect/boundary c-theorem for arbitrary p and d has been proposed for RG flows

localised to the defect/boundary [49], however, rigorous proofs have only appeared for a subset of these [55–57].

For CFTs in $d > 4$, power counting forbids any interacting local Lagrangian, so naïvely we expect the only local, reflection-positive $d = 6$ CFTs to be free, massless fields, namely scalars, fermions, self-dual three-forms, and combinations thereof. However, string theory has revealed that intrinsically strongly-interacting supersymmetric CFTs, or superconformal field theories (SCFTs), exist in $d = 6$. Despite lacking a Lagrangian description, all evidence to date suggests these SCFTs are local. These special properties suggest $d = 6$ SCFTs may be “parent theories” that, upon compactification and (super)symmetry breaking, give rise to many QFTs in lower d [58]. Moreover, refs. [59–65] proposed a classification of 6d SCFTs, making them an especially promising starting point for classifying QFTs. The 6d SCFTs with maximal SUSY are especially challenging to study, being isolated, strongly-interacting fixed points, and having no continuous free parameters. Very little is known about their local operator spectrum. However, string theory arguments suggest that these theories admit superconformal co-dimension two and four defect operators. Studying these defects provides a direct path towards a better understanding of these SCFTs. It is likely that some of these lessons will indicate a way towards the characterisation and classification of QFTs more generally.

The work presented in this thesis aims to take a step towards this broad goal. The scarcity of non-perturbative tools, however, makes it challenging to obtain exact expressions for physical observables. Some of the techniques available in DCFT include numerical [66–68] and perturbative [69] methods. By the celebrated anti-de Sitter (AdS)/CFT correspondence [70], some CFTs are holographically dual to string theory on AdS space in one dimension higher. Remarkably, this is a strong-weak duality, meaning that a strongly coupled CFT has a dual weakly coupled gravitational description. Conformal defects have been studied in this context, e.g. in refs. [50, 71–73]. However, the correspondence typically assumes the existence of a discrete parameter in the CFT, often called N , which is taken to be large. As a consequence, results derived using the AdS/CFT correspondence are perturbative in $1/N$.

The focus of this thesis will be on *exact* methods for DCFTs. The main subjects of investigation are the defect central charges mentioned in the previous paragraphs. We will derive novel universal results about a large class of defects. Some of these results will be illustrated in examples of simple yet non-trivial conformal defects in free CFTs. Using existing exact methods for free fields, we can determine various physical properties of these defects. Beyond free fields, non-perturbative tools are limited. They include the analytic conformal bootstrap, or require further symmetries. We will take the latter approach and impose SUSY in addition to conformal invariance. We

show how SUSY allows us to develop non-perturbative methods to compute defect central charges exactly, without any limits or approximations.

This thesis is organised as follows. Chapters 2, 3, 4, and 5 contain condensed reviews of CFT, DCFT, EE, and SUSY, respectively. We will be selective in our presentation, and only introduce concepts that are required for the following chapters. Motivated by the co-dimension two defect of the 6d SCFT with maximal SUSY, we study 4d conformal defects in chapter 6. We derive the defect's general contribution to the Weyl anomaly, allowing the ambient CFT to have arbitrary dimension $d \geq 5$. We then determine how some of the defect central charges appear in flat and curved space correlation functions of the stress tensor and the displacement operator. We also determine the defect contribution to EE, and derive a novel constraint on one of these defect central charges. In chapter 7, we study a simple co-dimension two defect in the theories of a complex scalar field and a Dirac fermion. The defect under consideration is constructed by introducing a monodromy in the ambient fields as they are rotated around a distinguished submanifold of dimension $p = d - 2$. We use various free field methods to compute correlation functions exactly. When the defect dimension $p = 2, 4$, we show how defect central charges can be extracted from these correlation functions. For $p = 2$, we can obtain all of them in this way. As a consistency check we compute the defect contribution to the EE when $p = 2$. In chapter 8, we study defects in SCFTs. We argue that central charges of 2d defects must appear in SUSY partition functions on backgrounds of the type S^d and $S^1 \times S^{d-1}$. Using a non-perturbative method called SUSY localisation [23, 24], these partition functions are exactly computable. We introduce new methods to extract these central charges without approximations. Our methods are broadly applicable, and we illustrate them in a number of examples of 4d and 6d SCFTs, including the 2d and 4d defects of the 6d SCFT with maximal SUSY. Finally, we make a few concluding remarks in chapter 9.

Chapter 2

Conformal Field Theory in $d > 2$

In this section we review CFT in $d > 2$. The case of $d = 2$ is special as the (local) conformal algebra is the infinite-dimensional Virasoro algebra, which contains the global conformal group as a subalgebra. The discussion below applies to the global subalgebra.

This section is a lightning review of standard textbook material. We found the following references useful in writing this section: [74–80]. We will assume Euclidean signature throughout, unless stated otherwise.

2.1 Conformal symmetry

A conformal transformation is a diffeomorphism $x \rightarrow x'(x)$ that leaves the metric $g_{\mu\nu}$ invariant up to a scale

$$g'_{\mu\nu}(x') = g_{\rho\sigma}(x) \frac{\partial x^\rho}{\partial x'^\mu} \frac{\partial x^\sigma}{\partial x'^\nu} = \Lambda^2(x') g_{\mu\nu}(x'), \quad (2.1.1)$$

where $\Lambda(x)$ is a position-dependent scale factor, and $\mu = 1, \dots, d$. Under an infinitesimal coordinate transformation generated by a vector ϵ^μ , such that $x'^\mu \rightarrow x'^\mu = x^\mu + \epsilon^\mu(x)$, metric invariance up to a scale translates to the following condition

$$D_\mu \epsilon_\nu(x) + D_\nu \epsilon_\mu(x) = -2\sigma(x) g_{\mu\nu}(x) = \frac{2}{d} D \cdot \epsilon(x) g_{\mu\nu}(x), \quad (2.1.2)$$

where D is the Levi-Civita connection and $\Lambda(x) = e^{\sigma(x)}$. The final equality follows from tracing the first equality, solving for $\sigma(x)$ and substituting it back into the equation. In Euclidean space with Cartesian coordinates, this reduces to

$$\partial_\mu \epsilon_\nu(x) + \partial_\nu \epsilon_\mu(x) = \frac{2}{d} \partial \cdot \epsilon(x) \delta_{\mu\nu}. \quad (2.1.3)$$

It is straightforward to show that this condition only has the following solutions:

$$\epsilon_\mu = a_\mu, \quad (2.1.4a)$$

$$\epsilon_\mu = \omega_{\mu\nu} x^\nu, \quad (2.1.4b)$$

$$\epsilon_\mu = \lambda x_\mu, \quad (2.1.4c)$$

$$\epsilon_\mu = 2(x \cdot b)x_\mu - b_\mu x^2, \quad (2.1.4d)$$

where a and b are constant vectors, ω is an anti-symmetric matrix with constant entries, and λ is a constant. The first two transformations correspond to ordinary translations and rotations. The third transformation implements a dilatation, whereas the fourth one is called a special conformal transformation. It can be thought of as an inversion $x^\mu \rightarrow x^\mu/x^2$, followed by a translation by $-b$, followed by another inversion.

The infinitesimal conformal transformations can be exponentiated to give finite transformations. The only non-trivial ones are the special conformal transformations, which are given by

$$x'^\mu = \beta(x)(x^\mu - b^\mu x^2), \quad \beta(x) = \frac{1}{1 - 2b \cdot x + b^2 x^2}. \quad (2.1.5)$$

A general conformal transformation has the following Jacobian

$$\frac{\partial x'^\mu}{\partial x^\nu} = \Lambda(x) R^\mu{}_\nu(x), \quad (2.1.6)$$

where $R^\mu{}_\nu$ is a position-dependent $SO(d)$ rotation matrix, i.e. a conformal transformation is a local rescaling and rotation. The metric then transforms as in eq. (2.1.1).

Invariance of the action I under (infinitesimal) conformal transformations ensures that there exists an improved stress tensor which obeys

$$\partial_\mu T^{\mu\nu} = 0, \quad T^{\mu\nu} = T^{\nu\mu}, \quad T^\mu{}_\mu = 0 \quad (2.1.7)$$

on-shell, see e.g. ref. [79].¹ Via Noether's theorem, translations, rotations, dilatations, and special conformal transformations give rise to conserved currents

$$(j_P^\nu)^\mu = T^{\mu\nu}, \quad (j_M^{\nu\rho})^\mu = x^\nu T^{\mu\rho} - x^\rho T^{\mu\nu}, \quad (j_D)^\mu = x_\nu T^{\mu\nu}, \quad (j_K^\nu)^\mu = x^2 T^{\mu\nu} - 2x^\nu x_\rho T^{\mu\rho}, \quad (2.1.8)$$

¹We assumed the existence of an action for convenience but this is not a requirement. Indeed, some of the CFTs that we will consider in this thesis do not have a (known) Lagrangian description. However, if the CFT is sufficiently local (and non-topological), it will have a spin-two local operator with the properties in eq. (2.1.7). For all CFTs (without defects), we will always assume the existence of a local stress tensor.

respectively, where $T_{\mu\nu}$ is the improved symmetric and conserved (on-shell) stress tensor.² The associated charges generate the conformal algebra

$$[D, P_\mu] = iP_\mu, \quad (2.1.9a)$$

$$[D, K_\mu] = -iK_\mu, \quad (2.1.9b)$$

$$[K_\mu, P_\nu] = 2i(\eta_{\mu\nu}D - M_{\mu\nu}), \quad (2.1.9c)$$

$$[K_\rho, M_{\mu\nu}] = i(\eta_{\rho\mu}K_\nu - \eta_{\rho\nu}K_\mu) \quad (2.1.9d)$$

$$[P_\rho, M_{\mu\nu}] = i(\eta_{\rho\mu}P_\nu - \eta_{\rho\nu}P_\mu) \quad (2.1.9e)$$

$$[M_{\mu\nu}, M_{\rho\sigma}] = i(\eta_{\nu\rho}M_{\mu\sigma} + \eta_{\mu\sigma}M_{\nu\rho} - \eta_{\mu\rho}M_{\nu\sigma} - \eta_{\nu\sigma}M_{\mu\rho}). \quad (2.1.9f)$$

Note that the generators $M_{\mu\nu}$ form the Lorentz algebra $\mathfrak{so}(d)$ in Euclidean signature (or $\mathfrak{so}(d-1, 1)$ in Lorentzian signature) as a subalgebra of the conformal algebra. The conformal algebra itself can be shown to be isomorphic to $\mathfrak{so}(d+1, 1)$ in Euclidean signature (or $\mathfrak{so}(d, 2)$ in Lorentzian signature). Let \tilde{M}_{IJ} be the generators of $\mathfrak{so}(d+1, 1)$, where $I, J = 0, 1, \dots, d+1$. The generators for $(I, J) = (\mu, \nu)$ are identified with the $\mathfrak{so}(d)$ Lorentz generators $M_{\mu\nu}$. $\tilde{M}_{0(d+1)}$ is identified with D , whereas $\tilde{M}_{\mu 0}$ and $\tilde{M}_{\mu(d+1)}$ are identified with the linear combinations $\frac{1}{2}(P+K)_\mu$ and $\frac{1}{2}(P-K)_\mu$. This algebra exponentiates to the Euclidean conformal group $SO(d+1, 1)$ (or $SO(d, 2)$ in Lorentzian signature).

The emergence of $SO(d+1, 1)$ suggests that one should consider its action on $\mathbb{R}^{d+1,1}$ rather than the physical spacetime \mathbb{R} . In fact, $SO(d+1, 1)$ acts naturally on the space of light-rays through the origin of $\mathbb{R}^{d+1,1}$, and \mathbb{R}^d can be obtained as a section of the lightcone. This gives rise to the embedding space formalism in CFT, which is a powerful formalism that makes the kinematical constraints of conformal symmetry easier to implement on correlation functions. See e.g. [75, 81] for an introduction.

2.2 States and operators

In a quantum theory, operators sit in representations of the global symmetries. In Lorentz-invariant QFT, local operators at the origin are in representations of the Lorentz group $SO(d)$. In a scale-invariant theory, it is convenient to also diagonalise the dilatation operator D , such that local operators also carry a label Δ , called the scaling dimension.

²In theories that are only Poincaré and scale invariant, dilatations are necessarily constant. Under a constant dilatation σ , the action I changes like $\delta I = -\int \sigma \delta_{\mu\nu} T^{\mu\nu}$. Requiring that the action is invariant under constant dilatations implies that $T^\mu{}_\mu = \partial_\mu V^\mu$ for some current V^μ , often called the virial current. The conserved dilatation current then is $(j_D)^\mu = x_\nu T^{\mu\nu} - V^\mu$. It is really the special conformal transformations which allow for spacetime dependent dilatations. Invariance of the action can then only be guaranteed if $\partial_\mu V^\mu = 0$, i.e. V^μ is a conserved current, in which case $T^\mu{}_\mu = 0$.

Consider a scalar operator \mathcal{O} with scaling dimension Δ . Under a constant scale transformation, it transforms as

$$\mathcal{O}(x) \rightarrow \mathcal{O}'(\lambda x) = \Lambda^{-\Delta} \mathcal{O}(x). \quad (2.2.10)$$

Conformal transformations, however, generically involve position-dependent scale transformations, and it is not immediately obvious how to generalise the above transformation rule eq. (2.2.10). A scalar operator \mathcal{O} is said to be primary if it transforms homogeneously,

$$\mathcal{O}(x) \rightarrow \mathcal{O}'(x') = \Lambda(x)^{-\Delta} \mathcal{O}(x), \quad (2.2.11)$$

under a general conformal transformation. The scale factor Λ is the one appearing in eq. (2.1.6). Note that $\partial_\mu \mathcal{O}_\Delta$ cannot transform homogeneously, as it will pick up contributions involving $\partial_\mu \Lambda(x)$.

By eq. (2.1.6), conformal transformations also involve rotations. An operator \mathcal{O} in an n -dimensional representation ρ of the Lorentz group $SO(d)$ and with scaling dimension Δ is said to be primary if it transforms as

$$\mathcal{O}_\alpha(x) \rightarrow \mathcal{O}'_\alpha(x') = \Lambda^{-\Delta}(x) \rho[R^\mu_\nu(x)]_\alpha^\beta \mathcal{O}_\beta(x), \quad (2.2.12)$$

where α, β are representation indices and $\rho[R^\mu_\nu(x)]_\alpha^\beta$ is the $n \times n$ matrix representative of $R^\mu_\nu(x)$, i.e. it implements the action of $R^\mu_\nu(x)$ in the $SO(d)$ representation ρ . E.g. for an operator in the vector representation, $\mathcal{O}'_\mu(x') = \Lambda^{-\Delta}(x) R^\nu_\mu(x) \mathcal{O}_\nu$.

Using the infinitesimal coordinate transformations in eq. (2.1.4), one finds the following action of the conformal charges on primary fields

$$[P_\mu, \mathcal{O}(x)] = -i \partial_\mu \mathcal{O}(x) \quad (2.2.13a)$$

$$[M_{\mu\nu}, \mathcal{O}(x)] = -i (\Sigma_{\mu\nu} - x_\mu \partial_\nu + x_\nu \partial_\mu) \mathcal{O}(x) \quad (2.2.13b)$$

$$[D, \mathcal{O}(x)] = -i (\Delta + x^\mu \partial_\mu) \mathcal{O}(x) \quad (2.2.13c)$$

$$[K_\mu, \mathcal{O}(x)] = -i (2x_\mu \Delta + 2x^\nu \Sigma_{\nu\mu} + 2x_\mu x^\nu \partial_\nu - x^2 \partial_\mu) \mathcal{O}(x), \quad (2.2.13d)$$

where we suppressed the $SO(d)$ representation indices. The $n \times n$ matrix $(\Sigma_{\mu\nu})_\alpha^\beta$ satisfies eq. (2.1.9f) and implements an infinitesimal $SO(d)$ transformation. E.g. in the vector representation, $(\Sigma_{\mu\nu})_\alpha^\beta = \delta_{\mu\alpha} \delta_\nu^\beta - \delta_\mu^\beta \delta_{\nu\alpha}$. If the primary is inserted at the origin, then $[K_\mu, \mathcal{O}(0)] = 0$, which may be regarded as the defining property of a primary. From the algebra eq. (2.1.9), it is clear that the translation generators P_μ raise the dimension by 1 whereas the special conformal generators K_μ lower it by 1. Therefore, from each primary operator one can construct operators of higher scaling dimension by repeatedly acting with P_μ . Such operators are called descendants.

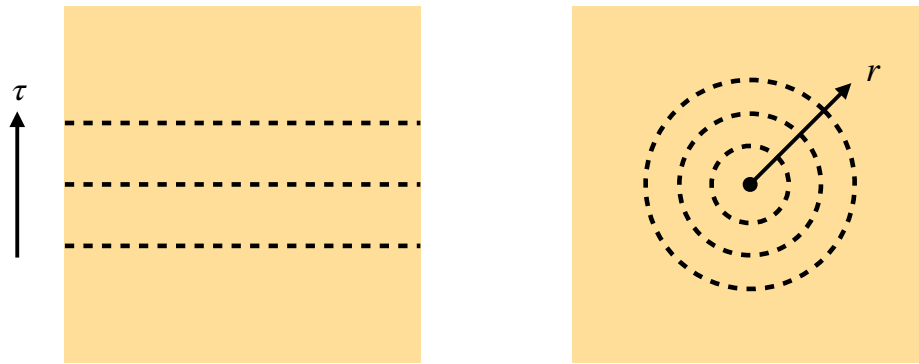


FIGURE 2.1: *Left:* Illustration of quantisation on spatial slices. The Euclidean time coordinate $\tau \in [-\infty, +\infty]$ extends along the vertical axis. Dashed lines are hypersurfaces of constant τ . *Right:* Illustration of radial quantisation. The radial coordinate $r = |x|$ plays the role of time. Dashed lines are hypersurfaces of constant $r \in [0, +\infty]$. Note that the Hilbert spaces associated with the spatial slices in the two quantisation schemes are different, however, there exists an isomorphism between them. In particular, the two Hilbert spaces have the same dimension.

In QFT, one associates a Hilbert space with each spatial slice in a foliation of spacetime. Usually, one picks spatial slices, and the generator of (Euclidean) time translations plays the role of the Hamiltonian. In Euclidean CFT, it is more convenient to pick a radial foliation around a distinguished point, typically the origin $x = 0$. One then quantises radially around this point, with the dilatation generator D playing the role of the Hamiltonian. See figure 2.1 for an illustration of the two quantisation choices. We will work in radial quantisation henceforth.

States form irreducible representations of the conformal algebra, and they are labelled by the scaling dimension Δ and their spin J ,

$$D|\Delta, J\rangle = -i\Delta|\Delta, J\rangle, \quad M_{\mu\nu}|\Delta, J\rangle = -i\Sigma_{\mu\nu}|\Delta, J\rangle. \quad (2.2.14)$$

Consider an operator $\mathcal{O}_{\Delta, J}$ with scaling dimension Δ and spin J . One can then create an initial state $|\Delta, J\rangle$ from the vacuum $|0\rangle$ as follows

$$|\Delta, J\rangle = \mathcal{O}_{\Delta, J}(0)|0\rangle. \quad (2.2.15)$$

This so-called in-state can then be evolved to a later slice via Hamiltonian evolution.

Our choice of quantisation comes with a notion of Hermitean conjugation. In radial quantisation for real $\mathcal{O}_{\Delta, J}$,³ Hermitean conjugation can be identified with an inversion

³A real operator in Euclidean signature is the analogue of a Hermitean operator in Lorentian QFT. For a complex operator, $\mathcal{O}^\dagger = \mathcal{O}^*$.

$x^\mu \rightarrow x'^\mu = \frac{x^\mu}{x^2}$, such that

$$\mathcal{O}_{\Delta,J}^{\mu_1 \dots \mu_J}(x^\mu)^\dagger = I^{\mu_1 \nu_1}(x) \dots I^{\mu_J \nu_J}(x) |x|^{-2\Delta} \mathcal{O}_{\Delta,J}^{\nu_1 \dots \nu_J} \left(\frac{x^\mu}{x^2} \right), \quad (2.2.16)$$

where $\frac{\partial x'^\mu}{\partial x^\nu} = |x|^{-2} \left(\delta_\nu^\mu - \frac{2x^\mu x_\nu}{x^2} \right) \equiv |x|^{-2} I^\mu{}_\nu(x)$.⁴ An out-state is then defined as

$$\langle \Delta, J | = \langle 0 | \mathcal{O}_{\Delta,J}(0)^\dagger = \lim_{y \rightarrow \infty} |y|^{2\Delta} \langle 0 | \mathcal{O}_{\Delta,J}(y). \quad (2.2.17)$$

Note that the factor of $|x|^{-2\Delta}$ in eq. (2.2.16) ensures that the norm of a state, i.e. the inner product of an in-state $|\Delta, J\rangle$ with the associated out-state $\langle \Delta, J|$ is well-defined. Hermitean conjugation exchanges in and out states, and thus the roles of origin and infinity. Since the conformal generators P_μ and K_μ fix the point at infinity and the origin, respectively, they must be interchanged under Hermitean conjugation:

$$P_\mu^\dagger = K_\mu, \quad M_{\mu\nu}^\dagger = M_{\mu\nu}, \quad D^\dagger = -D, \quad K_\mu^\dagger = P_\mu. \quad (2.2.18)$$

Radial quantisation allows for a one-to-one correspondence between states and local operators in CFT, known as the state-operator correspondence. A local operator inserted at the origin trivially maps to a state on a radial slice surrounding it via Hamiltonian evolution, or equivalently by performing the path integral on the region enclosed by the spatial slice. We have assumed this direction in writing eq. (2.2.15). In a CFT, one may also go the other way. To define a local operator, one needs to specify its correlation functions with other local operators. Given eigenstates of the dilatation operator $|\mathcal{O}_{\Delta_i}\rangle$, one can define a correlation function by excising spherical regions and assigning a state $|\mathcal{O}_{\Delta_i}\rangle$ to the boundary of each ball, and performing the path integral outside. The spheres can then be brought arbitrarily far apart by a dilatation. This defines a correlator of local operators, and one can show that it respects conformal invariance.

Conformal primary operators at the origin are annihilated by K . By the state operator correspondence, one may equivalently think of primary states

$$K_\mu |\Delta, J\rangle = 0, \quad D |\Delta, J\rangle = -i |\Delta, J\rangle, \quad M_{\mu\nu} |\Delta, J\rangle = -i \Sigma_{\mu\nu} |\Delta, J\rangle. \quad (2.2.19)$$

In a reflection-positive QFT, the Hamiltonian must be bounded from below.⁵ In radial

⁴Under an appropriate conformal transformation, the standard notion of Hermitian conjugation of a CFT on the cylinder quantised on spatial slices maps to inversion in a radially quantised CFT in flat space, see e.g. ref. [78], thus justifying the above identification.

⁵Reflection positivity is the Euclidean analogue of Lorentzian unitarity, $\langle \psi | \psi \rangle \geq 0$ for any state $|\psi\rangle$. By the Osterwalder-Schrader reconstruction theorem [82], a collection of reflection-positive Euclidean correlation functions can be analytically continued to unitary correlation functions in a Lorentzian QFT under certain technical assumptions. Ref. [83] recently proved this statement for CFT 2-, 3-, and 4-point functions assuming only Euclidean CFT axioms. In particular, their work relies on the convergence of the Euclidean operator product expansion (OPE), which will be introduced in section 2.3.

quantisation, the Hamiltonian is identified with the dilatation operator. This implies that reflection-positive representations must be of lowest-weight type. The conformal primary is the lowest weight since it is annihilated by K_μ , and the other weights in the module are obtained by acting with an arbitrary number of P_μ 's. In fact, one can do even better: reflection positivity/unitarity imposes bounds on the scaling dimensions of primary operators. E.g. for a primary state $|\Delta\rangle \equiv |\Delta, J = 0\rangle$,

$$|P_\mu|\Delta\rangle|^2 = \langle\Delta|K_\mu P_\mu|\Delta\rangle = 2\Delta \geq 0 \quad (2.2.20)$$

for fixed μ . Thus, $\Delta \geq 0$. When $d > 2$, this bound can in fact be strengthened by considering the norm of $P^2|\Delta\rangle$ to show that reflection positivity implies that primary operators have $\Delta = 0$ or $\Delta \geq \frac{d-2}{2}$. The unique operator with $\Delta = J = 0$ is the identity operator $\mathbb{1}$. For non-zero spin J , a similar argument shows that $\Delta \geq J + d - 2$ in a reflection-positive theory, see e.g. ref. [78] for a derivation. Note that conserved currents saturate the unitarity bounds. E.g. the stress tensor $T^{\mu\nu}$ is a primary with $\Delta = d$ and $J = 2$.⁶

2.3 Correlation functions and CFT data

Conserved currents in classical field theory give rise to Ward identities in QFT. Inside correlation functions, the currents are conserved away from other operator insertions. For j_P^ν , $j_M^{\nu\rho}$ and j_D defined in eq. (2.1.8) one finds the following Ward identities

$$\langle\partial_\mu T^\mu{}_\nu(x)\mathcal{O}_1(x_1)\dots\mathcal{O}_n(x_n)\rangle = -\sum_{i=1}^n\delta(x-x_i)\frac{\partial}{\partial x_i^\nu}\langle\mathcal{O}_1(x_1)\dots\mathcal{O}_n(x_n)\rangle, \quad (2.3.21a)$$

$$\langle(T^{\mu\nu}-T^{\nu\mu})(x)\mathcal{O}_1(x_1)\dots\mathcal{O}_n(x_n)\rangle = -\sum_{i=1}^n\delta(x-x_i)\Sigma_i^{\mu\nu}\langle\mathcal{O}_1(x_1)\dots\mathcal{O}_n(x_n)\rangle, \quad (2.3.21b)$$

$$\langle T^\mu{}_\nu(x)\mathcal{O}_1(x_1)\dots\mathcal{O}_n(x_n)\rangle = -\sum_{i=1}^n\delta(x-x_i)\Delta_i\langle\mathcal{O}_1(x_1)\dots\mathcal{O}_n(x_n)\rangle, \quad (2.3.21c)$$

where $\Sigma_i^{\mu\nu}$ is the rotation matrix in the representation of \mathcal{O}_i . See e.g. ref. [74] for a derivation. Note in particular that $T^\mu{}_\mu = 0$ away from other operator insertions.

Let us now consider the constraints of conformal invariance on correlation functions of primary operators. This is often called kinematics in the literature. The simplest correlation function is the one-point function. By Lorentz invariance, only scalar operators can acquire one-point functions. Translational invariance implies that such a one-point function must be constant. Scale invariance then fixes this constant to zero unless the operator has $\Delta = 0$. Thus, the only operator which can acquire a non-zero

⁶In 2d CFT, the stress tensor is a *Virasoro* descendant of the identity. It is not a descendant under the global conformal algebra.

one-point function is the identity. It is convenient to normalise the path integral such that $\langle \mathbb{1} \rangle = 1$.

Conformal invariance fixes the form of the two-point function in a CFT. For scalar primary operators, invariance under translations, rotations, and dilatations fixes

$$\langle \mathcal{O}_1(x) \mathcal{O}_2(y) \rangle \propto |x - y|^{-\Delta_1 - \Delta_2}. \quad (2.3.22)$$

Invariance under special conformal operators then implies that the two-point function vanishes unless $\Delta_1 = \Delta_2$. By choosing an orthonormal basis of primary operators, the constant of proportionality can be set to 1 for the two-point function of conjugate operators, and zero otherwise.

Two-point functions of spinning primary operators are more involved. E.g. the two-point function of spin $J = 2$ primaries with scaling dimension Δ is

$$\langle \mathcal{O}_1^{\mu\nu}(0) \mathcal{O}_2^{\rho\sigma}(x) \rangle = c_{12} \frac{I^{\mu\rho}(x) I^{\nu\sigma}(x) + I^{\mu\sigma}(x) I^{\nu\rho}(x) - \frac{2}{d} \delta^{\mu\nu} \delta^{\rho\sigma}}{|x|^{2\Delta}}, \quad (2.3.23)$$

where $I^{\mu\nu}(x)$ was defined below eq. (2.2.16), and c_{12} can be set to 1 or 0 by a suitable choice of basis. Note that the tensor structures are consistent with $\mathcal{O}_{1,2}^\mu = 0$. When $\mathcal{O}^{\mu\nu}$ is the stress tensor $T^{\mu\nu}$, the normalisation contains physical information. There is a canonical choice which ensures that the Noether charges of conformal symmetry, i.e. the conformal generators, are correctly normalised. By reflection-positivity, the coefficient of the two-point function $c_{12} = c_T$ must be positive semi-definite.

The three-point function is the first correlation function whose coefficient(s) cannot be normalised away. They are said to contain dynamical information. E.g. the correlation function of three scalar primaries is

$$\langle \mathcal{O}_1(x_1) \mathcal{O}_2(x_2) \mathcal{O}_3(x_3) \rangle = \frac{\lambda_{123}}{|x_{12}|^{\Delta_1 + \Delta_2 - \Delta_3} |x_{13}|^{\Delta_1 + \Delta_3 - \Delta_2} |x_{23}|^{\Delta_2 + \Delta_3 - \Delta_1}}, \quad (2.3.24)$$

where $x_{ij} \equiv x_i - x_j$. Three-point functions of spinning correlators can have multiple tensor structures, each appearing with their own coefficient. They are most easily dealt with in the embedding space formalism where conformal symmetry acts linearly, see e.g. [78].

Four- and higher-point functions have non-trivial dependence on the positions of the operator insertions. They can depend on conformally invariant scalar combinations of points, called cross ratios. Correlation functions depend on these cross ratios through known functions. Remarkably, these functions only depend on the scaling dimensions, spins, and three point-functions of the operators in the CFT. The spectrum of local operators and their three-point functions is commonly referred to as CFT data.

To demonstrate this, it is useful to introduce the operator product expansion (OPE). Consider two operators $\mathcal{O}_1(x_1), \mathcal{O}_2(x_2)$ inserted inside a spherical region centred on $\mathcal{O}_2(x_2)$. The path integral inside this region with the operator insertions defines a state on the sphere surrounding the operators. By the state-operator correspondence, this state defines a local operator at point x_2 . Since every local operator in a CFT is a linear combination of primaries and descendants, one can write

$$\mathcal{O}_1(x_1)\mathcal{O}_2(x_2) = \sum_k C_{12k}(x_{12}, \partial^{(x_2)})\mathcal{O}_k(x_2), \quad (2.3.25)$$

where the sum runs over all conformal primaries \mathcal{O}_k ,⁷ and C_{12k} are differential operators which take into account the contributions of the descendants of \mathcal{O}_k . The form of the C_{ijk} is fixed by conformal symmetry up to an overall coefficient, called the OPE coefficient, and depends on the scaling dimensions and spins of the operators involved. We have suppressed spin indices for readability.

The OPE is an operator equation that holds inside correlation functions. By applying it inside the three point function $\langle \mathcal{O}_1\mathcal{O}_2\mathcal{O}_3 \rangle$ (and assuming an orthonormal basis for the two-point function of primaries), the OPE coefficients are fixed in terms of the coefficient(s) of the three-point function λ_{123} . More generally, an n -point function decomposed as a sum of $(n - 1)$ -point functions

$$\langle \mathcal{O}_1(x_1)\mathcal{O}_2(x_2) \dots \mathcal{O}_n(x_n) \rangle = \sum_k C_{12k} \langle \mathcal{O}_k(x_2) \dots \mathcal{O}_n(x_n) \rangle. \quad (2.3.26)$$

Iterating the procedure, one finds that there is no new data in the higher-point functions: all the dynamical information is in the three-point functions. Together with the scaling dimensions of local operators, they determine all higher-point correlation functions.

The OPE can be applied to pairs of operators inside correlation functions in different orders, leading to different decompositions. However, the correlator cannot depend on the order in which the OPE is taken, i.e. the OPE must be associative. E.g. the four-point function can be decomposed in the following ways, which must be equal by associativity

$$\langle \mathcal{O}_1(x_1)\mathcal{O}_2(x_2)\mathcal{O}_3(x_3)\mathcal{O}_4(x_4) \rangle = \langle \mathcal{O}_1(x_1)\mathcal{O}_2(x_2)\mathcal{O}_3(x_3)\mathcal{O}_4(x_4) \rangle, \quad (2.3.27)$$

⁷This sum turns out to be convergent in CFT. The radius of convergence is given by the radius of the largest sphere that surrounds both \mathcal{O}_1 and \mathcal{O}_2 , and no other operators. See e.g. ref. [84] as well as ref. [85] for a more comprehensive discussion.

where the square brackets denote replacement with the OPE. This can be recast as an equation on the OPE coefficients

$$\begin{aligned} & \sum_k C_{12k}(x_{12}, \partial^{(x_2)}) C_{34k}(x_{34}, \partial^{(x_4)}) \langle \mathcal{O}_k(x_2) \mathcal{O}_k(x_4) \rangle \\ &= \sum_k C_{14k}(x_{14}, \partial^{(x_4)}) C_{23k}(x_{23}, \partial^{(x_3)}) \langle \mathcal{O}_k(x_3) \mathcal{O}_k(x_4) \rangle. \end{aligned} \quad (2.3.28)$$

Substituting the two-point functions and effecting the derivatives inside C_{ijk} , one finds two different decompositions of the four-point function. Each term contains two factors of λ multiplying a function of cross ratios, called a conformal block. The two different conformal block expansions must be equal by associativity of the OPE. This condition is called the crossing equation. It is a highly non-trivial consistency condition that any set of scaling dimensions, spins and three-point functions must satisfy to define a CFT. The goal of the conformal bootstrap programme is to carve out the space of allowed CFT data inside the space of all parameters using these consistency conditions. One can show that it is sufficient to impose associativity of the OPE on the four-point functions. No new constraints appear for higher-point functions, see e.g. ref. [75] for a diagrammatic argument. Thus, by solving the crossing equation of sufficiently many four-point functions of primary operators, one hopes to constrain the allowed CFT data to a point in parameter space, thus, solving the theory. For a discussion of recent progress, see e.g. [86,87] and refs. therein.

2.4 Curved background

So far we have considered CFTs on \mathbb{R}^d . We can put the theory on a curved background by turning on a non-trivial background metric $g_{\mu\nu}$. We denote the resulting Riemannian manifold (\mathcal{M}, g) . Note that the metric is treated as classical, i.e. it is non-dynamical and not integrated over in the path integral.

We will be interested in QFTs on non-trivial metric backgrounds that have Weyl invariance. Under a Weyl transformation,

$$g_{\mu\nu}(x) \rightarrow g'_{\mu\nu}(x) = \Omega^2(x) g_{\mu\nu}(x), \quad (2.4.29)$$

or infinitesimally

$$\delta g_{\mu\nu}(x) = 2g_{\mu\nu}(x) \delta\omega(x). \quad (2.4.30)$$

This is a local transformation with finite parameter $\Omega(x)$, and infinitesimal parameter $\delta\omega(x)$. It is a re-scaling of all lengths but not a coordinate transformation: unlike eq. (2.1.1), the transformed metric still depends on coordinates x , and not x' .

Consider a classical action I , which is a functional of some fields Ψ_i and the metric $g_{\mu\nu}$. On a curved background, the stress tensor is defined as the response to a small metric

perturbation

$$T^{\mu\nu} = -\frac{2}{\sqrt{g}} \frac{\delta I}{\delta g_{\mu\nu}} \quad (2.4.31)$$

It is symmetric by construction and covariantly conserved when the matter fields are on-shell by diffeomorphism invariance.

To couple spinors to a non-trivial background metric, one needs to introduce an orthonormal frame $e^M = e^M{}_\mu dx^\mu$ obeying

$$e^M{}_\mu e^N{}_\nu g^{\mu\nu} = \delta^{MN}, \quad e^M{}_\mu e^N{}_\nu \delta_{MN} = g_{\mu\nu}. \quad (2.4.32)$$

Its matrix inverse is $e_M{}^\mu = \delta_{MN} g^{\mu\nu} e^N{}_\nu$. The covariant derivative acting on a spinor then acquires an additional term involving the spin connection $\omega^M{}_N = \omega^M{}_{N\mu} dx^\mu$, which depends on e^M and its first derivative.⁸ The stress tensor is defined as

$$T^\mu{}_M = -\frac{1}{e} \frac{\delta S}{\delta e^M{}_\mu}, \quad (2.4.33)$$

where $e = \det e^M{}_\mu$, from which one can build the symmetric stress tensor

$$T^{\mu\nu} = \frac{1}{2} (T^\mu{}_M e^{M\nu} + T^\nu{}_M e^{M\mu}). \quad (2.4.34)$$

For a diffeomorphism and Lorentz invariant action, the stress tensor is conserved, see e.g. [88] for a proof.

A classical action I , which is a functional of some fields Ψ_i with scaling dimensions Δ_i and a metric $g_{\mu\nu}$, is said to be Weyl invariant if $I[\Omega^{-\Delta_i} \Psi_i, \Omega^2 g] = I[\Psi_i, g]$. A simple argument shows that Weyl, diffeomorphism and Lorentz invariant theories on curved space become CFTs on flat space. For simplicity, assume that Ψ_i are scalars, so Lorentz invariance is automatic. Let ϵ^μ be a vector field generating an infinitesimal diffeomorphism. Then

$$\int d^d x \left(\mathcal{L}_\epsilon \Psi_i(x) \frac{\delta}{\delta \Psi_i(x)} + (D_\mu \epsilon_\nu + D_\nu \epsilon_\mu)(x) \frac{\delta}{\delta g_{\mu\nu}(x)} \right) I[\Psi_i, g] = 0, \quad (2.4.35)$$

where \mathcal{L}_ϵ is the Lie derivative with respect to ϵ , D_μ is the Levi-Civita connection, and we have used that the change in the metric under a diffeomorphism is

$(\mathcal{L}_\epsilon g)_{\mu\nu} = D_\mu \epsilon_\nu + D_\nu \epsilon_\mu$. If ϵ is a conformal Killing vector, i.e. $D_\mu \epsilon_\nu + D_\nu \epsilon_\mu = 2\delta\omega g_{\mu\nu}$, then

$$\int d^d x \left(\mathcal{L}_\epsilon \Psi_i(x) \frac{\delta}{\delta \Psi_i(x)} + 2\delta\omega g_{\mu\nu}(x) \frac{\delta}{\delta g_{\mu\nu}(x)} \right) I[\Psi_i, g] = 0. \quad (2.4.36)$$

⁸We assume that $\omega^M{}_N$ is torsion-free.

But Weyl invariance of I means

$$\int d^d x \delta\omega \left(-\sum_i \Delta_i \Psi_i(x) \frac{\delta}{\delta \Psi_i(x)} + 2g_{\mu\nu}(x) \frac{\delta}{\delta g_{\mu\nu}(x)} \right) I[\Psi_i, g] = 0. \quad (2.4.37)$$

Thus, the infinitesimal diffeomorphism generated by the conformal Killing vector ϵ^μ can be written as

$$\int d^d x \sum_i (\mathcal{L}_\epsilon \Psi_i(x) + \delta\omega \Delta_i \Psi_i(x)) \frac{\delta}{\delta \Psi_i(x)} I[\Psi_i, g] = 0. \quad (2.4.38)$$

Taking $g_{\mu\nu} = \delta_{\mu\nu}$, this is simply the statement that under a conformal coordinate transformation $x'^\mu = x^\mu + \epsilon^\mu$, the action is invariant if the field Ψ_i transforms with scaling dimension Δ_i under a conformal transformation with $\Lambda = e^{\delta\omega}$. Thus, every Weyl and diffeomorphism invariant action on curved space gives rise to a classical CFT in flat space.

Going the other way requires care. E.g. a free scalar field ϕ on flat space is conformal. Coupling it to a non-trivial background metric in a Weyl invariant way, requires an additional term. The full action is

$$I[\phi, g] = \frac{1}{2} \int d^d x \sqrt{g} \left((\partial\phi)^2 + \frac{d-2}{4(d-1)} R\phi^2 \right), \quad (2.4.39)$$

where R is the Ricci scalar built out of the background metric $g_{\mu\nu}$.

A theory with a classically Weyl invariant action I has a traceless on-shell stress tensor and vice versa. For an infinitesimal re-scaling $\delta\omega$, eq. (2.4.37) becomes

$$0 = \int d^d x \delta\omega \left(-\sum_i \Delta_i \Phi_i(x) \frac{\delta I[\Phi_i, g]}{\delta \Phi_i(x)} - \sqrt{g} T^\mu{}_\mu(x) \right), \quad (2.4.40)$$

Taking the matter fields on-shell, one finds $T^\mu{}_\mu = 0$.

In a full QFT, one defines the stress tensor as the response of correlation functions to metric variations. Inside the path integral

$$\int \mathcal{D}\Phi e^{-I[\Phi, g]} T^{\mu\nu}(x) \dots = \frac{2}{\sqrt{g}(x)} \frac{\delta}{\delta g_{\mu\nu}(x)} \int \mathcal{D}\Phi e^{-I[\Phi, g]} \dots, \quad (2.4.41)$$

where the ellipsis stands for other operator insertions. If the other operators are just the identity, then

$$\langle T^{\mu\nu}(x) \rangle = -\frac{2}{\sqrt{g}(x)} \frac{\delta \mathcal{W}[g]}{\delta g_{\mu\nu}(x)}, \quad (2.4.42)$$

where $\mathcal{W} = -\log Z$ is the effective action, and correlation functions are normalised by the partition function Z .

2.5 Weyl anomaly

We saw that Weyl invariance leads to a classically traceless stress tensor. In QFT, however, symmetries that are present in a trivial background may not be symmetries of the theory on a generic background. Indeed, Weyl invariance is typically anomalous in CFT leading to a non-zero trace of the stress tensor. Since the Weyl anomaly will be a major focus of this thesis, we will review it in detail here.

A familiar example of an anomalous symmetry in a non-trivial background is the chiral anomaly of a 4d free, massless Dirac fermion. This theory has two global symmetries: a $U(1)_V$ vector and a $U(1)_A$ axial symmetry,

$$\psi \rightarrow e^{i\alpha_V} \psi, \quad \bar{\psi} \rightarrow \bar{\psi} e^{-i\alpha_V}, \quad (2.5.43a)$$

$$\psi \rightarrow e^{i\gamma_5 \alpha_A} \psi, \quad \bar{\psi} \rightarrow \bar{\psi} e^{i\gamma_5 \alpha_A}, \quad (2.5.43b)$$

where $\gamma_5 = -\gamma^1 \dots \gamma^4$, γ^M satisfy the Dirac algebra $\{\gamma^M, \gamma^N\} = 2\delta^{MN}$, and $\alpha_{V,A}$ are symmetry transformation parameters for $U(1)_{V,A}$. This theory has a mixed vector-axial anomaly. The path integral is UV divergent and needs regulating. Choosing a scheme that preserves $U(1)_V$, the mixed anomaly can be written as

$$\partial_\mu j_A^\mu = \frac{1}{16\pi^2} \epsilon^{\mu\nu\rho\sigma} F_{\mu\nu} F_{\rho\sigma}, \quad (2.5.44)$$

where j_A^μ is the axial current and $F_{\mu\nu} = \partial_\mu A_\nu - \partial_\nu A_\mu$ for a classical background $U(1)_V$ gauge field A_μ . This is an operator equation which holds inside correlation functions. Notice that the axial current is conserved for a flat $U(1)_V$ background connection A_μ . It is only in the presence of a non-trivial $U(1)_V$ background that charge conservation is spoiled in a specific way. Such an anomaly is called an 't Hooft anomaly. In this scheme, $U(1)_V$ can be gauged by making the background gauge field A_μ dynamical. Indeed, the anomaly eq. (2.5.44) persists and does not receive any radiative corrections. Had we chosen a scheme in which the axial current was conserved but the vector current was anomalous, then $U(1)_A$ can be gauged by making its gauge field dynamical. However, both $U(1)$'s cannot be gauged simultaneously. In this sense, an 't Hooft anomaly is an obstruction to gauging a global symmetry. See e.g. [88, 89] for a detailed discussion of anomalies.

In a similar way, Weyl symmetry may be anomalous on a curved background.⁹ To see how this could come about, consider the stress tensor one-point function on a background slightly perturbed away from the flat metric $g_{\mu\nu} = \delta_{\mu\nu} + h_{\mu\nu}$. For

⁹Note that Weyl and 't Hooft anomalies are qualitatively very different. We will comment more on some of the differences and similarities in this section and again in section 5.3.

simplicity, let $d = 2$. Then,

$$\langle T^\mu{}_\mu(x) \rangle_{\delta+h} = \frac{1}{2} \int d^2y \langle T^\mu{}_\mu(x) T^{\rho\sigma}(y) \rangle_{\delta} h_{\rho\sigma}(y) + \mathcal{O}(h^2). \quad (2.5.45)$$

Given the two-point function of a spin $J = 2$ primary with $\Delta = d = 2$ in flat space eq. (2.3.23), one would naively expect the right-hand side to vanish identically.

However, the y -integral is over all of spacetime, including the point $y = x$ where the operators become coincident and the two-point function clearly diverges. Therefore, we should regularise the two-point function in an appropriate way before substituting it in. Choosing to preserve diffeomorphism invariance, the unique way to regularise is to write

$$\langle T^{\mu\nu}(x) T^{\rho\sigma}(y) \rangle = -\frac{c_T}{6} (\partial_x^\mu \partial_x^\nu - \delta^{\mu\nu} \partial_x^2) (\partial_y^\rho \partial_y^\sigma - \delta^{\rho\sigma} \partial_y^2) \log(m|x-y|), \quad (2.5.46)$$

where m is a constant. Using $\partial_x^2 \log(m|x-y|) = 2\pi\delta^2(x-y)$, integrating by parts twice, and performing the y -integral, we find

$$\langle T^\mu{}_\mu(x) \rangle_{\delta+h} = \frac{c_T \pi}{6} (\partial^\mu \partial^\nu - \delta^{\mu\nu} \partial^2) h_{\mu\nu}(x), \quad (2.5.47)$$

which is finite. Note that $(\partial^\mu \partial^\nu - \delta^{\mu\nu} \partial^2) h_{\mu\nu} = R$, the Ricci scalar of the Levi-Civita connection D_μ , to leading order in h . This is manifestly diffeomorphism invariant. However, diffeomorphism invariance came at the cost of the dimensionful constant m breaking Weyl invariance. In 2d CFT, it is common to write the coefficient of the stress tensor two-point function $c_T = \frac{c^{(2d)}}{4\pi^2}$ such that the holomorphic stress tensor $T(z) = -2\pi T_{zz}$ has two-point function $\langle T(z) T(0) \rangle = \frac{c^{(2d)}/2}{z^4}$. In terms of $c^{(2d)}$, the stress tensor one-point function becomes

$$\langle T^\mu{}_\mu \rangle = \frac{c^{(2d)}}{24\pi} R. \quad (2.5.48)$$

This is the Weyl anomaly in $d = 2$ [90,91]. Even though we only computed the one-point function of the trace of the stress tensor, eq. (2.5.48) holds as an operator statement inside correlation functions. On flat space, eq. (2.5.48) vanishes.

Nonetheless, flat space correlation functions involving $T^\mu{}_\mu$ are modified. Indeed, the regularised two-point function of the stress tensor with its trace can be written as

$$\langle T^\mu{}_\mu(x) T^{\rho\sigma}(y) \rangle = \frac{c_T \pi}{3} (\partial_y^\rho \partial_y^\sigma - \delta^{\rho\sigma} \partial_y^2) \delta^2(x-y), \quad (2.5.49)$$

which is a contact term.

On a general curved background, the Weyl anomaly appears in the Weyl variation of the effective action

$$\delta_\omega \mathcal{W} = - \int d^d x \sqrt{g} \langle T^\mu{}_\mu \rangle \delta\omega. \quad (2.5.50)$$

It is useful to define the integrated anomaly

$$\mathcal{A} = \int d^d x \sqrt{g} \langle T^\mu{}_\mu \rangle, \quad (2.5.51)$$

such that by $\delta_{\omega_0} \mathcal{W}[g] = -\mathcal{A} \delta\omega_0$ for a constant Weyl transformation $\delta g_{\mu\nu} = 2\delta\omega_0 g_{\mu\nu}$. In computing the effective action, one typically encounters divergences. On a compact manifold, the characteristic length-scale L acts as an IR cut-off. The short-distance divergent terms must be diffeomorphism invariant local functionals of the background fields which can diverge no stronger than ϵ^{-d} as the short-distance cut-off $\epsilon \rightarrow 0$. If the metric is the only background field, then each power law divergent term must be of the form

$$\int d^d x \sqrt{g} \epsilon^{2k-d} \tilde{R}^{(k)} \sim \left(\frac{L}{\epsilon}\right)^{d-2k}, \quad (2.5.52)$$

where $k = 1, \dots, \lfloor \frac{d}{2} \rfloor$, and $\tilde{R}^{(k)}$ is a scalar built out of k Riemann tensors or pairs of derivatives acting on the curvatures. Schematically,

$$\mathcal{W}[g] = \# \left(\frac{L}{\epsilon}\right)^d + \# \left(\frac{L}{\epsilon}\right)^{d-2} + \dots - \mathcal{A} \log\left(\frac{L}{\epsilon}\right) + (-1)^{\frac{d+1}{2}} F[g], \quad (2.5.53)$$

where the logarithmic divergence in ϵ only appears when d is even, and F stands for finite terms [80, 92]. The power law divergent terms can be removed by local counter-terms built out of the metric. The log-term, however, is physical. Its coefficient is fixed to be the integrated Weyl anomaly since a re-scaling of the characteristic size of the system L must give $\delta_{\omega_0} \mathcal{W} = -\mathcal{A} \delta\omega_0$. The finite term F is a scheme-independent non-local functional of $g_{\mu\nu}$ in odd dimensions. In even dimensions, however, it is scheme-dependent.

The general form of the Weyl anomaly is very strongly constrained. This is most easily seen by considering an infinitesimal Weyl transformation of the effective action eq. (2.5.50). We saw that the Weyl anomaly arises from regularising short-distance divergences in a diffeomorphism invariant way, which is a local effect. Thus, $\delta_\omega \mathcal{W}$ should be a *local* functional of the background fields.¹⁰ Demanding that the trace of the stress tensor be diffeomorphism and Lorentz invariant, it must be built out of scalar combinations of background fields.¹¹ The stress tensor has scaling dimension $\Delta = d$. The anomaly must therefore have d derivatives acting on the metric to match the scaling dimension of $T_{\mu\nu}$. There is a finite number of terms which meet these criteria.

¹⁰Note that typically \mathcal{W} is a highly non-local functional of background fields. In fact, any non-trivial dependence on background terms is encoded in these non-local terms, as they must be scheme-independent. The requirement that $\delta_\omega \mathcal{W}$ be local is highly restrictive. Nonetheless, the Weyl anomaly knows about the non-locality of the effective action. Indeed, the Weyl anomaly completely determines the difference $\mathcal{W}[e^{2\sigma}g] - \mathcal{W}[g]$ as a non-local functional of $g_{\mu\nu}$. See e.g. [84] for a detailed discussion of the 2d case.

¹¹In principle, a theory could have many background fields which could contribute to the trace anomaly. We will only look for universal contributions coming from a non-trivial background metric.

Any anomaly must also satisfy the algebra of the anomalous symmetry. This principle goes by the name of Wess-Zumino (WZ) consistency [93]. Weyl transformations are Abelian, which means that the anomaly must satisfy $[\delta_1, \delta_2]\mathcal{W} = 0$. A simple argument shows that the integrated anomaly \mathcal{A} must therefore be Weyl invariant itself.¹² WZ consistency implies

$$\delta_\omega \delta_{\omega_0} \mathcal{W} = \delta_{\omega_0} \delta_\omega \mathcal{W} \quad (2.5.54)$$

for an arbitrary, spacetime dependent Weyl transformation $\delta\omega$, and a constant Weyl transformation $\delta\omega_0$. The left-hand side evaluates to

$$\delta_\omega (\mathcal{A} \delta\omega_0) = \delta\omega_0 \delta_\omega \mathcal{A}, \quad (2.5.55)$$

whereas the right-hand side is equal to

$$-\delta_{\omega_0} \int d^d x \sqrt{g} \langle T^\mu{}_\mu \rangle \delta\omega = - \int d^d x \sqrt{g} (d \langle T^\mu{}_\mu \rangle \delta\omega_0 + \delta_{\omega_0} \langle T^\mu{}_\mu \rangle) \delta\omega. \quad (2.5.56)$$

where we have used $\delta_{\omega_0} \sqrt{g} = d \sqrt{g} \delta\omega_0$. If we turn on a non-trivial background for the metric only, then $\langle T^\mu{}_\mu \rangle$ must be built out of the metric and d derivatives. Each derivative has one downstairs index which needs to be soaked up. If there are n metrics and m inverse metrics, then equating the number of upstairs and downstairs indices gives $2m = 2n + d$. An immediate consequence of this is that the Weyl anomaly can only exist when $d \in 2\mathbb{Z}$. Under a constant Weyl transformation, each inverse metric contributes $-2\delta\omega_0$ times itself, whereas each metric contributes $+2\delta\omega_0$ times itself. Therefore, $\sqrt{g} \delta_{\omega_0} \langle T^\mu{}_\mu \rangle = (2n - 2m) \sqrt{g} \langle T^\mu{}_\mu \rangle \delta\omega_0 = -d \sqrt{g} \langle T^\mu{}_\mu \rangle \delta\omega_0$, which precisely cancels the term coming from the variation of \sqrt{g} , i.e. $\delta\omega_0 \delta_\omega \mathcal{A} = 0$. Since this must hold for any constant Weyl variation $\delta\omega_0$, we conclude that $\delta_\omega \mathcal{A} = 0$ for an arbitrary spacetime dependent Weyl variation $\delta\omega$.

In QFT, physical observables are only defined up to local counter-terms. For instance, we are free to add a counter-term action \mathcal{W}_{CT} to \mathcal{W} consisting of a linear combination of scalars built out of background fields with arbitrary coefficients. Taking $\delta_\omega (\mathcal{W} + \mathcal{W}_{\text{CT}})$, and adjusting coefficients appropriately, one can remove some of the terms appearing in the Weyl anomaly. Whatever cannot be removed by local counter-terms constitutes the physical Weyl anomaly. This gives rise to cohomology-type problem formalised in ref. [95].

The above considerations lead to the following three-step algorithm to determine the form of the Weyl anomaly:

1. **Find a basis of terms for the anomaly $\delta_\omega \mathcal{W}$.** This amounts to enumerating all possible terms that may appear in $\delta_\omega \mathcal{W}$ to linear order in the Weyl

¹²See e.g. ref. [94] for a particularly clear discussion.

transformation parameter $\delta\omega$. We insist that the terms appearing in $\delta\omega\mathcal{W}$ are local, diffeomorphism and Lorentz invariant. Each term must contain d derivatives acting on the metric $g_{\mu\nu}$, or the Weyl variation parameter $\delta\omega$. However, not all of these terms are linearly independent due to geometric relations. One must choose a linearly independent basis, and each basis element is then included in the integrand of $\delta\omega\mathcal{W}$, with free coefficients.

2. **Impose WZ consistency.** The WZ consistency condition forces the anti-symmetrisation of two independent Weyl variations of \mathcal{W} to vanish, i.e., $[\delta_{\omega_1}, \delta_{\omega_2}]\mathcal{W} = 0$. As we will see, solving WZ consistency sets to zero some of the coefficients of the linearly independent anomaly basis, or it fixes some coefficients in terms of others.
3. **Determine which terms in the Weyl anomaly are scheme-independent.** To do so, we introduce in the effective action \mathcal{W} all possible local, diffeomorphism and Lorentz invariant counterterms with d derivatives acting on $g_{\mu\nu}$. Including each of these terms with their own free coefficient builds up the counterterm action, \mathcal{W}_{CT} . Taking an infinitesimal Weyl transformation of \mathcal{W}_{CT} , one can shift the anomaly $\delta\omega\mathcal{W} \mapsto \delta\omega\mathcal{W} + \delta\omega\mathcal{W}_{\text{CT}}$. Since the coefficients in \mathcal{W}_{CT} are free, one can then tune them so as to cancel terms appearing in $\delta\omega\mathcal{W}$. The WZ consistent terms that cannot be removed by any choice of counterterms are the scheme-independent contribution to the Weyl anomaly.

This algorithm implies that the anomaly takes the schematic form

$$T^\mu{}_\mu = \frac{1}{(4\pi)^{\frac{d}{2}}} \left((-1)^{\frac{d}{2}-1} a_{\mathcal{M}}^{(\text{dim})} E_d + \sum_n c_n^{(\text{dim})} I_n \right), \quad (2.5.57)$$

where we omitted any scheme-dependent contributions. The coefficients $a_{\mathcal{M}}$ and $c_n^{(\text{dim})}$ are called central charges, and I_n are a set of conformal invariants that are generally expressed as rank- $\frac{d}{2}$ scalar monomials built from contractions of Weyl tensors and their derivatives. E_d is the Euler density

$$E_d = \frac{1}{2^{d/2}} \delta_{\rho_1\sigma_1\dots\rho_{d/2}\sigma_{d/2}}^{\mu_1\nu_1\dots\mu_{d/2}\nu_{d/2}} R^{\rho_1\sigma_1}{}_{\mu_1\nu_1} R^{\rho_2\sigma_2}{}_{\mu_2\nu_2} \dots R^{\rho_{d/2}\sigma_{d/2}}{}_{\mu_{d/2}\nu_{d/2}}, \quad (2.5.58)$$

where $\delta_{\rho_1\sigma_1\dots}^{\mu_1\nu_1\dots}$ is the generalised Kronecker delta. It is a topological density and transforms as a total derivative under Weyl transformation, whereas the I_n are trivially Weyl invariant. We will call the former ‘‘A-type’’ anomalies and the latter ‘‘B-type’’ anomalies. Since we will discuss central charges of CFTs and defects of various dimensions, we use the superscript $^{(\text{dim})}$ to distinguish the dimension in which the central charges are defined, and the subscripts on $a_{\mathcal{M}}$ and a_Σ to distinguish the ambient CFT and intrinsic defect/boundary A-type central charges, respectively.

The nomenclature of A- and B-type anomalies was originally introduced in ref. [96]. There, the authors study CFTs on curved backgrounds deformed away from flat space. They distinguish two types of conformal anomalies based on whether the integrated anomaly \mathcal{A} vanishes on this background. If $\mathcal{A} = 0$, then the anomaly is A-type, and if $\mathcal{A} \neq 0$, then the anomaly is B-type. Since they consider generic small deformations away from flat space, A-type anomalies must necessarily be associated with topological densities. In parity-preserving CFTs, ref. [96] argues that the only such density is the Euler density, E_d , which transforms into a total derivative under a Weyl transformation. The remaining B-type terms are Weyl invariant scalar polynomials built out of curvatures and suitably contracted derivatives. Note that our definition below eq. (2.5.58) is not necessarily equivalent to the original definition of ref. [96].¹³ They happen to agree in the parity-preserving case. However, if one allows for parity-breaking, there exist topological densities, such as the Pontryagin density, whose integral vanishes on deformations around flat space *and* which are exactly Weyl invariant. We will classify these terms as B-type in accord with our definition below eq. (2.5.58).

Let us briefly comment on the physical origin of the different types of anomalies in a parity-preserving CFT on flat space. Since the integrated Euler density vanishes on small deformations around flat space, the A-type anomaly preserves scale invariance (but breaks the special conformal generators). Importantly, it is not related to a genuine UV divergence as can be seen from the way it is encoded in the effective action $\mathcal{W}[g]$. Recall that $\mathcal{W}[g]$ is a non-local functional of g arising from loop integrations. In dimensional regularisation, where $\varepsilon \ll 1$ parametrises the deviation from the physical dimension, UV divergences manifest themselves as $1/\varepsilon$ poles multiplying (non-local) geometrical structures. For the A-type anomaly, these geometrical structures vanish identically in the physical dimension $\varepsilon = 0$ [96]. Thus, the overall result is finite by itself, and the anomaly doesn't contribute to the logarithmic divergence in eq. (2.5.53). This is analogous to the chiral ('t Hooft) anomaly, which is finite by a similar mechanism. Note that the existence of such a "0/0" mechanism is also often quoted as the defining feature of an A-type anomaly, see e.g. ref. [99].¹⁴

When $d = 2(1 + \varepsilon)$, this "0/0" mechanism can equivalently be seen from the flat space two-point function of the stress tensor. As argued earlier, its coefficient is proportional to the coefficient $c^{(2d)}$ of the Euler density. Integrating over internal loop momenta produces a $1/\varepsilon$ pole in the momentum space two-point function multiplying an evanescent tensor structure. When $d = 2$ exactly, this structure vanishes identically,

¹³Our definition below eq. (2.5.58) is by no means original. To our knowledge, it first appeared in ref. [97]. See also ref. [98].

¹⁴By this definition, any term that is exactly Weyl invariant is classed as type-B as it cannot be associated with a "0/0" mechanism. This includes the parity-breaking Pontryagin density. Conversely, it is less clear whether all terms transforming into a total derivative under a Weyl transformation are necessarily associated with a "0/0" mechanism.

thus cancelling the divergence. See e.g. refs. [99, 100] for a pedagogical treatment. This is consistent with our earlier discussion in position space. To arrive at eq. (2.5.46), we employed differential regularisation which required introducing a scale m . Nonetheless, a logarithmic derivative with respect to m vanishes, and so the two-point function is indeed scale invariant. Similar “0/0” structures appear inside certain higher-point functions in larger d . See e.g. refs. [99, 101] for the stress tensor three-point function in $d = 4$.

In contrast, B-type anomalies are associated with genuine UV divergences. They manifest themselves as divergent terms in $\mathcal{W}[g]$ for which the geometrical structures do not vanish in the physical dimension. To cancel the divergence, one must introduce a scale-dependent counter-term, thus breaking scale invariance of the CFT. A simple example is the two-point function of the stress tensor when the physical dimension is even and greater than 2. In that case, the two-point function is not saved by a “0/0” mechanism. It is divergent and requires regularisation, thus introducing a scale. E.g. when $d = 4$, the stress tensor two-point function in differential regularisation can be found in ref. [101]. Unlike the $d = 2$ case, its logarithmic derivative with respect to the scale does not vanish, thus showing that scale invariance is truly broken when $d = 4$.

We now return to our discussion of Weyl anomalies on more general backgrounds. The fact that, by our definition, A-type anomalies transform as total derivatives immediately implies that its coefficient cannot depend on marginal couplings [38]. Consider a deformation by an exactly marginal operator \mathcal{O} by inserting $\int d^d x \sqrt{g} \lambda \mathcal{O}(x)$ into the path integral. By making λ spacetime-dependent, it acts as a source for the operator \mathcal{O} : varying $\mathcal{W}[g, \lambda]$ with respect to $\lambda(x)$ inserts $\mathcal{O}(x)$ into a correlation function. Now that λ is an additional background field, the Weyl anomaly will pick up additional terms. Since λ is dimensionless, it could also enter in the coefficients $a_{\mathcal{M}}^{(\text{dim})}$ and $c_n^{(\text{dim})}$. However, since E_d transforms into a total derivative, $\int d^d x \sqrt{g} a_{\mathcal{M}}^{(\text{dim})} E_d$ cannot be WZ consistent unless $a_{\mathcal{M}}^{(\text{dim})}$ is a constant and independent of λ . Thus, the A-type central charge must be independent of marginal couplings. The B-type central charges, however, can and do depend on marginal couplings.

Let us now illustrate this algorithm with a number of simple examples.

Step 1: In 2d, the only term that meets the criteria above is

$$\delta_{\omega_2} \mathcal{W} = \int d^2 x \sqrt{g} b_1 R \delta \omega_2, \quad (2.5.59)$$

where we have ignored a total derivative $D^2 \delta \omega_2$. In 2d, R is equal to the Euler density E_2 of the manifold, i.e. the Euler characteristic

$$\chi = \frac{1}{4\pi} \int d^2 x \sqrt{g} R \quad (2.5.60)$$

by the Gauss-Bonnet theorem.

Step 2: We now compute a second Weyl variation δ_{ω_1} and anti-symmetrise in 1 and 2. One finds

$$[\delta_{\omega_1}, \delta_{\omega_2}] \mathcal{W} = -2b_1 \int d^2x \sqrt{g} (\delta\omega_2 (D^2 \delta\omega_1) - \delta\omega_1 (D^2 \delta\omega_2)) = 0 \quad (2.5.61)$$

after integration by parts. Thus, the term $\int d^d x \sqrt{g} b_1 R \delta\omega$ is WZ consistent.¹⁵

Step 3: Finally, we may introduce a local counter-term $\mathcal{W}_{\text{CT}} = \int d^2x \sqrt{g} c_1 R$. However, $\delta_\omega \mathcal{W}_{\text{CT}} \propto \int d^2x \sqrt{g} D^2 \delta\omega = 0$, and thus the anomaly cannot be removed. Therefore, the full physical anomaly is of the form in (2.5.48) with $b_1 = \frac{c^{(2d)}}{24\pi}$.¹⁶

The coefficient $c^{(2d)}$ is called the central charge of the CFT. We already showed that it is proportional to the stress tensor two-point function. In fact, one can show that it controls all self-correlators of the stress tensor [102]. Moreover, it determines various other physical observables, including the thermal entropy for a CFT on $S_L^1 \times S_\beta^1$

$$S_{\text{thermo}} = (1 - \beta \partial_\beta) \log Z \xrightarrow{LT \gg 1} \frac{\pi}{6} c^{(2d)} TL, \quad (2.5.62)$$

where β, L are the circumference of $S_{\beta,L}^1$, respectively, and $T = \frac{1}{\beta}$ is the temperature [25, 26]. As we will see in section 4.4, $c^{(2d)}$ also controls the universal contribution to the EE of an interval [28].¹⁷ If the CFT is also supersymmetric, $c^{(2d)}$ has further properties that we will discuss in section 5.4.

The central charge $c^{(2d)}$ is essential for characterising and classifying $d = 2$ CFTs and QFTs. Famously, it obeys what is called a c-theorem [31]. At the RG fixed points of a reflection-positive/unitary QFT, scale invariance typically enhances to the full

¹⁵If b_1 had non-trivial dependence on a marginal coupling $\lambda(x)$, we wouldn't have been allowed to take b_1 out of the integral. Integrating by parts would then give

$$[\delta_{\omega_1}, \delta_{\omega_2}] \mathcal{W} = 2 \int d^2x \sqrt{g} (\delta\omega_2 (D^\mu b_1) (D_\mu \delta\omega_1) - \delta\omega_1 (D^\mu b_1) (D_\mu \delta\omega_2)) \neq 0,$$

in conflict with WZ consistency.

¹⁶Note that $\langle T^\mu{}_\mu \rangle$ is not Weyl invariant: it transforms into a total derivative. The integrated anomaly \mathcal{A} , however, is Weyl invariant after integration by parts, as it must.

¹⁷The central charge $c^{(2d)}$ also appears as the central extension of the Virasoro algebra, giving rise to the term 'central charge'.

conformal group.¹⁸ The theorem states that in a reflection-positive QFT, there exists a function of couplings g_i built from correlators of $T^{\mu\nu}$, called the c-function $c^{(2d)}(g_i)$, which monotonically decreases along a gradient under the RG flow. The c-function is stationary only at RG fixed points, where it reduces to the central charge of the CFT at the fixed point. This implies that $c_{\text{UV}}^{(2d)} \geq c_{\text{IR}}^{(2d)}$. Moreover, since $c^{(2d)}$ is the coefficient of the stress tensor two-point function (at the fixed points), reflection-positivity implies that $c^{(2d)}(g_i) \geq 0$ along the flow. In this sense, $c^{(2d)}(g_i)$ counts DOF along the flow.¹⁹ The original proof crucially uses the conservation of the stress tensor and certain special properties of 2d CFT. Relaxing these assumptions, a weaker version of the c-theorem can be proven, $c_{\text{UV}}^{(2d)} \geq c_{\text{IR}}^{(2d)}$ [34]. Note that this is a statement about the fixed points only, and not the entire flow.

The same algorithm can be used to determine the general form of the trace anomaly in a 4d CFT.

Step 1: The most general form of $\delta_\omega \mathcal{W}$ is

$$\begin{aligned} \delta_{\omega_2} \mathcal{W} = \int d^4x \sqrt{g} & (\mathfrak{b}_1 R^2 + \mathfrak{b}_2 R_{\mu\nu} R^{\mu\nu} + \tilde{\mathfrak{b}}_1 W_{\mu\nu\rho\sigma} W^{\mu\nu\rho\sigma} + \tilde{\mathfrak{b}}_2 \epsilon^{\mu\nu\rho\sigma} R_{\mu\nu\lambda\kappa} R_{\rho\sigma}{}^{\lambda\kappa} \\ & + \mathfrak{d}_1 R D^2) \delta\omega_2, \end{aligned} \quad (2.5.63)$$

where $R_{\mu\nu\rho\sigma}$ is the curvature tensor of D_μ , $R_{\mu\nu} = R^\rho{}_{\mu\rho\nu}$ is the Ricci tensor, $W_{\mu\nu\rho\sigma}$ is the Weyl tensor, and $\epsilon^{\mu\nu\rho\sigma}$ is the totally anti-symmetric Levi-Civita tensor. We have made sure to select a linearly independent basis of terms by using geometric identities. E.g. the divergence-free property of the Einstein tensor implies $R^{\mu\nu} D_\mu D_\nu \delta\omega = \frac{1}{2} R D^2 \delta\omega$ up to total derivatives. As we are looking for Weyl invariant combinations, it is convenient to replace $R_{\mu\nu\rho\sigma} R^{\mu\nu\rho\sigma}$ by $W_{\mu\nu\rho\sigma} W^{\mu\nu\rho\sigma}$ plus a linear combination of $R_{\mu\nu} R^{\mu\nu}$ and R^2 . We have included a parity-breaking term proportional to the Pontryagin density, which can also be written as $\epsilon^{\mu\nu\rho\sigma} R_{\mu\nu\lambda\kappa} R_{\rho\sigma}{}^{\lambda\kappa} = \epsilon^{\mu\nu\rho\sigma} W_{\mu\nu\lambda\kappa} W_{\rho\sigma}{}^{\lambda\kappa}$. We've denoted the coefficients of trivially Weyl invariant terms as $\tilde{\mathfrak{b}}_i$. Notice that the second line involves terms which vanish for a constant Weyl transformation.

¹⁸In $d = 2$ this can be rigorously proven by showing that the stress tensor on flat space is exactly traceless in all correlation functions, see e.g. [80, 103]. The proof comes with a small caveat: a key assumption is that the spectrum of operator dimensions is gapped and discrete, which is known to be violated by some CFTs, e.g. Liouville theory. For $d \geq 3$, there is no complete non-perturbative proof, however, there are no non-trivial counter-examples. See e.g. [104] for a review. In non-unitary theories, scale invariance need not enhance to conformal symmetry. E.g. the theory of elasticity in $d = 2$ is a physical non-unitary theory that has scale but not conformal invariance [105]. Reflection-positivity/unitarity appears to be a sufficient condition for the enhancement to conformal invariance, however, it is not necessary. E.g. the Lee-Yang minimal model is non-unitary but does have full conformal invariance.

¹⁹More precisely, it counts non-topological DOF because of its definition as the response to metric perturbations.

Step 2: Performing a second Weyl transformation, the (Weyl)² terms (including the Pontryagin density) vanish, leaving only

$$[\delta_{\omega_1}, \delta_{\omega_2}] \mathcal{W} = \int d^4x \sqrt{g} \left[-4(3\mathfrak{b}_1 + \mathfrak{b}_2) R \delta\omega_2 D^2 \delta\omega_1 + 4\mathfrak{b}_2 R^{\mu\nu} D_\mu \delta\omega_1 D_\nu \delta\omega_2 \right. \\ \left. - 2\mathfrak{b}_2 R D_\mu \delta\omega_1 D^\mu \delta\omega_2 - 6\mathfrak{d}_1 D^2 \delta\omega_1 D^2 \delta\omega_2 \right. \\ \left. + 2\mathfrak{d}_1 R D^\mu \delta\omega_1 D_\mu \delta\omega_2 \right] - (1 \leftrightarrow 2). \quad (2.5.64)$$

All but the first term vanish in the anti-symmetrisation, and so Wess-Zumino consistency requires $\mathfrak{b}_2 = -3\mathfrak{b}_1$, while $\tilde{\mathfrak{b}}_1$, $\tilde{\mathfrak{b}}_2$, and \mathfrak{d}_1 remain unfixed.

Step 3: The most general counter-term action is

$$\mathcal{W}_{\text{CT}} = \int d^4x \sqrt{g} (\mathfrak{c}_1 R^2 + \mathfrak{c}_2 R_{\mu\nu} R^{\mu\nu} + \mathfrak{c}_3 W_{\mu\nu\rho\sigma} W^{\mu\nu\rho\sigma} + \mathfrak{c}_4 \epsilon^{\mu\nu\rho\sigma} R_{\mu\nu\lambda\kappa} R_{\rho\sigma}{}^{\lambda\kappa}). \quad (2.5.65)$$

A first Weyl variation gives

$$\delta_\omega \mathcal{W}_{\text{CT}} = -4 \int d^4x \sqrt{g} (3\mathfrak{c}_1 + \mathfrak{c}_2) R D^2 \delta\omega. \quad (2.5.66)$$

Setting $\mathfrak{c}_1 = -\frac{\mathfrak{c}_2}{3} + \frac{\mathfrak{d}_1}{12}$, one then has

$$\delta_\omega (\mathcal{W} + \mathcal{W}_{\text{CT}}) = \int d^d x \sqrt{g} (\mathfrak{b}_1 (R^2 - 3R_{\mu\nu} R^{\mu\nu}) + \tilde{\mathfrak{b}}_1 W_{\mu\nu\rho\sigma} W^{\mu\nu\rho\sigma} \\ + \tilde{\mathfrak{b}}_2 \epsilon^{\mu\nu\rho\sigma} R_{\mu\nu\lambda\kappa} R_{\rho\sigma}{}^{\lambda\kappa}) \delta\omega, \quad (2.5.67)$$

i.e. the Weyl anomaly involves three linearly independent terms. In 4d, the Euler density can be written as

$$E_4 = \frac{2}{3} R^2 - 2R_{\mu\nu} R^{\mu\nu} + W_{\mu\nu\rho\sigma} W^{\mu\nu\rho\sigma}. \quad (2.5.68)$$

Therefore, the full anomaly is often written as

$$\delta_\omega \mathcal{W} = -\frac{1}{(4\pi)^2} \int d^d x \sqrt{g} (-a_{\mathcal{M}}^{(4d)} E_4 + c^{(4d)} W_{\mu\nu\rho\sigma} W^{\mu\nu\rho\sigma} + \tilde{c}^{(4d)} \epsilon^{\mu\nu\rho\sigma} R_{\mu\nu\lambda\kappa} R_{\rho\sigma}{}^{\lambda\kappa}) \delta\omega, \quad (2.5.69)$$

where $a_{\mathcal{M}}^{(4d)} = \frac{3(4\pi)^2}{2} \mathfrak{b}_1$, $c^{(4d)} = -(4\pi)^2 (\tilde{\mathfrak{b}}_1 - \frac{3}{2} \mathfrak{b}_1)$ and $\tilde{c}^{(4d)} = -(4\pi)^2 \tilde{\mathfrak{b}}_2$, and we have re-labelled $\mathcal{W} + \mathcal{W}_{\text{CT}} \rightarrow \mathcal{W}$. Equivalently, in terms of the stress tensor

$$\langle T^\mu{}_\mu \rangle = \frac{1}{(4\pi)^2} \left(-a_{\mathcal{M}}^{(4d)} E_4 + c^{(4d)} W_{\mu\nu\rho\sigma} W^{\mu\nu\rho\sigma} + \tilde{c}^{(4d)} \epsilon^{\mu\nu\rho\sigma} R_{\mu\nu\lambda\kappa} R_{\rho\sigma}{}^{\lambda\kappa} \right). \quad (2.5.70)$$

The coefficients $a_{\mathcal{M}}^{(4d)}$, $c^{(4d)}$, and $\tilde{c}^{(4d)}$ are commonly referred to as central charges. The coefficient of the Euler density, $a_{\mathcal{M}}^{(4d)}$, is A-type as it is the analogue of $c^{(2d)}$. The central charges $c^{(4d)}$ and $\tilde{c}^{(4d)}$ are coefficients of Weyl invariants, and are thus B-type. For reflection-positive, local $d = 4$ CFTs, the A-type central charge $a_{\mathcal{M}}^{(4d)}$ obeys the

a -theorem: $a_{\text{UV}}^{(4d)} \geq a_{\text{IR}}^{(4d)}$, which was conjectured by [35, 36] and proven decades later [34, 39]. Explicit examples are known in which the parity-even B-type central charge, $c^{(4d)}$, can decrease or increase along an RG flow [32, 106]. Unlike $d = 2$ CFTs, no single central charge determines all of $T^{\mu\nu}$'s self-correlators. Instead, the B-type anomaly $c^{(4d)}$ fixes $T^{\mu\nu}$'s two-point function, while $a_{\mathcal{M}}^{(4d)}$ and $c^{(4d)}$ are two of the three numbers that fix $T^{\mu\nu}$'s three-point function [101, 107]. The third number in the three-point function is not related to an anomaly. Reflection positivity then requires $c^{(4d)} \geq 0$. If $T^{\mu\nu}$ is the unique conserved spin-2 operator, then the conformal bootstrap and other CFT “first principles” bound the ratio $a_{\mathcal{M}}^{(4d)}/c^{(4d)}$ [108, 109], so that in particular $a_{\mathcal{M}}^{(4d)} \geq 0$. Somewhat like a $d = 2$ CFT, the $d = 4$ central charges determine the universal contribution to EE [29], see section 4.4. Further properties of $a_{\mathcal{M}}^{(4d)}$ and $c^{(4d)}$ in supersymmetric theories will be discussed in section 5.4. In contrast to $a_{\mathcal{M}}^{(4d)}$ and $c_{\mathcal{M}}^{(4d)}$, little is known about the parity-odd B-type central charge, $\tilde{c}^{(4d)}$. E.g. there is no consensus in the literature whether $\tilde{c}^{(4d)} \neq 0$ for a chiral fermion, see refs. [110–122].

As in 2d, the Weyl anomaly affects correlation functions in flat space through contact terms. In fact, varying eq. (2.5.70) twice with respect to the metric gives the three-point function $\langle T^\mu{}_\mu(x) T^{\rho\sigma}(y) T^{\lambda\kappa}(z) \rangle$. It consists of contact terms with singularities at $x = y$ and $x = z$ coming from the Ward identity eq. (2.3.21c) and additional anomalous terms analogous to the right-hand side of eq. (2.5.49). The exact expression can be found e.g. in [76]. All the structures appearing are controlled by the Weyl anomaly coefficients $a_{\mathcal{M}}^{(4d)}$ and $c_{\mathcal{M}}^{(4d)}$, such that the contact terms vanish when $a_{\mathcal{M}}^{(4d)} = c_{\mathcal{M}}^{(4d)} = 0$.

The same algorithm applied in 6d yields

$$\langle T^\mu{}_\mu \rangle = \frac{1}{(4\pi)^3} (a_{\mathcal{M}}^{(6d)} E_6 + c_1^{(6d)} I_1 + c_2^{(6d)} I_2 + c_3^{(6d)} I_3) . \quad (2.5.71)$$

where the B-type Weyl invariants are [95, 123]

$$I_1 = W_{\mu\lambda\rho\nu} W^{\lambda\sigma\tau\rho} W_{\sigma}{}^{\mu\nu}{}_{\tau} , \quad (2.5.72a)$$

$$I_2 = W_{\mu\nu}{}^{\lambda\rho} W_{\lambda\rho}{}^{\sigma\tau} W_{\sigma\tau}{}^{\mu\nu} , \quad (2.5.72b)$$

$$I_3 = W_{\mu\nu\lambda\rho} \left(D^2 \delta_\sigma^\nu - \frac{6}{5} R \delta_\sigma^\nu + 4R^\nu{}_\sigma \right) W^{\sigma\nu\lambda\rho} . \quad (2.5.72c)$$

The central charge $a_{\mathcal{M}}^{(6d)}$ appears in $T^{\mu\nu}$'s 4-point function, $c_1^{(6d)}$ and $c_2^{(6d)}$ are related to the two free parameters in $T^{\mu\nu}$'s 3-point function, and $c_3^{(6d)}$ fixes $T^{\mu\nu}$'s 2-point function [101, 107, 124]. Reflection positivity then requires $c_3^{(6d)} \geq 0$. Whether $a_{\mathcal{M}}^{(6d)}$ generically obeys a c -theorem remains an open question. For the state of the art, see refs. [125–130] and refs. therein. We will comment on constraints from SUSY in section 5.4. As in lower d , the $d = 6$ central charges determine the universal contribution to EE [131, 132].²⁰

²⁰Note that parity-odd terms do not exist in the 6d Weyl anomaly for the same reason that 4d QFTs cannot have gravitational, i.e. diffeomorphism/Lorentz, anomalies: there are no Lorentz-invariant cubic

Before closing this section, let us remark that the discussion in the present thesis focusses on Weyl anomalies that are universal in CFT, i.e. the ones associated with the metric. However, these are not the only conformal anomalies that can appear. Indeed, if a CFT has certain operators in its spectrum, correlation functions of these operators can be anomalous. The first such example was found in refs. [38, 107] and systematically studied in ref. [133]: the two-point function of a local scalar operator \mathcal{O} has a conformal anomaly if its scaling dimension $\Delta \in \frac{d}{2} + \mathbb{N}$. Correlation functions in CFT must be well-defined distributions, and, in particular, their Fourier transform must exist. For these Δ , however, the two-point function does not admit a Fourier transform due to short distance singularities. Regularising and renormalising the two-point function requires the introduction of a scale. A logarithmic derivative with respect to this scale then reveals the conformal anomaly. Since these anomalies are associated with genuine UV divergences, they are B-type in the classification of ref. [96].

These anomalies obey an interesting non-renormalisation theorem: the ratio of the anomaly and the overall constant of the two-point function does not renormalise provided that the scaling dimensions are protected [133]. Indeed, it turns out that the ratio only depends on Δ and the spacetime dimension d . Moreover, when a source for such \mathcal{O} is turned on, the trace of the stress tensor receives additional contributions. These terms are built out of the sources, and their coefficients are the above conformal anomalies.

In a similar vein, n -point correlation functions can be anomalous. For a detailed discussion of three-point functions of scalar and spinning operators, see refs. [133–135]. Note that for scalar three-point functions an analogous non-renormalisation theorem exists [133]. For conformal anomalies in higher-point functions, see ref. [136] where the authors study tree-level holographic four-point functions of scalar operators.

Finally, let us make a brief remark about odd-dimensional CFTs. In that case, there is no Weyl anomaly associated with the metric. However, the finite piece of the effective action, $F[g]$ in eq. (2.5.53), is physically meaningful, and one may wonder if it has any special properties. On a d -sphere, $F[g]$ is the renormalised sphere free energy. Refs. [137–139] proposed a monotonicity theorem for $F[g]$ when $d = 3$, called the F-theorem: the sphere free energy must decrease along an RG flow to an IR fixed point. Indeed, the F-theorem was proven in refs. [40, 140]. Moreover, ref. [141] proposed that F- and c-theorems can be combined into a monotonicity theorem in continuous d , called the generalised F-theorem, however, that remains conjectural.

polynomials in the 2-form curvature tensor. The only options are $\text{Tr}R \wedge R \wedge R$, $\text{Tr}(R \wedge R) \wedge \text{Tr}R$ and $(\text{Tr}R)^3$, where the trace is taken over the $\mathfrak{so}(d)$ indices M, N of $R^M_N = \frac{1}{2}R^M_{N\mu\nu}dx^\mu \wedge dx^\nu$. However, all of these terms vanish by anti-symmetry.

Chapter 3

Conformal Defects

Our discussion so far has focussed on local operators. However, QFTs also admit extended operators, often referred to as defects. Defects may come in numerous different types, with various properties and constructions, however, a classification scheme is currently unavailable.

The focus of this thesis is on defects in CFT, which partly preserve the conformal group. Concretely, a p -dimensional conformal defect in a d -dimensional CFT breaks the conformal group

$$SO(d+1,1) \rightarrow SO(p+1,1) \times SO(d-p), \quad (3.0.1)$$

i.e. the defect is invariant under conformal symmetry on its support, and transverse rotations.¹ The unbroken generators are $\{D, P_a, K_a, M_{ab}, M_{ij}\}$, where $a, b = 1, \dots, p$ are indices along the defect directions, and $i, j = p+1, \dots, d$ are indices in the transverse directions. Note that in \mathbb{R}^d these symmetries can only be preserved by a flat or spherical defect. The parallel coordinates x^a are labelled x_{\parallel} collectively. The normal directions x^i are labelled x_{\perp} , and the defect is located at $x^i = 0$. It will be useful to introduce unit normals $\hat{x}^i = \frac{x^i}{|x_{\perp}|}$, where $|x_{\perp}| = \sqrt{x^i x_i}$. The co-dimension of the defect is denoted $q = d - p$.

3.1 Correlation functions and DCFT data

We now turn to correlation functions of local operators in the presence of a conformal defect whose study was pioneered by refs. [142–146]. The constraints from the residual conformal symmetry were systematically studied in refs. [147, 148]. A p -dimensional defect can be thought of as an extended operator \mathcal{D} with support Σ_p

¹Invariance under transverse rotations is sometimes relaxed, however, we will typically assume it unless stated otherwise.

inserted inside a correlation function of local operators. We define a correlation function in the presence of \mathfrak{D} as

$$\langle \mathcal{O}_1 \dots \mathcal{O}_n \rangle_{\mathfrak{D}} = \frac{\langle \mathcal{O}_1 \dots \mathcal{O}_n \mathfrak{D} \rangle}{\langle \mathfrak{D} \rangle}, \quad (3.1.2)$$

where the local operators can be inserted either in the bulk or on Σ_p . The normalisation ensures that $\langle \mathbb{1} \rangle_{\mathfrak{D}} = 1$. In the subsequent discussion, we will drop the subscript $\langle \dots \rangle_{\mathfrak{D}} \rightarrow \langle \dots \rangle$ as it will be clear from context if a defect is inserted or not.

In the presence of a defect of any co-dimension, bulk operators can acquire non-vanishing one-point functions as there is now a scale: the distance from the defect. For a bulk scalar operator $\mathcal{O}_{\Delta, J=0}$, scale invariance implies

$$\langle \mathcal{O}_{\Delta, J=0}(x) \rangle = \frac{a_{\mathcal{O}}}{|x_{\perp}|^{\Delta}}, \quad (3.1.3)$$

where $a_{\mathcal{O}}$ is a dimensionless constant, and $x = (x_{\parallel}, x_{\perp})$. Note that bulk operators are normalised such that their two-point function in the absence of a defect is canonical. Thus, the coefficient of the one-point function with a defect, $a_{\mathcal{O}}$, contains dynamical information.

In a parity preserving theory, spin $J = 1$ bulk primaries sit in the vector representation of $SO(d+1, 1)$, and cannot acquire a one-point function. Invariance under scale transformations, translations along the defect, Lorentz invariance on the defect, and rotations around it require the putative one-point function to be

$$\langle \mathcal{O}_{\Delta}^a(x) \rangle = 0, \quad \langle \mathcal{O}_{\Delta}^i(x) \rangle = \frac{a_{\mathcal{O}} \hat{x}^i}{|x_{\perp}|^{\Delta}}. \quad (3.1.4)$$

However, invariance under the unbroken special conformal transformations K_a sets $a_{\mathcal{O}} = 0$. Indeed, under a special conformal transformation eq. (2.1.5) with $b_i = 0$, the normal components of \mathcal{O}^i transform as

$$\langle \mathcal{O}_{\Delta}^i(x') \rangle = \beta^{-\Delta} (\delta_j^i - 2\beta |b|^2 x^i x_j) \langle \mathcal{O}_{\Delta}^j(x) \rangle = \beta^{-\Delta} \langle \mathcal{O}_{\Delta}^i(x) \rangle - 2a_{\mathcal{O}} \frac{\beta^{1-\Delta} |b|^2 \hat{x}^i}{|x_{\perp}|^{\Delta-2}}. \quad (3.1.5)$$

But also

$$\langle \mathcal{O}_{\Delta}^i(x') \rangle = \frac{a_{\mathcal{O}} \hat{x}'^i}{|x'_{\perp}|^{\Delta}} = \beta^{-\Delta} \frac{a_{\mathcal{O}} \hat{x}^i}{|x_{\perp}|^{\Delta}} = \beta^{-\Delta} \langle \mathcal{O}_{\Delta}^i(x) \rangle. \quad (3.1.6)$$

These two equations are only consistent if $a_{\mathcal{O}} = 0$. Thus, a spin $J = 1$ primary cannot acquire a one-point function.

An important exception occurs in parity violating theories. Pseudo vectors sit in representations of $O(d+1, 1)$. These may acquire one-point functions, which necessarily involve an ϵ -tensor. E.g. when $q = 2$, a spin $J = 1$ operator can acquire the

following one-point function

$$\langle \mathcal{O}_\Delta^a(x) \rangle = 0, \quad \langle \mathcal{O}_\Delta^i(x) \rangle = \frac{a_{\mathcal{O}} \epsilon_{ij} \hat{x}^j}{|x_\perp|^\Delta}, \quad (3.1.7)$$

where ϵ is the Levi-Civita tensor in the transverse directions. Indeed, computing a special conformal transformation similarly to eq. (3.1.5), one finds that the second term vanishes by anti-symmetry of ϵ_{ij} . This is compatible with eq. (3.1.6) for any $a_{\mathcal{O}}$.

Next, consider operators with spin $J = 2$. For now, we'll keep the scaling dimension Δ general but we'll eventually take $\Delta = d$ to consider the stress tensor. Using scale invariance, translational invariance in the directions parallel to the defect, and covariance under rotations in the plane of the defect and the transverse directions, the most general form of the one-point function is

$$\langle \mathcal{O}_\Delta^{ab}(x) \rangle = c_1 \frac{\delta^{ab}}{|x_\perp|^\Delta}, \quad \langle \mathcal{O}_\Delta^{ai}(x) \rangle = \langle \mathcal{O}_\Delta^{ia}(x) \rangle = 0, \quad (3.1.8a)$$

$$\langle \mathcal{O}_\Delta^{ij}(x) \rangle = c_2 \frac{\delta^{ij}}{|x_\perp|^\Delta} + c_3 \frac{\hat{x}^i \hat{x}^j}{|x_\perp|^\Delta}, \quad (3.1.8b)$$

where $c_{1,2,3}$ are dimensionless coefficients to be fixed. A spin $J = 2$ operator has vanishing trace, thus $\delta_{\mu\nu} \langle \mathcal{O}_\Delta^{\mu\nu} \rangle = 0$. This imposes the following condition on the coefficients $c_{1,2,3}$

$$p c_1 + q c_2 + c_3 = 0. \quad (3.1.9)$$

Invariance under the special conformal transformations K_a imposes another constraint. A spin $J = 2$ primary transforms as

$$\mathcal{O}_\Delta^{\prime\mu\nu}(x') = \beta^{-\Delta}(x) R^\mu{}_\rho(x) R^\nu{}_\sigma(x) \mathcal{O}_\Delta^{\rho\sigma}(x), \quad (3.1.10)$$

where $R^\mu{}_\nu$ is an $SO(d)$ rotation matrix. A simple calculation gives for the normal-normal components

$$\begin{aligned} \mathcal{O}_\Delta^{\prime ij}(x') = & \beta^{-\Delta} \mathcal{O}_\Delta^{ij}(x) - 4\beta^{-\Delta} (c_2 + c_3) \frac{\hat{x}^i \hat{x}^j}{|x_\perp|^{\Delta-2}} (\beta |b|^2 - \beta^2 |b|^4 |x_\perp|^2) \\ & + 4c_1 \beta^{-\Delta+2} |b|^2 (1 - 2(b \cdot x) + |b|^2 |x_\parallel|^2) \frac{\hat{x}^i \hat{x}^j}{|x_\perp|^{\Delta-2}}. \end{aligned} \quad (3.1.11)$$

The ansatz eq. (3.1.8b) transforms simply by an overall factor, $\langle \mathcal{O}_\Delta^{ij}(x) \rangle \rightarrow \beta^{-\Delta} \langle \mathcal{O}_\Delta^{ij}(x) \rangle$. Matching both expressions, one finds the following constraint

$$c_1 = c_2 + c_3. \quad (3.1.12)$$

This gives a system of two linear equations in three variables, and thus the one-point function is fixed up to a single overall coefficient $a_{\mathcal{O}} = -\frac{c_1}{q-1}$ with $c_2 = (d - q + 1)a_{\mathcal{O}}$

and $c_3 = -d a_{\mathcal{O}}$.²

In the above we implicitly assumed that the co-dimension q is greater than 1. The $q = 1$ case is special as both tensor structures in the normal-normal components in eq. (3.1.8b) are identical. In this case, the only solution is the trivial solution $\langle \mathcal{O}_{\Delta}^{\mu\nu}(x) \rangle = 0$. Indeed, in that case both $c_1 = 0$ and $c_2 + c_3 = 0$.

For the stress tensor $T^{\mu\nu}$, it is common to write $a_T \equiv h$ such that the non-zero components are

$$\langle T^{ab} \rangle = -h \frac{(q-1)\delta^{ab}}{|x_{\perp}|^d}, \quad \langle T^{ij} \rangle = h \frac{(d-q+1)\delta^{ij} - d\hat{x}^i\hat{x}^j}{|x_{\perp}|^d}. \quad (3.1.13)$$

Note that $\partial_{\mu}\langle \mathcal{O}^{\mu a} \rangle = 0$ and $\partial_{\mu}\langle \mathcal{O}^{\mu i}(x) \rangle = (q-1)(\Delta-d)a_{\mathcal{O}}\frac{\hat{x}^i}{|x_{\perp}|^{\Delta+1}}$, which vanishes when $\mathcal{O}^{\mu\nu} = T^{\mu\nu}$ and $\Delta = d$. Therefore, this one-point function is compatible with conservation of the stress tensor away from the defect.

The form of the two- and higher-point functions of bulk primary operators in the presence of a defect are less constrained by conformal symmetry: they can depend on functions of dimensionless cross ratios. We will see an explicit example in section 7.2, where we will examine the two-point function of a scalar in the presence of a co-dimension two defect. See also ref. [147] for details.

So far we have discussed *bulk* operators in the presence of a defect. However, a conformal defect comes with a set of local operators that only live on the defect. Physically, they correspond to local excitations of the defect. An example of such an operator is the displacement operator \mathcal{D}^i , which exists for any non-trivial and non-topological DCFT. A defect breaks translational invariance in the directions transverse to it. Therefore, the Ward identities for translations normal to the defect are modified, and the stress tensor is no longer conserved in these directions at the location of the defect

$$\partial_{\mu} T^{\mu i}(x_{\parallel}, x_{\perp}) = \delta^{(q)}(x_{\perp}) \mathcal{D}^i(x_{\parallel}). \quad (3.1.14)$$

The displacement operator \mathcal{D}^i captures this non-conservation. It has scaling dimension $\hat{\Delta} = p + 1$,³ no spin in the defect direction, $\hat{j} = 0$, and spin $\hat{s} = 1$ in the transverse directions. By acting with K_a on eq. (3.1.14), one can show that \mathcal{D}^i is a primary under the conformal group preserved by the defect. Using the Jacobi identity, the algebra eq. (2.1.9), and eq. (2.2.13), one finds after a few lines of algebra that

$$[K_a, [P_{\mu}, T^{\mu i}(0, x_{\perp})]] = \delta^{(q)}(x_{\perp})(2x^j \Sigma_{aj} + |x_{\perp}|^2 \partial_a) \mathcal{D}^i(0) = 0, \quad (3.1.15)$$

²The same form can be derived in a much neater way using the embedding space formalism, see [147] for details.

³The delta function $\delta^{(q)}(x_{\perp})$ has scaling dimension q .

where the last equality follows from the identity $x\delta(x) = 0$. Thus, $[K_a, \mathcal{D}^i(0)] = 0$, and \mathcal{D}^i is a defect primary.⁴

In the co-dimension $q = 1$ case, a Gauss law pillbox argument [53] shows that the displacement operator may be identified with the defect limit of the normal-normal component of the stress tensor

$$\mathcal{D}(x_{\parallel}) \equiv \mathcal{D}^n(x_{\parallel}) = \lim_{x_{\perp} \rightarrow 0} T_{nn}(x_{\parallel}, x_{\perp}), \quad (3.1.16)$$

where n labels the single normal direction. Note that when $q = 1$, the scaling dimension $\hat{\Delta} = (d - 1) + 1 = d$, in agreement with that of the stress tensor.⁵

Invariance under the unbroken conformal generators implies

$$\langle \mathcal{D}^i(x_{\parallel}) \mathcal{D}^j(y_{\parallel}) \rangle = \frac{c_{\mathcal{D}\mathcal{D}} \delta^{ij}}{|x_{\parallel} - y_{\parallel}|^{2(p+1)}}. \quad (3.1.17)$$

The normalisation of the displacement operator two-point function $c_{\mathcal{D}\mathcal{D}}$ is physically meaningful as it is fixed by the ambient CFT's stress tensor.

More generally, a defect that breaks a continuous bulk symmetry induces a defect local operator via the associated current's modified Ward identity. In particular, this holds for flavour and global internal symmetries. Bulk currents have scaling dimension $\Delta = d - 1$. Therefore, the associated defect primary has scaling dimension $\hat{\Delta} = p$, i.e. it is exactly marginal.

Correlation functions of defect primary operators are completely analogous to those in ordinary CFT. It is again customary to canonically normalise two-point functions. E.g.

⁴If the defect additionally breaks rotational invariance in the transverse directions, the stress tensor no longer needs to be symmetric at the location of the defect,

$$T^{[ij]}(x_{\parallel}, x_{\perp}) = \delta^{(q)}(x_{\perp}) \lambda^{ij}(x_{\parallel}),$$

where λ^{ij} is a defect primary in the anti-symmetric representation of $SO(d - p)$ [147,149]. We will typically assume rotational invariance in the transverse directions such that λ^{ij} will play no role in this thesis.

⁵The argument goes as follows: Consider the boundary as an interface with the empty theory and introduce a cylindrical Gaussian pillbox $I \times B_{\delta}^{d-1}$ centred on the interface, where I is a closed interval in the normal direction, $x_{\perp} \in [-\varepsilon, \varepsilon]$ and B_{δ}^{d-1} is the solid $(d - 1)$ -ball of radius δ whose boundary is $\partial B_{\delta}^{d-1} = S_{\delta}^{d-2}$. By the divergence theorem,

$$\int_{I \times B_{\delta}^{d-1}} \partial_{\mu} T^{\mu n} = \int_{B_{\delta, \varepsilon}^{d-1}} T^{nn} - \int_{B_{\delta, -\varepsilon}^{d-1}} T^{nn} + \int_{I \times S_{\delta}^{d-1}} T^{rn},$$

where r is the index of the radial coordinate in the boundary direction, and $B_{\delta, \pm\varepsilon}$ are the solid balls at the endpoints of I , i.e. $x_{\perp} = \pm\varepsilon$. Now, the second term vanishes as $T^{nn} = 0$ for the empty theory, and the third term can be made arbitrarily small by taking $\varepsilon \rightarrow 0$. Substituting eq. (3.1.14) on the left-hand side, one has

$$\int_{B_{\delta, 0}^{d-1}} \mathcal{D} = \int_{B_{\delta, \varepsilon}^{d-1}} T^{nn},$$

where $B_{\delta, 0}^{d-1}$ is the solid ball located entirely within the interface at $x_{\perp} = 0$. This must hold for arbitrarily small δ , which implies eq. (3.1.16).

for an orthonormal basis of defect scalar primaries,

$$\langle \hat{\mathcal{O}}_1(x_1) \hat{\mathcal{O}}_2(x_2) \rangle = \frac{\delta_{1,2}}{|x_{12}^a|^{2\hat{\Delta}}}. \quad (3.1.18)$$

This only applies to operators whose normalisation is not physically meaningful, unlike eq. (3.1.17). Three-point functions are again fixed by kinematics up to a single coefficient, $\hat{\lambda}_{123}$. The only novel ingredient is that defect operators may carry spin with respect to the transverse rotation group. This may be regarded as a global $SO(q)$ symmetry from the defect's point of view.

For correlation functions mixing bulk and defect primaries, the conformal symmetry preserved by the defect fixes the kinematic dependence of the bulk-defect two-point function. E.g. the two-point function of a bulk scalar primary and a defect scalar primary is

$$\langle \mathcal{O}_{\Delta, J=0}(x_1) \hat{\mathcal{O}}_{\hat{\Delta}, \hat{j}=0, \hat{s}=0}(x_2) \rangle = \frac{b_{\mathcal{O}\hat{\mathcal{O}}}}{(|x_1^i|^2 + |x_{12}^a|^2)^{\hat{\Delta}} |x_1^i|^{\Delta-\hat{\Delta}}}, \quad (3.1.19)$$

where $x_1 = (x_1^a, x_1^i)$, $x_2 = (x_2^a, 0)$, and the coefficients $b_{\mathcal{O}\hat{\mathcal{O}}}$ are constants. Since both \mathcal{O} and $\hat{\mathcal{O}}$ are canonically normalised, the coefficients $b_{\mathcal{O}\hat{\mathcal{O}}}$ carry dynamical information. Note that when the defect operator is the identity, the two-point function reduces to the one-point function of \mathcal{O} with $b_{\mathcal{O}\hat{1}} = a_{\mathcal{O}}$.

Two-point functions of spinning operators like $\mathcal{O} = T^{\mu\nu}$ or $\hat{\mathcal{O}} = \mathcal{D}^i$ are slightly more involved. E.g. the two-point function of a bulk scalar primary and a defect primary with transverse spin $s = 1$ is

$$\langle \mathcal{O}_{\Delta, J=0}(x_1) \hat{\mathcal{O}}_{\hat{\Delta}, j=0, s=1}^i(x_2) \rangle = \frac{b_{\mathcal{O}\hat{\mathcal{O}}x_1^i}}{(|x_1^i|^2 + |x_{12}^a|^2)^{\hat{\Delta}} |x_1^i|^{\Delta-\hat{\Delta}+1}}. \quad (3.1.20)$$

Explicit expressions for other mixed two-point functions can be found in ref. [147]. Higher-point correlation functions mixing bulk and defect primaries have much more complicated coordinate dependence as they are functions of cross ratios.

Just like in a standalone CFT, the defect local operators have an OPE. When two defect operators are brought close to each other, they can be expanded as a linear combination of defect local operators, which again assemble into a sum over defect primaries and their descendants. Using associativity of this OPE, one can show exactly like in standard CFT that the higher-point correlation functions of defect primary operators are (fixed) functions that depend on the scaling dimensions $\hat{\Delta}_i$, spins \hat{j} and \hat{s} , and the three-point functions of defect primaries $\hat{\lambda}_{123}$.

Similarly to the bulk OPE, a bulk local operator close to the defect can be expanded in terms of defect local operators as a consequence of the state-operator correspondence,

$$\mathcal{O}(x^a, x^i) = \sum_{\hat{\mathcal{O}}} C_{\mathcal{O}\hat{\mathcal{O}}}(x^i, \partial_{\parallel}) \hat{\mathcal{O}}(x^a). \quad (3.1.21)$$

The coefficients $C_{\mathcal{O}\hat{\mathcal{O}}}(x^i, \partial_{\parallel})$ are differential operators which take into account the contributions from descendants of $\hat{\mathcal{O}}$ such that the sum can be taken to run over defect primaries only. The sum is convergent as can be shown by quantising radially around a point on the defect [66, 146, 147, 150]. This expansion of a single *bulk* operator in terms of *defect* local operators is often called the defect OPE, or defect operator expansion, and should not be confused with the OPE of *two* defect local operators discussed above. Physically, the defect OPE states that a bulk excitation near the defect is indistinguishable from an excitation localised on the defect. Applying the defect OPE inside the bulk-defect two-point function, one finds that the $C_{\mathcal{O}\hat{\mathcal{O}}}(x^i, \partial_{\parallel})$ must be proportional to $b_{\mathcal{O}\hat{\mathcal{O}}}$.

Given some bulk CFT data, mixed bulk-defect higher-point functions can be reduced to correlation functions of defect local operators only by repeatedly using the defect OPE. These can then be reduced further into three point functions of defect primaries. Thus, to be able to completely solve for all correlation functions of local operators in the presence of a defect, one needs to know the spectrum of defect local operators $\hat{\mathcal{O}}$, the defect three-point functions $\hat{\lambda}_{123}$, and the bulk-defect two-point functions $b_{\mathcal{O}\hat{\mathcal{O}}}$. These are called the DCFT data.

Associativity of the (defect) OPE gives rise to a number of consistency conditions that should hold in the presence of any conformal defect. Firstly, the bulk CFT must be consistent by itself, and thus its data must satisfy the crossing equations. Similarly, the spectrum of defect local operators and their three-point functions $\hat{\lambda}_{123}$ must obey their crossing equations. Lastly, there are consistency conditions that arise from bulk or bulk-defect correlation functions. E.g. the bulk two-point function $\langle \mathcal{O}_1 \mathcal{O}_2 \rangle$ can be decomposed in two ways. In the first decomposition, we use the bulk OPE on \mathcal{O}_1 and \mathcal{O}_2 first, and then the one-point function. This gives an expansion, where each term contains a factor of $\lambda_{12k} a_k$ times a function of cross ratios, called a defect conformal block. In the second decomposition, we first use the defect OPE on \mathcal{O}_1 and \mathcal{O}_2 separately, and then the defect two-point function. This results in an expansion where each term contains a factor $b_{1k} b_{2k}$ times another type of conformal block. We will see an explicit example of the latter defect conformal block expansion in chapter 7. Further consistency conditions, which involve the defect three-point functions $\hat{\lambda}_{123}$, can be obtained from $\langle \mathcal{O}_1 \mathcal{O}_2 \hat{\mathcal{O}}_3 \rangle$. Using these consistency conditions to identify the space of allowed DCFT data is the goal of the defect conformal bootstrap programme [66, 68, 147, 148, 151, 152].

3.2 Examples of conformal defects

Conformal defects typically fall into two classes, commonly called order- and disorder-type defects.

Order-type defects are engineered by introducing local DOF on a p -dimensional submanifold Σ_p . Consider pure Maxwell theory in \mathbb{R}^4 with action

$$I = \frac{1}{4e^2} \int d^4x F_{\mu\nu} F^{\mu\nu}, \quad (3.2.22)$$

where the field strength $F_{\mu\nu} = \partial_\mu A_\nu - \partial_\nu A_\mu$, and A_μ is the $U(1)$ gauge field. A simple example of an order-type conformal defect is the straight infinite Wilson line. It is defined by inserting

$$W_n[A] = \exp\left(in \int dx^\mu A_\mu\right) \quad (3.2.23)$$

into the path integral, where n is an integer. Physically, the Wilson line describes a heavy, i.e. non-dynamical, particle with electric charge ne . The one-point function of the bulk stress tensor in the presence of the Wilson line can be easily computed, and indeed takes the form of eq. (3.1.13) with $h = \frac{n^2 e^2}{96\pi^2}$ [153].

More generally, one can introduce a new set of fields ψ which only have support on Σ_p in addition to the bulk CFT fields Ψ , and insert the following deformation in the path integral

$$\exp\left(-\int_{\Sigma_p} d^p x \mathcal{L}_{\mathcal{D}}[\psi, \Psi]\right), \quad (3.2.24)$$

where the defect Lagrangian $\mathcal{L}_{\mathcal{D}}$ is some local functional of Ψ and ψ . If $\mathcal{L}_{\mathcal{D}}$ is conformal, its insertion in the path integral engineers a conformal defect. An example of such a defect is mixed-dimensional quantum electrodynamics (QED), where the charged fermions are confined to the boundary of a 4d spacetime [53]. This can be viewed as the IR fixed point of an infinite sheet of graphene. However, if $\mathcal{L}_{\mathcal{D}}$ has dimensionful couplings, they will flow under a defect RG flow.⁶ The IR fixed point will then correspond to a conformal defect. We will encounter such defects in chapter 8.

Disorder-type defects are introduced by prescribing singularity or boundary conditions for the ambient fields. The simplest example of this type of defect is the straight infinite 't Hooft line in 4d Maxwell theory. It is defined by imposing singularity conditions in the gauge field A_μ . Choose polar coordinates $\{\tau, r, \theta, \phi\}$ where the 't Hooft line is extended along Euclidean time τ , r is the radial direction away from it, and θ and ϕ are the polar and azimuthal angles, respectively. Pick a

⁶Couplings of the bulk CFT are unaffected due to locality.

gauge in which $A_r = 0$. Then the 't Hooft line is defined by the following singularity condition as $r \rightarrow 0$

$$A_\phi \rightarrow \frac{m(1 - \cos \theta)}{4\pi r \sin \theta}, \quad (3.2.25)$$

where m is the integer quantised magnetic charge.⁷ Physically, this boundary condition corresponds to a heavy Dirac monopole of quantised charge m . To compute correlation functions in the presence of such a defect, one is instructed to perform the path integral only over field configurations that satisfy the appropriate boundary or singularity condition. To find the stress tensor one-point function for the 't Hooft line in free Maxwell theory it suffices to evaluate the classical stress tensor on the unique solution of the equations of motion (EOM) that satisfies the boundary conditions. The result is again of the form in eq. (3.1.13) with $h = \frac{m^2}{24e^2}$ [153].⁸

Another example of a disorder-type defect is the monodromy defect, which will be studied in detail in chapter 7. It is a co-dimension $q = 2$ defect that can be introduced whenever there is a global symmetry group G in the bulk theory. If the bulk is a CFT, then a straight monodromy defect is conformal. Let $x^\mu = \{\tau, \vec{x}, \rho, \theta\}$ be cylindrical coordinates on \mathbb{R}^d , where τ is Euclidean time, \vec{x} denotes the spatial flat directions, ρ the radial coordinate, and θ the polar angle. A monodromy defect at $\rho = 0$ along \vec{x} is engineered by declaring that bulk operators

$$\Psi_i(\tau, \vec{x}, \rho, \theta) \rightarrow \Psi'_i(\tau, \vec{x}, \rho, \theta + 2\pi) = g_i \Psi_i(\tau, \vec{x}, \rho, \theta), \quad (3.2.26)$$

i.e. each field Ψ_i experiences a monodromy $g_i \in G$ as it is rotated around the defect in the transverse directions. From another point of view, monodromy defects can be thought of as co-dimension two operators on which topological domain walls that implement flavour symmetry rotations can end. This type of construction of defects in QFTs fits into a larger class of topological defects effecting generalised global symmetry transformations [154]. In free theories, monodromy defects are special. E.g. in the theory of a 4d free scalar field, the only reflection-positive defects that can have interesting dynamics are monodromy defects. All other defects must have trivial dynamics, i.e. all connected n -point functions of the bulk field remain zero, even in the presence of the defect. [155, 156].^{9,10} Monodromy defects in free theories will be discussed in detail in chapter 7.

In the discussion above, we introduced order and disorder as a broad partitioning of defects. However, it is unlikely that this partitioning will form the basis for a classification because order and disorder-type defects can sometimes be related. E.g.

⁷This expression only holds in the patch including the north pole $\theta = 0$. An analogous expression exists for the patch with the south pole. On the overlap of the patches, the two gauge fields are related by a gauge transformation.

⁸Maxwell theory famously enjoys electric-magnetic duality $F_{\mu\nu} \rightarrow \epsilon_{\mu\nu\rho\sigma} F^{\rho\sigma}$ and $e^2 \rightarrow \frac{4\pi^2}{e^2}$. Under this map, Wilson and 't Hooft lines are exchanged as can be seen from their values of h .

⁹In dimensions $d \geq 5$, there can exist non-trivial non-monodromy defects if the co-dimension $q = 3$.

¹⁰In 4d Maxwell theory it was shown that *all* surface defects have trivial dynamics [157].

we may be able to integrate out DOF on Σ_p to obtain singular behaviour of the ambient fields at Σ_p . We will discuss an example in chapter 8 for which this happens.

3.3 Submanifold geometry

We would now like to put our DCFT on a curved background to study the Weyl anomaly in the presence of the defect. Before we can do so, we need to review the geometry of embedded submanifolds.

Let \mathcal{M}_d be a smooth d -dimensional Riemannian manifold. \mathcal{M}_d with $d \geq 2$ is the background geometry into which we will embed a defect, or introduce a boundary. We refer to this background as the *ambient* space. Let x^μ be the coordinates on \mathcal{M}_d , where $\mu = 1, \dots, d$, and let $g_{\mu\nu}$ be the metric on \mathcal{M}_d . The Levi-Civita connection on \mathcal{M}_d is denoted by D_μ , and its connection coefficients are the Christoffel symbols $\Gamma_{\mu\nu}^\rho$. The associated curvature tensors are denoted by R , i.e. $R^\mu{}_{\nu\rho\sigma}$ is the Riemann tensor, $R_{\mu\nu} = R^\rho{}_{\mu\rho\nu}$ is the Ricci tensor, and R is the Ricci scalar on \mathcal{M}_d . The ambient Weyl tensor is denoted by $W_{\mu\nu\rho\sigma}$.

The defects that we will study are supported on a p -dimensional embedded submanifold, $\Sigma_p \hookrightarrow \mathcal{M}_d$. Let σ^a be coordinates on Σ_p , where $a = 1, \dots, p$. The embedding induces various intrinsic geometric quantities on Σ_p that we distinguish from their counterparts on \mathcal{M}_d with a bar. In particular, let $\bar{g}_{ab} = e_a^\mu e_b^\nu g_{\mu\nu}$ denote the induced metric, where $e_a^\mu = \partial_a X^\mu$, and $X^\mu(\sigma^a)$ are the embedding functions. The matrix e_a^μ acts to pull back ambient tensors onto Σ_p , e.g. the pullback of the ambient Ricci tensor is $R_{ab} = e_a^\mu e_b^\nu R_{\mu\nu}$.

On Σ_p we denote the induced Levi-Civita connection as \bar{D}_a , with its connection coefficients being the Christoffel symbols $\bar{\Gamma}_{bc}^a$ built out of \bar{g}_{ab} . The Riemann curvature tensor constructed from \bar{D}_a is $\bar{R}^a{}_{bcd}$, and similarly for the Ricci tensor and scalar. We further introduce a covariant derivative that acts on tensors with mixed indices. We will abuse notation and also refer to it as \bar{D}_a , e.g. $\bar{D}_a w_b^\mu = \partial_a w_b^\mu + \Gamma_{\nu a}^\mu w_b^\nu - \bar{\Gamma}_{ab}^c w_c^\mu$ for a mixed tensor w_b^μ , where $\Gamma_{\nu a}^\mu = e_a^\rho \Gamma_{\nu\rho}^\mu$. From \bar{D}_a , we define the second fundamental form, $\Pi_{ab}^\mu \equiv \bar{D}_a e_b^\mu$. It is symmetric in a and b , and it obeys $E_\mu^c \Pi_{ab}^\mu = 0$. Its traceless version is denoted as $\hat{\Pi}_{ab}^\mu \equiv \Pi_{ab}^\mu - \frac{1}{p} \bar{g}_{ab} \Pi^\mu$, with $\Pi^\mu \equiv \bar{g}^{cd} \Pi_{cd}^\mu$.

The embedding $\Sigma_p \hookrightarrow \mathcal{M}_d$ splits the ambient space's tangent bundle $T\mathcal{M}_d \simeq T\Sigma_p \oplus N\Sigma_p$ into a sum of the defect submanifold's tangent bundle, $T\Sigma_p$, and the normal bundle, $N\Sigma_p$. We will often replace tensor indices μ, ν, \dots that are only valued in the normal bundle by i, j, \dots for emphasis, e.g. $\Pi^\mu \rightarrow \Pi^i$.

The important geometric features of the normal bundle $N\Sigma_p$ derive from the totally antisymmetric normal tensor,

$$n_{\mu_1 \dots \mu_q} = \frac{1}{p!} \epsilon^{a_1 \dots a_p} \epsilon_{\nu_1 \dots \nu_p \mu_1 \dots \mu_q} e_{a_1}^{\nu_1} \dots e_{a_p}^{\nu_p}, \quad (3.3.27)$$

where $\epsilon_{a_1 \dots a_p}$ and $\epsilon_{\mu_1 \dots \mu_d}$ are Levi-Civita tensors on Σ_p and \mathcal{M}_d respectively. From $n_{\mu_1 \dots \mu_q}$, we define a projector onto $N\Sigma_p$,

$$N_{\mu\nu} \equiv \frac{1}{(q-1)!} n_{\mu\sigma_2 \dots \sigma_q} n_{\nu}^{\sigma_2 \dots \sigma_q}. \quad (3.3.28)$$

We can similarly define a projector onto $T\Sigma_p$, also called the first fundamental form,

$$h_{\mu\nu} \equiv g_{\mu\nu} - N_{\mu\nu}. \quad (3.3.29)$$

Note that $h_{\mu\nu} = E_{\mu}^a E_{\nu}^b \bar{g}_{ab}$, where E_{μ}^a is a matrix which obeys $E_{\mu}^a e_b^{\mu} = \delta_b^a$. The decomposition eq. (3.3.29) implies for example

$$\bar{g}^{ab} R_{ab} = h^{\mu\nu} R_{\mu\nu} = R - N^{\mu\nu} R_{\mu\nu}, \quad (3.3.30)$$

and

$$D^2 f = h^{\mu\nu} D_{\mu} D_{\nu} f + N^{\mu\nu} D_{\mu} D_{\nu} f = \bar{D}^2 f - \Pi^{\mu} D_{\mu} f + N^{\mu\nu} D_{\mu} D_{\nu} f, \quad (3.3.31)$$

for some scalar function f .

On a non-trivial normal bundle, one can also define a covariant derivative on normal vectors descending from D_{μ} . We denote it as D_a^{\perp} . Its associated curvature $(R^{\perp})^{\mu}_{\nu ab}$ is anti-symmetric under $(a \leftrightarrow b)$ and $(\mu \leftrightarrow \nu)$ separately.

The curvature tensors of D_{μ} , D_a^{\perp} , and \bar{D}_a are related via the Gauss-Codazzi-Ricci equations. The Gauss equation relates the intrinsic Riemann tensor \bar{R}_{abcd} on the submanifold and the pullback of the ambient Riemann tensor R_{abcd} . Together with the equation's contractions with the induced metric \bar{g}^{ab} , they read

$$R^a{}_{bcd} = \bar{R}^a{}_{bcd} - 2\Pi_{\mu[c}{}^a \Pi_{d]b}^{\mu}, \quad (3.3.32a)$$

$$R_{ab} = \bar{R}_{ab} - \Pi_{\mu ab} \Pi^{\mu} + \Pi_{\mu ac} \Pi^{\mu}{}_b{}^c + N^{\rho\sigma} R_{\rho b \sigma}, \quad (3.3.32b)$$

$$R = \bar{R} - \Pi_{\mu} \Pi^{\mu} + \Pi_{\mu ab} \Pi^{\mu ba} + 2N^{\mu\nu} R_{\mu\nu} - N^{\mu\rho} N^{\nu\sigma} R_{\mu\nu\rho\sigma}. \quad (3.3.32c)$$

The Codazzi relation and its contraction with \bar{g}^{ab} read

$$N_{\nu}^{\mu} R^{\nu}{}_{abc} = N_{\nu}^{\mu} (\bar{D}_b \Pi_{ca}^{\nu} - \bar{D}_c \Pi_{ba}^{\nu}), \quad (3.3.33a)$$

$$N_{\nu}^{\mu} R^{\nu}{}_b = N_{\nu}^{\mu} (\bar{D}_b \Pi^{\nu} - \bar{D}_c \Pi_b^{\nu c}) + N^{\mu\nu} N^{\rho\sigma} R_{b\sigma\nu\rho}. \quad (3.3.33b)$$

Finally, we also have the Ricci equation

$$N_p^\mu N_V^\sigma R^\rho{}_{\sigma ab} = (R^\perp)^\mu{}_{\nu ab} - \Pi_{ac}^\mu \Pi_{\nu b}{}^c + \Pi_{bc}^\mu \Pi_{\nu a}{}^c. \quad (3.3.34)$$

When $q = 1$, i.e. for a boundary or interface, $N\Sigma_p$ is a trivial bundle. In that case, $(R^\perp) = 0$ and the Ricci eq. (3.3.34) becomes trivial. Moreover, the normal projector becomes $N_{\mu\nu} = n_\mu n_\nu$, where n_μ is the outward pointing unit normal co-vector. Moreover, $h_{\mu\nu}$ reduces to the usual hypersurface metric, $h_{\mu\nu} = g_{\mu\nu} - n_\mu n_\nu$. We define the extrinsic curvature as $K_{\mu\nu} \equiv \frac{1}{2} \mathcal{L}_n h_{\mu\nu}$, where \mathcal{L}_n is the Lie derivative along n^μ , which satisfies $n^\mu K_{\mu\nu} = 0$, and is related to the second fundamental form by $K_{ab} = -n_\mu \Pi_{ab}^\mu$, where $K_{ab} = e_a^\mu e_b^\nu K_{\mu\nu}$. We define the traceless version $\mathring{K}_{ab} \equiv K_{ab} - \frac{1}{p} \bar{g}_{ab} K$, with $K \equiv \bar{g}^{ab} K_{ab}$.

Finally, we define two notions of parity. By ‘‘parity along the defect’’, we mean simultaneous orientation reversal of the submanifold and the ambient space, such that $\epsilon^{a_1 \dots a_p} \rightarrow -\epsilon^{a_1 \dots a_p}$ and $\epsilon^{\mu_1 \dots \mu_d} \rightarrow -\epsilon^{\mu_1 \dots \mu_d}$, such that $n^{\mu_1 \dots \mu_q}$, as defined by eq. (3.3.27), is invariant. Intuitively, this corresponds to reversing parity in the directions parallel to the defect. By ‘‘parity in the normal bundle’’ we mean orientation reversal of the ambient space alone. Under this transformation, $\epsilon^{\mu_1 \dots \mu_d} \rightarrow -\epsilon^{\mu_1 \dots \mu_d}$ while $\epsilon^{a_1 \dots a_p}$ is invariant, such that $n^{\mu_1 \dots \mu_q} \rightarrow -n^{\mu_1 \dots \mu_q}$. This corresponds to reversing parity in the directions normal to the defect.

3.4 Defect Weyl anomaly

Consider a d -dimensional CFT on a curved background \mathcal{M}_d with a p -dimensional conformal defect supported on $\Sigma_p \hookrightarrow \mathcal{M}_d$. The embedding functions $X^\mu(\sigma)$ now play the role of background fields in the path integral. Under an infinitesimal variation of $\mathcal{W}[g, X]$ with respect to $g_{\mu\nu}$ and X^μ ,

$$\begin{aligned} \delta \mathcal{W}[g, X] = & -\frac{1}{2} \int_{\mathcal{M}_d} d^d x \sqrt{\bar{g}} \delta g_{\mu\nu} \langle T^{\mu\nu} |_{\mathcal{M}_d} \rangle \\ & - \frac{1}{2} \int_{\Sigma_p} d^p \sigma \sqrt{\bar{g}} \left(\delta g_{\mu\nu} \langle T^{\mu\nu} |_{\Sigma_p} \rangle + 2\delta X^\mu(\sigma^a) \langle \mathcal{D}_\mu \rangle \right), \end{aligned} \quad (3.4.35)$$

where $T^{\mu\nu}|_{\mathcal{M}_d}$ and $T^{\mu\nu}|_{\Sigma_p}$ denote the contributions to the stress tensor from the ambient CFT and the defect, respectively. The response of the path integral to deformations of Σ_p is denoted very suggestively as \mathcal{D}^μ . Consider a diffeomorphism of \mathcal{M}_d parametrised by ξ^μ . This induces a variation of both $g_{\mu\nu}$ and X^μ . Indeed, the variation of $\mathcal{W}[g, X]$ under ξ^μ allows one to identify \mathcal{D}^μ with the displacement operator defined in eq. (3.1.14), with $\partial_\mu \rightarrow D_\mu$. Moreover, reparametrisation invariance of Σ_p on its own implies that one can set $e_a^\mu \mathcal{D}_\mu = 0$. I.e. only \mathcal{D}^i is non-trivial, where i is a normal bundle index [147]. This ultimately gives the

displacement operator its name: it “displaces” a point on the defect in a normal direction. Note that generically the defect does not have its own intrinsically defined, conserved stress tensor. However, the components of the full stress tensor along Σ_p , containing both ambient and defect contributions, are conserved everywhere on \mathcal{M}_d , including Σ_p , i.e. $D_\mu T^{\mu a} = 0$.

If we instead consider an infinitesimal Weyl rescaling without affecting the defect’s embedding, then the Weyl anomaly picks up a contribution localised to Σ_p ,

$$T^\mu{}_\mu = T^\mu{}_\mu|_{\mathcal{M}_d} + \delta_{\Sigma_p}^{(q)} T^\mu{}_\mu|_{\Sigma_p}. \quad (3.4.36)$$

Here we indicate by $T^\mu{}_\mu|_{\mathcal{M}_d}$ the contributions to the Weyl anomaly purely from the ambient CFT, and by $T^\mu{}_\mu|_{\Sigma_p}$ we denote the defect/boundary Weyl anomaly, which will be the primary focus of the following sections. The delta function $\delta_{\Sigma_p}^{(q)}$ is defined as $\int_{\mathcal{M}_d} d^d x \sqrt{g} f(x) \delta_{\Sigma_p}^{(q)} = \int_{\Sigma_p} d^p \sigma \sqrt{\bar{g}} f(X(\sigma))$ for some test function f . Importantly, $T^\mu{}_\mu|_{\Sigma_p}$ is built out of structures that involve (derivatives of) the metric $g_{\mu\nu}$ and the embedding functions $X^\mu(\sigma^a)$. This leads to a much richer basis for conformal invariants, and hence novel defect Weyl anomalies.

The form of the defect Weyl anomaly $\delta_\omega \mathcal{W} = \int_{\Sigma_p} (\dots) \delta\omega$ can be determined algorithmically by modifying the three-step algorithm in section 2.5 on page 26. The main novelty is that each term in $\delta_\omega \mathcal{W}[g, X]$ may also contain X^μ and its derivatives. In particular, each term must contain p derivatives acting on the metric $g_{\mu\nu}$, the pullbacks e_a^μ , or the Weyl variation parameter $\delta\omega$. Ensuring that all the terms in step 1 are linearly independent can become rather cumbersome as there are new geometric relations stemming from the decomposition of the metric in eq. (3.3.29) and the Gauss-Codazzi-Ricci eqs. (3.3.32), (3.3.33), and (3.3.34). Moreover, when $p \geq 3$, the second Bianchi identity can be combined with the Gauss-Codazzi-Ricci equations, to produce additional geometric relations, which can be further adorned with extra derivatives. Each linearly independent term is then added to the defect Weyl anomaly with an unfixed coefficient. The remaining steps involving WZ consistency and local counter-terms go through unchanged.

The defect/boundary Weyl anomaly has been determined in four cases: $p = 1$ in $d = 2$ [84], $p = 2$ in $d \geq 3$ [50, 71, 72, 97, 98, 158–160], $p = 3$ in $d = 4$ [51, 52], and $p = 4$ in $d = 5$ [161]. In the rest of this section we will review the first three cases. In chapter 6, we review the fourth case and generalise it to $d \geq 6$. This turns out to be rather involved due to an abundance of additional tensor structures.

For a $p = 1$ defect, applying the algorithm is straightforward. The only allowed tensor structures are $\int_{\Sigma_1} d\sigma \sqrt{g} K \delta\omega$ and $\int_{\Sigma_1} d\sigma \sqrt{g} n^\mu D_\mu \delta\omega$. The former is not WZ consistent on its own and the latter can be removed by a counter-term. Thus, for $p = 1$ in a $d > 2$ CFT the defect Weyl anomaly vanishes. However, when $d = 2$, WZ consistency of the

bulk anomaly eq. (2.5.48) requires the following boundary term [84]

$$T^\mu{}_\mu|_{\Sigma_1} = \frac{c^{(2d)}}{12\pi} K. \quad (3.4.37)$$

Note that its coefficient is fixed by the bulk central charge $c^{(2d)}$. More generally, if the ambient CFT has even d , and the defect has co-dimension $q = 1$, then WZ consistency of the ambient Euler density induces a term in the defect's Weyl anomaly whose coefficient is fixed in terms of the ambient CFT's A-type central charge. We will see this feature again for $p = 3$ in $d = 4$, see eq. (3.4.45). In fact, these boundary terms are known for all even d [51].

Applying the algorithm to determine the Weyl anomaly of a $p = 2$ defect in a $d \geq 3$ CFT is less trivial since defect Weyl anomalies are much richer compared to their counterparts in standalone CFTs. E.g. for a $p = 2$ defect in $d = 4$, a linearly independent basis of terms is 10-dimensional. Contrast this with the case of a standalone 2d CFT, which only allowed for a single term, see eq. (2.5.59). We summarise the computation in appendix A.1. It is convenient to turn the process of eliminating scheme-dependent terms into a linear algebra problem, which we also illustrate there. The result is [50, 71, 72, 97, 98, 158–160]

$$T^\mu{}_\mu|_{\Sigma_2} = \frac{1}{24\pi} (a_\Sigma^{(2d)} \bar{R} + d_1^{(2d)} \mathring{\Pi}^2 + d_2^{(2d)} W^{ab}{}_{ab}) + \frac{\delta_{q,2}}{24\pi} \epsilon^{ab} n_{ij} (\tilde{d}_1^{(2d)} (R^\perp)^{ij}{}_{ab} + \tilde{d}_2^{(2d)} \mathring{\Pi}_{ac}^i \mathring{\Pi}_b^j{}^c), \quad (3.4.38)$$

where $\delta_{q,2}$ is a Kronecker delta. Within the first set of parentheses, the first term is an A-type central charge, while the remaining two are B-type. The term $d_2^{(2d)} W^{ab}{}_{ab}$ does not exist for $q = 1$ because the ambient Weyl tensor W vanishes identically when $d = 3$. In that term, the trace over the indices is performed with the induced metric \bar{g}_{ab} , hence $W^{ab}{}_{ab}$ is generically non-vanishing when $d \geq 4$. In the second set of parentheses, both terms exist only when $q = 2$. They are B-type, and odd under parity along the defect and separately under parity in the normal bundle. The indices i, j, \dots are valued in the normal bundle. We often use them instead of μ, ν, \dots to denote projection onto the normal bundle. Note that even if d is odd, and hence the ambient CFT has no Weyl anomaly, the defect Weyl anomaly in eq. (3.4.38) still exists.

Like their CFT counterparts, the defect/boundary central charges should appear in a number of observables, besides $T^\mu{}_\mu$ itself. We will review what is known to date. The central charge $a_\Sigma^{(2d)}$ appears in the free energy of a spherical defect. Consider a defect supported on an equatorial $S^2 \hookrightarrow S^d$, and let L be the radius of the sphere. For a CFT on a round S^{2k} , the free energy has a log divergence proportional to the integrated Weyl anomaly \mathcal{A} . From eq. (3.4.38), it is clear that only the A-type anomalies of the ambient CFT and the defect contribute. In particular, S^{2k} is conformally flat, and so its Weyl tensor vanishes. This implies that all the ambient B-type anomalies vanish, and further $W_{ab}{}^{ab} = 0$. The second fundamental form for $S^2 \hookrightarrow S^{2k}$ is pure trace, so $\mathring{\Pi}_{ab}^\mu = 0$

as well. The Ricci eq. (3.3.34) can be rewritten in terms of the Weyl tensor, the traceless second fundamental form and the normal bundle curvature, implying that when $q = 2$ all the parity-odd terms vanish, too. Denoting the partition functions with and without defect by Z^{DCFT} and Z^{CFT} , respectively, one finds

$$F^{\text{def}}|_{\log \frac{\ell}{\epsilon}} \equiv (-\log Z^{\text{DCFT}} + \log Z^{\text{CFT}})|_{\log \frac{\ell}{\epsilon}} = -\frac{a_{\Sigma}^{(2d)}}{3}. \quad (3.4.39)$$

The central charge $d_1^{(2d)}$ controls \mathcal{D}^i 's two-point function in flat space. For example, for a flat defect in \mathbb{R}^4 [162, 163],

$$\langle \mathcal{D}^i(x_{\parallel}) \mathcal{D}^j(0) \rangle = \frac{4}{3\pi^2} \frac{d_1^{(2d)}}{|x_{\parallel}|^6}. \quad (3.4.40)$$

This can be seen from the fact that $\Pi^\mu \sim \partial_a \partial_b X^\mu$ close to flat space, and varying \mathcal{W} with respect to X^μ inserts the displacement operator into correlation functions. We will make this argument precise in section 6.2.1.1. Reflection positivity then requires $d_1^{(2d)} \geq 0$. When $q > 1$, the central charge $d_2^{(2d)}$ controls $T^{\mu\nu}$'s one-point function eq. (3.1.13). As shown in refs. [50, 162, 163], the coefficient h is determined by $d_2^{(2d)}$,

$$h = -\frac{1}{6\pi(d-1)\text{vol}(S^{d-3})} d_2^{(2d)}, \quad (3.4.41)$$

where $\text{vol}(S^d)$ is the volume of a unit d -sphere. Heuristically, $W^{ab}{}_{ab} \sim \partial^2 g$, and taking a variation of \mathcal{W} with respect to $g_{\mu\nu}$ computes the one-point function of the stress tensor. This argument will be made precise in section 6.2.2.1. If we Wick-rotate to Minkowski space, then the average null energy condition (ANEC) states

$$\int_{-\infty}^{\infty} du \langle T_{\mu\nu} \rangle v^\mu v^\nu \geq 0, \quad (3.4.42)$$

where v^μ is a null vector in $\mathbb{R}^{1,d-1}$ with affine parameter u . If the ANEC holds in the presence of a defect, then $d_2^{(2d)} \leq 0$ [50].¹¹ To show this, consider a null ray skew to the defect and parametrised by

$$t = \ell u, \quad x^1 = \ell u \cos \psi, \quad x^2 = \ell u \sin \psi, \quad x^3 = \ell, \quad x^4 = \dots = x^{d-1} = 0, \quad (3.4.43)$$

where the defect is extended along t and x^1 , ℓ is the shortest distance between the defect and the null ray, and ψ is the angle between them. See figure 3.1 for an illustration of the set-up. By plugging eq. (3.4.43) and eq. (3.1.13) into the ANEC and

¹¹The proofs of the ANEC in refs. [164–166] have not yet been extended to include defects. Nevertheless, in unitary DCFTs we expect the ANEC to hold for defects, because physically a defect should not change the fact that the total energy measured by a null observer should be non-negative.

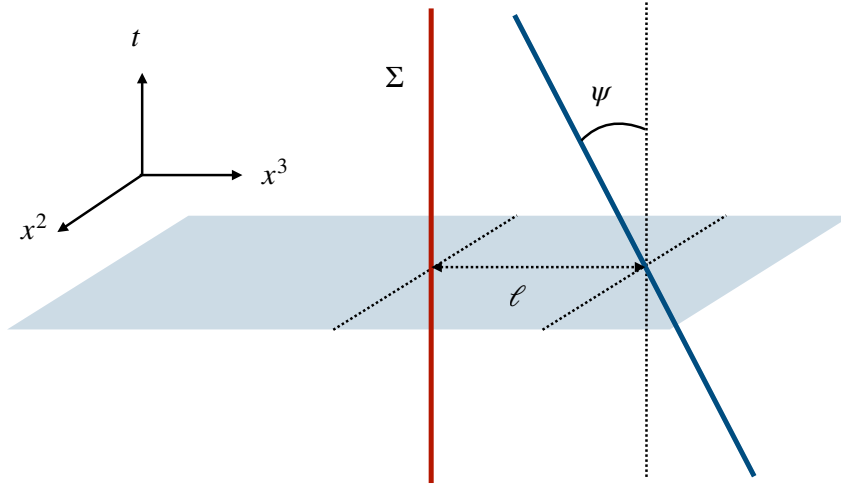


FIGURE 3.1: Configuration for the null geodesic v^μ described in eq. (3.4.43). The null geodesic (blue) passes by the defect (red, labelled Σ) at an angle ψ in the $x^1 - x^2$ plane and at a distance ℓ away in the x^3 direction.

using eq. (3.4.41), we obtain

$$\int_{-\infty}^{\infty} du \langle T_{\mu\nu} \rangle v^\mu v^\nu = -d_2^{(2d)} \frac{|\sin \psi| \Gamma\left(\frac{d-1}{2}\right)}{6\sqrt{\pi} \ell^d \text{vol}(S^{d-3}) \Gamma\left(\frac{d}{2}\right)} \geq 0. \quad (3.4.44)$$

Since the fraction is strictly positive, $d_2^{(2d)} \leq 0$.

The A-type defect central charge, $a_\Sigma^{(2d)}$, shares a few key features with the $d = 2$ CFT central charge, $c^{(2d)}$. For instance, under a defect RG flow, $a_\Sigma^{(2d)}$ obeys a c-theorem: $a_{\Sigma,UV}^{(2d)} \geq a_{\Sigma,IR}^{(2d)}$ [55]. This is a direct generalisation of the proof of the weak c-theorem in 2d CFT by ref. [34], which does not rely on a conserved stress tensor. By the same argument as in section 2.5, WZ consistency implies that $a_\Sigma^{(2d)}$ is independent of *defect* marginal couplings. However, the similarities seem to end there. For example, $a_\Sigma^{(2d)}$ can depend on marginal couplings of the *ambient* CFT [167–169]. The argument is evaded due to a scale anomaly in the one-point functions of marginal bulk operators as $|x_\perp| \rightarrow 0$. The one-point functions can depend on marginal couplings, and they diverge as the operator approaches the defect. This requires regularisation and introduction of a scale. As a result, the Weyl anomaly picks up contributions dependent on the bulk marginal couplings. WZ consistency of the full anomaly then requires that also all the defect central charges depend on these bulk marginal couplings, including the A-type anomaly. Unlike $c^{(2d)}$, $a_\Sigma^{(2d)}$ is not necessarily positive semi-definite, even in reflection-positive theories. In particular, a free, massless scalar with Dirichlet boundary conditions in $d = 3$ has $a_\Sigma^{(2d)} < 0$ [48, 55, 170]. This raises the question of in what sense $a_\Sigma^{(2d)}$ is counting defect/boundary DOF. More generally, what bounds $a_\Sigma^{(2d)}$ obeys, if any, remains an open question.

The Weyl anomaly of the $p = 3$ boundary in a $d = 4$ CFT is [51,52]

$$T^\mu{}_\mu|_{\Sigma_3} = \frac{1}{16\pi^2} \left(a_{\mathcal{M}}^{(4d)} E_4|_{\partial\mathcal{M}} + b_1^{(3d)} \overset{\circ}{K}^3 + b_2^{(3d)} \overset{\circ}{K}^{ab} W^c{}_{acb} \right). \quad (3.4.45)$$

As anticipated below eq. (3.4.37), the first term in the parentheses in eq. (3.4.45) is the Chern-Simons (CS)-like boundary term of the bulk A-type anomaly,

$$E_4|_{\partial\mathcal{M}} = \delta_{def}^{abc} \left(2K^d{}_a R^{ef}{}_{bc} + \frac{8}{3} K^d{}_a K^e{}_b K^f{}_c \right), \quad (3.4.46)$$

with a coefficient determined entirely by the ambient CFT's A-type central charge, $a_{\mathcal{M}}^{(4d)}$. It is required by WZ consistency of the ambient CFT's Weyl anomaly in the presence of the boundary. The boundary thus has only two new central charges, $b_1^{(3d)}$ and $b_2^{(3d)}$, which are both B-type and parity odd in the normal bundle. In free field CFTs, $b_2^{(3d)}$ is fixed in terms of the ambient CFT's B-type central charge, $c^{(4d)}$, specifically, $b_2^{(3d)} = -8c^{(4d)}$, independent of the boundary conditions [171–173]. However, ref. [53] showed that the same is not true in interacting CFTs. The other boundary central charge, $b_1^{(3d)}$, does depend on boundary conditions, even for free fields [174, 175].

Similarly to the $p = 2$ defect/boundary, the B-type central charges $b_1^{(3d)}$ and $b_2^{(3d)}$ determine correlation functions of the boundary displacement operator, \mathcal{D} . In particular, $b_2^{(3d)}$ controls \mathcal{D} 's two-point function for a flat defect in flat space [52, 53]:

$$\langle \mathcal{D}(x_{\parallel}) \mathcal{D}(0) \rangle = -\frac{15}{2\pi^4} \frac{b_2^{(3d)}}{|x_{\parallel}|^8}. \quad (3.4.47)$$

Reflection positivity then requires $b_2^{(3d)} \leq 0$. Further, $b_1^{(3d)}$ controls \mathcal{D} 's three-point function [52]:

$$\langle \mathcal{D}(x_{\parallel}) \mathcal{D}(y_{\parallel}) \mathcal{D}(0) \rangle = -\frac{35}{2\pi^6} \frac{b_1^{(3d)}}{|x_{\parallel}|^4 |y_{\parallel}|^4 |x_{\parallel} - y_{\parallel}|^4}. \quad (3.4.48)$$

Chapter 4

Entanglement Entropy

In this chapter, we review the role of entanglement entropy (EE) in QFT and CFT. As we will see, EE is an immensely useful tool, and e.g. provides a way to prove c-theorems. We will take a pedestrian approach inspired by refs. [92, 176]. Excellent modern reviews with a more algebraic treatment are [177, 178].

4.1 Entanglement in finite quantum systems

Given a quantum mechanical system in a pure state $|\Psi\rangle$ in the Hilbert space \mathcal{H} , we can construct its density matrix

$$\rho = |\Psi\rangle\langle\Psi|. \quad (4.1.1)$$

If $\langle\Psi|\Psi\rangle = 1$, then $\text{Tr}\rho = 1$. Suppose the Hilbert space admits a factorisation, $\mathcal{H} = \mathcal{H}_A \otimes \mathcal{H}_B$, where A and $B = \bar{A}$ are complementary subsystems. Using the Schmitt decomposition theorem, one can write

$$|\Psi\rangle = \sum_{k=1}^m \sqrt{p_k} |\psi_k\rangle_A \otimes |\psi_k\rangle_B, \quad (4.1.2)$$

where $p_k \in \mathbb{R}^+$ satisfying $\sum_k p_k = 1$, the states $|\psi_k\rangle_{A,B}$ are orthonormal, and $m = \min(\dim \mathcal{H}_A, \dim \mathcal{H}_B)$. By tracing over \mathcal{H}_B , one defines a reduced density matrix

$$\rho_A = \text{Tr}_B \rho = \sum_{|\psi\rangle_B \in \mathcal{H}_B} {}_B\langle\psi|\rho|\psi\rangle_B, \quad (4.1.3)$$

such that $\text{Tr}_A \rho_A = 1$, and similarly for ρ_B . Note that ρ_A is generically not a pure state on A . The reduced density matrices ρ_A can be used to compute correlation functions of operators of the subsystem A , i.e. $\mathcal{O} = \mathcal{O}_A \otimes \mathbb{1}_B$. E.g. $\langle\mathcal{O}\rangle = \text{Tr}\rho\mathcal{O} = \text{Tr}_A \rho_A \mathcal{O}_A$.

The EE measures the entanglement between A and its complement. It is defined as the von Neumann entropy of the reduced density matrix ρ_A

$$S_A = -\text{Tr}_A \rho_A \log \rho_A, \quad (4.1.4)$$

where \log denotes the matrix logarithm. The von Neumann entropy vanishes if and only if the state is pure. Since ρ_A is generically mixed, the EE $S_A \neq 0$. If ρ is a pure state, then $S_A = S_B$. The EE is bounded from above, $S_A \leq \log m$.

A simple example in quantum mechanics (QM) is a system of two spins $|s_1\rangle_A \otimes |s_2\rangle_B$, where the spins $s_{1,2}$ can be either up or down, denoted 0 and 1. The Hilbert spaces have dimension $\dim \mathcal{H}_A = \dim \mathcal{H}_B = 2$. Consider the four Bell states

$$|\Psi_{\pm}\rangle = \frac{1}{\sqrt{2}} (|0\rangle_A |0\rangle_B \pm |1\rangle_A |1\rangle_B), \quad (4.1.5)$$

$$|\Phi_{\pm}\rangle = \frac{1}{\sqrt{2}} (|0\rangle_A |1\rangle_B \pm |1\rangle_A |0\rangle_B). \quad (4.1.6)$$

The reduced density matrix for each state is

$$\rho_A = \frac{1}{2} (|0\rangle_{AA} \langle 0| + |1\rangle_{AA} \langle 1|). \quad (4.1.7)$$

Matrix logarithms are typically hard to compute. Luckily, the reduced density matrix is diagonal, and thus $S_A = \log 2$ for each state. The Bell pairs saturate the bound $S_A \leq m = 2$, and are said to be maximally entangled.

For more complicated states in more complex quantum systems, it is useful to compute the EE via their Rényi entropies

$$S_n(A) = \frac{1}{1-n} \log \text{Tr}_A \rho_A^n, \quad (4.1.8)$$

where the integer n is often called the replica number. The Rényi entropies are easier to compute than the EE as they do not contain a matrix logarithm. Assuming one can analytically continue n , one finds that the $n \rightarrow 1$ limit reduces to the EE

$$\lim_{n \rightarrow 1} S_n(A) = -\lim_{n \rightarrow 1} \frac{\partial}{\partial n} \log \text{Tr}_A \rho_A^n = S_A. \quad (4.1.9)$$

For the Bell pairs, $S_n(A) = \frac{1}{1-n} \log(2^{-n} \text{Tr}_A \mathbb{1}_A) = \log 2$ for all integer $n > 1$.

Analytically continuing and taking the $n \rightarrow 1$ limit becomes trivial, and we recover S_A .

4.2 Entanglement in QFT

The Bell states can be thought of as states of a spin chain with two sites. The partition into subsystems A and B then corresponds to chopping the chain in two. In more general lattice models, this is a natural way to partition a system: given a spatial slice with an associated Hilbert space, separate the lattice sites by introducing a co-dimension 1 surface. The sites enclosed by the surface form subsystem A . In the full lattice model including the (possibly Euclidean) time direction, this is a co-dimension 2 surface. It is often called the entangling surface. Taking the continuum limit, one defines EE entropy in QFT geometrically in this way.¹

Consider a quantum field $\phi(x)$, where $x^\mu = (\tau, \vec{x})$ are coordinates on spacetime \mathcal{M}_d , which we take to be flat for the moment. A spatial slice at time $\tau = 0$ has an associated Hilbert space. Let $|\Psi\rangle$ be a pure state in this Hilbert space. We can define the density matrix of $|\Psi\rangle$ as in eq. (4.1.1). The QFT analogue of a quantum mechanical wavefunction is the wavefunctional of field configurations at $\tau = 0$, $\Psi[\phi(\vec{x})] = \langle \phi(\vec{x}) | \Psi \rangle$. Consider a formal basis of field configurations at $\tau = 0$ labelled by the indices R, S . E.g. $\phi_R(\vec{x})$ is a basis vector. Formally, ρ can be thought of as a linear map on the space of field configurations, with matrix elements

$$\rho_{RS} = \langle \phi_R(\vec{x}) | \rho | \phi_S(\vec{x}) \rangle = \Psi^*[\phi_R(\vec{x})] \Psi[\phi_S(\vec{x})]. \quad (4.2.10)$$

If $|\Psi\rangle$ is the vacuum, the wavefunctionals can be computed by performing the following path integral over half of spacetime

$$\Psi[\phi_S] = \frac{1}{\sqrt{Z}} \int_{\phi(0^-, \vec{x}) = \phi_S(\vec{x})} \mathcal{D}\phi(x) \exp\left(-\int_{-\infty}^{0^-} d\tau \int d^{d-1}\vec{x} \mathcal{L}[\phi, \partial\phi]\right), \quad (4.2.11)$$

where \mathcal{L} is the QFT Lagrangian, and Z is the partition function. Note that the field configuration $\phi_S(\vec{x})$ at $\tau = 0^-$ becomes a boundary condition in the integration. Intuitively, this path integral computes the transition amplitude from the vacuum in the far past to a reference state $\phi_S(\vec{x})$ at $\tau = 0^-$. The wavefunctional $\Psi^*[\phi_R]$ can be computed by performing a similar path integral on the other half of spacetime.

One can obtain the reduced density matrix ρ_A on a subregion of space A by fixing boundary conditions at $\tau = 0^-$ and $\tau = 0^+$ that only have support on A . In the complement, boundary conditions should be identified and integrated over. One can write this path integral in a compact form as an integral over all field configurations

¹As we will see, EE in QFT suffers from short-distance divergences which are state-independent. In our discussion of QM, we assumed that the Hilbert space factorises. In QFT, this is not true, and the UV divergences arise a consequence. They are state-independent because at short distances, every state looks like the vacuum. What does factorise, is the algebra of observables. See e.g. [177, 178] for a modern review. We will ignore these subtleties here.

with delta functions imposing the boundary conditions at $\tau = 0^-$ and $\tau = 0^+$,

$$\begin{aligned} \langle \phi_r(\vec{x}_A) | \rho_A | \phi_s(\vec{x}_A) \rangle &= \int \mathcal{D}\phi(x) \delta(\phi(0^+, \vec{x}_A) - \phi_r(\vec{x}_A)) \\ &\quad \times \delta(\phi(0^-, \vec{x}_A) - \phi_s(\vec{x}_A)) \exp\left(-\int_{-\infty}^{+\infty} d\tau \int d^{d-1}\vec{x} \mathcal{L}[\phi, \partial\phi]\right), \end{aligned} \quad (4.2.12)$$

where the delta function constraints are imposed at every point in A , and $\phi_r(\vec{x}_A)$ form a basis of boundary field configurations on A only.

Equipped with the matrix elements of ρ_A , we can now compute the Rényi entropies eq. (4.1.8). Matrix multiplication amounts to identifying the boundary field configurations $\phi_r(\vec{x}_A)$ of adjacent matrices and path integrating over all possible configurations. $\text{Tr}\rho_A^n$ can then be written as a single path integral on the n -sheeted cover of spacetime $\mathcal{M}_d^{(n)}$, where the spatial region ($\tau = 0^+, \vec{x}_A$) on one sheet is identified with the spatial region ($\tau = 0^-, \vec{x}_A$) of the next sheet. See figure 4.1 for a pictorial representation of the reduced density matrix and the n -sheeted cover. We denote this path integral by Z_n such that

$$\text{Tr}\rho_A^n = \frac{Z_n}{Z^n}, \quad (4.2.13)$$

where the denominator ensures that the path integral is unit normalised. The n -sheeted and appropriately glued cover of spacetime has a conical singularity around the $(d-2)$ -dimensional surface $\Sigma_{d-2} = \partial A$, called the entangling surface or twist defect, with conical deficit angle $2\pi(1-n)$. We then obtain the EE via eq. (4.1.9),

$$S_A^{\text{QFT}} = \lim_{n \rightarrow 1} \frac{\partial}{\partial n} (\mathcal{W}_n - n\mathcal{W}), \quad (4.2.14)$$

where $\mathcal{W}_n = -\log Z_n$, and \mathcal{W} is the ordinary effective action. This procedure is called the replica trick [27, 28].

4.3 Entanglement in free QFTs and the heat kernel

The replica trick eq. (4.2.14) instructs us to compute the full path integral on \mathcal{M}_d and $\mathcal{M}_d^{(n)}$ in order to determine the EE. For interacting QFTs, this is often out of reach. In free CFTs, however, the path integral reduces to a functional determinant of the kinetic operator Δ ,

$$\mathcal{W} = \frac{1}{2} \log \det' \Delta, \quad (4.3.15)$$

where the $'$ indicates that zero eigenvalues are omitted. It is useful to write this determinant in terms of the heat kernel, see ref. [179] for a detailed review. The heat

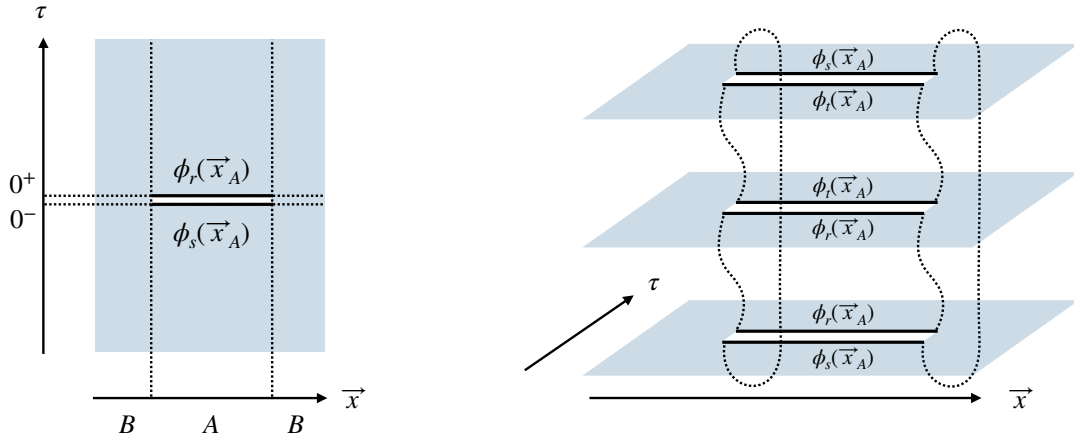


FIGURE 4.1: *Left:* Illustration of the path integral representation of the matrix elements of the reduced density matrix ρ_A . The path integral is evaluated over the blue region with boundary conditions $\phi_s(\vec{x}_A)$ and $\phi_r(\vec{x}_A)$ at $\tau = 0^-$ and $\tau = 0^+$, respectively, which are only supported on the spatial region A . *Right:* Illustration of the replica trick. The Rényi entropy $S_n(A)$ is mapped to the path integral over the n -sheeted cover of spacetime, with sheets glued together along the cuts as indicated by dashed lines. Repeated subscripts on ϕ on adjacent cuts indicate that the boundary conditions are identified and integrated over in the path integral, thus effecting matrix multiplication of ρ_A .

kernel of Δ with eigenvalues λ_n is defined as

$$K(s; \Delta) = e^{-s\Delta}. \quad (4.3.16)$$

If Δ is the Laplacian $-D^2$, then the heat kernel in position space,

$$K(s; x, y; \Delta) = \langle x | K(s; \Delta) | y \rangle, \quad (4.3.17)$$

satisfies the following differential equation and initial condition

$$\left(\partial_s - D_{(x)}^2 \right) K(s; x, y; \Delta) = 0, \quad (4.3.18a)$$

$$K(0; x, y; \Delta) = \delta^{(d)}(x, y). \quad (4.3.18b)$$

This is the heat equation, which lends the heat kernel its name. Notice that these equations imply that the Green's function of Δ , i.e. the propagator $G(x, y)$, obeying

$$\Delta^{(x)} G(x, y) = \delta^{(d)}(x, y), \quad (4.3.19)$$

can be written as

$$G(x, y) = \int_0^\infty ds K(s; x, y, \Delta). \quad (4.3.20)$$

Therefore, if one is given a propagator, one can deduce the heat kernel by performing a spectral decomposition.

To relate the functional determinant of Δ to the heat kernel, we introduce the zeta-function

$$\mathfrak{Z}_\Delta(t) = \sum_n' \lambda_n^{-t}, \quad (4.3.21)$$

where the prime means that the sum is only taken over strictly positive eigenvalues λ_n . This sum is convergent for $t > t^* \in \mathbb{R}$. Taking a derivative with respect to t gives

$$\mathfrak{Z}'_\Delta(t) = \sum_n' \lambda_n^{-t} \log \lambda_n. \quad (4.3.22)$$

To regularise the functional determinant, we analytically continue $\mathfrak{Z}_\Delta(t)$ to the complex t -plane. The functional determinant of Δ is then defined in terms of the analytic continuation to the origin:

$$\det' \Delta = \prod_{n=0}^{\infty} \lambda_n = \exp(-\mathfrak{Z}'_\Delta(0)), \quad (4.3.23)$$

where the product is over non-zero eigenvalues, as indicated by the prime. This is called zeta-function regularisation.

The zeta-function is the Mellin transform of the trace of the heat kernel,²

$$\mathfrak{Z}_\Delta(t) = \frac{1}{\Gamma(t)} \int_0^\infty ds s^{t-1} (\text{Tr}K(s; \Delta) - n_\Delta^0), \quad (4.3.24)$$

where n_Δ^0 is the number of zero modes of Δ , and

$$\text{Tr}K(s; \Delta) = \sum_n e^{-s\lambda_n} = \int d^d x \sqrt{g} \langle x | K(s; \Delta) | x \rangle. \quad (4.3.25)$$

Differentiating with respect to t and taking $t \rightarrow 0$, one finds

$$\mathcal{W} = \frac{1}{2} \log \det' \Delta = -\frac{1}{2} \mathfrak{Z}'_\Delta(0) = -\frac{1}{2} \int_{\epsilon^2}^\infty \frac{ds}{s} \text{Tr}K(s; \Delta), \quad (4.3.26)$$

where $\epsilon > 0$ is a UV cut-off, and we have subtracted the zero modes of the Laplacian to IR regulate the integral.³

To compute the EE via eq. (4.2.14), one also needs the form of the heat kernel on a space with conical singularity. This is related to the heat kernel in the absence of conical singularities via the Sommerfeld formula [181, 182]. Consider polar coordinates around the entangling surface, writing $\tau = r \sin \phi$ and $x^1 = r \cos \phi$ with $0 \leq \phi \leq 2\pi$. In this coordinate system the conical singularity is introduced by making

²The following integral identity is useful:

$$\lambda^{-t} = \frac{1}{\Gamma(t)} \int_0^\infty ds s^{t-1} e^{-s\lambda}.$$

³For a careful treatment of UV and IR divergences in simple examples, see e.g. [180].

ϕ periodic with period $2\pi n$. The heat kernel in the presence of such a conical singularity is

$$K_n(s; \phi, \phi'; \Delta) = K(s; \phi - \phi'; \Delta) + \frac{i}{4\pi n} \int_{\Gamma} d\omega \cot\left(\frac{\omega}{2n}\right) K(s; \phi - \phi' + \omega; \Delta), \quad (4.3.27)$$

where the contour Γ is given by two vertical lines going from $(-\pi + i\infty)$ to $(-\pi - i\infty)$ and from $(\pi - i\infty)$ to $(\pi + i\infty)$. It intersects the real axis twice between the poles of $\cot \omega / (2n)$, once between $-2\pi n$ and 0 , and once between 0 and $2\pi n$. As $n \rightarrow 1$, the integral is $\mathcal{O}(1 - n)$. Substituting eq. (4.3.27) into eq. (4.2.14) using the representation eq. (4.3.26), one can explicitly compute the EE. We will present two examples in chapter 7.

4.4 Entanglement in CFT

The EE is bounded by the dimensions of the subsystem Hilbert spaces. However, in QFT, those are infinite, and indeed, the EE is typically divergent. Intuitively, the EE in the vacuum of a QFT arises from virtual Bell pairs that are produced near the $(d - 2)$ -dimensional entangling surface Σ , with one spin on either side of Σ . Thus, one expects the EE to grow with the $(d - 2)$ -dimensional volume of Σ_{d-2} . In a CFT on flat space, there are no other dimensionful constants, and so one expects that the leading UV divergence of $S_A^{\text{CFT}} \sim \epsilon^{2-d}$ as the short-distance cut-off $\epsilon \rightarrow 0$ [183, 184].⁴

We have expressed eq. (4.2.14) in terms of the effective action \mathcal{W} whose UV divergent structure is given in eq. (2.5.53). The leading divergence comes from a term proportional to the volume of spacetime, $\int_{\mathcal{M}_d} d^d x \sqrt{g} \epsilon^{-d}$, where we are allowing for a non-trivial metric background. Since

$$\int_{\mathcal{M}_d^{(n)}} d^d x \sqrt{g} = n \int_{\mathcal{M}_d} d^d x \sqrt{g}, \quad (4.4.28)$$

the terms diverging as $\sim \epsilon^{-d}$ in \mathcal{W}_n and $n\mathcal{W}$ cancel. The same argument does not apply to the subleading divergences involving integrals of curvatures. These do not cancel as we will see. Thus, the leading UV divergence of S_A^{CFT} in a CFT is $\sim \epsilon^{2-d}$, as expected.

In even d , the coefficient of the log term in \mathcal{W} is the Weyl anomaly. Thus, the logarithmic part of the EE must be related to the CFT's central charges. Consider a rescaling of the characteristic length scale L of the entangling surface Σ_{d-2} . This is

⁴When $d = 4$, the volume of Σ_{d-2} is two-dimensional. For this reason the leading divergence of the EE is often called an area law, even in general d .

equivalent to performing a Weyl transformation eq. (2.4.29). Thus, the EE changes as

$$L \frac{\partial}{\partial L} S_A^{\text{CFT}} = \lim_{n \rightarrow 1} \frac{\partial}{\partial n} \left(\int_{\mathcal{M}_d^{(n)}} d^d x \sqrt{g} \langle T^\mu{}_\mu \rangle - n \int_{\mathcal{M}_d} d^d x \sqrt{g} \langle T^\mu{}_\mu \rangle \right). \quad (4.4.29)$$

Away from the conical singularity, the two expressions cancel against each other. The only contributions must be coming from the region near the tip, i.e. the entangling surface Σ_{d-2} . By regularising the conical singularity, ref. [30] showed that as $n \rightarrow 1$,

$$\int_{\mathcal{M}_d^{(n)}} d^d x \sqrt{g} \tilde{R}^{(k)} - n \int_{\mathcal{M}_d} d^d x \sqrt{g} \tilde{R}^{(k)} \sim (1-n) \int_{\Sigma_{d-2}} d^{d-2} \sigma \sqrt{\bar{g}} \widetilde{R^{(\ell)} \Pi^{(m)}} \quad (4.4.30)$$

to leading order in $(1-n)$, where $\widetilde{R^{(\ell)} \Pi^{(m)}}$ is linear combination of scalars built out of ℓ curvature tensors and m second fundamental forms Π_{ab}^μ with $2\ell + m = 2k - 2$.

The replica trick with this regularisation can then be used to compute the EE between an interval and its complement in a 2d CFT. In 2d, the Weyl anomaly eq. (2.5.48) only depends on the 2d Ricci scalar R , for which

$$\int_{\mathcal{M}_2^{(n)}} d^2 x \sqrt{g} R - n \int_{\mathcal{M}_2} d^2 x \sqrt{g} R = 4\pi(1-n). \quad (4.4.31)$$

Taking $\lim_{n \rightarrow 1} \frac{\partial}{\partial n}$, one finds that

$$L \frac{\partial}{\partial L} S_A^{\text{CFT}} = \frac{c^{(2d)}}{3}, \quad (4.4.32)$$

where the extra factor of 2 comes from the fact that there are two conical defects in 2d, one at each end point of the interval. Integrating, one finds

$$S_A^{\text{CFT}} = \frac{c^{(2d)}}{3} \log \left(\frac{L}{\epsilon} \right) + \dots, \quad (4.4.33)$$

where ϵ is a UV cut-off and the ellipsis stands for scheme-dependent terms [27, 28].

This relation allows for an alternative proof of the c-theorem. Indeed, ref. [33] found a c-function related to S_A^{CFT} and showed that it monotonically decreases along an RG flow using quantum information techniques.

In 2d, there exists a conformal map from the plane to the infinite cylinder whose base has circumference β . Thus one would expect that the EE is related to the thermodynamic entropy defined in eq. (2.5.62). This indeed turns out to be the case. Consider an interval of length L extended along the axis of the cylinder. Applying the replica trick, one finds an EE on the cylinder that interpolates between the flat space result for the EE eq. (4.4.33) for $\beta \gg L$ and the thermodynamic entropy eq. (2.5.62) for $\beta \ll L$, where L is identified with the size of the system [28].

Now consider EE in 4d CFT. Ref. [30] found for the 4d Euler density E_4 ,

$$\int_{\mathcal{M}_4^{(n)}} d^4x \sqrt{\bar{g}} E_4 - n \int_{\mathcal{M}_4} d^4x \sqrt{\bar{g}} E_4 = 8\pi(1-n) \int_{\Sigma_2} d^2\sigma \sqrt{\bar{g}} \bar{R} + \mathcal{O}(1-n)^2, \quad (4.4.34)$$

and for the (Weyl)² term

$$\begin{aligned} & \int_{\mathcal{M}_4^{(n)}} d^4x \sqrt{\bar{g}} W_{\mu\nu\rho\sigma} W^{\mu\nu\rho\sigma} - n \int_{\mathcal{M}_4} d^4x \sqrt{\bar{g}} W_{\mu\nu\rho\sigma} W^{\mu\nu\rho\sigma} \\ &= 8\pi(1-n) \int_{\Sigma_2} d^2\sigma \sqrt{\bar{g}} \left(W_{ab}{}^{ab} + \mathring{\Pi}_{ab}{}^\mu \mathring{\Pi}_\mu{}^{ab} \right) + \mathcal{O}(1-n)^2. \end{aligned} \quad (4.4.35)$$

For the Pontryagin density, the appropriate computation was performed in [160],

$$\begin{aligned} & \int_{\mathcal{M}_4^{(n)}} d^4x \sqrt{\bar{g}} \epsilon^{\mu\nu\rho\sigma} R_{\mu\nu\lambda\kappa} R_{\rho\sigma}{}^{\lambda\kappa} - n \int_{\mathcal{M}_4} d^4x \sqrt{\bar{g}} \epsilon^{\mu\nu\rho\sigma} R_{\mu\nu\lambda\kappa} R_{\rho\sigma}{}^{\lambda\kappa} \\ &= \pi(1-n) \int_{\Sigma_2} d^2\sigma \sqrt{\bar{g}} \epsilon^{ab} n^{ij} (R^\perp)_{ijab} + \mathcal{O}(1-n)^2. \end{aligned} \quad (4.4.36)$$

These are precisely the terms that appeared in the contribution of a 2d conformal defect to the Weyl anomaly in eq. (3.4.38). The coefficient of the log term in the EE takes the form of the integrated Weyl anomaly of a co-dimension 2 defect, with coefficients fixed in terms of *bulk* central charges. Indeed, in 4d the coefficient of the logarithm is [29]⁵

$$S_A^{\text{CFT}} \Big|_{\log \frac{1}{\epsilon}} = \int_{\Sigma_2} d^2\sigma \sqrt{\bar{g}} \left[\frac{a^{(4d)}}{2\pi} \bar{R} - \frac{c^{(4d)}}{2\pi} \left(W_{ab}{}^{ab} + \mathring{\Pi}_{ab}{}^\mu \mathring{\Pi}_\mu{}^{ab} \right) + \frac{4\tilde{c}^{(4d)}}{\pi} \epsilon^{ab} n^{ij} (R^\perp)_{ijab} \right], \quad (4.4.37)$$

In particular, if the ambient geometry is conformally flat and Σ is a round sphere, then the only contribution comes from the Euler density. For a 2-sphere, $\chi = \frac{1}{4\pi} \int_{S^2} \bar{R} = 2$, and thus the universal part of the EE is $S_A^{\text{CFT}} \Big|_{\log \frac{1}{\epsilon}} = 4a_{\mathcal{M}}^{(4d)}$.

In $d = 6$, however, the relation between the universal part of the EE and the $p = 4$ defect Weyl anomaly is less understood, partly because the general form of the Weyl anomaly was unknown until recently. The EE has only been determined in special cases: an entangling surface Σ_4 without extrinsic curvature [131] or with only extrinsic curvature, i.e. a curved Σ_4 in flat space [132]. Our result of the $p = 4$ defect Weyl anomaly in section 6.1 allows for determination of the EE in a $d = 6$ standalone CFT with Σ_4 of arbitrary shape.

⁵It is clear from the effective action that UV divergences of EE must be of order $\sim \epsilon^{2k-d}$ for integer $0 \leq k \leq \lfloor \frac{d}{2} \rfloor$. Naively, however, one would expect that divergences could appear in integer steps, since local counter-terms on the entangling surface could take the form $\int_{\Sigma_{d-2}} \partial^{(i)} R^{(j)} \Pi^{(k)}$. The integrand has mass dimension $i + 2j + k$, which can be odd. However, the EE of region A must be equal to the EE of region $B = \bar{A}$. In both cases Σ_{d-2} is the same but it must have opposite orientation. This implies that the second fundamental forms have opposite sign, and therefore, the coefficient of a term with an odd number of Π 's must be zero.

Finally, let us comment briefly on the relation of EE with two other physical quantities: Firstly, when d is odd, the EE has no logarithmic term. In particular, if $\mathcal{M}_d = S^d$, the renormalised sphere free energy F in eq. (2.5.53) is identified with the constant term in the EE, which is now universal. As mentioned in section 2.5, F was conjectured to be monotonic under RG flows. By employing the relation between F and EE, and using quantum information techniques, ref. [140] proved a weak form of the F-theorem when $d = 3$. To my knowledge, this EE based argument is the only proof of the 3d F-theorem to date. Secondly, note that a conformal transformation maps Euclidean space to $S^1_\beta \times \mathbb{H}^{d-1}$. The vacuum state of the CFT on \mathbb{R}^d maps to a thermal state on \mathbb{H}^{d-1} at temperature $T = \frac{1}{\beta}$, where β is the circumference of S^1_β . As a result, the EE of a spherical ball in \mathbb{R}^d can be shown to be equal to the thermal entropy on \mathbb{H}^{d-1} [185].

4.5 Entanglement in DCFT

We now turn to the EE in the presence of boundaries and defects. In the case of a 2d CFT on half-space, i.e. with a 1d boundary, ref. [28] computed the EE of an interval of length $\frac{L}{2}$ with one endpoint on the boundary using eq. (4.2.14). The result is

$$S_A^{\text{BCFT}} = \frac{c^{(2d)}}{6} \log \left(\frac{L}{\epsilon} \right) + c' + \mathcal{O}(\epsilon), \quad (4.5.38)$$

where c' is the finite piece. Like in the case of an interval of length L in a CFT without boundary in eq. (4.4.33), the EE again depends on the central charge. The coefficient, however, is half of that in eq. (4.4.33) since the interval in the BCFT case only has one endpoint in the bulk. In eq. (4.4.33), we omitted the finite piece as we argued that it is scheme-dependent. In the BCFT case, however, the finite piece *does* contain physical information. Assuming that S_A^{BCFT} and eq. (4.4.33) are computed in the same scheme, then the scheme-dependence and the logarithmic divergence cancel,

$$S^{\text{bdy}} \equiv S_A^{\text{BCFT}} - \frac{1}{2} S_A^{\text{CFT}} = \log g. \quad (4.5.39)$$

The finite piece, $\log g$, is commonly called the boundary entropy. By construction, it only depends on boundary DOF. In 2d, one can conformally map a CFT on half-space to the semi-infinite cylinder where the radial direction has circumference β .

Computing the EE of an interval of length $\frac{L}{2}$ along the axis and anchored on the boundary, ref. [28] found an expression interpolating between the flat space EE eq. (4.5.38) as $\beta \gg L$ and the thermodynamic entropy eq. (2.5.62) as $\beta \ll L$, with the replacement $L \rightarrow \frac{L}{2}$. Ref. [186] argued that the thermal entropy of a 2d CFT with boundary has a finite piece that is independent of the size of the system. Let $Z[S^1_\beta \times I]$ be the thermal partition function on a finite interval I of length $\frac{L}{2}$. Then the thermal

entropy has a physical finite piece,

$$S_{\text{thermo}} = \left(1 - \beta \frac{\partial}{\partial \beta}\right) \log Z = \frac{c^{(2d)} \pi L}{6 \beta} + \log g. \quad (4.5.40)$$

If one of the two boundary states is the vacuum, then $\log g$ only depends on the non-trivial boundary condition at the other end. In that case $\log g$ can be identified with the right-hand side of eq. (4.5.39).

Ref. [186] conjectured that $\log g$ decreases under boundary RG flows, $\log g_{\text{UV}} \geq \log g_{\text{IR}}$. A non-perturbative proof of the conjecture was given in ref. [187]. The authors showed that $\log g$, defined through the thermal entropy, actually decreases monotonically,

$$\mu \frac{\partial}{\partial \mu} \log g \leq 0, \quad (4.5.41)$$

where μ is the RG scale. This is called the g -theorem, in analogy to the c -theorem for the 2d central charge $c^{(2d)}$. An entropic version of the g -theorem was proved in [188] using quantum information techniques. There the authors show that $\log g$, defined through the EE, decreases monotonically along the boundary RG flow. Note that the two proofs are logically independent: they prove monotonicity theorems for different quantities, which only agree at the fixed points.

Conformal interfaces in 2d CFT can be mapped to the boundary case above using the folding trick [189, 190]. A conformal interface between CFT_1 and CFT_2 is equivalent to $\text{CFT}_1 \otimes \text{CFT}_2$ on half-space joined together at the boundary, with the orientation of one of the CFTs reversed. The discussion also applies to line defects in 2d CFTs without boundaries. An interval with one endpoint on the defect has the form eq. (4.5.38). If both endpoints are in the CFT, then the logarithmic part has an extra factor of 2.

For line defects in higher-dimensional CFTs, ref. [191] argued that $S^{\text{def}} \equiv S_A^{\text{DCFT}} - S_A^{\text{CFT}}$ for a spherical ball A receives an additional term from the stress tensor one-point function eq. (3.1.13). As a result, the defect contribution to the EE is no longer required to decrease along a defect RG flow, see e.g. ref. [49] for an example. However, one can still define an analogue of the thermodynamic defect entropy. In a $d \geq 3$ CFT, one can conformally map \mathbb{R}^d to the cylinder $\mathbb{R} \times S^{d-1}$, where the sphere has radius R and the defect is located at the equator. Ref. [192] showed that the quantity

$$\left(1 - R \frac{\partial}{\partial R}\right) (\log Z^{\text{DCFT}} - \log Z^{\text{CFT}}), \quad (4.5.42)$$

decreases monotonically under a defect RG flow, where Z^{DCFT} and Z^{CFT} are the partition functions with and without defect insertion, respectively. Note that this quantity no longer agrees with the defect contribution to the EE, not even at the fixed points.

Next consider a conformal boundary in a 3d CFT. When $d = 3$, the boundary Weyl anomaly in eq. (3.4.38) fully determines the coefficient of the logarithmic divergence of the effective action \mathcal{W} . To compute the EE, one can again use the replica trick eq. (4.2.14). Recall that the only contributions to the EE come from the tip of the conical singularity, which is identified with the entangling surface. If it intersects the boundary, then the EE will pick up logarithmic contributions from the boundary Weyl anomaly. Otherwise, the logarithmic part vanishes. The boundary contribution to the EE was determined in refs. [47, 48] for an arbitrary entangling surface intersecting the boundary. Generically,

$$S_A^{\text{bdy}} \equiv S_A^{\text{BCFT}} - \frac{1}{2} S_A^{\text{CFT}} = \frac{1}{6} \left(N a_{\Sigma}^{(2d)} - d_1^{(2d)} \sum_{k=1}^N f(\alpha_k) \right) \log \left(\frac{L}{\epsilon} \right) + \dots, \quad (4.5.43)$$

where the entangling surface intersects the boundary N times, each time at an angle α_k , and f is a known function. $a_{\Sigma}^{(2d)}$ and $d_1^{(2d)}$ are two of the defect central charges in eq. (3.4.38). For a round half-disk centred on the boundary, this reduces to

$$S_A^{\text{bdy}} = \frac{a_{\Sigma}^{(2d)}}{3} \log \left(\frac{L}{\epsilon} \right) + \dots. \quad (4.5.44)$$

The coefficient of the logarithm defines a function along a boundary RG flow that coincides with $a_{\Sigma}^{(2d)}$ at the fixed points. Using quantum information theory arguments, ref. [56] gave an entropic proof of the c-theorem for $a_{\Sigma}^{(2d)}$, i.e. $a_{\Sigma,UV}^{(2d)} \geq a_{\Sigma,IR}^{(2d)}$ under a boundary RG flow. It is equivalent to the proof of ref. [55] when $d = 3$, which we discussed in section 3.4.

Consider the contribution to the EE of a flat $p = 2$ defect in a CFT on \mathbb{R}^d , where $d \geq 4$ and the entangling region is taken to be a sphere of radius L centred on the defect, see figure 4.2. Ref. [49] argued that the coefficient of the logarithm has two contributions. The first one is related to the defect contribution to the free energy on S^d of radius L with the defect wrapping an equatorial S^2 . The second contribution is proportional to the stress tensor one-point function eq. (3.1.13). Ref. [50] argued that these are in turn related to the defect central charges $a_{\Sigma}^{(2d)}$ and $d_2^{(2d)}$ via eqs. (3.4.39) and (3.4.40), respectively, such that the defect's contribution to the universal part of the EE is

$$S_A^{\text{def}} \Big|_{\log \frac{L}{\epsilon}} \equiv (S_A^{\text{DCFT}} - S_A^{\text{CFT}}) \Big|_{\log \frac{L}{\epsilon}} = \frac{1}{3} \left(a_{\Sigma}^{(2d)} + \frac{d-3}{d-1} d_2^{(2d)} \right). \quad (4.5.45)$$

Again, the universal defect contribution to the EE no longer serves as a good c-function. The appearance of the stress tensor one-point function spoils its monotonicity. Indeed, refs. [49, 193] provides multiple examples where S_A^{def} increases along a defect RG flow. However, F^{def} is always found to decrease, prompting the authors to conjecture that it is a good c-function for any defect and ambient space dimensions. This putative c-theorem reduces to the monotonicity theorems for $\log g$

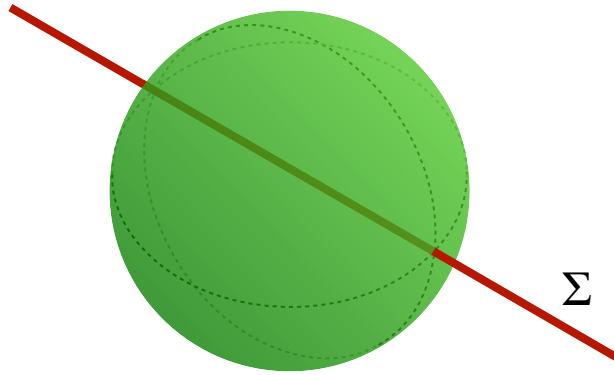


FIGURE 4.2: A spherical entangling surface in $d = 4$ centred on the $p = 2$ defect at time $\tau = 0$. The defect's contribution to the universal EE of the region enclosed is given by eq. (4.5.45).

and $a_{\Sigma}^{(2d)}$ when the defect dimension is $p = 1$ and $p = 2$, respectively. It is the defect version of the generalised F-theorem mentioned in section 2.5.⁶

More generally, ref. [49] argues that the universal part of the EE of a spherical region centred on a defect of any dimension p is related to the universal part of the sphere free energy and the stress tensor one-point function,

$$S_A^{\text{def}}|_{\text{univ.}} = -F^{\text{def}}|_{\text{univ.}} - \frac{2(d-p-1)\pi^{\frac{d}{2}+1}}{\sin\left(\frac{p}{2}\pi\right)\Gamma\left(\frac{p}{2}+1\right)\Gamma\left(\frac{d-p}{2}\right)}h. \quad (4.5.46)$$

When p is odd, the finite pieces of S_A^{def} and F^{def} are universal. When p is even, it is the coefficients of $\log\frac{L}{\epsilon}$ that appear in eq. (4.5.46). The pole in the second term for even p arises from the choice of a dimensional regularisation scheme. It maps to a logarithmic divergence in the UV cut-off ϵ in a short distance expansion around the intersection $\partial A \cap \Sigma$. Explicitly in $p = n - \epsilon$ dimensions for integer n , $\frac{1}{\epsilon} \rightarrow \log\frac{L}{\epsilon}$. In section 6.2.2.1 we will use eq. (4.5.46) to relate the logarithmic contribution to the EE of a $p = 4$ dimensional defect to two defect central charges.

⁶A boundary version of the F-theorem when $d = 3$ was originally proposed by refs. [170,194]

Chapter 5

Supersymmetry

In this chapter, we review several aspects of supersymmetry (SUSY) and superconformal symmetry as well as defects preserving parts of these symmetries.

5.1 Flat space supersymmetry

In this section, we review relevant concepts of SUSY in flat space. Excellent introductions can be found e.g. in refs. [195–197]. In flat space, SUSY is an extension of the Poincaré algebra by fermionic, i.e. spinorial and Grassmann, generators Q^I , where $I = 1, \dots, \mathcal{N}$. The integer \mathcal{N} counts the number of minimal spinors-worth of generators. By minimal spinor we mean the smallest irreducible spin representation of the Lorentz group. These are dependent on the spacetime dimension d and the signature. Commonly \mathcal{N} refers to the number of minimal spinors of $SO(d-1, 1)$. The number of real components of all of the Q^I combined is called the total number of supercharges.¹ The types of minimal $SO(d-1, 1)$ spinors and the corresponding number of real supercharges are summarised in table 5.1.

¹In Euclidean signature, it is customary to count the number of real supercharges using the same \mathcal{N} as in Lorentzian signature. This may seem misleading at first, since the irreducible spinor representations of $SO(d-1, 1)$ and $SO(d)$ have different dimensions. In particular, a Majorana condition is typically identified with a reality condition on the Clifford algebra basis. The spacetime dimensions d in which such a condition can be imposed are different for Euclidean and Lorentzian signature. While this is technically correct, it misses the point. Often one considers Euclidean QFT as an arena to study questions about Lorentzian physics in a more controlled setting. By the Osterwalder-Schrader reconstruction theorem [82], reflection-positive Euclidean correlation functions can be Wick rotated to give unitary correlators in Minkowski space. Rather than imposing an ordinary Majorana condition in Euclidean signature, one should instead consider an alternative Majorana condition which ensures that the Euclidean path integral of Grassmann valued fermions computes correlation functions which, upon Wick rotation, coincide with the correlation functions of (ordinary Lorentzian) Majorana spinors. Such a “physical” Majorana condition can be shown to exist in the same spacetime dimensions as the ordinary Majorana condition in Lorentzian signature [198]. The same applies to symplectic and pseudo-Majorana fermions [199], and, of course, Weyl conditions are signature independent too.

d	minimal spinor	# real components	SUSY	# real supercharges
2	MW	1	$\mathcal{N} = (p, q)$	$p + q$
3	M	2	\mathcal{N}	$2\mathcal{N}$
4	M	4	\mathcal{N}	$4\mathcal{N}$
5	SM	8	\mathcal{N}	$8\mathcal{N}$
6	SMW	8	$\mathcal{N} = (p, q)$	$8(p + q)$

TABLE 5.1: Minimal spinors of $SO(d - 1, 1)$ and SUSY for $2 \leq d \leq 6$. The spinors obey Majorana (M), Majorana-Weyl (MW), symplectic Majorana (SM), and symplectic Majorana-Weyl (SMW) conditions depending on d as summarised in the second column. The number of real components of each minimal spinor is reported in the third column. $\mathcal{N} \in \mathbb{Z}$ counts the number of minimal spinors-worth of SUSY generators. When $d = 2, 6$, minimal spinors are chiral. We write $\mathcal{N} = (p, q)$ for $p, q \in \mathbb{Z}$ to keep track of chiralities. The number of real supercharges for given \mathcal{N} is reported in the last column.

Since spinorial representations of the Lorentz group depend on d and the signature, the precise form of the algebra takes on slightly different forms across dimensions. In our discussion we will encounter SUSY QFTs (SQFTs) in various dimensions and with different amounts of SUSY. Schematically,

$$[P, Q^I] = 0, \quad [M, Q^I] \sim Q^I, \quad \{Q^I, Q^J\} \sim P + \mathcal{Z}, \quad (5.1.1)$$

where P_μ and $M_{\mu\nu}$ are the Poincaré generators introduced in chapter 2, and \mathcal{Z} is a collection of c-numbers, which commute with all generators.

Representations of the SUSY algebra are often called multiplets. Since the supercharges are fermionic, their action on a bosonic state results in a fermion, and vice versa. States sit in highest-weight representations of the SUSY algebra. Half of the supercharges act as raising, and half as lowering operators for spin or helicity. Acting with lowering operators results in a finite-dimensional representation. It is finite because the Q 's are Grassmann valued. In a SUSY multiplet, the number of bosonic and fermionic states are equal. Assembling the states into the on-shell modes of single particles, one finds that SUSY multiplets contain particles of different spins, which must sit in the same representations of global and gauge symmetries. Their dynamics can be described by Lagrangians whose field contents can be elegantly described diagrammatically in so-called quiver diagrams. We will see examples of these in chapter 8.

In a SQFT, flavour symmetry generators commute with all the generators of the SUSY algebra eq. (5.1.1). However, not all global symmetries in SQFT are flavour symmetries. The SUSY algebra has a non-trivial automorphism group, called the R-symmetry, which acts non-trivially on the SUSY generators Q^I . In SQFT, R-symmetry is partly optional: a given theory need not realise the full R-symmetry group. However, if present, states in a SUSY multiplet must have different R-charges since states are related by the action of Q 's.

Let us briefly discuss some of the SQFTs that we will encounter later in this thesis. Many of the SQFTs that we will study are gauge theories for some gauge group G . SUSY gauge theories are built out of multiplets containing a gauge boson. The types of accompanying fields depend on the amount of SUSY and the dimension. E.g. a 2d $\mathcal{N} = (2, 2)$ vector multiplet contains a gauge boson, a Dirac fermion and a complex scalar, all of which are in the adjoint of G . The simplest action for this multiplet is the super-Yang-Mills (SYM) action, a SUSY version of ordinary YM theory. The simplest $\mathcal{N} = (2, 2)$ matter multiplets are so called chiral multiplets, which contain one complex scalar and a Weyl fermion. One can build 2d $\mathcal{N} = (2, 2)$ SUSY gauge theories by taking chiral multiplets in a representation of G , coupling them to a vector multiplet, and turning on a potential for the matter fields, called a superpotential, often denoted by W . If G is reductive, i.e. it contains $U(1)$ factors, one can also turn on a twisted superpotential for each $U(1)$. It is a deformation by two real parameters. One of them is called a Fayet-Iliopoulos (FI) parameter, ξ , which corresponds to a particular deformation of the scalar potential. The other one is a 2d θ -angle for the Abelian part of the field strength. The resulting gauge theory is often called a gauged linear sigma model (GLSM). See e.g. ref. [21, 200] for a detailed discussion. We will meet examples of GLSMs in chapter 8.

Another set of examples are 4d $\mathcal{N} = 2$ gauge theories. The most fundamental building block is a 4d $\mathcal{N} = 2$ vector multiplet, which contains one gauge boson, two Weyl fermions, and one complex scalar. Again, one can write a SYM action for each vector multiplet. $\mathcal{N} = 2$ SUSY preserving matter must be in a so-called hypermultiplet, which contains two Weyl fermions and two complex scalars. A simple example of a 4d SUSY gauge theory is $\mathcal{N} = 2$ supersymmetric QCD (SQCD) with $G = SU(N)$ and $2N$ flavours, i.e. two hypermultiplets in the fundamental representation of $SU(N)$. It turns out that for this theory, the YM coupling g_{YM}^2 is exactly marginal. Another example is the case of a gauge theory consisting of a vector multiplet coupled to a single hypermultiplet in the adjoint representation. In that case, the vector and hypermultiplets combine into an $\mathcal{N} = 4$ vector multiplet to form $\mathcal{N} = 4$ SYM theory. Again, g_{YM}^2 is exactly marginal and the theory is conformal.

It is an immediate consequence of the algebra eq. (5.1.1) that a vacuum state preserves SUSY if and only if it has zero energy. Typically, SQFTs with R-symmetry have multiple SUSY vacua. Sometimes, there can be infinitely many neighbouring vacua corresponding to flat directions in the scalar potential. Such a vacuum manifold is called a (classical) moduli space. Each flat direction in the potential corresponds to a massless field, called a modulus. At energy scales below the mass of the lightest massive particle, only moduli remain. Thus, the classical moduli space of vacua describes the naïve IR dynamics of the SQFT. Moduli spaces are typically stable, i.e. they are not lifted by quantum corrections. However, they do receive interesting quantum corrections, both perturbatively and non-perturbatively. These corrections

can alter the moduli space drastically, and e.g. lead to singularities. Nonetheless, compatibility with SUSY requires the moduli space to admit certain geometric structures which depend on the number of supercharges. The full quantum corrected moduli space encodes the low energy dynamics of the theory. The moduli space can be given a natural metric, and the IR dynamics is dictated by a non-linear sigma model (NLSM) whose target space is the moduli space.

Generically, determining the IR phase of a QFT is difficult. SUSY, however, imposes powerful constraints that can provide tools to study a given QFT. E.g. non-renormalisation theorems heavily constrain the IR dynamics of theories with four supercharges [201]. Where couplings do run, SUSY may still allow for computation of the beta functions. E.g. in 4d $\mathcal{N} = 1$ SUSY gauge theory, ref. [202,203] derived a compact formula for the beta function to all loop orders and non-perturbatively. Gauge theories with eight supercharges have moduli spaces which typically have two branches, where the IR gauge theory either exhibits long-range Coulomb interactions, or the gauge group is fully higgsed. These are called Coulomb and Higgs branches, respectively. The Higgs branch is classically exact, however, the Coulomb branch can receive quantum corrections. E.g. in 4d $\mathcal{N} = 2$ SYM, g_{YM}^2 is marginally relevant. Non-renormalisation theorems imply that the coupling can only receive corrections at one-loop in perturbation theory and non-perturbatively. The moduli space only consists of a Coulomb branch, which receives quantum corrections. Nonetheless, SUSY allows for exact determination of the theory's IR dynamics. Ref. [19] argued for the $SU(2)$ theory that the moduli space has two singularities in the interior of the moduli space, where additional DOF become light. The type of additional particles is encoded in the monodromies around the points. By studying the monodromies, they were able to construct holomorphic differentials on an auxiliary complex curve, whose integrals along 1-cycles exactly determine the metric on the moduli space. This auxiliary curve is often called the Seiberg-Witten (SW) curve. Similar curves and differentials have been found for gauge theories with matter content, e.g. in ref. [20]. See ref. [204] for a review with many other examples.

5.2 Supersymmetric localisation

QFT in flat space suffers from IR divergences. These can be cured by putting the theory on a compact manifold. In order to preserve SUSY on a curved background, additional couplings to the background curvature need to be introduced. This lifts the moduli space of vacua. Nonetheless, SUSY still allows for explicit computation of various observables. These include the renormalised partition functions Z_{S^d} and the $Z_{S^1 \times S^{d-1}}$ if the theory preserves enough SUSY.

The technique that allows for these computations is SUSY localisation. See e.g. ref. [205] for a pedagogical introduction, and ref. [24] for a comprehensive review. The localisation principle was first formulated in ref. [13]. Let $I[\Phi]$ be the action of a SQFT, and let \mathcal{Q} be a fermionic symmetry of I , i.e. $\mathcal{Q}I = 0$. \mathcal{Q} can be any Grassmann valued charge that squares to a linear combination of bosonic spacetime, global and gauge symmetry charges, $\mathcal{Q}^2 = \mathcal{B}$. One may then consider the deformed action $I + t\mathcal{Q}V$, for some fermionic functional $V[\Phi]$ that is invariant under \mathcal{B} , i.e. $\mathcal{B}V = 0$. The path integral, with SUSY invariant measure $\mathcal{D}\Phi$, is unchanged by this deformation

$$\begin{aligned} \frac{\partial}{\partial t} Z(t) &= \frac{\partial}{\partial t} \int \mathcal{D}\Phi e^{-I-t\mathcal{Q}V} = - \int \mathcal{D}\Phi \mathcal{Q}V[\Phi] e^{-I-t\mathcal{Q}V} \\ &= - \int \mathcal{D}\Phi \mathcal{Q} \left(V e^{-I-t\mathcal{Q}V} \right) = 0, \end{aligned} \quad (5.2.2)$$

where the last equality holds because \mathcal{Q} is a differential in field space, and we are assuming that $V[\Phi]$ falls off sufficiently fast at infinity in field space. Thus, the path integral can be computed at any value of t , $Z(t) = Z(0) = Z$. At large t , the path integral is dominated by field configurations that extremise $\mathcal{Q}V$, and we can perform a saddle-point approximation around these points. In the $t \rightarrow \infty$ limit, this approximation becomes exact. Note that the argument also applies to correlation functions of observables \mathcal{O} obeying $\mathcal{Q}\mathcal{O} = 0$.

One choice of \mathcal{Q} and $V[\Phi]$, reduces the path integral to a sum over the Bogomol'nyi-Prasad-Sommerfield (BPS) locus of bosonic \mathcal{Q} -invariant field configurations, i.e. configurations for which all fermionic fields and their \mathcal{Q} -variations vanish. In the case of an $\mathcal{N} \geq 2$ gauge theory on S^4 , the sum over saddle points then reduces to a finite-dimensional integral of the vacuum expectation value (VEV) of the vector multiplet scalar, a , over the Cartan subalgebra \mathfrak{t}_{4d} of the gauge algebra \mathfrak{g}_{4d} . Since a parametrises the Coulomb branch of the moduli space in flat space, this choice of \mathcal{Q} and V is often called Coulomb branch localisation. The localised partition function takes the following schematic form [23]

$$Z_{S^4} = \int_{\mathfrak{t}_{4d}} da Z_{\text{class}} Z_{1\text{-loop}} |Z_{\text{inst}}|^2. \quad (5.2.3)$$

It consists of a classical part Z_{class} , a 1-loop part $Z_{1\text{-loop}}$, and an instanton part Z_{inst} . Each of these is parametrised by a , valued in the Cartan subalgebra.² Often, localisation is performed on a squashed sphere, $S^4_{\mathfrak{b}}$, where $\mathfrak{b}^2 = \frac{\epsilon_1}{\epsilon_2}$ are squashing parameters. The round sphere partition function can be obtained by taking $\mathfrak{b} \rightarrow 1$. We will comment more on the squashed case in section 8.2.

²The instanton part will not play much of a role in this thesis. Let us just point out that it was first determined by ref. [22] by deforming the theory on \mathbb{R}^4 in a way that preserves a $U(1)^2$ subgroup of the original $SO(4)$ Lorentz group. This is called the Ω -background, $\mathbb{R}^4_{\epsilon_1, \epsilon_2}$, where $\epsilon_{1,2}$ are the deformation parameters. Using this deformation, ref. [22] was able to give a microscopic derivation of the full IR dynamics of $\mathcal{N} = 2$ SYM theory without resorting to an analysis of the moduli space via the SW curve.

For a 2d GLSM, one can also localise onto the BPS locus, where field configurations are parametrised by a quantised 2d gauge flux $m = \frac{1}{2\pi} \int_{S^2} F$ and the VEV of one of the two real vector multiplet scalars, σ . The Coulomb branch localised partition function on S^2 takes the schematic form [206,207]

$$Z_{S^2} = \frac{1}{|\mathcal{W}_{\mathfrak{g}_{2d}}|} \sum_{m \in \mathfrak{t}_{2d}^{\mathbb{Z}}} \int_{\mathfrak{t}_{2d}} d\sigma Z_{\text{class}} Z_{1\text{-loop}}^{\text{gauge}} Z_{1\text{-loop}}^{\text{matter}}, \quad (5.2.4)$$

where $\mathcal{W}_{\mathfrak{g}_{2d}}$ is the Weyl group of \mathfrak{g}_{2d} , and $\mathfrak{t}_{2d}^{\mathbb{Z}}$ is the charge lattice.³

Another common choice of \mathcal{Q} and $V[\Phi]$ exists when the gauge group is completely higgsed in flat space by turning on a non-zero FI parameter. In this case the path integral reduces to a discrete sum over BPS configurations which correspond to a finite number of points on the Higgs branch. E.g. in 2d, the partition function again depends on classical and 1-loop parts but now also receives contributions from vortex and anti-vortex excitations. This choice is called Higgs branch localisation [206,207]. The different localisation schemes all give the same answer, as they must.

5.3 Superconformal symmetry

In QFT in flat space, invariance under both SUSY and conformal symmetry typically implies invariance under the larger superconformal group. For pedagogical introductions to superconformal symmetry, see e.g. refs. [76,208]. Importantly, R-symmetry is no longer optional for superconformal field theories (SCFTs): it is part of the superconformal algebra (SCA), which is a super-Lie algebra composed of bosonic and fermionic generators. Its bosonic subalgebras are the conformal algebra eq. (2.1.9) and the R-symmetry algebra. In addition to the fermionic supercharges Q^I , the SCA also contains an equal number of fermionic superconformal generators S^I . A subset of the non-trivial commutation relations is

$$\begin{aligned} [D, Q] &= +\frac{i}{2}Q, & [D, S] &= -\frac{i}{2}S, & [K, Q] &\sim S, & [P, S] &\sim Q \\ \{Q, Q\} &\sim P, & \{S, S\} &\sim K, & [Q, S] &\sim D + R + M, \end{aligned} \quad (5.3.5)$$

where R is an R-symmetry generator. Thus, Q and S have scaling dimension $\Delta = +\frac{1}{2}$ and $\Delta = -\frac{1}{2}$, respectively. SCA have been classified under mild physical assumptions, and have been shown to only exist for spacetime dimensions $d \leq 6$ [209], i.e. there are no SCFTs in $d > 6$.

In 6d, there are two SCAs: one with 6d $\mathcal{N} = (2, 0)$ and $\mathfrak{usp}(4)$ R-symmetry, and the other with $\mathcal{N} = (1, 0)$ SUSY and $\mathfrak{usp}(2)$ R-symmetry. There is no SCA with $\mathcal{N} = (1, 1)$

³In practical terms, one may think of $m \in \mathfrak{t}_{2d}^{\mathbb{Z}}$ as having integer eigenvalues on any representation of the gauge group G_{2d} .

SUSY. The most famous interacting 6d SCFTs are the $\mathcal{N} = (2, 0)$ theories, which are labelled by an ADE Lie algebra \mathfrak{g}_{6d} [210, 211]. The low energy effective theory on a generic point on the moduli space contains a two-form gauge field whose field strength is self-dual. These SCFTs are believed to be the unique 6d SCFTs with maximal SUSY. String and M-theory suggest that these SCFTs describe the IR dynamics of certain extended objects, called branes. There is ample evidence that these are healthy, local SCFTs (see e.g. ref. [212]) but an explicit QFT description is lacking. There is no known Lagrangian description.

In 5d, the situation is even more restrictive: the unique SCA $\mathfrak{f}(4)$ only has $\mathcal{N} = 1$ SUSY with $\mathfrak{su}(2)$ R-symmetry. The only known examples of interacting 5d SCFTs come from string theory constructions, including webs of intersecting branes [213] and geometric engineering [214, 215]. Moreover, string theory suggests that all 5d SCFTs descend from 6d $\mathcal{N} = (1, 0)$ SCFTs via compactification [216]. Conversely, compactifying the 6d $\mathcal{N} = (2, 0)$ theory on a circle gives 5d $\mathcal{N} = 2$ SYM theory, which is not conformal. The radius of the S^1 is identified with the YM coupling g_{YM}^2 , which is irrelevant in $d \geq 5$.

In 4d, there is one SCA with maximal $\mathcal{N} = 4$ SUSY and $\mathfrak{su}(4)$ R-symmetry. $\mathcal{N} = 4$ SYM theory is believed to be the unique 4d SCFT with that SCA, and indeed the only SQFT with maximal SUSY. In addition to its large spacetime symmetry, $\mathcal{N} = 4$ SYM theory has an $SL(2, \mathbb{Z})$ duality group, a generalisation of electromagnetic duality in Maxwell theory. SCAs with $\mathcal{N} \leq 3$ have $\mathfrak{su}(\mathcal{N}) \oplus \mathfrak{u}(1)$ R-symmetry.⁴ A large class of 4d $\mathcal{N} = 2$ SCFTs are the class \mathcal{S} theories [217], which arise from the (partially twisted) compactification of the A_{N-1} 6d $\mathcal{N} = (2, 0)$ SCFT on punctured Riemann surfaces. We will review them briefly in section 8.1.

In 3d, there exist SCAs with $\mathcal{N} \leq 8$ and $\mathfrak{so}(\mathcal{N})$ R-symmetry. A famous example is the Aharony-Bergman-Jafferis-Maldacena (ABJM) theory [218]. ABJM theory is a CS-matter theory which includes two non-dynamical $U(N)$ gauge fields with CS terms at levels k and $-k$ as well as charged matter. For generic $k \in \mathbb{Z}$, ABJM has $\mathcal{N} = 6$ SUSY, which enhances to the maximal $\mathcal{N} = 8$ when $k = 1, 2$. Another class of examples are the so-called class \mathcal{R} theories of ref. [219]. They are 3d $\mathcal{N} = 2$ SCFTs obtained by compactifying the 6d $\mathcal{N} = (2, 0)$ SCFTs on a three-manifold.

The case of $d = 2$ is special: the conformal group factorises into chiral and anti-chiral halves. The chiral halves can be invariant under different SCAs. In fact, there exist three infinite families of chiral SCAs as well as three exceptional SCAs, one of which is labelled by a continuous parameter.

Local operators in unitary CFTs sit in lowest-weight representations of the conformal algebra. The lowest-weight is a conformal primary \mathcal{O} , obeying $[K_\mu, \mathcal{O}(0)] = 0$. In

⁴When $\mathcal{N} = 4$, the R-symmetry generator of the $\mathfrak{u}(1)$ part becomes central and can be quotiented out, giving the aforementioned SCA with $\mathfrak{su}(4)$ R-symmetry.

unitary SCFTs, local operators sit in lowest-weight representations of the SCA. Since both K_μ and S lower the scaling dimension, a lowest-weight should obey

$$[K_\mu, \mathcal{O}(0)] = 0, \quad [S^I, \mathcal{O}(0)] = 0. \quad (5.3.6)$$

Here, $[\cdot, \cdot]$ denotes the commutator if \mathcal{O} is bosonic, and the anti-commutator if it is Grassmann valued. Such a local operator \mathcal{O} is called a superconformal primary.

Superconformal descendants are obtained by taking nested (anti-)commutators $[Q, \cdot]$ of \mathcal{O} , each commutator raising the scaling dimension of \mathcal{O} by $\frac{1}{2}$. E.g. the first superconformal descendant of \mathcal{O} , with scaling dimension $\Delta_{\mathcal{O}}$, is $\mathcal{O}' = [Q, \mathcal{O}]$ whose scaling dimension $\Delta_{\mathcal{O}'} = \Delta_{\mathcal{O}} + \frac{1}{2}$. As the Q 's are Grassmann, there are finitely many superconformal descendants. Note that all superconformal descendants are conformal primaries. This can be seen by using $[K_\mu, Q] \sim S$, and using the Jacobi identity repeatedly. Thus each superconformal descendant gives rise to an infinite family of conformal descendants linked by the supercharges Q .

The representation theory of SCAs is much richer than their non-SUSY counterparts [220–222]. As for ordinary CFTs, superconformal primaries in SCFTs must obey unitarity bounds. Unitarity allows for scaling dimensions $\Delta \geq \Delta_A$ for some Δ_A as well as $\Delta = \Delta_B, \Delta_C, \dots$, where $\Delta_{B,C,\dots} < \Delta_A$ are a discrete set. Superconformal primaries with $\Delta = \Delta_A, \Delta_B, \Delta_C, \dots$ obey shortening conditions, i.e. at least one superconformal descendant is annihilated by at least one supercharge Q . As continuous parameters in the SCFT are varied, the scaling dimension of long multiplets can reach the unitarity bound Δ_A from above. At this point the long multiplet splits into a short multiplet with Δ_A and another short multiplet (of any type) containing the null states of the former. Short multiplets that do not appear in the fragmentation of long multiplets at the unitarity bound are said to be absolutely protected. They must necessarily have $\Delta = \Delta_B, \Delta_C, \dots$. Conversely, some short multiplets may recombine into long multiplets and leave the unitarity bound as continuous parameters are tuned. This process is called recombination. See e.g. ref. [222] for more details.

An important example of a superconformal multiplet is the stress tensor multiplet. It is a protected multiplet that exists in any SCFT.⁵ On general grounds, this multiplet consists of the stress tensor, the R-symmetry current and the supercurrents whose charges are the fermionic generators of the SCA. The stress tensor is the

⁵The existence of a stress tensor multiplet imposes strong constraints on the admissible SCAs. Nahm's classification [209] allows for an arbitrary number of supercharges \mathcal{N} in $d = 3, 4, 6$. A standard argument states that theories with more than 16 real supercharges must necessarily include gravity. However, this argument assumes the existence of weakly coupled one-particle states. Clearly, this requirement is not met for non-Lagrangian SCFTs. The reason that any SCFT in $d = 4, 6$ can have no more than 16 real supercharges is precisely the requirement of the existence of a suitable stress tensor multiplet. In $d = 3$, theories with more than 16 supercharges admit a stress tensor multiplet but they are necessarily free [222]. We have implicitly assumed the existence of such a multiplet in our previous discussion, and we will continue to do so in the remainder of this thesis.

superconformal descendant with the largest scaling dimension $\Delta = d$ in this multiplet. Conserved flavour symmetry currents also sit in superconformal multiplets. Since a flavour symmetry charge must commute with all the supercharges, the conserved current must be the component which is annihilated by all further Q 's, and so it must have the largest scaling dimension.

The BPS local operators in a SCFT, i.e. operators which are annihilated by at least one Q , form an important subsector of the theory. One can define a formal index that counts them graded by their quantum numbers. This is the superconformal index (SCI), specified by a choice of supercharge Q . In radial quantisation, it is defined as

$$\mathcal{I}(\beta_i) = \text{Tr}_{\mathcal{H}_Q} (-1)^F e^{-\sum_j \beta_j \mathfrak{t}_j}, \quad (5.3.7)$$

where β_i are real parameters called chemical potentials for each generator \mathfrak{t}_i of the Cartan subalgebra of the superconformal and flavour symmetry commuting with Q , and $\mathcal{H}_Q \subset \mathcal{H}$ is the subspace of the radial quantisation Hilbert space that is annihilated by Q and $Q^\dagger = S$.⁶ These states, or equivalently, operators via the state-operator correspondence, sit in short representations which generically have $\Delta = \Delta_A, \Delta_B, \Delta_C, \dots$. SUSY indices should be invariant under continuous deformations of the theory. For the SCI in eq. (5.3.7), one might worry that two short multiplets could recombine and leave the unitarity bound, thus changing the index. However, it turns out that contributions to the SCI from any such pair evaluate to zero, and it indeed is invariant under continuous deformations of the theory that preserve Q [223–225]. Thus, more precisely, the index counts BPS operators modulo recombination.

Via a standard argument [226], the Hamiltonian $\{Q, Q^\dagger\} \sim D + R + M$ can be inserted with some coefficient β in the exponential of eq. (5.3.7) at no cost. The modified SCI is independent of β . This modification of the SCI suggests that one may be able to compute it via a path integral. Studying a CFT on \mathbb{R}^d in radial quantisation is equivalent to placing the theory on $\mathbb{R} \times S^{d-1}$, where \mathbb{R} is the (radial, Euclidean) time direction: the Hilbert spaces are the same. By compactifying \mathbb{R} to S^1_β , where the circumference β is identified with the coefficient of the Hamiltonian, one maps the SCI to the path integral on $S^1_\beta \times S^{d-1}$, with anti-periodic boundary conditions along the S^1_β for the fermions. In fact, the path integral computes the SCI up to a factor,

$$Z_{S^1 \times S^{d-1}}(\beta, \mu_j) = e^{-\beta E_c(\mu_j)} \mathcal{I}(\beta \mu_j), \quad (5.3.8)$$

where $\mu_j = \frac{\beta_j}{\beta}$, and $E_c(\mu_j)$ is a polynomial in μ_j called the SUSY Casimir energy (SCE) [227–229].

⁶Different Q 's have different commutants, and the exponent on the right-hand side changes accordingly. The full SCI, however, turns out to be independent of this choice.

In ordinary 2d CFT, one typically defines the Casimir energy as the ground state energy on the circle $\int_{S^1_L} dx \sqrt{g} \langle T_{\tau\tau} \rangle = -\frac{\pi}{6L} c^{(2d)}$, where τ is the Euclidean time coordinate along \mathbb{R} , see e.g. ref. [84]. For higher-dimensional CFTs, the direct analogue $\int_{S^{d-1}} d^{d-1}x \sqrt{g} \langle T_{\tau\tau} \rangle$ turns out to be scheme-dependent [230]. For SCFTs, one can define an alternative Casimir energy by reducing on the S^{d-1} to obtain a SUSY QM (SQM). The expectation value of the 1d theory's Hamiltonian, $\langle H_{\text{SQM}} \rangle$, turns out to be scheme-independent, and can be identified with the SCE E_c appearing in eq. (5.3.8) by taking the $\beta \rightarrow \infty$ limit [230].

5.4 Weyl anomaly in SCFTs

In chapter 2 we discussed the CFT Weyl anomaly and briefly mentioned 't Hooft anomalies. Both anomalies correspond to non-conservation of currents (the dilatation current for the stress tensor and the ordinary Noether current of a global symmetry) in a non-trivial background.⁷ Weyl and 't Hooft anomalies share some similarities, e.g. both must obey the WZ consistency condition, however, they are fundamentally different in QFT.

For 't Hooft anomalies, imposing WZ consistency can be recast as a Becchi-Rouet-Stora-Tyutin (BRST) cohomology problem, see e.g. refs. [88, 89, 237, 238] for a pedagogical introduction.. Physical anomalies that cannot be removed by local counter-terms correspond to BRST cohomology classes. A remarkably simple way to solve the BRST problem is called the descent mechanism. 't Hooft anomalies can be obtained from $(d+2)$ -form characteristic classes, i.e. gauge invariant polynomials of (background) field strength tensors that are closed under the exterior derivative d and whose integrals are topological invariants. The sum of these characteristic classes is called the anomaly polynomial $\mathcal{A}_{d+2}(\mathcal{M}_d)$. The 't Hooft anomalies of the d -dimensional QFT are obtained via the descent equations, which reduce the $(d+2)$ -form to a BRST-closed d -form. The combinations of field strength tensors appearing in each characteristic class determine the anomalous symmetries. The Hodge dual of the BRST-closed d -form parametrises the non-conservation of the anomalous symmetry's current, like in eq. (2.5.44). The coefficients of the characteristic classes descend to 't Hooft anomaly coefficients. This is in contrast to Weyl anomalies, for which it is believed that no anomaly polynomial exists.⁸ The 't Hooft anomaly coefficients are not fixed by descent, they need to be computed

⁷Our discussion will focus on continuous symmetries, however, 't Hooft anomalies of discrete symmetries have received considerable interest recently, see e.g. refs. [231–233]. Further, various recent generalisations of symmetry typically involve discrete groups or more general algebraic structures, see e.g. refs. [154, 234–236].

⁸Given the resemblance of the Euler anomaly to the chiral anomaly, as discussed in section 2.5, ref. [96] speculated that it should satisfy a descent identity. Indeed, refs. [239, 240] proved somewhat recently that the Euler anomaly is the unique density obeying a non-trivial descent mechanism.

separately. Since 't Hooft anomalies typically arise from 1-loop fermion diagrams [241, 242], they can be straightforwardly computed. This is unlike Weyl anomalies which are not one-loop effects and also exist in CFTs without fermions. Moreover, 't Hooft anomalies are invariant under RG flows, and may be computed at any point along the flow. This is known as 't Hooft anomaly matching [243]. This is in stark contrast to Weyl anomalies, which only exist at the fixed points of RG flows, and the c-theorems discussed in section 2.5.

Nonetheless, in SCFTs, the stress tensor and R-symmetry current sit in the same superconformal multiplet, and one might wonder if there exists a relation between the 't Hooft anomaly of the R-symmetry and the Weyl anomaly coefficients. Indeed, this turns out to be the case. E.g. in 2d $\mathcal{N} = (2, 0)$ SCFTs, refs. [244, 245] found

$$c^{(2d)} = 3k, \quad (5.4.9)$$

where k is the pure 't Hooft anomaly coefficient of the superconformal R-symmetry. The proportionality factor is normalisation-dependent, and we have chosen the same conventions as refs. [244, 245]. Similarly, the central charges $a_{\mathcal{M}}^{(4d)}$ and $c^{(4d)}$ of 4d $\mathcal{N} = 1$ SCFTs can be related to combinations of R-symmetry anomalies [106]. E.g. for $\mathcal{N} = 4$ SYM theory, this implies that $a_{\mathcal{M}}^{(4d)} = c^{(4d)}$. The central charges are independent of marginal couplings and are given by the free field result, see e.g. the review [246]. Similar statements hold for the central charges of $\mathcal{N} = 2$ SCFTs with a Lagrangian description, see e.g. the recent review [247]. For 6d $\mathcal{N} = (1, 0)$ SCFTs, SUSY imposes a linear relation on the three B-type central charges in eq. (2.5.71), so that only two are independent. $\mathcal{N} = (2, 0)$ SUSY imposes a second linear relation, so that only one is independent [123, 248, 249].⁹ Similarly to the 4d case, refs. [249, 251] found linear relations between 6d central charges and mixtures of R-symmetry and gravitational 't Hooft anomalies, which are consistent with the reduction in the number of independent central charges.

Often when studying SCFTs, one only has access to a weakly coupled Lagrangian description at some energy scale and would like to ask questions about its strongly coupled IR fixed point. Given that 't Hooft anomalies are RG invariants, one might hope that computing the anomalies in the weakly coupled SQFT fixes the central charges of the IR SCFT. However, the $U(1)$ R-symmetry of the weakly coupled theory can mix with other $U(1)$ flavour symmetries along the flow to produce an equally good R-symmetry in the IR. It is this superconformal R-symmetry that determines the central charges. Refs. [244, 245, 252] showed that, provided there are no accidental $U(1)$ symmetries in the IR,¹⁰ the superconformal R-symmetry in $d = 2$ and $d = 4$ can

⁹SUSY has also been shown to constrain RG flows in $d = 6$. E.g. RG flows triggered by non-zero expectation values in a SUSY vacuum for scalars in the gauge multiplet obey a c-theorem for $a_{\mathcal{M}}^{(6d)}$ [250, 251].

¹⁰This is in fact a rather strong assumption. In particular, most 4d IR $\mathcal{N} = 2$ SCFTs have accidental $U(1)$ symmetries, and one must resort to other techniques to compute $a_{\mathcal{M}}^{(4d)}$ and $c^{(4d)}$. See e.g. ref. [253] for 4d $\mathcal{N} = 2$ SCFTs that can be reached via RG flow from $\mathcal{N} = 2$ gauge theories.

be determined by an extremisation principle: one first defines a trial central charge $a_{\mathcal{M},\text{trial}}^{(\text{dim})}$ by replacing the R-symmetry anomalies in eq. (5.4.9) and its higher-dimensional analogues by the anomalies of a general admixture of R- and $U(1)$ flavour symmetries with arbitrary coefficients. The coefficients that extremise the value of $a_{\mathcal{M},\text{trial}}^{(\text{dim})}$ then correspond to the superconformal R-symmetry. A similar extremisation principle was also proved for the sphere free energy F in 3d $\mathcal{N} = 2$ SCFTs, which have an $SO(2) \simeq U(1)$ R-symmetry [254].

In section 2.5, we argued that central charges control various observables in a given CFT. In SCFTs, there are additional observables that depend on them. In particular, a SUSY localisation computation on S^1 times a squashed S^3 showed that the SCE E_c introduced in eq. (5.3.8) is proportional to the Weyl anomaly coefficients $a_{\mathcal{M}}^{(4d)}$ and $c^{(4d)}$,

$$\begin{aligned} E_c(\mu_j) &\equiv -\lim_{\beta \rightarrow \infty} \partial_\beta \log Z(\beta, \mu_j) \\ &= \frac{4\pi}{3} (|\mu_1| + |\mu_2|) \left((a_{\mathcal{M}}^{(4d)} - c^{(4d)}) + \frac{(|\mu_1| + |\mu_2|)^2}{|\mu_1||\mu_2|} (3c^{(4d)} - 2a_{\mathcal{M}}^{(4d)}) \right), \end{aligned} \quad (5.4.10)$$

where $\mu_{1,2}$ are chemical potentials for $SO(2)_{1,2}$ rotations preserved in squashing the S^3 [227, 230]. Since Weyl anomalies in SCFTs are related to 't Hooft anomalies, ref. [229] conjectured, that the SCE is given by the equivariant integration of the anomaly polynomial,

$$E_c = \int \mathcal{A}_{d+2}(\mathcal{M}_d), \quad (5.4.11)$$

Indeed, ref. [255] demonstrated in 4d $\mathcal{N} = 1$ examples on more general backgrounds that the SCE depends on $U(1)$ global and mixed gravitational 't Hooft anomalies. However, we reiterate that eq. (5.4.11) remains a conjecture, albeit one strongly supported by evidence from a number of examples in various dimensions [229].

Finally, let us point out a peculiar feature of 4d $\mathcal{N} \geq 2$ and 6d $\mathcal{N} = (2, 0)$ SCFTs on flat space: there exists a protected subsector of local operators that is isomorphic to a 2d chiral algebra, also called vertex operator algebra (VOA) [256–258]. This VOA can be identified by choosing a suitable admixture of supercharges and superconformal generators \mathbb{Q} and passing to its cohomology. The cohomology of these operators consists of the so-called Schur operators, which are the operators appearing in a certain limit of the SCI, called the Schur limit [259]. See e.g. ref. [260] for a pedagogical discussion. The choice of supercharge picks out a 2d plane inside the 4d or 6d SCFT, on which the anti-holomorphic 2d global conformal generators are \mathbb{Q} -exact. In particular the anti-holomorphic translation generator \bar{L}_{-1} is \mathbb{Q} -exact, and so the anti-holomorphic coordinate dependence in correlation functions of operators in cohomology drops out. Thus, the operators in cohomology are holomorphic and form a VOA.

In the case of a 4d $\mathcal{N} = 2$ SCFT, the 2d global conformal symmetry can be shown to enhance to Virasoro symmetry with central charge $c_{\text{VOA}}^{(2d)} \propto -c^{(4d)} \leq 0$, where $c^{(4d)}$ is the B-type central charge of the 4d SCFT. Unitarity of the ambient SCFT can be used to infer properties of the VOA. Conversely, certain properties of the VOA can be used to learn about a subsector of the ambient SCFT and its correlation functions. See e.g. [261] for a pedagogical review. For the 6d $\mathcal{N} = (2, 0)$ theories, 2d global conformal symmetry enhances to \mathcal{W} -symmetry, an enlargement of the Virasoro algebra by holomorphic higher spin currents. In 6d $\mathcal{N} = (2, 0)$, there is only one independent B-type central charge, and the Virasoro central charge $c_{\text{VOA}}^{(2d)} \geq 0$ is fixed in terms of it [258]. Note that unlike in 4d, the VOA is unitary in 6d $\mathcal{N} = (2, 0)$ SCFTs.

5.5 Superconformal defects

A p -dimensional superconformal defect preserves a subalgebra of the ambient SCA which is itself a SCA in p dimensions. More precisely, let $\mathfrak{G} = \mathfrak{G}_s \oplus \mathfrak{G}_f$ be the total symmetry algebra of the ambient SCFT, where \mathfrak{G}_s is the SCA and \mathfrak{G}_f is the flavour symmetry algebra. Then a superconformal defect preserves $\mathfrak{g} = \mathfrak{g}_s \oplus \mathfrak{g}_b \oplus \mathfrak{g}_f \subset \mathfrak{G}$, where $\mathfrak{g}_s \subset \mathfrak{G}_s$ is the SCA preserved by the defect, $\mathfrak{g}_b \subset \mathfrak{G}_s$ is the bosonic subalgebra generated by R-symmetry and transverse rotation generators that leave the defect invariant and commute with \mathfrak{g}_s , and $\mathfrak{g}_f \subset \mathfrak{G}_f$ is the flavour symmetry preserved by the defect.

Defect local operators sit in superconformal multiplets of \mathfrak{g}_s . Given a superconformal defect primary, i.e. a local operator annihilated by the K_a and S^I generators preserved by the defect, its defect superconformal multiplet is generated by acting with the supercharges Q^I preserved by the defect. Such operators carry additional quantum numbers of $\mathfrak{g}_b \oplus \mathfrak{g}_f$. A number of theorems about the representation theory of defect multiplets were proved in ref. [149]. The displacement operator \mathcal{D}^i is an example of a defect local operator in DCFT. It is a defect conformal primary which arises from broken translations in the transverse directions to the defect and therefore exists for every (non-topological) defect. In an SCFT, a defect also breaks superconformal generators, giving rise to additional defect primaries. Together, they form the displacement supermultiplet, where the displacement operator is the superconformal descendant with the highest scaling dimension. The coefficients of the two-point functions of these additional primaries in the displacement multiplet are fixed in terms of the displacement operator two-point function $c_{\mathcal{D}\mathcal{D}}$. Similarly, any broken flavour generator that commutes with the supercharges in \mathfrak{g}_s gives rise to a defect primary proportional to the non-conservation of the current at the defect. This operator must sit in a defect superconformal multiplet.

Let us now briefly comment on superconformal defects across dimensions. We begin with $p = 1$, i.e. line defects. Ref. [149] recently classified the superconformal subalgebras of line defects, and their unitary representations. One of their results is that superconformal lines do not exist in 3d, 4d, and 6d $\mathcal{N} = 1$ SCFTs because their SCAs do not admit 1d superconformal subalgebras. Superconformal lines in the 6d $\mathcal{N} = (2, 0)$, if they exist, must break the transverse rotational symmetry.

Superconformal line defects have been studied in a host of SCFTs. They include 3d CS-matter theories and ABJM theory, see e.g. [262–268] and the review [269]. For line defects in 4d SCFTs, see e.g. refs. [191, 270–274], and refs. [275–277] for investigations without relying on a Lagrangian description. There has also been renewed interest from the bootstrap and integrability communities, see e.g. [278–282] and refs. therein.

A famous example of a superconformal line defect is the round $\frac{1}{2}$ -BPS Wilson-Maldacena loop in 4d $SU(N)$ $\mathcal{N} = 4$ SYM theory

$$W_R[A] = \frac{1}{N} \text{Tr}_R \mathcal{P} \exp \left(i \oint d\sigma (\dot{x}^\mu A_\mu + \theta^I \Phi^I |\dot{x}|) \right), \quad (5.5.12)$$

where Tr_R denotes the trace in the representation R , \mathcal{P} denotes path ordering, σ parametrises the line, $\dot{x}^\mu = \partial_\sigma x^\mu$, Φ^I with $I = 1, \dots, 6$ are the six real vector multiplet scalars, and θ^I is a constant $SO(6)$ R-symmetry vector [270]. It is a stable IR fixed point under a defect RG flow from an ordinary Wilson line in $\mathcal{N} = 4$ SYM theory [283, 284]. Since it is BPS, the localisation argument in section 5.2 applies, and its expectation value can be computed exactly [23]. The expectation values of similar line defects in 3d SUSY CS-matter theories were computed in [285].

A Wilson-Maldacena line with a sharp bend, or cusp, at one point can be viewed as a quark that is made to accelerate at one point. In a medium with massless DOF, accelerating charges emit bremsstrahlung. For a small cusp, the bremsstrahlung was shown to be proportional to the coefficient of the displacement operator two-point function $c_{\mathcal{DD}}$ [273]. Since $c_{\mathcal{DD}}$ is related to an energy, ref. [191] conjectured that, in an SCFT, it is proportional to the coefficient of the stress tensor one-point function h . Indeed ref. [286] proved that this relation is universal for $\frac{1}{2}$ -BPS superconformal line defects in 4d $\mathcal{N} = 2$ SCFTs.

Superconformal defects of higher dimension are less explored. A novel feature of $p = 2$ superconformal defects compared to line defects is that they have Weyl anomalies that are not fixed by the bulk, see eq. (3.4.38). Ref. [287] argued that for a 2d defect preserving at least $\mathcal{N} = (2, 0)$ SUSY, the A-type central charge $a_\Sigma^{(2d)}$ and the defect superconformal R-symmetry 't Hooft anomaly coefficient k_Σ are proportional. In particular,

$$a_\Sigma^{(2d)} = 3k_\Sigma \quad (5.5.13)$$

in the absence of gravitational anomalies. This is the same relation obeyed by standalone 2d SCFTs, i.e. eq. (5.4.9), for the same choice of normalisation. Moreover, there exists an extremisation principle that determines the defect superconformal R-symmetry analogously to the ordinary 2d SCFT case of refs. [244, 245]. As explained in section 6.1.1, WZ consistency implies that $a_{\Sigma}^{(2d)}$ is independent of defect marginal couplings but for a generic surface defect it can depend on bulk marginal couplings. If the defect preserves at least 2d $\mathcal{N} = (2, 0)$ SUSY, however, then the A-type anomaly cannot depend on *any*, neither defect nor bulk, marginal couplings [169].

A relation between $c_{\mathcal{D}\mathcal{D}}$ and h was proved in [288] for a 2d defect with (at least) $\mathcal{N} = (2, 0)$ SUSY preserving transverse rotations in a 4d $\mathcal{N} \geq 1$ SCFT. This is completely analogous to the line defect case. For the Weyl anomaly coefficients, this implies

$$d_1^{(2d)} = -d_2^{(2d)} \quad (5.5.14)$$

via eqs. (3.4.40) and (3.4.41). The authors conjectured that this relation holds for a surface defect in a SCFT in any $d \geq 4$. Indeed ref. [289] showed that it holds for $\frac{1}{2}$ -BPS defects in $d = 6$ with $\mathcal{N} = (2, 0)$ SUSY. More generally, ref. [288] conjectured a general relation between $c_{\mathcal{D}\mathcal{D}}$ and h for any defect dimension p and any co-dimension q

$$c_{\mathcal{D}\mathcal{D}} = \frac{2^{p+1}(q+p-1)(p+2)\Gamma(\frac{p+1}{2})}{(q-1)\pi^{\frac{p-q+1}{2}}\Gamma(\frac{q}{2})}h. \quad (5.5.15)$$

Note that the proportionality factor is manifestly positive for $q \geq 2$. This relation encompasses the line defect case and passes other consistency checks [72, 163].

A VOA perspective on 2d $\mathcal{N} = (2, 2)$ superconformal defects in 4d $\mathcal{N} \geq 2$ SCFTs was given in refs. [288, 290]. A flat surface defect intersecting the chiral algebra plane at the origin (and infinity) preserves the cohomological supercharge. The defect then defines a local operator in the VOA whose scaling dimension is determined by h , or equivalently $d_2^{(2d)}$. The superconformal primary of the displacement multiplet is a Virasoro descendant of the defect identity in the VOA.

We now present a number of examples of superconformal surface defects. SUSY boundary conditions of 3d SCFTs have been studied e.g. in refs. [287, 291, 292]. Superconformal surface defects in 4d SCFTs with varying amounts of SUSY have been discussed e.g. in refs. [45, 293–300]. The best studied example of a surface defect in 4d is the Gukov-Witten defect originally introduced in $\mathcal{N} = 4$ SYM theory in ref. [293]. It is a disorder-type defect where the singularity in the ambient fields determines the amount of gauge symmetry preserved by the defect. We will discuss this type of defect in detail in chapter 8. Order type defects in class \mathcal{S} theories were discussed e.g. in refs. [45, 296, 298]. Such defects will also be discussed in chapter 8. In 6d, interacting SCFTs are non-Lagrangian and scarce. Most examples of surface defects in 6d theories come from string theory arguments. They are difficult to study in QFT given the

absence of a Lagrangian description in the interacting case. For the free case see e.g. refs. [97, 158]. Importantly, string and M-theory arguments suggest that the 6d $\mathcal{N} = (2, 0)$ SCFT with algebra \mathfrak{g}_{6d} admits dimension two defects which are $\frac{1}{2}$ -BPS, i.e. they preserve half of the supercharges, and are labelled by representations of \mathfrak{g}_{6d} . Under dimensional reduction to 5d $\mathcal{N} = 2$ SYM, they become $\frac{1}{2}$ -BPS Wilson lines, similar to eq. (5.5.12). For this reason, the 2d defects in the 6d SCFT are often called Wilson surfaces. We will study these defects in chapter 8. Also, see refs. [289, 301] for recent progress.

Most examples of 3d superconformal defects are either boundaries or interfaces of 4d SCFTs. A simple example of a 3d superconformal defect is a SUSY version of mixed-dimensional QED [302]. Another set of examples are the $\frac{1}{2}$ -BPS superconformal interfaces and boundary conditions of 4d $\mathcal{N} = 4$ SYM theory constructed in ref. [303, 304]. In studying the S-duality transformations of Dirichlet boundary conditions, the authors discovered a class of 3d boundary SCFTs coupled to the bulk gauge theory which allow for algorithmic determination of S-dual boundary conditions [305]. Conformal domain walls in $\mathcal{N} = 4$ SYM at large N have also been studied using integrability techniques [306]. This allows for computation of one-point functions of certain non-protected local operators. In the large N limit, these one-point functions can be computed to all orders perturbatively [307] and non-perturbatively [308] in the 't Hooft coupling $\lambda = Ng_{YM}^2$.¹¹

We now move on to 4d boundaries and defects in higher-dimensional SCFTs. Ref. [57] argued that for a defect with $\mathcal{N} \geq 1$, the defect analogous of $a_{\mathcal{M}}^{(4d)}$ and $c^{(4d)}$ have the same dependence on defect R-symmetry 't Hooft anomalies as their counterparts in standalone 4d SCFT [106]. Ref. [57] also extended the extremisation principle of ref. [287] to 4d defects, analogously to the standalone 4d case [252].

String and M-theory arguments suggest that the 6d $\mathcal{N} = (2, 0)$ SCFTs admit co-dimension two defects in addition to the surface defects mentioned above. They are $\frac{1}{2}$ -BPS, of disorder-type, and they are labelled by nilpotent orbits of \mathfrak{g}_{6d} . They play a crucial role in the construction of the 4d $\mathcal{N} = 2$ class \mathcal{S} theories, which are obtained by compactification on a Riemann surface. However, the absence of a Lagrangian description makes it prohibitively difficult to study them. Most results have been obtained via their compactification to $d \leq 5$, see e.g. [310, 311]. In particular, the superconformal fixed point has not been explored using DCFT techniques.

Note that 4d is the largest defect dimension in SCFT: there are no superconformal boundaries or interfaces in 6d SCFTs because the 5d SCA $\mathfrak{f}(4)$ is not a subalgebra of the 6d SCAs [149].

¹¹A similar programme of study was recently initiated for the domain walls in ABJM theory [309].

Part II

Research

Chapter 6

Weyl Anomaly of 4d Conformal Defects

This chapter is based on ref. [1], which I co-authored. Motivated by the co-dimension two defects of the 6d $\mathcal{N} = (2, 0)$ SCFTs, we study conformal defects of dimension $p = 4$ in an ambient CFT of dimension $d \geq 5$. In section 6.1, we determine the form of the defect Weyl anomaly of a conformal defect of dimension $p = 4$ in a $d \geq 5$ CFT. When the ambient space dimension $d = 5$, we extend the findings of ref. [312] by parity-breaking terms. When $d \geq 6$, our result eq. (6.1.1) is novel. We find 23 parity-even terms in the defect Weyl anomaly. The number of parity-odd terms is co-dimension q dependent, and determined for all q .¹ In section 6.2, we then determine how the defect central charges appear in flat and curved space correlation functions. In particular, we relate one defect central charge to the flat space displacement operator two-point function in eq. (6.2.20), and another one to the flat space stress tensor one-point function in eq. (6.2.39). As a result, we argue that these central charges must have definite sign. In the case of a flat boundary in curved space, we determine the leading divergences of the stress tensor one-point function in eq. (6.2.52). We also express the defect contribution to the EE of a spherical ball centred on the defect in terms of two defect central charges, see eq. (6.2.45).

6.1 Defect Weyl anomaly

In this section we present our results for the Weyl anomaly of a $p = 4$ conformal defect of arbitrary co-dimension $q \geq 1$. We determine the anomaly through the three-step algorithm discussed in sections 2.5 and 3.4. Applying the algorithm is computationally involved, so we do not present all the details here. Typically, the

¹Determining the full defect Weyl anomaly for all q was my main contribution to the paper.

algorithm grows more difficult to implement as the defect's dimension, p , increases. In particular, the number of diffeomorphism and Lorentz invariant terms with p derivatives increases sharply with p . Moreover, ensuring that the terms are linearly independent becomes increasingly involved, because geometric relations can be adorned with derivatives in numerous ways.

In appendix A.1, we illustrate the algorithm with the simple example of a $p = 2$ defect in a $d = 4$ ambient CFT. For such a surface defect, there are 10 terms in step 1. After step 2 there are 7 terms, of which 5 are scheme-independent and remain in the end. By contrast, for a defect of dimension $p = 4$, those numbers are larger by an order of magnitude, as we explain in the following subsections and in appendix B.1. We employ the `xAct` package for Mathematica [313] to facilitate dealing with these large numbers of terms. In a supplemental Mathematica notebook available from ref. [1], we also derive many intricate geometric relations which ensure that our basis is linearly independent.

6.1.1 Defect Weyl anomaly for $d \geq 6$

Following the algorithm for arbitrary q , in step 1 we find a 101-dimensional basis of terms. We report this basis of terms in appendix B.1.1. Step 2, WZ consistency, selects linear combinations of these terms with 61 unfixed coefficients. In step 3, we find that of these 61 contributions, 29 are scheme independent, and thus make up the Weyl anomaly of a $p = 4$ conformal defect.

These 29 terms comprise the expected A-type anomaly of the induced connection on the defect, \bar{E}_4 , as well as 28 B-type terms. The Weyl variation of \bar{E}_4 is a total derivative that cannot be removed by a counter-term, whereas the Weyl variations of the B-type terms are either exactly zero or a total derivative that can be removed by a counter-term² Of the 28 B-type terms, 22 are of even parity. The remaining 6 break parity along the defect because they contain a defect Levi-Civita tensor ϵ^{abcd} .

All of the terms mentioned above are admissible in any co-dimension q . The case $q = 1$, however, is special as the symmetry properties of curvature tensors cause many terms to vanish identically. Moreover, terms that are distinct for general q may reduce to the same term when $q = 1$. The 23 parity-even terms in general q reduce to 9 different terms when $q = 1$, and of the 6 parity-odd terms, only 3 are non-zero when $q = 1$.

In addition to the terms that exist for any co-dimension $q \geq 2$, for special values of q certain additional terms may appear that contain the totally anti-symmetric tensor in the normal bundle, $n^{\mu_1 \dots \mu_q}$. As explained in section 3.3, we refer to these terms as being

²We have checked this statement explicitly for the non-trivial conformal invariants \mathcal{I} in eq. (6.1.10) and \mathcal{J}_1 in eq. (6.1.1). However, we have not confirmed that this is true for \mathcal{J}_2 .

parity-odd in the normal bundle. We find that for $q = 2$, there is 1 additional such term, and for $q = 4$ there are 8. For $q = 3$ and $q \geq 5$, the index structure is too restrictive, and rules out the existence of such terms.

We now present the full Weyl anomaly of a $p = 4$ defect. After implementing the algorithm outlined above, and using the same normalisation as in eq. (2.5.57), we arrive at

$$\begin{aligned}
T^\mu{}_\mu|_{\Sigma_4} = & \frac{1}{(4\pi)^2} \left(-d_\Sigma^{(4d)} \bar{E}_4 + d_1^{(4d)} \mathcal{J}_1 + d_2^{(4d)} \mathcal{J}_2 + d_3^{(4d)} W_{abcd} W^{abcd} + d_4^{(4d)} (W_{ab}{}^{ab})^2 \right. \\
& + d_5^{(4d)} W_{aibj} W^{aibj} + d_6^{(4d)} W^b{}_{iab} W_c{}^{iac} + d_7^{(4d)} W_{ijkl} W^{ijkl} + d_8^{(4d)} W_{aijk} W^{aijk} \\
& + d_9^{(4d)} W_{abjk} W^{abjk} + d_{10}^{(4d)} W_{iabc} W^{iabc} + d_{11}^{(4d)} W^c{}_{acb} W_d{}^{adb} + d_{12}^{(4d)} W^a{}_{iaj} W_b{}^{ibj} \\
& + d_{13}^{(4d)} W_{ab}{}^{ab} \hat{\Pi}_{cd}{}^i \hat{\Pi}_i{}^{cd} + d_{14}^{(4d)} W^a{}_{bij} \hat{\Pi}_{ac}{}^i \hat{\Pi}^{jbc} + d_{15}^{(4d)} W^a{}_{ibj} \hat{\Pi}_{ac}{}^i \hat{\Pi}^{jbc} \\
& + d_{16}^{(4d)} W^{abcd} \hat{\Pi}_{ac}{}^i \hat{\Pi}_{ibd} + d_{17}^{(4d)} W_a{}^{bac} \hat{\Pi}_{ba}{}^i \hat{\Pi}_{ic}{}^d + d_{18}^{(4d)} W^c{}_{icj} \hat{\Pi}_{ab}{}^i \hat{\Pi}^{jab} \\
& + d_{19}^{(4d)} \text{Tr} \hat{\Pi}^i \hat{\Pi}_i \hat{\Pi}^j \hat{\Pi}_j + d_{20}^{(4d)} \text{Tr} \hat{\Pi}^i \hat{\Pi}^j \hat{\Pi}_i \hat{\Pi}_j + d_{21}^{(4d)} (\text{Tr} \hat{\Pi}^i \hat{\Pi}_i)^2 \\
& + d_{22}^{(4d)} (\text{Tr} \hat{\Pi}^i \hat{\Pi}^j) (\text{Tr} \hat{\Pi}_i \hat{\Pi}_j) \\
& + \tilde{d}_1^{(4d)} W_{abcd} W^{ab}{}_{ef} \epsilon^{cdef} + \tilde{d}_2^{(4d)} W_{ijab} W^{ij}{}_{cd} \epsilon^{abcd} + \tilde{d}_3^{(4d)} \bar{D}_a \hat{\Pi}_{bf}{}^i \bar{D}_c \hat{\Pi}_{id}{}^j \epsilon^{abcd} \\
& \left. + \tilde{d}_4^{(4d)} W_{abcd} \hat{\Pi}^i{}_{ef} \hat{\Pi}^j{}_{ef} \epsilon^{cdef} + \tilde{d}_5^{(4d)} W_{ijab} \hat{\Pi}_c{}^{ie} \hat{\Pi}_d{}^{jf} \epsilon^{abcd} + \tilde{d}_6^{(4d)} \hat{\Pi}_a{}^i \hat{\Pi}_{be}{}^j \hat{\Pi}_{ic}{}^f \hat{\Pi}_{jd}{}^f \epsilon^{abcd} \right). \tag{6.1.1}
\end{aligned}$$

The only A-type term is the first term, involving the intrinsic Euler density, whose coefficient defines $a_\Sigma^{(4d)}$. The next 22 terms, with coefficients $(d_1^{(4d)}, \dots, d_{22}^{(4d)})$, are B-type and parity-even. The final 6 terms, with coefficients $(\tilde{d}_1^{(4d)}, \dots, \tilde{d}_6^{(4d)})$, are B-type and parity-odd along the defect.

In what follows, for B-type central charges, $d^{(\text{dim})}$ or $\tilde{d}^{(\text{dim})}$ with subscripts denote defect central charges, as in eq. (6.1.1) above, and $b^{(\text{dim})}$ or $\tilde{b}^{(\text{dim})}$ with subscripts denote boundary central charges, as in eq. (6.1.10) below. A handy mnemonic device is then “ d for defect and b for boundary”.

As we noted in sections 2.5 and 3.4, solving WZ consistency can sometimes relate the coefficients of the linearly independent terms in our basis to one another, which leads to non-trivial conformal invariants built out of a linear combination of basis elements. For a $p = 4$ defect, there are indeed two such WZ consistent non-trivial conformal invariants, \mathcal{J}_1 and \mathcal{J}_2 , which appear in the first line of eq. (6.1.1), with coefficients $d_1^{(4d)}$ and $d_2^{(4d)}$, and take the form

$$\begin{aligned}
\mathcal{J}_1 = & \frac{1}{d-1} R \hat{\Pi}_{ab}{}^i \hat{\Pi}_i{}^{ab} - \frac{1}{d-2} N^{\mu\nu} R_{\mu\nu} \hat{\Pi}_{ab}{}^i \hat{\Pi}_i{}^{ab} - \frac{2}{d-2} R^a{}_b \hat{\Pi}_{ac}{}^i \hat{\Pi}_i{}^{bc} - \frac{1}{2} W^c{}_{acb} \hat{\Pi}_i \hat{\Pi}^i \\
& + \frac{4}{9} W^c{}_{ica} \bar{D}^b \hat{\Pi}_{ab}{}^i + \hat{\Pi}^{iab} D_i W^c{}_{acb} - \frac{1}{2} \hat{\Pi}^i \text{Tr} \hat{\Pi}_i \hat{\Pi}^j \hat{\Pi}_j + \frac{1}{16} \hat{\Pi}^i \hat{\Pi}_i \text{Tr} \hat{\Pi}^j \hat{\Pi}_j \\
& + \frac{2}{9} \bar{D}^b \hat{\Pi}_{ab}{}^i \bar{D}^c \hat{\Pi}_{ic}{}^a, \tag{6.1.2}
\end{aligned}$$

$$\begin{aligned}
\mathcal{J}_2 = & \frac{d-4}{d-2} W_{ab}{}^{ab} N^{\mu\nu} R_{\mu\nu} - \frac{d-4}{d-1} R W_{ab}{}^{ab} + \frac{4(d-5)}{3(d-2)} R_{ab} W_c{}^{acb} \\
& - \frac{5(d-4)}{48} W_{ab}{}^{ab} \Pi^i \Pi_i + \frac{2(d-5)}{3} W_c{}^{ica} \bar{D}^b \dot{\Pi}_{ab}^i + \frac{4(d+1)}{9} \dot{\Pi}^{iab} D_i W_c{}^{acb} \\
& - \frac{1}{3} W_{ic}{}^{ac} \bar{D}_a \Pi^i - \frac{2(d-5)}{3} \Pi^i \text{Tr} \dot{\Pi}_i \dot{\Pi}^j \dot{\Pi}_j + \frac{(d-10)}{12} \Pi^i D_i W_{ab}{}^{ab} + \frac{1}{3} D^i D_i W_{ab}{}^{ab},
\end{aligned} \tag{6.1.3}$$

where for example $D^i D_i W_{ab}{}^{ab} = N^{\mu\nu} h^{\rho\tau} h^{\sigma\kappa} D_\mu D_\nu W_{\rho\sigma\tau\kappa}$.

Also as noted above, even though our basis elements for the defect Weyl anomaly are linearly independent, the basis is not unique. To illustrate this, consider the square of the intrinsic Weyl tensor $\bar{W}_{abcd} \bar{W}^{abcd}$. The Gauss eq. (3.3.32) implies

$$\begin{aligned}
\bar{W}_{abcd} \bar{W}^{abcd} = & W_{abcd} W^{abcd} + \frac{1}{3} (W_{ab}{}^{ab})^2 - 2 W_c{}^{acb} W_d{}^{adb} - \frac{2}{3} W_{ab}{}^{ab} \dot{\Pi}_{cd}^i \dot{\Pi}_i{}^{cd} \\
& + 4 W^{abcd} \dot{\Pi}_{ac}^i \dot{\Pi}_{ibd}^i + 4 W_a{}^{bac} \dot{\Pi}_{bd}^i \dot{\Pi}_{ic}^d - 2 \text{Tr} \dot{\Pi}^i \dot{\Pi}_i \dot{\Pi}^j \dot{\Pi}_j - 2 \text{Tr} \dot{\Pi}^i \dot{\Pi}^j \dot{\Pi}_i \dot{\Pi}_j \\
& + \frac{1}{3} (\text{Tr} \dot{\Pi}^i \dot{\Pi}_i)^2 + 2 (\text{Tr} \dot{\Pi}^i \dot{\Pi}^j) (\text{Tr} \dot{\Pi}_i \dot{\Pi}_j).
\end{aligned} \tag{6.1.4}$$

Thus, in eq. (6.1.1), replacing any of the terms that appear on the right-hand side in eq. (6.1.4) with $\bar{W}_{abcd} \bar{W}^{abcd}$ yields an equally admissible basis. One could also consider replacing the intrinsic Euler density \bar{E}_4 with the scheme-independent part of the defect's intrinsic four-dimensional Q -curvature [314], which can be written as³

$$\int d^4\sigma \sqrt{\bar{g}} \bar{Q} \delta\omega = \frac{1}{4} \int d^4\sigma \sqrt{\bar{g}} \left(\bar{E}_4 - \bar{W}_{abcd} \bar{W}^{abcd} \right) \delta\omega, \tag{6.1.5}$$

where we have put a bar on Q to emphasise that it is constructed with intrinsic curvatures of the submanifold. In eq. (6.1.1), the effect of replacing \bar{E}_4 with Q -curvature and using eq. (6.1.4) amounts to scaling the A-type coefficient by a factor of 4 and shifting several B-type anomaly coefficients. Specifically, replacing \bar{E}_4 with \bar{Q} in eq. (6.1.1) shifts

$$\begin{aligned}
d_3^{(4d)} & \rightarrow d_3^{(4d)} + a_\Sigma^{(4d)}, & d_4^{(4d)} & \rightarrow d_4^{(4d)} + \frac{1}{3} a_\Sigma^{(4d)}, & d_{11}^{(4d)} & \rightarrow d_{11}^{(4d)} - 2a_\Sigma^{(4d)}, & d_{13}^{(4d)} & \rightarrow d_{13}^{(4d)} - \frac{2}{3} a_\Sigma^{(4d)}, \\
d_{16}^{(4d)} & \rightarrow d_{16}^{(4d)} + 4a_\Sigma^{(4d)}, & d_{17}^{(4d)} & \rightarrow d_{17}^{(4d)} + 4a_\Sigma^{(4d)}, & d_{19}^{(4d)} & \rightarrow d_{19}^{(4d)} - 2a_\Sigma^{(4d)}, & d_{20}^{(4d)} & \rightarrow d_{20}^{(4d)} - 2a_\Sigma^{(4d)}, \\
d_{21}^{(4d)} & \rightarrow d_{21}^{(4d)} + \frac{1}{3} a_\Sigma^{(4d)}, & d_{22}^{(4d)} & \rightarrow d_{22}^{(4d)} + 2a_\Sigma^{(4d)}.
\end{aligned} \tag{6.1.6}$$

³The full form of Branson's Q -curvature in $d = 4$ contains a total derivative,

$$Q = \frac{1}{6} (R^2 - 3R_{\mu\nu} R^{\mu\nu} - \square R).$$

The $\square R$ term linearises the Weyl variation, and ensures that δQ is a total derivative linear in $\delta\omega$, with all terms at higher order in $\delta\omega$ vanishing identically. Since the Weyl transformation of Q is a total derivative, $\int Q$ is Weyl invariant. In eq. (6.1.5), we consider the Q -curvature of a $p = 4$ submanifold obtained by replacing $R \rightarrow \bar{R}$ and $\square \rightarrow \bar{\square}$. The $\bar{\square} \bar{R}$ term plays no role in our discussion as it can be removed by a local counterterm on the defect.

Note that a number of coefficients are unaffected by the change to Q -curvature. Furthermore, several linear combinations of $d_n^{(4d)}$ in eq. (6.1.6) are invariant under the change to Q -curvature.

In eq. (6.1.1), we emphasise the presence of the non-trivial parity-odd anomalies, with coefficients $(\tilde{d}_1^{(4d)}, \dots, \tilde{d}_6^{(4d)})$. The term whose coefficient is $\tilde{d}_3^{(4d)}$ can be written as a linear combination of a total derivative plus the terms whose coefficients are $\tilde{d}_4^{(4d)}$ and $\tilde{d}_5^{(4d)}$. The anomalous variation of \mathcal{W} , however, includes an additional factor of $\delta\omega$. The $\tilde{d}_3^{(4d)}$ term is not a total derivative in $\delta\mathcal{W}$ because the derivative does not act on $\delta\omega$. If one were to try to absorb the $\tilde{d}_3^{(4d)}$ term into a shift of the $\tilde{d}_4^{(4d)}$ and $\tilde{d}_5^{(4d)}$ terms via partial integration, one would be left with a parity-odd Weyl invariant in $\delta_\omega\mathcal{W}$ with derivatives acting on the Weyl variation parameter $\delta\omega$. Concretely, that term is \mathcal{D}_{41} in eq. (B.1.3). This term is also WZ consistent and cannot be removed by a counterterm. So, we find it convenient to write the anomaly with the $\tilde{d}_3^{(4d)}$ term instead of \mathcal{D}_{41} .

Just as in the case for the parity-even anomalies, the basis of independent terms for the parity-odd defect anomalies is not unique. To illustrate this, we could use the form of the intrinsic Pontryagin density, which can be expressed as

$$\bar{R}_{abcd}\bar{R}^{ab}{}_{ef}\epsilon^{cdef} = W_{abcd}W^{ab}{}_{ef}\epsilon^{cdef} + 4W_{abcd}\mathring{\Pi}^i{}_e\mathring{\Pi}^b{}_f\epsilon^{cdef} - 4\mathring{\Pi}^i{}_a\mathring{\Pi}^j{}_b\mathring{\Pi}^c{}_i\mathring{\Pi}^d{}_f\epsilon^{abcd}, \quad (6.1.7)$$

to rewrite the parity odd part of eq. (6.1.1). The net effect would again be to shift and possibly rescale $\tilde{d}_1^{(4d)}$, $\tilde{d}_4^{(4d)}$, and $\tilde{d}_6^{(4d)}$, depending on the term in eq. (6.1.1) that we replace.

As mentioned above, additional parity-odd terms may appear in the defect Weyl anomaly, for special values of the co-dimension q . More specifically, using our definitions of parity in section 3.3, these terms are parity-odd in the normal bundle, and their existence depends on q by construction, because the totally antisymmetric normal tensor has q indices. The requirement that each term has $p = 4$ derivatives, and the symmetry properties of the curvature tensors are so restrictive, that only when $q = 2$ and $q = 4$ can eq. (6.1.1) pick up such parity-odd contributions. When $q = 2$, in step 1 we find 41 parity-odd terms in the normal bundle. We list them in appendix B.1.2. However, only one of these is WZ consistent and scheme-independent:

$$T^\mu{}_\mu|_{\Sigma_4} \supset \frac{\delta_{q,2}}{(4\pi)^2} \tilde{d}_7^{(4d)} W_{ajbk} \mathring{\Pi}_i{}^{ac} \mathring{\Pi}_c{}^{bj} n^{ik}. \quad (6.1.8)$$

When $q = 4$, in step 1 the basis of parity-odd terms in the normal bundle is 6-dimensional. All 6 terms are WZ consistent and scheme-independent. They are

$$\begin{aligned}
T^\mu{}_\mu|_{\Sigma_4} \supset \frac{\delta_{q,4}}{(4\pi)^2} & \left(\tilde{d}_8^{(4d)} \epsilon^{abcd} n^{ijkl} W_{abij} W_{cdkl} + \tilde{d}_9^{(4d)} n^{ijkl} W_{abij} W_{kl}^{ab} \right. \\
& + \tilde{d}_{10}^{(4d)} n^{ijkl} W_{mirj} W_{k\ell}^{m\ell} + \tilde{d}_{11}^{(4d)} n^{ijkl} W_{aimj} W_{k\ell}^{a\ell} \\
& \left. + \tilde{d}_{12}^{(4d)} n_{ijkl} \epsilon_{abcd} W^{abij} \overset{\circ}{\Pi}_f{}^{ck} \overset{\circ}{\Pi}{}^{fd\ell} + \tilde{d}_{13}^{(4d)} n_{ijkl} W^{abij} \overset{\circ}{\Pi}_{ac}{}^k \overset{\circ}{\Pi}_b{}^{c\ell} \right). \tag{6.1.9}
\end{aligned}$$

To date, little to nothing is known about the $p = 4$ defect central charges we have found in eqs. (6.1.1), (6.1.8), and (6.1.9). The one exception is the A-type central charge, $a_\Sigma^{(4d)}$. Indeed, ref. [57] showed that $a_\Sigma^{(4d)}$ obeys a c-theorem, for RG flows localised to the defect. Furthermore, if the defect preserves at least 4d $\mathcal{N} = 1$ SUSY, then there is an extremisation principle for $a_\Sigma^{(4d)}$ which determines the defect superconformal R-symmetry.

6.1.2 Boundary Weyl anomaly for $d = 5$

Here we employ the algorithm outlined above to construct the most general expression for the boundary Weyl anomaly in $d = 5$. In doing so, we will recover the expression for the parity even anomalies found in ref. [161].⁴ We also identify three previously unknown parity odd anomalies, whose coefficients we denote $(\tilde{b}_1^{(4d)}, \tilde{b}_2^{(4d)}, \tilde{b}_3^{(4d)})$. The full anomaly is

$$\begin{aligned}
T^\mu{}_\mu|_{\Sigma_4} = \frac{1}{(4\pi)^2} & \left(-a_\Sigma^{(4d)} \bar{E}_4 + b_1^{(4d)} \mathcal{I} + b_2^{(4d)} (\text{Tr } \overset{\circ}{K}^2)^2 + b_3^{(4d)} \text{Tr } \overset{\circ}{K}^4 + b_4^{(4d)} W_{abcd} W^{abcd} \right. \\
& + b_5^{(4d)} W_{anbn} W^a{}_n{}^b{}_n + b_6^{(4d)} W_{abcd} \overset{\circ}{K}{}^{ac} \overset{\circ}{K}{}^{bd} + b_7^{(4d)} W_{anbn} \overset{\circ}{K}{}^a{}_c \overset{\circ}{K}{}^{cb} \\
& + b_8^{(4d)} W_{nabc} W_n{}^{abc} + \tilde{b}_1^{(4d)} \bar{D}_a \overset{\circ}{K}_b{}^e \bar{D}_c \overset{\circ}{K}_{de} \epsilon^{abcd} \\
& \left. + \tilde{b}_2^{(4d)} W_{ab}{}^{ef} W_{cdef} \epsilon^{abcd} + \tilde{b}_3^{(4d)} W_{abcd} \overset{\circ}{K}{}^a{}_e \overset{\circ}{K}{}^b{}_f \epsilon^{cdef} \right), \tag{6.1.10}
\end{aligned}$$

where $W_{anbn} = e_a^\mu n^\nu e_b^\rho n^\sigma W_{\mu\nu\rho\sigma}$, and similarly for W_{nabc} . The conformal invariant \mathcal{I} is

$$\begin{aligned}
\mathcal{I} = -\frac{2}{3} R_{ab} \overset{\circ}{K}{}^a{}_c \overset{\circ}{K}{}^{cb} + \frac{1}{4} R \text{Tr } \overset{\circ}{K}^2 - \frac{1}{3} R_{mn} \text{Tr } \overset{\circ}{K}^2 + \frac{1}{2} W_{anbn} K \overset{\circ}{K}{}^{ab} + \frac{1}{16} K^2 \text{Tr } \overset{\circ}{K}^2 \\
+ \overset{\circ}{K}{}^{ab} D_n W_{anbn} - \frac{1}{2} K \text{Tr } \overset{\circ}{K}^3 + \frac{2}{9} \bar{D}^a \overset{\circ}{K}_{ab} \bar{D}_c \overset{\circ}{K}{}^{bc}, \tag{6.1.11}
\end{aligned}$$

where $D_n W_{anbn} = n^\tau e_a^\mu n^\nu e_b^\rho n^\sigma D_\tau W_{\mu\nu\rho\sigma}$.

⁴The dictionary between our central charges and those in ref. [161] is (Here \rightarrow There): $-a_\Sigma^{(4d)} \rightarrow a/5760$, $b_1^{(4d)} \rightarrow c_8/5760$, $b_2^{(4d)} \rightarrow (c_1 - \frac{1}{3}c_8)/5760$, $b_3^{(4d)} \rightarrow (c_2 + c_8)/5760$, $b_i^{(4d)} \rightarrow c_{i-1}/5760$ for $i = 4, \dots, 6$, $b_7^{(4d)} \rightarrow (c_6 + c_8)/5760$, and $b_8^{(4d)} \rightarrow c_7/5760$. Note the different sign convention for the A-type anomaly, where here the $a_\Sigma^{(4d)}$ -theorem goes the usual way, $a_{\Sigma,UV}^{(4d)} \geq a_{\Sigma,IR}^{(4d)}$.

One can also deduce the form of eq. (6.1.10) from eq. (6.1.1) by setting $q \rightarrow 1$. Most of the terms in eq. (6.1.1) do not have analogous $q = 1$ structures: they vanish due to various symmetry properties of the curvature tensors. Furthermore, some of the $q > 1$ structures have identical $q = 1$ analogues, and so a linear combination of their coefficients end up determining the $q = 1$ anomaly coefficients. The exact dictionary for mapping the B-type central charges is as follows, where \rightarrow indicates taking $q \rightarrow 1$:

$$\begin{aligned} d_1^{(4d)} &\rightarrow b_1^{(4d)}, & d_{21}^{(4d)} + d_{22}^{(4d)} &\rightarrow b_2^{(4d)}, & d_{19}^{(4d)} + d_{20}^{(4d)} &\rightarrow b_3^{(4d)}, & d_3^{(4d)} &\rightarrow b_4^{(4d)}, \\ d_5^{(4d)} + d_{11}^{(4d)} &\rightarrow b_5^{(4d)}, & d_{16}^{(4d)} &\rightarrow b_6^{(4d)}, & d_{15}^{(4d)} - d_{17}^{(4d)} &\rightarrow b_7^{(4d)}, & d_{10}^{(4d)} &\rightarrow b_8^{(4d)}, \\ \tilde{d}_3^{(4d)} &\rightarrow \tilde{b}_1^{(4d)}, & \tilde{d}_1^{(4d)} &\rightarrow \tilde{b}_2^{(4d)}, & \tilde{d}_4^{(4d)} &\rightarrow \tilde{b}_3^{(4d)} \end{aligned} \quad (6.1.12)$$

with all other $q > 1$ terms vanishing when $q = 1$.

6.2 Defect central charges from observables

In this section, we connect some of the coefficients that appear in the defect Weyl anomaly in eq. (6.1.1) to various physical quantities. In subsection 6.2.1 we will find a relation between the coefficient of the flat space two-point function of the displacement operator, $\langle \mathcal{D}\mathcal{D} \rangle$ in eq. (3.1.17), and the defect central charge $d_1^{(4d)}$. In a reflection-positive DCFT, we will then argue that $d_1^{(4d)}$ is a negative semi-definite c-number, by reflection positivity of $\langle \mathcal{D}\mathcal{D} \rangle$. In subsection 6.2.2 we will relate the coefficient, h , in the flat space one-point function of the stress tensor in the presence of a co-dimension $q > 1$ defect, $\langle T^{\mu\nu} \rangle$ in eq. (3.1.13), to the defect central charge $d_2^{(4d)}$. Assuming that the defect ANEC is true, we then argue that $d_2^{(4d)}$ must be negative semi-definite. Further, we will be able to show that since $h \propto -d_2^{(4d)}$, the defect contribution to the universal part of EE for a spherical region centred on the defect, as computed in ref. [49], contains a linear combination of $a_\Sigma^{(4d)}$ and $d_2^{(4d)}$, similar to the $p = 2$ result in eq. (4.5.45) [50]. Finally, in subsection 6.2.2.2, for $d = 5$ BCFTs we compute $\langle T^{\mu\nu} \rangle$ for a flat boundary of an ambient space with non-trivial curvature, and relate the coefficients of the first two leading divergent terms to linear combinations of the boundary central charges in eq. (6.1.10).

6.2.1 Displacement operator two-point function

In this subsection, we connect the anomalous scale dependence in the displacement two-point function to a particular term in the Weyl anomaly. For a flat defect, conformal invariance on the defect determines the two- and three-point functions of defect primaries up to constants. In particular, the displacement operator two-point function takes the form of eq. (3.1.17) with constant coefficient $c_{\mathcal{D}\mathcal{D}}$. There is a variety of techniques for isolating the scale dependence of the correlator in eq. (3.1.17), and

hence matching to the Weyl anomaly in eq. (6.1.1) or eq. (6.1.10). In subsection 6.2.1.1 we use some of them to fix $c_{\mathcal{D}\mathcal{D}}$ in terms of the defect central charge $d_1^{(4d)}$ in eq. (6.1.1), or boundary central charge $b_1^{(4d)}$ in eq. (6.1.10). In subsection 6.2.1.2 we check our result in the case of the free scalar BCFT in $d = 5$. In subsection 6.2.1.3 we comment on other correlators of \mathcal{D}^i and their possible relation to defect/boundary central charges.

6.2.1.1 Relating $c_{\mathcal{D}\mathcal{D}}$ to $d_1^{(4d)}$ and $b_1^{(4d)}$

Here we consider an infinitesimal shape perturbation of the flat defect, $\delta X^i(x_{\parallel})$. In this subsection we will keep p generic, and at the end set $p = 4$. Up to second order in the shape perturbation, the variation of the effective action reads

$$\delta_X \mathcal{W} = -\frac{1}{2} \int_{\Sigma_p} d^p x_{\parallel} d^p y_{\parallel} \langle \mathcal{D}_i(x_{\parallel}) \mathcal{D}_j(y_{\parallel}) \rangle \delta X^i(x_{\parallel}) \delta X^j(y_{\parallel}) + \mathcal{O}(\delta X^3), \quad (6.2.13)$$

where by translational invariance along the flat defect, $\langle \mathcal{D}_i \rangle = 0$. To isolate the logarithmic divergence we first define $s_{\parallel} \equiv x_{\parallel} - y_{\parallel}$ and substitute eq. (3.1.17) into eq. (6.2.13) obtaining

$$\begin{aligned} \delta_X \mathcal{W} &= -\frac{c_{\mathcal{D}\mathcal{D}}}{2} \int_{\Sigma_p} d^p x_{\parallel} \int_{\Sigma_p} d^p s_{\parallel} \frac{1}{|s_{\parallel}|^{2p+2}} \delta X^i(x_{\parallel}) \delta X^i(x_{\parallel} - s_{\parallel}) + \mathcal{O}(\delta X^3) \\ &\supset -\frac{c_{\mathcal{D}\mathcal{D}}}{2} \int_{\Sigma_p} d^p x_{\parallel} \int_{\Sigma_p} d^p s_{\parallel} \frac{1}{|s_{\parallel}|^{2p+2}} \frac{s^{a_1} \dots s^{a_{p+2}}}{(p+2)!} \delta X^i(x_{\parallel}) \partial_{a_1} \dots \partial_{a_{p+2}} \delta X^i(x_{\parallel}), \end{aligned} \quad (6.2.14)$$

where we are summing over the repeated i indices. In the second line, we Taylor expanded $\delta X^i(x_{\parallel} - s_{\parallel})$ up to order $p+2$ in s_{\parallel} , and only kept the highest order to isolate the logarithmic part. For even p , the integral over s_{\parallel} can be computed using the identity

$$\int d^p s_{\parallel} \frac{1}{|s_{\parallel}|^{2p+2}} s^{a_1} \dots s^{a_{p+2}} = \text{vol}(S^{p-1}) \frac{(p-2)!!}{(2p)!!} \int_{\epsilon}^L ds \frac{1}{s} [\delta^{a_1 a_2} \dots \delta^{a_{p+1} a_{p+2}} + \text{perm}], \quad (6.2.15)$$

where ϵ and L are UV and IR cut-offs, respectively, and perm stands for permutations of indices excluding pairwise exchange on each δ^{ab} . For odd p , the integral over s_{\parallel} vanishes identically, so we will assume that p is even for the remainder of this computation. Using the fact that the number of permutations is $(p+1)!!$, we obtain for the coefficient of $\log \frac{L}{\epsilon}$

$$\delta_X \mathcal{W} \Big|_{\log \frac{L}{\epsilon}} = (-1)^{p/2} \frac{2^{-(p+2)} \pi^{\frac{p}{2}}}{p! \Gamma(\frac{p}{2} + 2)} c_{\mathcal{D}\mathcal{D}} \int_{\Sigma_p} d^p x_{\parallel} \partial^{a_1} \dots \partial^{a_{p/2+1}} \delta X^i \partial_{a_1} \dots \partial_{a_{p/2+1}} \delta X^i, \quad (6.2.16)$$

where we have used $\text{vol}(S^{p-1}) = 2\pi^{\frac{p}{2}} / \Gamma(\frac{p}{2})$. Let us rewrite the above equation in terms of the second fundamental form. At leading order we have $\delta \Pi_{ab}^i = \partial_a \partial_b \delta X^i$. We

thus find

$$\delta_X \mathcal{W}|_{\log \frac{L}{\epsilon}} = (-1)^{p/2} \frac{2^{-(p+2)} \pi^{\frac{p}{2}}}{p! \Gamma(\frac{p}{2} + 2)} c_{\mathcal{DD}} \int_{\Sigma_p} d^p x_{\parallel} \partial^{a_1} \dots \partial^{a_{p/2-1}} \delta \Pi^{icd} \partial_{a_1} \dots \partial_{a_{p/2-1}} \delta \Pi_{cd}^i. \quad (6.2.17)$$

Taking $p = 4$, we find for the logarithmically divergent part of $\delta_X \mathcal{W}$,

$$\delta_X \mathcal{W}|_{\log \frac{L}{\epsilon}} = -\frac{1}{2} \frac{\pi^2}{4608} c_{\mathcal{DD}} \int_{\Sigma_p} d^p x_{\parallel} \delta \Pi^{icd} \bar{\square} \delta \Pi_{cd}^i, \quad (6.2.18)$$

where $\bar{\square} \equiv \partial_a \partial^a$.

The next step is to relate $c_{\mathcal{DD}}$ to the coefficients in the defect or boundary Weyl anomaly, eq. (6.1.1) or (6.1.10), respectively. By eq. (2.5.53), the logarithmic divergence in the effective action needs to match the anomaly, so we should compute to second order the shape deformation of eq. (6.1.1) around the configuration of a flat defect embedded in a flat ambient space. Among all of the terms in the defect anomaly, only \mathcal{J}_1 contains an appropriate structure to contribute at second order in the variation, which reads

$$\begin{aligned} \delta_X \int_{\Sigma_4} d^4 x_{\parallel} \langle T^\mu{}_\mu \rangle &= \frac{d_1^{(4d)}}{72\pi^2} \int_{\Sigma_4} d^4 x_{\parallel} \partial^b \delta \Pi_{ab}^i \partial^c \delta \Pi_{ic}^a + \mathcal{O}(\delta \Pi^3) \\ &= \frac{d_1^{(4d)}}{72\pi^2} \int_{\Sigma_4} d^4 x_{\parallel} \frac{9}{16} \partial^a \partial^b \partial^c \delta X^i \partial_a \partial_b \partial_c \delta X^i + \mathcal{O}(\delta X^3). \end{aligned} \quad (6.2.19)$$

Comparing eq. (6.2.19) to (6.2.16) then gives our main result of this subsection,

$$c_{\mathcal{DD}} = -\frac{72}{\pi^4} d_1^{(4d)}. \quad (6.2.20)$$

Performing an identical computation in the boundary case using eq. (6.1.10), we find

$$c_{\mathcal{DD}} = -\frac{72}{\pi^4} b_1^{(4d)}. \quad (6.2.21)$$

As a check of our methods, let us consider $p = 2$. In that case, eq. (6.2.17) reduces to

$$\delta_X \mathcal{W}|_{\log \frac{L}{\epsilon}} = -\frac{\pi}{64} c_{\mathcal{DD}} \int_{\Sigma_2} d^2 x_{\parallel} \delta \Pi^{icd} \delta \Pi_{cd}^i, \quad (6.2.22)$$

and by direct comparison to the defect Weyl anomaly in eq. (3.4.38) we obtain $d_1^{(2d)} = \frac{3\pi^4 c_{\mathcal{DD}}}{4}$, reproducing the known result for $d = 4$ in eq. (3.4.40). In fact, our calculation shows that eq. (3.4.40) is valid for any d .

6.2.1.2 Check of the result for the free scalar BCFT in $d = 5$

We can check our result for the boundary case, eq. (6.2.21), using a free, massless scalar in $d = 5$, in the presence of a boundary. On the one hand, $b_1^{(4d)} = -\frac{1}{256}$ was computed in ref. [161] using heat kernel methods. This answer is in fact independent of the boundary conditions, Neumann or Dirichlet. On the other hand, we can compute the displacement operator two-point function in flat space using Wick's theorem. The displacement operator in the $q = 1$ case can be identified with the boundary limit of the T^{mn} component of the stress tensor, see eq. (3.1.16). For a conformally coupled scalar with action in eq. (2.4.39), the improved stress tensor takes the form

$$T^{\mu\nu} = (\partial^\mu\phi)(\partial^\nu\phi) - \frac{1}{2}\delta^{\mu\nu}(\partial_\rho\phi)(\partial^\rho\phi) - \frac{d-2}{4(d-1)}(\partial^\mu\partial^\nu - \delta^{\mu\nu}\square)\phi^2,$$

where we have set $g_{\mu\nu} = \delta_{\mu\nu}$. Using the scalar's EOM, the displacement operator follows from the boundary limit of T^{mn} :

$$\mathcal{D}_D = \frac{1}{2}(\partial_n\phi)(\partial_n\phi), \quad \mathcal{D}_N = -\frac{1}{2}(\partial_a\phi)(\partial^a\phi) + \frac{d-2}{4(d-1)}\partial_a\partial^a\phi^2, \quad (6.2.23)$$

with subscript D for Dirichlet and N for Neumann. If we normalise the two-point function of the scalar to take the form

$$\langle\phi(x_\parallel, x_\perp)\phi(0, 0)\rangle = \kappa \left(\frac{1}{(x_\perp^2 + |x_\parallel|^2)^{(d-2)/2}} \pm \frac{1}{(x_\perp^2 + |x_\parallel|^2)^{(d-2)/2}} \right),$$

with a plus sign for Neumann and minus sign for Dirichlet, then Wick's theorem yields

$$\langle\mathcal{D}(x_\parallel)\mathcal{D}(0)\rangle = \frac{2(d-2)^2\kappa^2}{|x_\parallel|^{2d}}, \quad (6.2.24)$$

in both cases. The standard normalisation, $\kappa^{-1} = (d-2)\text{vol}(S^{d-1})$, with $d = 5$ then gives $c_{\mathcal{D}\mathcal{D}} = \frac{9}{32\pi^4}$. Plugging this into eq. (6.2.21) then gives us $b_1^{(4d)} = -\frac{1}{256}$, in agreement with the heat kernel result, as expected.

6.2.1.3 Comments on other correlators of the displacement operator

Having successfully established a relationship between $c_{\mathcal{D}\mathcal{D}}$ and the Weyl anomaly for $p = 4$ defects, it is natural to wonder if additional relationships can be established between the Weyl anomaly and other displacement operator correlation functions. One natural candidate is the displacement operator three-point function,

$$\langle\mathcal{D}(x_\parallel)\mathcal{D}(y_\parallel)\mathcal{D}(z_\parallel)\rangle = \frac{c_{\mathcal{D}\mathcal{D}\mathcal{D}}}{|x_\parallel - y_\parallel|^5|y_\parallel - z_\parallel|^5|x_\parallel - z_\parallel|^5}, \quad (6.2.25)$$

with constant $c_{\mathcal{D}\mathcal{D}}$. In the $d = 4$ case with $p = 3$ dimensional boundary, such a correlation function determines the coefficient of the $\text{Tr } \mathring{K}^3$ term in the Weyl anomaly [52], as shown in eq. (3.4.48). However, in our $p = 4$ case, there are no terms in the Weyl anomaly with an odd number of derivatives and extrinsic curvatures, precluding the displacement three-point function from determining a piece of the Weyl anomaly.

Another obvious correlation function to investigate is $\langle T^{\mu\nu}(x_{\parallel}, x_{\perp}) \mathcal{D}^i(y_{\parallel}) \rangle$, which is also determined by conformal symmetry, up to two constants [147]. In the co-dimension $q = 1$ case, the tensor structures simplify and the correlation function is determined by a single overall constant, which turns out to be $c_{\mathcal{D}\mathcal{D}}$. After some work in the $q = 1$ case, we were able to check that the scale anomaly in $\langle T^{\mu\nu}(x_{\parallel}, x_{\perp}) \mathcal{D}(y_{\parallel}) \rangle$ is consistent with the coefficients of the $\mathring{K}^{ab} D_n W_{ambn}$ and $\bar{D}^a \mathring{K}_{ab} \bar{D}_c \mathring{K}^{bc}$ terms in eq. (6.1.11). In the higher co-dimension case, ref. [147] argued that $\langle T^{\mu\nu}(x_{\parallel}, x_{\perp}) \mathcal{D}^i(y_{\parallel}) \rangle$ is determined by both $c_{\mathcal{D}\mathcal{D}}$ and a_T . However, the tensor structures involved make the analysis more complicated, and we leave this as an exercise for the future.

Other correlation functions involving the stress tensor and displacement operator tend to involve undetermined functions of a cross ratio, as well as sums over tensor structures. We have not found useful candidates to explore, except for $\langle T^{\mu\nu} \rangle$, which we turn to next.

6.2.2 Stress-tensor one-point function

In this subsection, we compute the one-point function of the stress tensor, $\langle T^{\mu\nu} \rangle$, in two cases. First, in subsection 6.2.2.1, we consider $\langle T^{\mu\nu} \rangle$ for a flat $p = 4$ defect in a $d \geq 6$ ambient CFT. Our results will be similar to those for a $p = 2$ defect in $d > 3$, reviewed in sec. 3.4. By applying the method of ref. [162] (see also ref. [163]), we will show that the coefficient h in eq. (3.1.13) and the defect Weyl anomaly coefficient $d_2^{(4d)}$ in eq. (6.1.1) are related as $h \propto -d_2^{(4d)}$. Using this result, we will then Wick-rotate to Lorentzian signature and assume the ANEC applies in the presence of a defect to argue that $d_2^{(4d)} \leq 0$. By combining the relation between h and $d_2^{(4d)}$ with a result of ref. [49], we will also show that the defect contribution to the universal part of the EE of a region centred on the defect is a linear combination of $a_{\Sigma}^{(4d)}$ and $d_2^{(4d)}$. Second, in subsection 6.2.2.2, we will consider $\langle T^{\mu\nu} \rangle$ in a $d = 5$ BCFT with a curved boundary. In that case the near-boundary expansion of $\langle T^{\mu\nu} \rangle$ has a number of free coefficients [315, 316], which we determine in terms of some boundary central charges from eq. (6.1.10).

6.2.2.1 Relating h to d_2 for a flat defect in flat space

In the context of computing Rényi entropies, where the defect is the co-dimension $q = 2$ twist defect, the authors of ref. [162] consider the relation between $\langle T_{\mu\nu} \rangle$ and the anomaly term $\square W^{ij}_{ij}$ when $d = 6$.⁵ Here we repeat their analysis, now keeping the co-dimension of the defect arbitrary, provided $q > 1$. We will focus on \mathcal{J}_2 in eq. (6.1.1), the only term in the anomaly that contains $\square W^{ij}_{ij}$,

$$T^\mu{}_\mu \supset \frac{d_2^{(4d)}}{16\pi^2} \frac{1}{3} D^i D_i W^{ab}{}_{ab} \delta_{\Sigma_4}^{(q)} + \mathcal{O}(R^2), \quad (6.2.26)$$

where we used tracelessness of $W_{\mu\nu\rho\sigma}$ to swap freely between W^{ij}_{ij} and $W^{ab}{}_{ab}$. In eq. (6.2.26), $\mathcal{O}(R^2)$ stands for terms at least quadratic in the curvatures, which will not be important to establish that $h \propto -d_2^{(4d)}$.

The starting point for the computation is the ambient CFT on $\mathcal{M}_d = \mathbb{R}^d$ with metric $\delta_{\mu\nu}$ and a flat defect wrapping $\Sigma = \mathbb{R}^4 \hookrightarrow \mathbb{R}^d$. We then perturb the flat ambient metric so that $\delta_{\mu\nu} \rightarrow g_{\mu\nu} = \delta_{\mu\nu} + \delta g_{\mu\nu}$. To first order in the metric perturbation, the effective action changes as

$$\delta_g \mathcal{W} = -\frac{1}{2} \int d^d x \langle T^{\mu\nu} \rangle \delta g_{\mu\nu}. \quad (6.2.27)$$

Crucially, since we have assumed that the perturbation is about both a flat background and flat defect, we can employ the form of the stress tensor given in eq. (3.1.13).

Since in curved space the Weyl anomaly is generically non-trivial, we expect that eq. (6.2.27) will contain a logarithmic divergence of the form in eq. (2.5.53). In particular, consistency between eq. (6.2.27) and eq. (2.5.53) implies

$$\delta_g \int d^d x \sqrt{g} \langle T^\mu{}_\mu \rangle = \frac{1}{2} \int d^d x \langle T^{\mu\nu} \rangle \delta g_{\mu\nu} \Big|_{\log \frac{L}{\epsilon}}. \quad (6.2.28)$$

In the anomaly eq. (6.1.1), \mathcal{J}_2 is the only conformal invariant that contains terms at most linear in both the Weyl tensor and $\hat{\Pi}_{ab}^i$. The term in eq. (6.2.26) is the only one that contributes to the first-order perturbation about the flat configuration.

Let us analyse the expressions on either side of eq. (6.2.28) separately, starting with the left-hand side. The first order variation of the integral of eq. (6.2.26) over the defect's submanifold Σ_4 may be written as

$$\delta_g \int_{\Sigma_4} d^4 \sigma \sqrt{g} \langle T^\mu{}_\mu |_{\Sigma_4} \rangle = \frac{d_2^{(4d)}}{16\pi^2} \int_{\Sigma_4} d^4 x_{\parallel} \frac{1}{3} \partial^k \partial_k \delta W^{ab}{}_{ab}, \quad (6.2.29)$$

⁵See also ref. [131], which considered EE in a $d = 6$ dimensional CFT, but which has an error in the analysis of the contribution to the anomaly containing the $\square W^{ij}_{ij}$ term. Specifically, in the third line of eq. (2.28) of ref. [131], the variation of the term $I_3 = W_{\mu\rho\sigma\tau} (\square \delta^\mu{}_\nu + 4R^\mu{}_\nu - \frac{6}{5} R \delta^\mu{}_\nu) W^{\nu\rho\sigma\tau}$ in the ambient Weyl anomaly does not result in a conformally invariant term along the entangling surface. Indeed, a further Weyl variation vanishes up to terms that are total derivatives in the *normal* directions, but which cannot be dropped in the integral over the entangling surface's directions.

where we dropped terms that are higher order in curvature, or subleading in the perturbation such that the integral can be evaluated on \mathbb{R}^4 with coordinates x_{\parallel} . This short computation gives us all of the information that we will need about the left-hand side of eq. (6.2.28).

The evaluation of the right-hand side of eq. (6.2.28) is slightly more involved. Using the form of $\langle T^{\mu\nu} \rangle$ derived in section 3.1 leading to eq. (3.1.13), we can write the right-hand side of eq. (6.2.28) as

$$\int d^d x \langle T^{\mu\nu} \rangle \delta g_{\mu\nu} = h \int d^d x \left[\frac{(d-q+1)}{|x_{\perp}|^d} \delta^{ij} \delta g_{ij} - \frac{(q-1)}{|x_{\perp}|^d} \delta^{ab} \delta g_{ab} - \frac{d \hat{x}^j \hat{x}^i}{|x_{\perp}|^d} \delta g_{ij} \right], \quad (6.2.30)$$

where $\hat{x}^i = \frac{x^i}{|x_{\perp}|}$. The perturbed metric $g_{\mu\nu} = \delta_{\mu\nu} + \delta g_{\mu\nu}$ admits an expansion near the defect of the form in eq. (2.16) of ref. [317]. We observe that log-divergent contributions in eq. (6.2.30) can only arise from terms with near-defect behaviour like $1/|x_{\perp}|^d$. Since $d = q + 4$, we will need the fourth order in the perturbed metric's near-defect expansion, which has

$$\delta g_{ij} \supset -\frac{1}{20} \partial_m \partial_n \delta R_{ikj\ell} \Big|_{\Sigma_4} x^m x^n x^k x^\ell, \quad (6.2.31)$$

where $\delta R_{ikj\ell} \Big|_{\Sigma_4}$ is the Riemann tensor of the metric perturbed around flat space, $g_{\mu\nu}$, and evaluated on the defect. Note that terms of the form $\mathcal{O}(R^2)$ in the near defect expansion of the metric vanish for a first order perturbation around flat space. Since the orthogonal and transverse directions are independent, for computational ease we can simply match terms that have only transverse components. Plugging eq. (6.2.31) into eq. (6.2.30) and using the anti-symmetry of the Riemann tensor to eliminate the $x^i x^j \delta g_{ij}$ term, we then adopt cylindrical coordinates (ρ, θ_i) around the defect, located at $\rho = 0$, to write

$$\int d^d x \langle T^{\mu\nu} \rangle \delta g_{\mu\nu} \supset -\frac{h}{4} \int_{\Sigma_4} d^4 x_{\parallel} \partial_r \partial_s \delta R_{ikj\ell} \Big|_{\Sigma_4} \int_{\epsilon}^L d\rho \frac{1}{\rho} \int d\Omega_{q-1} \hat{x}^r \hat{x}^s \hat{x}^k \hat{x}^\ell, \quad (6.2.32)$$

where we introduced a UV cut-off ϵ and an IR cut-off L to regulate the ρ -integral around the location of the defect. The angular integral can easily be computed using the following relation,

$$\int d\Omega_{q-1} \hat{x}^{i_1} \dots \hat{x}^{i_n} = \frac{(q+n-2)!!}{(q-2)!!} \text{vol}(S^{q-1}) (\delta^{i_1 i_2} \dots \delta^{i_{n-1} i_n} + \text{perm}), \quad (6.2.33)$$

where perm denotes pairwise permutations in the i_n indices. Performing the angular integral in eq. (6.2.32) then allows us to compute the ρ -integral easily, which produces a logarithmic divergence in ϵ . The totally transverse part of the coefficient of $\log \epsilon$ is

$$\int d^d x \langle T^{\mu\nu} \rangle \delta g_{\mu\nu} \Big|_{\log \frac{L}{\epsilon}, \perp} = -\frac{h \text{vol}(S^{q-1})}{4 q(q+2)} \int_{\Sigma_4} d^4 x_{\parallel} [\partial^2 \delta R_{ikik} + 2\partial_k \partial_\ell \delta R_{ikj\ell}]. \quad (6.2.34)$$

Moreover, one can easily show that at first-order in the perturbation

$$2\partial_k\partial_\ell\delta R_{ikil} = \partial^2\delta R_{ikik}, \quad (6.2.35)$$

so that eq. (6.2.34) becomes

$$\int \mathbf{d}^d x \langle T^{\mu\nu} \rangle \delta g_{\mu\nu} \Big|_{\log \frac{\ell}{\epsilon}, \perp} = -\frac{h}{2q(q+2)} \text{vol}(S^{q-1}) \int_{\Sigma_4} \mathbf{d}^4 x_{\parallel} \partial^2 \delta R_{ikik}. \quad (6.2.36)$$

In order to compare eq. (6.2.36) to eq. (6.2.29), we use that at first order in the metric perturbation,

$$\delta W^{ab}{}_{ab} \Big|_{\perp} = \frac{12}{6+5q+q^2} \delta R_{ijij}, \quad (6.2.37)$$

where we have used the fact that we are perturbing around flat space, and we have only kept terms that solely have transverse components. Finally, by plugging eq. (6.2.37) into eq. (6.2.29), and comparing to eq. (6.2.36) through the relation eq. (6.2.28), we arrive at the generic relation between the coefficient h that fixes $\langle T^{\mu\nu} \rangle$ and the defect Weyl anomaly coefficient $d_2^{(4d)}$, for a co-dimension q conformal defect in a $d = q + 4$ CFT:

$$h = -\frac{\Gamma(\frac{q}{2} + 1)}{\pi^{\frac{q}{2}+2} (q+3)} d_2^{(4d)}. \quad (6.2.38)$$

For the special case of $q = 2$, which will be useful for the monodromy defects considered in chapter 7, eq. (6.2.38) becomes

$$h = -\frac{1}{5\pi^3} d_2^{(4d)}, \quad (6.2.39)$$

such that the conjecture for superconformal defects eq. (5.5.15) implies the following relation between defect central charges

$$d_1^{(4d)} = 2d_2^{(4d)}. \quad (6.2.40)$$

Upon taking into account the different conventions, this agrees with ref. [162].⁶

Following the example of a $p = 2$ defect in $d \geq 4$ reviewed in section 3.4, we can use our result for the $p = 4$ defect in eq. (6.2.38) to show that $d_2^{(4d)} \leq 0$, if we assume that the ANEC holds in the presence of the defect. We Wick-rotate to Lorentzian signature, and take Σ_4 to be a flat, static defect in $d \geq 6$ -dimensional Minkowski space. We consider a null geodesic passing at a minimal distance ℓ away from Σ_4 and oriented at

⁶The case of a $p = 2$ defect with Weyl anomaly in eq. (3.4.38) proceeds similarly. By the same arguments, h must depend on the defect Weyl anomaly coefficients of terms at most linear in the intrinsic and extrinsic curvature tensors. Since the Euler term is topological, it is invariant under metric perturbations. Thus, only the $W^{ab}{}_{ab}$ term can contribute. The remaining argument proceeds as in the $p = 4$ case, the only notable difference being that $\delta g_{ij} \supset -\frac{1}{3}\delta R_{ikj\ell}|_{\Sigma_2} x^k x^\ell$ suffices to obtain the logarithmic contribution.

an angle ψ out of the plane. We take the following family of null geodesics parametrised as

$$t = \ell u, \quad x_1 = \ell u \cos \psi, \quad x_4 = \ell u \sin \psi, \quad x_5 = \ell, \quad (6.2.41)$$

while all the other components are set to zero. Here t, x_1 are coordinates parallel to the defect and x_4, x_5 are orthogonal. By plugging eq. (6.2.41) and eq. (3.1.13) into the ANEC and using eq. (6.2.38), we obtain

$$\int_{-\infty}^{\infty} du \langle T_{\mu\nu} \rangle v^\mu v^\nu = -d_2^{(4d)} \frac{q \Gamma\left(\frac{d+1}{2}\right) \Gamma\left(\frac{q}{2}\right)}{(q+3) \Gamma\left(\frac{d}{2}\right) \pi^{\frac{q+3}{2}} \ell^{d-2}} |\sin \psi| \geq 0, \quad (6.2.42)$$

and hence $d_2^{(4d)} \leq 0$, as advertised.

Also following the example of a $p = 2$ defect in $d > 3$ in section 3.4, we can use our result in eq. (6.2.38), combined with a result of ref. [49], to show that $d_2^{(4d)}$ contributes to the universal part of the EE of a spherical region centred on the defect. Wick-rotating to Lorentzian signature and fixing the time, we consider a compact, spherical entangling region A of radius L that is co-original with Σ_4 , such that the intersection $\partial A \cap \Sigma_4$ is an equatorial S^2 . The general expression for the universal part of the defect EE for a p -dimensional conformal defect is given by eq. (4.5.46). When p is even, the universal part is the coefficient of $\log \frac{L}{\epsilon}$, and the pole for even p (arising from dimensional regularisation), maps to a logarithmic divergence in the UV cut-off ϵ . In particular, for $p = 4$, the universal part of the defect EE is

$$S_{A, \Sigma_4} = -4 \left[a_{\Sigma}^{(4d)} - \frac{(d-5)\pi^{d/2}}{2\Gamma\left(\frac{d}{2}-2\right)} h \right] \log\left(\frac{L}{\epsilon}\right), \quad (6.2.43)$$

where we used that

$$F^{(\text{def})} \Big|_{\log \frac{L}{\epsilon}} = \frac{a_{\Sigma}^{(4d)}}{(4\pi)^2} \int_{S^4} d^4\sigma \sqrt{\bar{g}} \bar{E}_4 = 4a_{\Sigma}^{(4d)}. \quad (6.2.44)$$

Using our result in eq. (6.2.38), we thus find for the universal part of the EE

$$S_{A, \Sigma_4} = -4 \left[a_{\Sigma}^{(4d)} + \frac{1}{4} \frac{(d-5)(d-4)}{d-1} d_2^{(4d)} \right] \log\left(\frac{L}{\epsilon}\right). \quad (6.2.45)$$

This result highlights the key fact that the universal part of the defect EE is not necessarily monotonic under defect RG flows. That is, in spite of the c-theorem for $a_{\Sigma}^{(4d)}$ proven in ref. [57], and since no c-theorems are known for B-type anomalies, the presence of $d_2^{(4d)}$ means eq. (6.2.45) is not necessarily monotonic under defect RG flows. Note that additional central charges may appear in the coefficient of the logarithmic divergence if one considers entangling regions with a generic shape intersecting the

defect, as discussed in refs. [47, 318] in the $d = 4$ case with a boundary. We leave the study of this more general case to future work.

6.2.2.2 Boundary Weyl anomalies and $\langle T^{\mu\nu} \rangle$ with curved boundaries

In this subsection, we consider a $d = 5$ dimensional ambient CFT on a curved background \mathcal{M}_5 with a boundary, $\partial\mathcal{M}_5 \neq \emptyset$. Since we assume that \mathcal{M}_5 is not flat, the stress-tensor picks up a non-trivial one-point function in the near-boundary expansion. We will thus find a relation between some of the boundary central charges in eq. (6.1.10) and the coefficients in the leading divergences of $\langle T_{\mu\nu} \rangle$.

Generically, when a CFT is defined on a background with a curved boundary, the near-boundary expansion of $\langle T_{\mu\nu} \rangle$ has divergences of the form [315, 316]

$$\langle T_{\mu\nu} \rangle = \frac{T_{\mu\nu}^{(d)}}{x_{\perp}^d} + \frac{T_{\mu\nu}^{(d-1)}}{x_{\perp}^{d-1}} + \frac{T_{\mu\nu}^{(d-2)}}{x_{\perp}^{d-2}} + \dots, \quad (6.2.46)$$

where x_{\perp} is the geodesic distance from the boundary located at $x_{\perp} = 0$. The first three divergences can be computed simply by requiring that $T_{\mu\nu}$ is conserved and traceless [315].

The residual conformal symmetry at the boundary is enough to constrain the leading $1/x_{\perp}^d$ divergence to vanish identically, $T_{\mu\nu}^{(d)} = 0$. The subleading divergences, however, have much richer structures determined by the Weyl and extrinsic curvatures:

$$(4\pi)^2 T_{\mu\nu}^{(d-1)} = A_T \check{K}_{\mu\nu}, \quad (6.2.47)$$

and

$$\begin{aligned} (4\pi)^2 T_{\mu\nu}^{(d-2)} = & \frac{A_T}{d-2} \left(n_{\mu} n_{\nu} - \frac{h_{\mu\nu}}{d-1} \right) \text{tr} \check{K}^2 - 2 \frac{A_T}{d-1} n_{(\mu} h_{\nu)}^{\rho} D_{\rho} K - \frac{2A_T}{d-2} n_{(\mu} h_{\nu)}^{\rho} R_{\rho n} \\ & - 2A_T \check{K}_{(\mu}^{\rho} K_{\nu)\rho} + \beta_1 W_{\mu\rho\nu\sigma} n^{\rho} n^{\sigma} + \beta_2 K \check{K}_{\mu\nu} + \beta_3 \left((K^2)_{\mu\nu} - \frac{h_{\mu\nu}}{d-1} \text{tr} K^2 \right), \end{aligned} \quad (6.2.48)$$

where parentheses indicate symmetrisation over the enclosed indices.⁷ In ref. [316], the authors related the coefficients A_T , β_1 , β_2 and β_3 to the boundary central charges for dimensions $d = 3$ and 4 . Below, we will find such relations for the case $d = 5$.

To relate the near-boundary data $(A_T, \beta_1, \beta_2, \beta_3)$ to the coefficients in eq. (6.1.10), we again employ eq. (6.2.28). We begin by evaluating the left-hand side of eq. (6.2.28), which requires a first-order metric variation of the integrated Weyl anomaly. For ease

⁷In ref. [316] the authors allowed for a term of the form $\bar{R}_{\mu\nu} - 1/4 \bar{R} \bar{g}_{\mu\nu}$, which is argued to be inconsistent with conformal symmetry in ref. [315]. In addition, ref. [316] found that this term is absent both when $d = 3$ and $d = 4$. The presence or absence of this term does not affect the calculation here.

of computation, and to facilitate matching with the right-hand side, we write the background metric in Gaussian normal coordinates,

$$ds^2 = dx_\perp^2 + g_{ab}(x_\perp, \sigma) d\sigma^a d\sigma^b. \quad (6.2.49)$$

We next write the near-boundary expansion of the components $g_{ab}(x_\perp, \sigma)$ in eq. (6.2.49) up to third order in the geodesic distance x_\perp from the boundary,

$$ds^2 = dx_\perp^2 + \left[\bar{g}_{ab} - 2K_{ab}x_\perp + (K_{ab}^2 - R_{anbn})x_\perp^2 + \right. \\ \left. - \frac{1}{3} (\partial_n R_{anbn} - R_{ancn}K^c{}_b - R_{cnbn}K^c{}_a) x_\perp^3 + \mathcal{O}(x_\perp^4) \right] d\sigma^a d\sigma^b. \quad (6.2.50)$$

On the right-hand side, the variations δK_{ab} and $\delta \bar{g}_{ab}$ around the background eq. (6.2.50) would contribute to the logarithmic divergence also at the orders $\mathcal{O}(1/x_\perp^2)$ and $\mathcal{O}(1/x_\perp)$, respectively, corresponding to $T_{\mu\nu}^{(2)}$ and $T_{\mu\nu}^{(1)}$. However, since the form of the one-point function of the stress tensor is only known up to order $\mathcal{O}(1/x_\perp^3)$, we need to restrict to metric perturbations that obey $\delta K_{ab} = \delta \bar{g}_{ab} = 0$, allowing only the variations δR_{anbn} and $\delta \partial_n R_{anbn}$ to be non-trivial. To simplify the computation further, we assume without loss of generality that the boundary metric is flat, $\bar{g}_{ab} = \delta_{ab}$, and we use x_\parallel to denote the boundary coordinates. With these assumptions, the left-hand side, i.e. the variation of the anomaly, gives

$$\delta_g \int d^5x \sqrt{g} \langle T^\mu{}_\mu \rangle = \frac{1}{(4\pi)^2} \int_{\partial\mathcal{M}_5} d^4x_\parallel \left\{ -b_1^{(4d)} \frac{2}{3} K^{ab} \delta \partial_n R_{anbn} + \left[\frac{2}{3} (b_6^{(4d)} + b_7^{(4d)} - 2b_1^{(4d)}) K^{ac} K^b{}_c \right. \right. \\ \left. \left. + \frac{1}{12} (b_6^{(4d)} + b_7^{(4d)}) K^2 \delta^{ab} + \frac{1}{6} (3b_1^{(4d)} - 2b_6^{(4d)} - 2b_7^{(4d)}) K K^{ab} \right. \right. \\ \left. \left. - \frac{1}{6} (b_1^{(4d)} + b_6^{(4d)} + b_7^{(4d)}) \text{tr} K^2 \delta^{ab} + \frac{4}{3} (2b_4^{(4d)} + b_5^{(4d)}) W^{anbn} \right] \delta R_{anbn} \right\}. \quad (6.2.51)$$

On the right-hand side of eq. (6.2.28), we need the log-divergent part of the integral of eq. (6.2.46) in the near-boundary expansion of the metric in eq. (6.2.50). A straightforward computation as in the previous subsection yields the same structure as in eq. (6.2.51), with the identifications

$$A_T = 4b_1^{(4d)}, \quad \beta_1 = -\frac{8}{3} (2b_4^{(4d)} + b_5^{(4d)}), \quad (6.2.52) \\ \beta_2 = \frac{2}{3} (b_6^{(4d)} + b_7^{(4d)}) + \frac{13}{3} b_1^{(4d)}, \quad \beta_3 = -\frac{4}{3} (2b_1^{(4d)} + b_6^{(4d)} + b_7^{(4d)}).$$

One interesting point to note about the relations in eq. (6.2.52) is that they are all invariant under the change of basis that replaces the intrinsic Euler density with Q -curvature. That is, the relations in eq. (6.2.52) are invariant under the shifts in eq. (6.1.6), after using the map from defect to boundary central charges in eq. (6.1.12). Specifically, under these shifts $b_1^{(4d)}$ and $b_8^{(4d)}$ are invariant, while all other boundary

central charges are shifted non-trivially by multiples of $a_{\Sigma}^{(4d)}$. This raises the question of whether the invariance of eq. (6.2.52) under this change of basis is universal to all orders, or if it is spoiled at fourth-order by contributions due to δK_{ab} and $\delta \bar{g}_{ab}$. We leave this question for future research.

6.3 Discussion

In this chapter, we determined the most general form of the Weyl anomaly for a conformal defect of dimension $p = 4$ in an arbitrary CFT of dimension $d \geq 6$. Our main result for the Weyl anomaly of a $p = 4$ conformal defect with co-dimension $q \geq 1$ is eq. (6.1.1), with 23 parity-even terms and 6 parity-odd terms, plus the additional parity-odd terms in eqs. (6.1.8) and (6.1.9) for $q = 2$ and $q = 4$, respectively. Among the 23 parity-even terms, one is A-type while all the others are B-type. The parity-odd terms are all B-type. Each of these terms comes with a coefficient that defines a defect central charge. For $p = 4$ conformal defects with $q = 1$, our result reduces to eq. (6.1.10), which reproduces the 9 parity-even terms first obtained by ref. [161]. This served as a non-trivial check of our results. Moreover, beyond the parity-even anomalies, we found 3 parity-odd terms that were previously unknown. We subsequently showed in section 6.2 how some of the defect central charges appear in physical observables (besides the Weyl anomaly itself), namely the two-point function of the displacement operator, the one-point function of the stress tensor, and the universal contribution to EE of a spherical region centred on a flat defect.

Our results raise a host of questions, and suggest many directions for future research. Many questions remain about how defect/boundary central charges appear in physical observables. For example, in the calculation of EE in a standalone $d = 6$ CFT for a region with arbitrary shape, the contribution to the universal part will have the form of the Weyl anomaly in eq. (6.1.1), but with defect central charges fixed by the ambient CFT's central charges in eq. (2.5.71). Establishing the full map between ambient and defect central charges remains an important open question.

Further, how do defect/boundary central charges appear in higher-point functions of the displacement operator, mixed correlators like $\langle TDD \rangle$, not to mention thermal entropy, heat capacity, conductivities, and so on? Answering these questions could be especially enlightening for the many parity-odd defect/boundary central charges we found, which remain particularly mysterious. More generally, answering these questions could allow us to compute all the defect/boundary central charges in many important examples, including free-field CFTs, like the monodromy defects discussed in chapter 7, as well as interacting CFTs, such as $p = 4$ defects in $d = 6$ SCFTs.

If we can determine how defect/boundary central charges enter physical observables, then we can ask whether any general principles provide bounds on them. In

eq. (6.2.20) we found that the normalisation of the displacement operator's two-point function was $\propto -d_1$ for a defect and $\propto -b_1$ for a boundary, hence reflection positivity requires $d_1 \leq 0$ or $b_1 \leq 0$, respectively. In eq. (6.2.38) we found that, for $q \geq 2$, the normalisation of the stress-tensor's one-point function was $\propto -d_2$, so that if the ANEC is valid in the presence of a defect, then $d_2 \leq 0$. Since the A-type central charge $a_{\Sigma}^{(4d)}$ obeys a c-theorem for boundary/defect RG flows [57], we can ask whether it is bounded from below. This bound cannot be zero, since $a_{\Sigma}^{(4d)} < 0$ in explicit (reflection-positive) examples, including a free scalar BCFT in $d = 5$ with Dirichlet boundary conditions (see [161]). Perhaps defect/boundary central charges are bounded by other defect/boundary central charges, in a similar fashion to the bounds on $a_{\mathcal{M}}^{(4d)}/c^{(4d)}$ [108, 109].

Do any of the other defect and boundary central charges obey c-theorems, for either defect/boundary or ambient RG flows? To date, c-theorems have only been proven for A-type central charge. However, nothing *a priori* forbids B-type central charges from also obeying c-theorems. Exploring more examples to identify candidate defect/boundary central charges that could obey c-theorems, and developing methods to prove them, remain important open questions.

Adding SUSY also raises a host of questions. For example, refs. [57, 287] showed for superconformal defects with $p = 2$ and $p = 4$ that $a_{\Sigma}^{(2d)}$ and $a_{\Sigma}^{(4d)}$ are fixed by certain 't Hooft anomaly coefficients, and obey an extremisation principle. Are other defect/boundary central charges fixed by 't Hooft anomaly coefficients? Are defect B-type central charges also extremised along RG flows to IR SCFTs? One of our main motivations was to study the $p = 4$ superconformal defects in the $d = 6$ $\mathcal{N} = (2, 0)$ SCFTs. Our main result for a $p = 4$ defect Weyl anomaly in eq. (6.1.1) provides a starting point for constructing the full defect super-Weyl anomaly, which should be crucial for characterising these important defects. More generally, fully characterising both co-dimension two and four defects in $d = 6$ SCFTs through their defect central charges will be crucial for exploring how, via (partially twisted) dimensional reduction, these data determine lower dimensional superconformal defects in class \mathcal{S} theories in $d = 4$ [217, 296, 319] and class \mathcal{R} theories in $d = 3$ [219].

Thinking more broadly, aside from the defect/boundary Weyl anomalies we reviewed in sec. 8.1, and our novel results for $p = 4$ defects/boundaries in sec. 6.1, what other defect/boundary Weyl anomalies are possible? Two obvious cases have yet to be studied. The first is $p = 3$ in $d > 4$ (examples appear for instance in refs. [320, 321]). In this case, our preliminary analysis suggests that a $p = 3$ defect in $d > 4$ has parity-odd Weyl anomalies, whose form depends on the co-dimension, similar to what we found for $p = 4$ in $d \geq 5$. The second is $p = 5$ in $d \geq 6$. Crucially, when $d = 6$ these must be non-SUSY, since the $d = 5$ superconformal algebra does not embed in any $d = 6$ superconformal algebra.

Chapter 7

Monodromy Defects in Free Field Theories

This chapter is primarily based on ref. [2] and partly on ref. [1], both of which I co-authored. We consider monodromy defects in free CFTs in d -dimensions. Monodromy defects are co-dimension $q = 2$ defects that can be introduced whenever the theory has a global symmetry. As mentioned in section 3.2, their construction is simple yet they may carry non-trivial dynamics, even in free CFTs. We provide more detailed background material in section 7.1. The simple nature of these defects allows us to obtain exact analytic results for certain one- and two-point correlation functions without requiring SUSY. Specifically, we compute the one-point functions of the stress tensor and flavour current, and the two-point function of the displacement operator for a free scalar field and a free Dirac fermion in sections 7.2 and 7.3, respectively.^{1,2} Using their data, we extract the defect central charges of monodromy defects in $d = 4$ and $d = 6$, in the latter case determining parts of the $p = 4$ defect Weyl anomaly discussed in chapter 6. Lastly, in section 7.4, we study the behaviour of monodromy defects under defect RG flows. Some of the details of the computations in these sections are expanded upon in appendix C.

7.1 Background

In section 3.2, we introduced monodromy defects as a disorder-type defect. The defect is defined by prescribing boundary conditions on ambient fields as they are rotated around the defect in the transverse plane, see eq. (3.2.26).

¹The computation of correlation functions in section 7.3 was my main contribution to the paper.

²While in the process of finishing the writing of [2], ref. [322] appeared, which has overlap with some of the computations of section 7.2. We will indicate which of our results also appeared there.

We begin with an ambient free field CFT with a global flavour symmetry group G . In what follows we will assume that $G = U(1)$. Let I_{CFT} be the action on $\mathcal{M}_d = \mathbb{R}^{1,d-1}$ with coordinates $x^\mu = \{t, \vec{x}_\parallel, \rho, \theta\}$ and metric $g_{\mu\nu}$,

$$ds^2 = g_{\mu\nu} dx^\mu dx^\nu = -dt^2 + d\vec{x}_\parallel^2 + d\rho^2 + \rho^2 d\theta. \quad (7.1.1)$$

In this chapter only, we will take $\mu = 0, 1, \dots, d-1$. In some computations, we will need to Wick rotate to Euclidean signature, i.e. \mathbb{R}^d , by taking $t \rightarrow -i\tau$. We insert a monodromy defect along $x^a = \{t, \vec{x}_\parallel\}$ located at $\rho = 0$ in the transverse $\{\rho, \theta\}$ -plane by imposing monodromies on the field Ψ as in eq. (3.2.26).³ Equivalently, one can introduce the defect by turning on a constant background gauge field for the $U(1)$ flavour symmetry along

$$A = \alpha d\theta. \quad (7.1.2)$$

The gauge background eq. (7.1.2) is a closed but not an exact form since it is singular at $\rho = 0$. In particular, we may perform a singular gauge transformation to gauge away A . This transformation affects any field $\Phi(x)$ with ordinary periodic boundary conditions and minimally coupled to A with unit charge in the following way

$$\Phi(x) \rightarrow \Phi'(x) = e^{-i\alpha\theta} \Phi(x) \equiv \Psi(x). \quad (7.1.3)$$

The gauge transformed field Ψ then behaves as in eq. (3.2.26). Thus, the introduction of the potential (7.1.2) is equivalent to ascribing a non-trivial monodromy to $\Psi(x)$, as claimed above. Notice that for generic α , the defect breaks parity in the transverse directions. The conserved current sourced by A , $J_\mu \equiv \frac{\delta I_{\text{CFT}}}{\delta A^\mu}$, may thus acquire a one-point function of the form in eq. (3.1.7). In polar coordinates this translates into

$$\langle J^\theta(x) \rangle = \frac{a_J}{\rho^d}, \quad (7.1.4)$$

with all other components vanishing and where the coefficient a_J is a function of the monodromy parameter $a_J \equiv a_J(\alpha)$.

From the relationship between the generating functional and the Weyl anomaly eq. (2.5.53), it is natural to expect that a_J in $d = \text{even}$ is related to defect central charges for monodromy defects. However, naively computing

$$-\frac{\partial}{\partial \alpha} \log Z^{\text{DCFT}}[\alpha] = \int d^d x \langle J^\theta(x) \rangle, \quad (7.1.5)$$

where $Z^{\text{DCFT}}[\alpha]$ is the generating functional for J^θ , we find no log divergences, only power law divergences. This is due to the fact that the defect we constructed above is flat and the integrated trace anomaly vanishes identically.

³Note that the cylindrical coordinates eq. (7.1.1) make manifest the preserved $SO(2) \simeq U(1)$ rotational symmetry around the defect submanifold $\Sigma_{d-2} \hookrightarrow \mathcal{M}_d$.

In order to obtain a non-trivial result in eq. (7.1.5), we can modify eq. (7.1.2) to include a non-trivial shape function

$$A_\mu = \alpha f_\mu(x), \quad (7.1.6)$$

where $f_\mu(x)$ are the components of a closed form that is singular on a co-dimension $q = 2$ submanifold. Repeating the computation above, we have

$$-\frac{\partial}{\partial \alpha} \log Z_f^{\text{DCFT}}[\alpha] = \int d^d x \langle J^\mu(x) \rangle_f f_\mu(x), \quad (7.1.7)$$

where $\langle \cdot \rangle_f$ denotes the expectation value in the presence of a defect of generic shape. A straightforward computation outlined in appendix C.1 shows that

$$\frac{\partial}{\partial \alpha} F^{\text{def}}|_{\text{univ.}} = -a_J(\alpha) \frac{2\pi^{\frac{d}{2}+1}}{\Gamma\left(\frac{d}{2}\right) \sin\left(\frac{\pi}{2}d\right)}, \quad (7.1.8)$$

where $F^{\text{def}} \equiv -\log Z_f^{\text{DCFT}}[\alpha] + \log Z^{\text{CFT}}$ is the defect sphere free energy. The above equation was originally found in [168, 169] where the authors studied how the defect free energy depends on bulk marginal couplings. The present case is slightly different from theirs since here the marginal operator $J^\theta(x)$ has explicit space-time dependence. We notice that eq. (7.1.8) has a simple pole when d is even. This reflects the fact that the sphere free energy contains a logarithmic divergence which corresponds to the A-type defect anomaly. In particular, in terms of the integrated anomaly \mathcal{A} in eq. (2.5.51),

$$\frac{\partial}{\partial \alpha} \mathcal{A} = (-1)^{d/2} a_J(\alpha) \frac{4\pi^{d/2}}{\Gamma\left(\frac{d}{2}\right)}. \quad (7.1.9)$$

When $d = 4$ and $d = 6$, this reduces to

$$\frac{\partial}{\partial \alpha} a_\Sigma^{(2d)}(\alpha) = 12\pi^2 a_J(\alpha), \quad (7.1.10)$$

$$\frac{\partial}{\partial \alpha} a_\Sigma^{(4d)}(\alpha) = \frac{\pi^3}{2} a_J(\alpha), \quad (7.1.11)$$

after using eqs. (3.4.39) and (6.2.44).

Due to the relatively simple construction of monodromy defects through eq. (7.1.2), higher point correlation functions of J^μ will be related to other important physical observables. Consider the stress tensor of a field theory coupled to A . With the insertion of a monodromy defect, $T_{\mu\nu}$ is no longer conserved at the location of the defect, and

$$\nabla^\mu T_{\mu\nu} = J^\mu F_{\mu\nu}. \quad (7.1.12)$$

From eq. (7.1.2), $F_{\mu\nu}$ is proportional to a Dirac delta function at $\rho = 0$. This is most clearly seen in Cartesian coordinates in the transverse space to the defect $x = \rho \cos \theta$, $y = \rho \sin \theta$, where now $F_{xy} = 2\pi\alpha\delta^2(x, y)$. Comparing eq. (7.1.12) to

eq. (3.1.14), we identify the displacement operator as

$$\mathcal{D}_x = -2\pi\alpha J_y|_{x,y=0}, \quad \mathcal{D}_y = 2\pi\alpha J_x|_{x,y=0}. \quad (7.1.13)$$

In the following sections it will be convenient to use complex coordinates $z = x + iy$, $\bar{z} = x - iy$ in the transverse space. In these coordinates we have

$$\mathcal{D}_z = -2\pi i\alpha J_z|_{z,\bar{z}=0}, \quad \mathcal{D}_{\bar{z}} = 2\pi i\alpha J_{\bar{z}}|_{z,\bar{z}=0}. \quad (7.1.14)$$

This brief computation has demonstrated a second important use for correlators of J_i . Since $\mathcal{D}_i \propto J_i$, we see that the displacement operator two-point function eq. (3.1.17) is computable through $\langle J_i J_j \rangle$. This in turn means that the defect limit of the current two-point function is controlled by $c_{\mathcal{D}\mathcal{D}}$, which is proportional to $d_1^{(2d)}$ in $d = 4$ by eq. (3.4.41) and to $d_1^{(4d)}$ in $d = 6$ by eq. (6.2.39).

One important caveat to this statement arises when non-trivial sources for relevant defect operators in the defect OPE are included. These modes will be central to the analysis in the subsequent sections. When they are turned on, the relationship between J_i and \mathcal{D}_i for monodromy defects no longer holds, and we will need to resort to other techniques to compute $c_{\mathcal{D}\mathcal{D}}$.

7.2 Free scalar

In this section, we study the monodromy defect in the theory of a free, conformally coupled complex scalar field, $\varphi(x)$, in d dimensions. As explained in section 7.1, we engineer this defect by turning on a constant background gauge field for the $U(1)$ global symmetry. We take the Euclidean action of the theory to be

$$I_{\text{scalar}} = \int d^d x \sqrt{g} \left[\nabla^\mu \varphi (\nabla_\mu \varphi)^\dagger + \frac{d-2}{4(d-1)} R |\varphi|^2 \right], \quad (7.2.15)$$

where the coupling to the scalar curvature R is needed to have a conformal and Weyl invariant action. We also define the gauge covariant derivative $\nabla_\mu \equiv D_\mu - ieA_\mu$.

Varying I_{scalar} with respect to the gauge field A_μ gives the conserved $U(1)$ current

$$J_\mu = \frac{1}{\sqrt{g}} \frac{\delta I_{\text{scalar}}}{\delta A^\mu} = -i \left(\varphi D_\mu \varphi^\dagger - D_\mu \varphi \varphi^\dagger + 2ieA_\mu |\varphi|^2 \right), \quad (7.2.16)$$

while the variation with respect to the metric $g_{\mu\nu}$ produces the stress tensor

$$\begin{aligned} T_{\mu\nu} &= \frac{2}{\sqrt{g}} \frac{\delta I_{\text{scalar}}}{\delta g^{\mu\nu}} \\ &= \nabla_\mu \varphi (\nabla_\nu \varphi)^\dagger + (\nabla_\mu \varphi)^\dagger \nabla_\nu \varphi - \frac{d-2}{2(d-1)} \left[D_\mu D_\nu + \frac{g_{\mu\nu}}{d-2} D^2 - R_{\mu\nu} \right] |\varphi|^2, \end{aligned} \quad (7.2.17)$$

where $R_{\mu\nu}$ is the Ricci tensor for the background geometry.

7.2.1 Mode expansion and propagator

In order to introduce a monodromy defect, we set A_μ to be as in eq. (7.1.2), and for simplicity we set the charge $e = 1$. In appendix C.2 we provide the detailed derivation of the mode expansion and the propagator. Here we report and discuss the results. In what follows we will restrict $\alpha \in (0, 1)$, and we will treat the limits $\alpha \rightarrow 0, 1$ carefully. We will also adopt complex coordinates transverse to the defect, i.e. $z = \rho e^{i\theta}$ and $\bar{z} = \rho e^{-i\theta}$. The mode expansion can be written as

$$\varphi = \varphi_{-\alpha} z^{-\alpha} + \varphi_{\alpha-1} \bar{z}^{\alpha-1} + \sum_{m=1}^{\infty} \varphi_{m-\alpha} z^{m-\alpha} + \sum_{m=0}^{\infty} \varphi_{m+\alpha} \bar{z}^{m+\alpha}. \quad (7.2.18)$$

The modes $\varphi_{m+\alpha}$ are defined for $m \geq 0$ and $\varphi_{m-\alpha}$ for $m \geq 1$ as follows:

$$\varphi_{m\pm\alpha} \equiv \int dk_\rho \int d^{d-3}\vec{k}_\parallel \left[f(k) a_{\mp m}(k) + f^*(k) b_{\mp m}^\dagger(k) \right] \frac{J_{m\pm\alpha}(k_\rho \rho)}{\rho^{m\pm\alpha}}, \quad (7.2.19)$$

where $J_\nu(\zeta)$ is the Bessel function of the first kind, and

$$f(k) = \frac{\sqrt{k_\rho}}{(\sqrt{2\pi})^{d-2} \sqrt{2\omega}} e^{-i\omega t + i\vec{k}_\parallel \cdot \vec{x}_\parallel}, \quad (7.2.20)$$

with $\omega^2 = k_\rho^2 + \vec{k}_\parallel^2$. Throughout we use the shorthand $k = (\vec{k}_\parallel, k_\rho)$. The modes φ_α and $\varphi_{1-\alpha}$ are special because they are naturally paired with two singular modes $\varphi_{-\alpha}$ and $\varphi_{\alpha-1}$, respectively. These modes can be included if one allows for divergences milder than $\mathcal{O}(\rho^{-1})$ as $\rho \rightarrow 0$ such that the mode is square integrable at the origin.⁴ In principle, we can introduce these four modes independently but the canonical commutation relation for φ fixes their coefficients in terms of two free parameters $\xi, \tilde{\xi} \in [0, 1]$ so that we have

$$\varphi_\alpha = \sqrt{1-\xi} \int dk_\rho \int d^{d-3}\vec{k}_\parallel \left[f(k) a_0^{(+)}(k) + f^*(k) b_0^{(+)\dagger}(k) \right] \frac{J_\alpha(k_\rho \rho)}{\rho^\alpha}, \quad (7.2.21a)$$

$$\varphi_{-\alpha} = \sqrt{\xi} \int dk_\rho \int d^{d-3}\vec{k}_\parallel \left[f(k) a_0^{(-)}(k) + f^*(k) b_0^{(-)\dagger}(k) \right] \frac{J_{-\alpha}(k_\rho \rho)}{\rho^{-\alpha}}, \quad (7.2.21b)$$

$$\varphi_{1-\alpha} = \sqrt{1-\tilde{\xi}} \int dk_\rho \int d^{d-3}\vec{k}_\parallel \left[f(k) a_1^{(+)}(k) + f^*(k) b_1^{(+)\dagger}(k) \right] \frac{J_{1-\alpha}(k_\rho \rho)}{\rho^{1-\alpha}}, \quad (7.2.21c)$$

$$\varphi_{\alpha-1} = \sqrt{\tilde{\xi}} \int dk_\rho \int d^{d-3}\vec{k}_\parallel \left[f(k) a_1^{(-)}(k) + f^*(k) b_1^{(-)\dagger}(k) \right] \frac{J_{\alpha-1}(k_\rho \rho)}{\rho^{\alpha-1}}. \quad (7.2.21d)$$

⁴Physically, we require the integrals of energy density and charge density to be finite in a neighbourhood around the defect. Indeed, energy and charge density are quadratic in the field ϕ and do not involve any radial derivatives. The measure of integration over the spatial directions involves a factor of ρ . Thus, each field must have a divergence milder than $\mathcal{O}(\rho^{-1})$ for the integral to converge at the origin. As we will see shortly, defect unitarity will impose exactly the same constraint.

Similar modes have been already discussed from an abstract defect CFT perspective in [155,288]. In order to make contact with these works it is useful to match our mode expansion with the defect OPE of the bulk field φ . The latter allows to expand any bulk operator in terms of defect primaries $\hat{\mathcal{O}}_m$ and their descendants, as in eq. (3.1.21). The coefficients of this expansion are the bulk-to-defect couplings $b_{\varphi\hat{\mathcal{O}}_m}$. For a monodromy defect, the allowed defect operators in the defect OPE of a bulk scalar in our conventions must have orthogonal spin $s \in \mathbb{Z} - \alpha$. Furthermore, in a free theory, the EOM for φ allow for two sets of defect operators in the defect OPE of φ . The dimensions of these two sets of operators were denoted in [155] as $\hat{\Delta}_s^+ = \frac{d}{2} - 1 + |s|$ and $\hat{\Delta}_s^- = \frac{d}{2} - 1 - |s|$. While the former are always allowed, the latter cannot be allowed for all s . Indeed defect operators must obey the same unitarity bounds stated below eq. (2.2.20) with $d \rightarrow p$. The operators with $\hat{\Delta}_s^-$ violate the unitarity bound for a $p = d - 2$ defect in $d > 4$ unless $|s| < 1$. For $d \leq 4$, unitarity requires $|s| < \frac{d-2}{2}$. The defect OPE then reads

$$\begin{aligned} \varphi = & \sum_{s \in \mathbb{Z} - \alpha} b_{\varphi\hat{\mathcal{O}}_s^+} \rho^{|s|} e^{is\theta} \mathcal{C}_s^+(\rho^2 \partial_{\parallel}^2) \hat{\mathcal{O}}_s^+(x_{\parallel}) \\ & + b_{\varphi\hat{\mathcal{O}}_{-\alpha}^-} \frac{e^{-i\alpha\theta}}{\rho^\alpha} \mathcal{C}_s^-(\rho^2 \partial_{\parallel}^2) \hat{\mathcal{O}}_{-\alpha}^-(x_{\parallel}) + b_{\varphi\hat{\mathcal{O}}_{1-\alpha}^-} \frac{e^{i(1-\alpha)\theta}}{\rho^{1-\alpha}} \mathcal{C}_s^-(\rho^2 \partial_{\parallel}^2) \hat{\mathcal{O}}_{1-\alpha}^-(x_{\parallel}), \end{aligned} \quad (7.2.22)$$

where $\partial_{\parallel}^2 = \partial_a \partial^a$. The differential operators $\mathcal{C}_s^\pm(\rho^2 \partial_{\parallel}^2)$ resum the contribution of all the conformal descendants, and are fixed by conformal invariance to be

$$\mathcal{C}_s^\pm(\rho^2 \partial_{\parallel}^2) \equiv \sum_{k=0}^{+\infty} \frac{(-4)^{-k} (\rho^2 \partial_{\parallel}^2)^k}{k! (1 \pm |s|)_k}, \quad (7.2.23)$$

where $(a)_k \equiv a(a+1) \dots (a+k-1)$ if $k \neq 0$ and $(a)_0 \equiv 1$ is the Pochhammer symbol. Comparing this expression with the small ρ expansion of eq. (7.2.18) after Wick rotation, one finds a one-to-one correspondence between the mode expansion and the defect OPE, thus establishing that each mode in eq. (7.2.18) creates a conformal family of defect operators. Including modes that are less singular than $\mathcal{O}(\rho^{-1})$ is equivalent to allowing for defect operators with dimension $\hat{\Delta}_s^-$ above the unitarity bound. Conversely, any mode that diverges like $\mathcal{O}(\rho^{\leq -1})$ at the origin would give rise to a defect primary below the unitarity bound. We will determine the bulk-to-defect couplings $b_{\varphi\hat{\mathcal{O}}}$ by comparing the propagator with the defect block expansion.

The propagator is computed in appendix C.2 where we find that the result consists precisely of a sum over defect blocks. A bulk two-point function can be expressed in terms of two cross ratios: the relative angle θ and the combination

$$\eta \equiv \frac{2\rho\rho'}{\rho^2 + \rho'^2 + |x_{\parallel}|^2}, \quad (7.2.24)$$

where we have set $x'_{\parallel} = 0$ by translational invariance along the defect. Note that in the coincident limit $\theta \rightarrow 0$ and $\eta \rightarrow 1$. A defect block is a function of these cross ratios:

$$F_{\hat{\Delta}_s}(\eta, \theta) = \left(\frac{\eta}{2}\right)^{\hat{\Delta}_s} {}_2F_1\left(\frac{\hat{\Delta}_s}{2}, \frac{\hat{\Delta}_s + 1}{2}; \hat{\Delta}_s + 2 - \frac{d}{2}; \eta^2\right) e^{is\theta}, \quad (7.2.25)$$

where ${}_2F_1(a, b; c; z)$ is the ordinary hypergeometric function. The propagator then takes the form

$$\begin{aligned} & \langle \varphi(x) \varphi^\dagger(0, \rho') \rangle \\ &= \left(\frac{1}{\rho\rho'}\right)^{\frac{d}{2}-1} \left(\sum_{s \in \mathbb{Z} - \alpha} c_s^+ F_{\hat{\Delta}^+, s}(\eta, \theta) + c_{-\alpha}^- F_{\hat{\Delta}^-, -\alpha}(\eta, \theta) + c_{1-\alpha}^- F_{\hat{\Delta}^-, 1-\alpha}(\eta, \theta) \right), \end{aligned} \quad (7.2.26)$$

with

$$c_s^+ = \frac{\Gamma\left(\frac{d}{2} - 1 + |s|\right)}{4\pi^{d/2} \Gamma(1 + |s|)} \quad \text{for } s \neq -\alpha, 1 - \alpha, \quad (7.2.27)$$

and special cases

$$c_{-\alpha}^+ = (1 - \zeta) \frac{\Gamma\left(\frac{d}{2} - 1 + \alpha\right)}{4\pi^{d/2} \Gamma(1 + \alpha)}, \quad c_{-\alpha}^- = \zeta \frac{\Gamma\left(\frac{d}{2} - 1 - \alpha\right)}{4\pi^{d/2} \Gamma(1 - \alpha)}, \quad (7.2.28a)$$

$$c_{1-\alpha}^+ = (1 - \tilde{\zeta}) \frac{\Gamma\left(\frac{d}{2} - \alpha\right)}{4\pi^{d/2} \Gamma(2 - \alpha)}, \quad c_{1-\alpha}^- = \tilde{\zeta} \frac{\Gamma\left(\frac{d}{2} - 2 + \alpha\right)}{4\pi^{d/2} \Gamma(\alpha)}. \quad (7.2.28b)$$

In section 7.3, we will find it advantageous to adopt an alternative notation for the scalar propagator in eq. (7.2.26), $G_{S, \alpha, \zeta, \tilde{\zeta}}(x, x') \equiv \langle \varphi(x) \varphi^\dagger(0, \rho') \rangle$. By applying the defect OPE eq. (7.2.22) to each scalar in the propagator, and matching with the defect block expansion eq. (7.2.26) using the normalisation

$$\langle \hat{\mathcal{O}}_s^\pm(x_{\parallel}) \hat{\mathcal{O}}_{s'}^{\pm\pm}(0) \rangle = \frac{\delta_{s, -s'}}{|x_{\parallel}|^{d-2 \pm 2|s|}} \quad (7.2.29)$$

for the defect operators, we immediately identify $c_s^\pm = b_{\varphi \hat{\mathcal{O}}_s^\pm} b_{\varphi^\dagger \hat{\mathcal{O}}_s^{\pm\pm}}$. Reflection positivity imposes that $c_s^\pm > 0$, which determines the range of the parameters ζ and $\tilde{\zeta}$ to be

$$0 \leq \zeta, \tilde{\zeta} \leq 1. \quad (7.2.30)$$

In $d < 4$, the unitarity bounds above eq. (7.2.22) impose further conditions on the range of α at non-zero ζ or $\tilde{\zeta}$. As an example consider $d = 3$, for which the unitarity bound reads $|s| < \frac{1}{2}$. This requires that either $\alpha \in [0, \frac{1}{2})$ if $\zeta \neq 0$ and $\tilde{\zeta} = 0$, or $\alpha \in (\frac{1}{2}, 1]$ if $\zeta = 0$ and $\tilde{\zeta} \neq 0$. Notice that since the two ranges of α don't overlap, one cannot turn on both deformations $\zeta, \tilde{\zeta} \neq 0$ without breaking unitarity.

At this point, we are ready to discuss what happens for the limiting values $\alpha \rightarrow 0$ and

$\alpha \rightarrow 1$. In the absence of the divergent modes, i.e. for $\zeta = \tilde{\zeta} = 0$, the defect OPE of φ simply reduces to the Taylor expansion of the free field φ around the co-dimension two surface $\rho = 0$. In other words, the defect reduces to the trivial defect as one would expect in the absence of a monodromy. The singular modes, instead, lead to a singular behaviour of eq. (7.2.22) either at $\alpha = 0$ or at $\alpha = 1$. For $\tilde{\zeta} = 0$ and $\zeta \neq 0$ the limit $\alpha \rightarrow 0$ is perfectly well-defined and leads again to the free field Taylor expansion, while the limit $\alpha \rightarrow 1$ is singular. This seems to be in contrast with our definition of the monodromy defect, which should reduce to the trivial defect for integer α . Nevertheless, a glance at (7.2.28a) shows that, at least for $d > 4$, the singular mode decouples from the bulk at $\alpha = 1$ since $c_{-1}^- = 0$. This leads to a two-dimensional theory, which is decoupled from the bulk free scalar. This is still not enough to affirm that the limit $\alpha \rightarrow 1$ is well-defined. Even though the singular mode decouples, the remaining bulk propagator still depends on ζ as the contribution of the φ_α mode gives a factor of $1 - \zeta$ to one of the terms in the propagator. Thus, the propagator does not reduce to that of a free complex scalar but has an extra term proportional to $-\zeta$ consisting of a single defect block. This bulk two-point function is not crossing invariant and therefore it does not lead to a consistent defect CFT. Therefore, we have to conclude that the limit $\alpha \rightarrow 1$ cannot be smooth for a constant value of ζ . Either ζ is a function of α or some discontinuous behaviour must be introduced at $\alpha = 1$ so that the periodicity in α is reinstated. In the following, we do not make any assumption on ζ and we will mention explicitly the places where we will assume that it is not a function of α . More generally, we keep an abstract point of view on this issue, assuming there could be a dynamical mechanism which causes the decoupling of this mode for $\alpha = 1$. For the case of $\zeta = 0$ but non-vanishing $\tilde{\zeta}$ as $\alpha \rightarrow 0$ an identical discussion applies.

We introduced ζ and $\tilde{\zeta}$ as abstract parameters in the defect OPE. Any value in the range eq. (7.2.30) gives rise to an admissible defect conformal block expansion. However, the physical meaning of these parameters and the defects that they define is less clear. The $U(1)$ monodromy defect is closely related to an Aharonov-Bohm solenoid, for which the gauge field outside has the same profile as eq. (7.1.2) [323–325]. By a similar computation to the one outlined here, one can solve the Klein-Gordon equation both inside and outside the solenoid. Physical boundary conditions at the solenoid correspond to continuity in the field and the first radial derivative. Then taking the size of the solenoid to zero, one obtains the field configurations in eqs. (7.2.19) and (7.2.21) with $\zeta = \tilde{\zeta} = 0$. For non-zero ζ or $\tilde{\zeta}$, the monodromy defect does not describe a solenoid but a more general defect for which particles experience the physics at the centre of the defect. In an Aharonov-Bohm-like experiment the particles wouldn't just acquire a phase but non-trivially scatter with the defect. To our knowledge, the possibility of more general field configurations as a function of continuous parameters ζ or $\tilde{\zeta}$ was first noted in ref. [324].

Another perspective on the modes with $\zeta = 1$ or $\tilde{\zeta} = 1$ is given by a Weyl transformation of the planar defect in \mathbb{R}^d to $S^1 \times H^{d-1}$, where H^{d-1} is the $(d-1)$ -dimensional hyperbolic space (i.e. the Euclidean version of anti-de Sitter space) [322]. The support of the defect is mapped to the boundary of H^{d-1} while the scalar field now has a monodromy around the S^1 . Performing a Kaluza-Klein reduction on the S^1 , one obtains massive scalars on H^{d-1} with masses $m_s^2 = s^2 - \frac{(d-2)^2}{4}$ in units of the hyperbolic radius, where $s \in \mathbb{Z} - \alpha$ as before. Each bulk massive scalar on H^{d-1} is holographically dual to an operator on the boundary, which can be identified with one of our defect primaries $\hat{\mathcal{O}}_s^\pm$. The defect operator's scaling dimension $\hat{\Delta}_s^\pm$ is related to the bulk scalar's mass as follows $m_s^2 = \hat{\Delta}_s^\pm (\hat{\Delta}_s^\pm - d + 2)$. The two possibilities $\hat{\Delta}_s^\pm$ for fixed spin s correspond to the two possible boundary conditions of a massive scalar in hyperbolic space. For m_s^2 above the Breitenlohner-Freedman bound $m_s^2 > -\frac{(d-2)^2}{4}$ and also $m_s^2 \leq -\frac{(d-2)^2}{4} + 1$, both solutions $\hat{\Delta}_s^\pm = \frac{d-2}{2} \pm \sqrt{\frac{(d-2)^2}{4} + m_s^2}$ are above the boundary theory's unitarity bound. For this range of m_s^2 , alternate quantisation is admissible, exchanging the usual role of source and VEV for the dual field theory operator. The only values of s for which m_s^2 lies in this range are $s = -\alpha$ and $s = 1 - \alpha$. These are precisely the singular modes with $\zeta = 1$ and $\tilde{\zeta} = 1$, respectively.

7.2.2 Correlation functions and central charges

We start by computing some relevant one-point functions by taking a suitable coincident limit of the propagator. A generic one-point function of a composite operator can be found by Wick contracting the fundamental fields and then taking the coincident limit, carefully regularising the short distance divergences. In the following, we consider only one-point functions of operators quadratic in the fundamental field φ . In this case, we only need to take the appropriate combinations of derivatives of the propagator, and then take the coincident limit.

To this end, it is convenient to start from the non-singular propagator ($\zeta = \tilde{\zeta} = 0$) for which we can use the form in eq. (C.2.25), which after a change of variables $\zeta = 2/(s\rho\rho')$ becomes

$$\left\langle \varphi(x) \varphi^\dagger(x') \right\rangle_{\zeta=\tilde{\zeta}=0} = \frac{1}{2(2\pi)^{d/2}} \frac{1}{(\rho\rho')^{d/2-1}} \int_{\frac{2\epsilon^2}{\rho\rho'}}^{+\infty} d\zeta e^{-\frac{1}{\eta\zeta}} \zeta^{-d/2} \sum_m e^{i(m-\alpha)\theta} I_{|m-\alpha|} \left(\frac{1}{\zeta} \right), \quad (7.2.31)$$

where $I_\nu(\zeta)$ is the modified Bessel function of the first kind. The integral is divergent in the coincident ($\eta \rightarrow 1$) limit. For this reason we introduce the UV cut-off ϵ . The one-point function will be a power expansion in terms of ϵ . If the divergent term is independent of α , the divergences can be consistently removed by subtracting the one-point function with $\alpha = 0$. After computing the contribution from the regular modes of φ , we will add the singular parts, which are proportional to ζ and $\tilde{\zeta}$.

7.2.2.1 One-point function of $|\varphi|^2$

Let us start with the simplest case: the one-point function of $|\varphi|^2$. Taking the coincident limit of eq. (7.2.31) we obtain

$$\langle \varphi(x)\varphi^\dagger(x') \rangle_{\xi=\bar{\xi}=0} = \frac{1}{2(2\pi)^{d/2}} \frac{1}{\rho^{d-2}} \int_{\frac{2\epsilon^2}{\rho^2}}^{+\infty} d\zeta e^{-\frac{1}{\zeta}} \zeta^{-d/2} \mathcal{I}_\alpha^{(1)}\left(\frac{1}{\zeta}\right), \quad (7.2.32)$$

where we defined⁵

$$\begin{aligned} \mathcal{I}_\alpha^{(1)}(\zeta) \equiv \sum_m I_{|m-\alpha|}(\zeta) &= \frac{1}{2\alpha} \left[e^\zeta \int_0^\zeta e^{-x} I_{-\alpha}(x) dx - \zeta I_{-\alpha}(\zeta) - \zeta I_{1-\alpha}(\zeta) \right] \\ &+ \frac{1}{2(1-\alpha)} \left[e^\zeta \int_0^\zeta e^{-x} I_{\alpha-1}(x) dx - \zeta I_{\alpha-1}(\zeta) - \zeta I_\alpha(\zeta) \right]. \end{aligned} \quad (7.2.33)$$

The integral over ζ in eq. (7.2.32) can be performed, and indeed one can see that it diverges for $\epsilon \rightarrow 0$. However, the divergences are independent of α and can be unambiguously subtracted. The final result is

$$\langle |\varphi(x)|^2 \rangle_{\xi=\bar{\xi}=0} = -\frac{\Gamma\left(\frac{d}{2}-\alpha\right)\Gamma\left(\frac{d}{2}+\alpha-1\right)\sin(\pi\alpha)}{2^{d-1}\pi^{\frac{d+1}{2}}(d-2)\Gamma\left(\frac{d-1}{2}\right)} \frac{1}{\rho^{d-2}}. \quad (7.2.34)$$

We observe that the one-point function vanishes both when $\alpha = 0$ and $\alpha = 1$. The former is obvious since it corresponds to the absence of a defect, while the latter reflects the fact that the flux is defined modulo integers. We now compute the contribution of the singular modes. The part of the propagator proportional to ξ can be deduced from eq. (7.2.26) and it reads

$$\langle \varphi(x)\varphi^\dagger(x') \rangle_\xi = \xi \left(\frac{1}{\rho\rho'}\right)^{\frac{d}{2}-1} \left(-\frac{\Gamma\left(\frac{d}{2}-1+\alpha\right)}{4\pi^{d/2}\Gamma(1+\alpha)} F_{\hat{\Delta}^+,-\alpha}(\eta,\theta) + \frac{\Gamma\left(\frac{d}{2}-1-\alpha\right)}{4\pi^{d/2}\Gamma(1-\alpha)} F_{\hat{\Delta}^-,-\alpha}(\eta,\theta) \right). \quad (7.2.35)$$

We are interested in the $\theta \rightarrow 0$ and $\eta \rightarrow 1$ limit. The former simply eliminates the exponential in eq. (7.2.25), while the latter gives a singular limit for the hypergeometric function in eq. (7.2.25). Actually, each defect block is logarithmically divergent in the limit $\eta \rightarrow 1$. However, these logarithms cancel in the combination eq. (7.2.35), leaving us only with power law divergences. After subtracting them we get

$$\langle |\varphi(x)|^2 \rangle_\xi = \xi \frac{\Gamma\left(\frac{d}{2}-\alpha-1\right)\Gamma\left(\frac{d}{2}+\alpha-1\right)\sin(\pi\alpha)}{2^{d-1}\pi^{\frac{d+1}{2}}\Gamma\left(\frac{d-1}{2}\right)} \frac{1}{\rho^{d-2}}. \quad (7.2.36)$$

⁵In the second equality we used eq. (C.4.43).

The result proportional to $\tilde{\xi}$ can be simply obtained by replacing $\alpha \rightarrow 1 - \alpha$:

$$\langle |\varphi(x)|^2 \rangle_{\tilde{\xi}} = \tilde{\xi} \frac{\Gamma\left(\frac{d}{2} + \alpha - 2\right) \Gamma\left(\frac{d}{2} - \alpha\right) \sin(\pi\alpha)}{2^{d-1} \pi^{\frac{d+1}{2}} \Gamma\left(\frac{d-1}{2}\right)} \frac{1}{\rho^{d-2}}. \quad (7.2.37)$$

Putting everything together we get the final result

$$\langle |\varphi(x)|^2 \rangle = \frac{\Gamma\left(\frac{d}{2} - \alpha\right) \Gamma\left(\frac{d}{2} + \alpha - 1\right) \sin(\pi\alpha)}{2^{d-1} \pi^{\frac{d+1}{2}} \Gamma\left(\frac{d-1}{2}\right)} \frac{1}{\rho^{d-2}} \left(-\frac{1}{d-2} + \frac{\xi}{\frac{d}{2} - \alpha - 1} + \frac{\tilde{\xi}}{\frac{d}{2} + \alpha - 2} \right). \quad (7.2.38)$$

As a special case we note that when $d = 4$, the one-point function becomes

$$\langle |\varphi(x)|^2 \rangle = -\frac{(1-\alpha)\alpha - 2\xi\alpha - 2\tilde{\xi}(1-\alpha)}{8\pi^2\rho^2}. \quad (7.2.39)$$

7.2.2.2 One-point function of $T_{\mu\nu}$

The one-point function of the stress tensor in the presence of a $p = d - 2$ dimensional conformal defect is fixed by conformal symmetry to be of the form in eq. (3.1.13).

Thus, we only need to compute the coefficient h to determine the full stress tensor one-point function. To do this, we can choose a particular component, and we pick

$$\langle T_{\rho\rho} \rangle = 2 \langle \partial_\rho \varphi \partial_\rho \varphi^\dagger \rangle - \frac{1}{2(d-1)} \left[(d-1) \partial_\rho^2 + \frac{1}{\rho} \partial_\rho \right] \langle |\varphi|^2 \rangle. \quad (7.2.40)$$

Having already found $\langle |\varphi|^2 \rangle$ above, we only need to compute the first term in eq. (7.2.40), i.e. the coincident limit of the propagator after taking derivatives with respect to ρ . Once again, we start from the regular part of the propagator ($\xi = \tilde{\xi} = 0$), for which we use the representation eq. (7.2.31),

$$\langle \partial_\rho \varphi(x) \partial_\rho \varphi^\dagger(x) \rangle_{\xi=\tilde{\xi}=0} = \frac{1}{8(2\pi)^{d/2}} \frac{1}{\rho^d} \int_{\frac{2\epsilon^2}{\rho^2}}^{+\infty} d\zeta e^{-1/\zeta} \frac{(d-2)^2 \zeta + 4}{\zeta^{\frac{d}{2}+1}} \mathcal{I}_\alpha^{(1)}\left(\frac{1}{\zeta}\right). \quad (7.2.41)$$

Just as above, we find that the divergences in ϵ are independent of α and can thus be subtracted unambiguously. The finite part reads

$$\langle \partial_\rho \varphi \partial_\rho \varphi^\dagger(x) \rangle_{\xi=\tilde{\xi}=0} = -\frac{((d-2)d^2 + 4(1-\alpha)\alpha) \sin(\pi\alpha) \Gamma\left(\frac{d}{2} - \alpha\right) \Gamma\left(\frac{d}{2} + \alpha - 1\right)}{2^{d+1} \pi^{\frac{d+1}{2}} d(2d-1) \Gamma\left(\frac{d-1}{2}\right)} \frac{1}{\rho^d}. \quad (7.2.42)$$

Performing the same analysis for the singular contributions we find

$$\left\langle \partial_\rho \varphi \partial_\rho \varphi^\dagger(x) \right\rangle_{\bar{\xi}} = \xi \frac{((d-2)^2 d - 8\alpha^2) \Gamma\left(\frac{d}{2} - \alpha - 1\right) \Gamma\left(\frac{d}{2} + \alpha - 1\right) \sin(\pi\alpha)}{2^{d+2} \pi^{\frac{d+1}{2}} ((d-2)^2 - 4\alpha^2) \Gamma\left(\frac{d+1}{2}\right)} \frac{1}{\rho^d}, \quad (7.2.43)$$

$$\left\langle \partial_\rho \varphi \partial_\rho \varphi^\dagger(x) \right\rangle_{\bar{\xi}} = \bar{\xi} \frac{((d-2)^2 d - 8(1-\alpha)^2) \Gamma\left(\frac{d}{2} + \alpha - 2\right) \Gamma\left(\frac{d}{2} - \alpha\right) \sin(\pi\alpha)}{2^{d+2} \pi^{\frac{d+1}{2}} ((d-2)^2 - 4(1-\alpha)^2) \Gamma\left(\frac{d+1}{2}\right)} \frac{1}{\rho^d}. \quad (7.2.44)$$

Thus, by plugging eqs. (7.2.38), (7.2.42), and (7.2.43) into eq. (7.2.40), we find the full one-point function of the stress tensor

$$\langle T_{\rho\rho}(x) \rangle = - \frac{\Gamma\left(\frac{d}{2} - \alpha\right) \Gamma\left(\frac{d}{2} + \alpha - 1\right) \sin(\pi\alpha) \left(\frac{\alpha(1-\alpha)}{d} + \frac{\alpha^2 \bar{\xi}}{\frac{d}{2} - \alpha - 1} + \frac{(1-\alpha)^2 \bar{\xi}}{\frac{d}{2} + \alpha - 2} \right)}{2^{d-1} \pi^{\frac{d+1}{2}} \Gamma\left(\frac{d+1}{2}\right)} \frac{1}{\rho^d}, \quad (7.2.45)$$

which is vanishing for $\alpha = 0$ and $\alpha = 1$ when $d > 4$, as expected. The contribution with $\bar{\xi} = \xi = 0$ was previously computed in [326]. Comparing with eq. (3.1.13), we find that h is expressed as

$$h = \frac{\Gamma\left(\frac{d}{2} - \alpha\right) \Gamma\left(\frac{d}{2} + \alpha - 1\right) \sin(\pi\alpha) \left(\frac{\alpha(1-\alpha)}{d} + \frac{\alpha^2 \bar{\xi}}{\frac{d}{2} - \alpha - 1} + \frac{(1-\alpha)^2 \bar{\xi}}{\frac{d}{2} + \alpha - 2} \right)}{2^{d-1} \pi^{\frac{d+1}{2}} \Gamma\left(\frac{d+1}{2}\right)}. \quad (7.2.46)$$

Note that $h \geq 0$ for the ranges $\alpha \in (0, 1)$, and $\bar{\xi}, \xi \in [0, 1]$ in $d \geq 4$. For $d < 4$, unitarity requires that the range of α be restricted in the presence of singular modes, as discussed below eq. (7.2.30). In that case h is manifestly non-negative.

Specialising to $d = 4$ and $d = 6$ in order to connect to defect central charges, we find using eqs. (3.4.41) and (6.2.39)

$$d_2^{(2d)} = -\frac{3}{2} \left((1-\alpha)^2 \alpha^2 + 4\bar{\xi} \alpha^3 + 4\xi (1-\alpha)^3 \right), \quad (7.2.47)$$

$$d_2^{(4d)} = -\frac{\alpha(1-\alpha^2)(2-\alpha)}{72} \left(\alpha(1-\alpha) + \frac{6\alpha^2 \bar{\xi}}{2-\alpha} + \frac{6(1-\alpha)^2 \bar{\xi}}{1+\alpha} \right). \quad (7.2.48)$$

Since $h \geq 0$, then $d_2^{(2d)} \leq 0$ and $d_2^{(4d)} \leq 0$. This is in agreement with the expectation that $d_2^{(2d)} \leq 0$ and $d_2^{(4d)} \leq 0$ if the ANEC holds in the presence of a $p = 2$ and $p = 4$ dimensional defect, respectively [50].

7.2.2.3 One-point function of J_θ

In this subsection, we consider the one-point function of the current $\langle J_\mu \rangle$. By computing the coefficient a_J , we can leverage eq. (7.1.10) in $d = 4$ to compute the defect central charge $a_\Sigma^{(2d)}$ and eq. (7.1.11) in $d = 6$ to compute $a_\Sigma^{(4d)}$.

We start again from the regular part of the propagator in the form of eq. (7.2.31), and consider the following expectation value

$$\langle J_\theta \rangle_{\tilde{\zeta}=\tilde{\zeta}=0} = -2i \langle \varphi \partial_\theta \varphi^\dagger \rangle = -\frac{1}{(2\pi)^{d/2}} \frac{1}{\rho^{d-2}} \int_{\frac{2\epsilon^2}{\rho^2}}^{+\infty} d\zeta e^{-\frac{1}{\zeta}} \zeta^{-d/2} \mathcal{I}_\alpha^{(2)} \left(\frac{1}{\zeta} \right), \quad (7.2.49)$$

where we have taken the coincident limit and defined the sum⁶

$$\begin{aligned} \mathcal{I}_\alpha^{(2)}(\zeta) &\equiv \sum_m (m - \alpha) I_{|m-\alpha|}(\zeta) \\ &= \frac{\zeta}{2} [I_{1-\alpha}(\zeta) + I_{-\alpha}(\zeta) - I_{1+\alpha}(\zeta) - I_\alpha(\zeta)] - \alpha I_\alpha(\zeta). \end{aligned} \quad (7.2.50)$$

Inserting the result of the sum in eq. (7.2.50) into eq. (7.2.49), we find that the ζ -integral is convergent in the limit $\epsilon \rightarrow 0$. For the regular modes, computing the ζ -integral and removing the UV cut-off gives⁷

$$\langle J_\theta \rangle_{\tilde{\zeta}=\tilde{\zeta}=0} = \frac{(1 - 2\alpha)\Gamma\left(\frac{d}{2} - \alpha\right)\Gamma\left(\frac{d}{2} + \alpha - 1\right)\sin(\pi\alpha)}{2^d \pi^{\frac{d+1}{2}} \Gamma\left(\frac{d+1}{2}\right)} \frac{1}{\rho^{d-2}}. \quad (7.2.51)$$

We note that $\langle J_\theta \rangle = 0$ both for $\alpha = 0, 1$, and for $\alpha = 1/2$. The former cases are expected as the monodromy becomes trivial, while the latter follows from symmetry considerations. More specifically, the Lagrangian in eq. (7.2.15) is manifestly invariant under the transformation $\theta \rightarrow -\theta$ provided that $\alpha \rightarrow -\alpha$. If φ is regular in the limit $\rho \rightarrow 0$, then $-\alpha$ and $1 - \alpha$ are identified by gauge invariance. This implies that $\langle J_\theta \rangle$ is odd under $\alpha \rightarrow 1 - \alpha$ in the range $\alpha \in [0, 1]$, and thus it vanishes when $\alpha = 1/2$. Equivalently, parity in the normal directions is restored at $\alpha = \frac{1}{2}$, which forces the one-point function of a vector to vanish as discussed in section 3.1. The contribution of the singular modes is

$$\langle J_\theta \rangle_{\tilde{\zeta}} = 2\tilde{\zeta} \frac{\alpha \Gamma\left(\frac{d}{2} - \alpha - 1\right)\Gamma\left(\frac{d}{2} + \alpha - 1\right)\sin(\pi\alpha)}{2^{d-1} \pi^{\frac{d+1}{2}} \Gamma\left(\frac{d-1}{2}\right)} \frac{1}{\rho^{d-2}}, \quad (7.2.52a)$$

$$\langle J_\theta \rangle_{\tilde{\zeta}} = 2\tilde{\zeta} \frac{(1 - \alpha) \Gamma\left(\frac{d}{2} + \alpha - 2\right)\Gamma\left(\frac{d}{2} - \alpha\right)\sin(\pi\alpha)}{2^{d-1} \pi^{\frac{d+1}{2}} \Gamma\left(\frac{d-1}{2}\right)} \frac{1}{\rho^{d-2}}. \quad (7.2.52b)$$

⁶This follows immediately from eq. (C.4.44).

⁷This one-point function was also computed by ref. [322].

Summing all the contributions we have

$$\langle J_\theta \rangle = \frac{\Gamma\left(\frac{d}{2} - \alpha\right) \Gamma\left(\frac{d}{2} + \alpha - 1\right) \sin(\pi\alpha) \left(1 - 2\alpha + \frac{2\alpha(d-1)\tilde{\zeta}}{\frac{d}{2} - \alpha - 1} + \frac{2(1-\alpha)(d-1)\tilde{\xi}}{\frac{d}{2} + \alpha - 2}\right)}{2^d \pi^{\frac{d+1}{2}} \Gamma\left(\frac{d+1}{2}\right)} \frac{1}{\rho^{d-2}}. \quad (7.2.53)$$

We observe that when $\tilde{\zeta}, \tilde{\xi} \neq 0$ the current is not vanishing at $\alpha = 1/2$. This is due to the singular modes, which break the invariance of the theory under the shift $\alpha \rightarrow \alpha + \mathbb{Z}$.

The integral of this function with respect to α leads to the universal part of the sphere free energy.⁸ When d and p are even, it is controlled by the A-type defect central charge. Setting $d = 4$ and $d = 6$, using eqs. (7.1.10) and (7.1.11) and integrating over the flux α , we obtain

$$a_\Sigma^{(2d)} = \frac{(1-\alpha)^2 \alpha^2 + 4\tilde{\zeta} \alpha^3 + 4\tilde{\xi} (1-\alpha)^3}{2}, \quad (7.2.54)$$

$$a_\Sigma^{(4d)} = \frac{\alpha^2}{720} (1-\alpha)^2 (3 + \alpha - \alpha^2) + \frac{\alpha^3}{360} (5 - 3\alpha^2) \tilde{\zeta} - \frac{(1-\alpha)^3}{360} (3\alpha^2 - 6\alpha - 2) \tilde{\xi}. \quad (7.2.55)$$

A few comments about this result are in order. First of all, when integrating the current one-point function with respect to α , we assumed that $\tilde{\zeta}$ and $\tilde{\xi}$ are not functions of α . Were $\tilde{\zeta}$ or $\tilde{\xi}$ function of α , the dependence of $a_\Sigma^{(2d)}$ and $a_\Sigma^{(4d)}$ on α would be affected by the dynamical source of $\tilde{\zeta}$ and $\tilde{\xi}$ and this unknown source would contribute to the derivative in eq. (7.1.10). Another important comment is that eq. (7.1.10) involves an integration constant which can be a function of $\tilde{\zeta}$ and $\tilde{\xi}$. This constant can be fixed by requiring that $a_\Sigma^{(2d)}$ and $a_\Sigma^{(4d)}$ vanish at $\alpha = 0$ if $\tilde{\xi} = 0$, and at $\alpha = 1$ if $\tilde{\zeta} = 0$, together with the requirement that its dependence on $\tilde{\zeta}$ and $\tilde{\xi}$ be linear. E.g. when $d = 4$, these requirements fix the integration constant to be $-2\tilde{\xi}$, giving precisely eq. (7.2.54). As a check of eq. (7.2.54), we will compute in section 7.2.3 the EE in the presence of the monodromy defect, and we will show that it vanishes for any value of α , $\tilde{\zeta}$ and $\tilde{\xi}$. This implies, in particular, that $a_\Sigma^{(2d)} + \frac{d_2^{(2d)}}{3} = 0$, which is consistent with eqs. (7.2.54) and (7.2.47).

7.2.2.4 Two-point function of \mathcal{D}_i

In this subsection we study the displacement operator of the monodromy defect of the complex scalar. Our final goal will be to identify the coefficient of its two-point function, which in $d = 4$ and $d = 6$ is related to the defect central charge $d_1^{(2d)}$ and $d_1^{(4d)}$, respectively.

⁸When $d = 3$ we can compare with the results obtained in Appendix A of [327], finding perfect agreement upon identification of the flux parameters ($\mu = 2\pi\alpha$).

Given the defect OPE of the fundamental field φ eq. (7.2.22) and of its conjugate φ^\dagger , we look for the displacement operator in the fusion of defect fields $\hat{\mathcal{O}}_{m-\alpha}^\pm$ and $\hat{\mathcal{O}}_{m+\alpha}^{\pm\dagger}$. We are looking for an operator of dimension $\hat{\Delta}_{\mathcal{D}} = d - 1$ and spin $s = 1$. To be precise, there are two operators \mathcal{D}_z and $\mathcal{D}_{\bar{z}}$ with the same dimension and opposite spin associated to the two broken translations in complex coordinates. The combination of defect operators fulfilling these requirements is

$$\mathcal{D}_z = A \hat{\mathcal{O}}_{1-\alpha}^+ \hat{\mathcal{O}}_\alpha^{\dagger+} + B \hat{\mathcal{O}}_{-\alpha}^- \hat{\mathcal{O}}_{1+\alpha}^{\dagger+} + C \hat{\mathcal{O}}_{2-\alpha}^+ \hat{\mathcal{O}}_{-1+\alpha}^{\dagger-} + D [\hat{\mathcal{O}}_\alpha^{\dagger-} \hat{\mathcal{O}}_{1-\alpha}^-]_2, \quad (7.2.56)$$

and their conjugates for the operator with spin $s = -1$. The last operator in eq. (7.2.56) is the conformal primary built out of $\hat{\mathcal{O}}_\alpha^{\dagger-}$, $\hat{\mathcal{O}}_{1-\alpha}^-$ and two derivatives,

$$[\hat{\mathcal{O}}_\alpha^{\dagger-} \hat{\mathcal{O}}_{1-\alpha}^-]_2 \equiv \left(\frac{1}{2(d-2)} - \frac{1}{4\alpha} \right) \hat{\mathcal{O}}_\alpha^{\dagger-} \partial_{\parallel}^2 \hat{\mathcal{O}}_{1-\alpha}^- + \frac{1}{d-2} \partial_a \hat{\mathcal{O}}_\alpha^{\dagger-} \partial^a \hat{\mathcal{O}}_{1-\alpha}^- \\ + \left(\frac{1}{2(d-2)} - \frac{1}{4(1-\alpha)} \right) \partial_{\parallel}^2 \hat{\mathcal{O}}_\alpha^{\dagger-} \hat{\mathcal{O}}_{1-\alpha}^-. \quad (7.2.57)$$

In eq. (7.2.56) the coefficients A , B , C and D are implicitly functions of α , ζ and $\tilde{\zeta}$. We denote their analogues for the spin $s = -1$ operator as A^\dagger , B^\dagger , C^\dagger and D^\dagger . Notice that only the first operator is present for $\zeta = \tilde{\zeta} = 0$. The second operator includes a mode $\hat{\mathcal{O}}_{-\alpha}^-$ so it must vanish for $\zeta = 0$, the third one includes $\hat{\mathcal{O}}_{-1+\alpha}^+$ and it must not appear for $\tilde{\zeta} = 0$. The last term appears only when both ζ and $\tilde{\zeta}$ are non-vanishing. Using this piece of information and consistency with the Ward identity eq. (2.3.21a)

$$\int d^{d-2} x_{\parallel} \langle |\varphi(0, z, \bar{z})|^2 \mathcal{D}_z(x_{\parallel}) \rangle = -\partial_z \langle |\varphi(0, z, \bar{z})|^2 \rangle, \quad (7.2.58)$$

we can fix the form of the displacement operator. Indeed, the two-point function in eq. (7.2.58) is fixed by conformal invariance to be of the form in eq. (3.1.20), which in complex coordinates transverse to the defect becomes

$$\langle |\varphi(0, z, \bar{z})|^2 \mathcal{D}_z(x_{\parallel}) \rangle = b_{\varphi^2 \mathcal{D}}(\alpha, \zeta, \tilde{\zeta}) \frac{\bar{z}}{(|x_{\parallel}|^2 + z\bar{z})^{d-1}}. \quad (7.2.59)$$

Thus by eq. (7.2.58),

$$b_{\varphi^2 \mathcal{D}}(\alpha, \zeta, \tilde{\zeta}) = -\frac{\Gamma(\frac{d}{2} - \alpha) \Gamma(\frac{d}{2} + \alpha - 1) \sin(\pi\alpha)}{4\pi^d} \left(1 - \frac{(d-2)\zeta}{\frac{d}{2} - \alpha - 1} - \frac{(d-2)\tilde{\zeta}}{\frac{d}{2} + \alpha - 2} \right). \quad (7.2.60)$$

Inserting the ansatz eq. (7.2.56) into the two-point function eq. (7.2.59) we find an equation for the coefficients in eq. (7.2.56), which has the solution

$$A = 4\pi\alpha(1-\alpha) b_{\varphi^\dagger \hat{\mathcal{O}}_\alpha^{\dagger+}} b_{\varphi \hat{\mathcal{O}}_{1-\alpha}^+}, \quad B = 4\pi\alpha(1+\alpha) b_{\varphi^\dagger \hat{\mathcal{O}}_{1+\alpha}^{\dagger+}} b_{\varphi \hat{\mathcal{O}}_{-\alpha}^-}, \quad (7.2.61)$$

$$C = 4\pi(1-\alpha)(2-\alpha) b_{\varphi^\dagger \hat{\mathcal{O}}_{-1+\alpha}^{\dagger-}} b_{\varphi \hat{\mathcal{O}}_{2-\alpha}^+}, \quad D = 4\pi\alpha(1-\alpha) b_{\varphi^\dagger \hat{\mathcal{O}}_\alpha^{\dagger-}} b_{\varphi \hat{\mathcal{O}}_{1-\alpha}^-}, \quad (7.2.62)$$

where the b coefficients are the bulk-to-defect couplings introduced in eq. (7.2.23). Similar expressions hold for A^\dagger , B^\dagger , C^\dagger and D^\dagger , with the bulk-to-defect couplings replaced by the ones for the conjugate operators. Using this data it is easy to see that the displacement two-point function in complex coordinates

$$\langle \mathcal{D}_z(x_\parallel) \mathcal{D}_{\bar{z}}(0) \rangle = \frac{c_{\mathcal{D}\mathcal{D}}}{2|x_\parallel|^{2d-2}} \quad (7.2.63)$$

is determined by a linear combination quadratic in the coefficients in eqs. (7.2.27), (7.2.28a) and (7.2.28b)⁹

$$\begin{aligned} c_{\mathcal{D}\mathcal{D}} &= AA^\dagger + BB^\dagger + CC^\dagger + DD^\dagger \frac{(\frac{d}{2} - 1 - \alpha)(\frac{d}{2} - 2 + \alpha)}{\alpha(1 - \alpha)} \\ &= 4\pi^{2-d} \Gamma\left(\frac{d}{2} - \alpha\right) \Gamma\left(\frac{d}{2} + \alpha - 1\right) \sin(\pi\alpha) \left(\alpha(1 - \alpha) + \frac{d\alpha^2\tilde{\zeta}}{\frac{d}{2} - \alpha - 1} + \frac{d(1-\alpha)^2\tilde{\zeta}}{\frac{d}{2} + \alpha - 2} \right). \end{aligned} \quad (7.2.64)$$

Note that it satisfies the relation (5.5.15) for $q = 2$, when compared with the explicit value of h in eq. (7.2.46), and so $c_{\mathcal{D}\mathcal{D}} \geq 0$ whenever $h \geq 0$. Specialising to $d = 4$ and $d = 6$ and using the normalisation eq. (3.4.40) and eq. (6.2.20), respectively, we find for a monodromy defect created by α units of flux in the theory of a complex free scalar

$$d_1^{(2d)} = \frac{3}{2} \left((1 - \alpha)^2 \alpha^2 + 4\tilde{\zeta} \alpha^3 + 4\tilde{\zeta}(1 - \alpha)^3 \right), \quad (7.2.65)$$

$$d_1^{(4d)} = -\frac{\alpha(1 - \alpha^2)(2 - \alpha)}{36} \left(\alpha(1 - \alpha) + \frac{6\alpha^2\tilde{\zeta}}{2 - \alpha} + \frac{6(1 - \alpha)^2\tilde{\zeta}}{1 + \alpha} \right). \quad (7.2.66)$$

As discussed in section 7.1, when $\zeta = \tilde{\zeta} = 0$, the displacement operator \mathcal{D}_i can be identified as the regular term in the defect OPE of the orthogonal components of the current J_i . However, we emphasise that the relation eq. (7.1.12) is not gauge invariant under the shift $\alpha \rightarrow \alpha + \mathbb{Z}$. Thus, expressing \mathcal{D}_i in terms of J_i makes sense only after we fix a specific gauge, which reflects in the choice of the range of α . If we choose the range to be $\alpha \in [0, 1)$ as above, we need to change the definition of the current to be

$$\begin{aligned} \alpha J_z &\rightarrow \mathcal{J}_z \equiv i \left((1 - \alpha) \varphi \partial_z \varphi^\dagger + \alpha \varphi^\dagger \partial_z \varphi \right), \\ \alpha J_{\bar{z}} &\rightarrow \mathcal{J}_{\bar{z}} \equiv -i \left((1 - \alpha) \varphi^\dagger \partial_{\bar{z}} \varphi + \alpha \varphi \partial_{\bar{z}} \varphi^\dagger \right). \end{aligned} \quad (7.2.67)$$

The displacement operator for $\zeta = \tilde{\zeta} = 0$ is then

$$\mathcal{D}_z = -2\pi i \mathcal{J}_z|_{z, \bar{z}=0}, \quad \mathcal{D}_{\bar{z}} = 2\pi i \mathcal{J}_{\bar{z}}|_{z, \bar{z}=0}. \quad (7.2.68)$$

Inserting in these expressions the defect OPE of φ and φ^\dagger , one finds agreement with the first term of eq. (7.2.56).

⁹The final expression for $\zeta = \tilde{\zeta} = 0$ also appeared in ref. [322].

7.2.3 Entanglement entropy

As a check of our computations, we will compute the EE contribution of the monodromy defect in the free complex scalar theory when $d = 4$. In the following, we assume that the defect is flat, and the region A is the half space orthogonal to the defect. More precisely, we take the defect to extend along the τ and the $x^{1, \dots, d-3}$ directions, and the entangling surface ∂A is defined by $\tau = x^1 = 0$ as depicted in figure 7.1. This configuration is the most symmetric case, and it is conformally related to a spherical entangling surface at $\tau = 0$ centred on the flat defect, which was discussed in section 4.5 and depicted in figure 4.2. When $d = 4$ the entangling surface intersects the monodromy defect in a single point and the EE shows a logarithmic divergence whose coefficient is given by [50]

$$S_A^{\text{def}} \Big|_{\log \frac{l}{\varepsilon}} = \frac{1}{6} \left(a_{\Sigma}^{(2d)} + \frac{d_2^{(2d)}}{3} \right). \quad (7.2.69)$$

Note that this is half of eq. (4.5.45) since the defect only intersects the entangling surface once.

Here we employ the heat kernel method following ref. [181] to show that the result is in perfect agreement with eq. (7.2.69). See section 4.3 for an introduction to heat kernel methods. As emphasised in [48, 191, 328–330], in the case of the conformal free scalar, the EE consists of two contributions, one that can be computed from the heat kernel and a second one coming from the coupling to the scalar curvature R . To show this, we can consider the coupling to R as a deformation of the theory. The conical singularity leads to a scalar curvature of the form $R = 2(1 - n)\delta(\rho)/(n\rho)$ [30] which implies the following contribution to the action

$$I_{\text{scalar}}^R[n] = \pi \frac{d-2}{d-1} (1-n) \int_{\partial A} d^2 x_{\perp} d^{d-4} \tilde{x}_{\parallel} |\varphi|^2, \quad (7.2.70)$$

where x_{\perp} denotes the coordinates transverse to the defect, and \tilde{x}_{\parallel} are the defect directions shared with the entangling surface. The delta function coming from R localised the integral over spacetime to the entangling surface ∂A . Thus the full partition function may be written as

$$Z_n = Z_n^{R=0} \left\langle e^{-I_{\text{scalar}}^R} \right\rangle, \quad (7.2.71)$$

where $Z_n^{R=0}$ denotes the partition function of the theory without the coupling to R . Given this factorisation, the replica trick eq. (4.2.14) implies that the EE splits into two contributions

$$S_A = S_A^{R=0} + S_A^R, \quad (7.2.72)$$

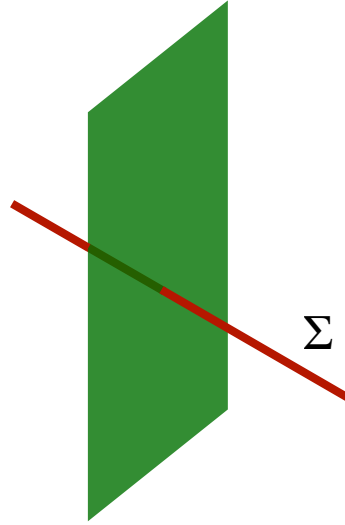


FIGURE 7.1: Sketch of the configuration we employ to compute the defect contribution to the EE in $d = 4$. The figure is an instance in time at $\tau = 0$. The defect (red) extends along the x^1 direction, while the entangling surface (green) extends along the remaining orthogonal directions and intersects the defect at $x^1 = 0$. The defect's contribution to the universal EE of the region to either side of the entangling surface is given by eq. (7.2.69).

where $S_A^{R=0}$ is the EE for the theory in the absence of the coupling to R , and S_A^R is the contribution of eq. (7.2.70) which reads [191, 328–330]

$$S_A^R = -\frac{\pi(d-2)}{(d-1)} \int_{\partial A} d^2 x_{\perp} d^{d-4} \tilde{x}_{\parallel} \langle |\varphi(x)|^2 \rangle. \quad (7.2.73)$$

This last contribution is straightforward to compute. Setting $d = 4$ and using eq. (7.2.39), we find

$$\begin{aligned} S_A^R &= \frac{(1-\alpha)\alpha - 2\tilde{\xi}\alpha - 2\tilde{\xi}(1-\alpha)}{12\pi} \int_{\partial A} d^2 x_{\perp} \frac{1}{\rho^2} = \frac{(1-\alpha)\alpha - 2\tilde{\xi}\alpha - 2\tilde{\xi}(1-\alpha)}{12\pi} \int_0^{2\pi} d\theta \int_{\epsilon}^L \frac{d\rho}{\rho} \\ &= \frac{(1-\alpha)\alpha - 2\tilde{\xi}\alpha - 2\tilde{\xi}(1-\alpha)}{6} \log\left(\frac{L}{\epsilon}\right). \end{aligned} \quad (7.2.74)$$

The first contribution to (7.2.72) can be computed with the heat kernel method as done in [181] for the case of a real scalar in a BCFT. For simplicity we will illustrate the computation only for the regular part of the propagator, namely for $\xi = \tilde{\xi} = 0$, being the generalisation to the singular part straightforward. Recall from section 4.3 that the heat kernel for the Laplacian $\Delta = -\nabla^2$ can be easily extracted from the propagator using eq. (4.3.20). In our case we have

$$K(s; x, x', \alpha) = \frac{1}{(4\pi s)^{\frac{d}{2}}} \sum_m e^{im\theta} e^{-(\rho^2 + \rho'^2 + (x_{\parallel} - x'_{\parallel})^2)/(4s)} I_{|m-\alpha|} \left(\frac{\rho\rho'}{2s} \right) + \text{c.c.}, \quad (7.2.75)$$

where c.c. stands for complex conjugate, and we have replaced the Δ label by α for clarity. We now compute the trace of the heat kernel on a space with conical singularity $\text{Tr}K_n$ via the Sommerfeld formula eq. (4.3.27). By setting $\rho = \rho'$ and $x_{\parallel} = x'_{\parallel}$ the integrals become

$$\begin{aligned} \text{Tr}K_n &= \frac{4\pi n}{(4\pi s)^{\frac{d}{2}}} \int_0^\infty d\rho \int_0^{2\pi} d\theta \int_0^\infty dr \int d^{d-4}\tilde{x}_{\parallel} \rho e^{-\rho^2/(2s)} \mathcal{I}_\alpha^{(1)}\left(\frac{\rho^2}{2s}\right) \\ &+ \frac{8\pi^2 n}{(4\pi s)^{\frac{d}{2}}} \frac{i}{4\pi n} \int_\Gamma d\omega \cot\frac{\omega}{2n} \left[\int_0^\infty d\rho \int_0^\infty dr \int d^{d-4}\tilde{x}_{\parallel} \rho r e^{-\rho^2/(2s) - r^2 \sin^2(\omega/2)/s} \mathcal{I}_\alpha^{(1)}\left(\frac{\rho^2}{2s}\right) \right], \end{aligned} \quad (7.2.76)$$

where r is a radial coordinate along the defect directions orthogonal to ∂A , $r = \sqrt{\tau^2 + (x^1)^2}$, and the function $\mathcal{I}_\alpha^{(1)}$ was defined in eq. (7.2.33). After a change of variables we have

$$\begin{aligned} \text{Tr}K_n &= \frac{4\pi n L^{d-2}}{(4\pi s)^{\frac{d}{2}}} s \int_0^{\frac{L^2}{2s}} d\zeta e^{-\zeta} \mathcal{I}_\alpha^{(1)}(\zeta) \\ &+ \frac{8\pi^2 n L^{d-4}}{(4\pi s)^{\frac{d}{2}}} s^2 \left[\frac{i}{8\pi n} \int_\Gamma d\omega \cot\left(\frac{\omega}{2n}\right) \frac{1}{\sin^2\frac{\omega}{2}} \right] \left[\int_0^{\frac{L^2}{2s}} d\zeta e^{-\zeta} \mathcal{I}_\alpha^{(1)}(\zeta) \right], \end{aligned} \quad (7.2.77)$$

where we introduced the cut-off L to regulate the IR divergence. The contour integral over ω can be evaluated exactly, and it gives

$$\frac{i}{8\pi n} \int_\Gamma d\omega \cot\left(\frac{\omega}{2n}\right) \frac{1}{\sin^2\frac{\omega}{2}} = \frac{1}{6n^2}(1 - n^2). \quad (7.2.78)$$

The heat-kernel contribution to the entanglement entropy $S_A^{R=0}$ can be found using

$$S_A^{R=0} = \lim_{n \rightarrow 1} \partial_n (\mathcal{W}_n^{R=0} - n\mathcal{W}^{R=0}). \quad (7.2.79)$$

The term linear in n in eq. (7.2.77) does not contribute. Thus, the whole contribution to the EE comes from the second line, and we find

$$S_A^{R=0} = \frac{1}{6} \int_{\epsilon^2}^{+\infty} ds \left[\frac{8\pi^2 L^{d-4}}{(4\pi s)^{\frac{d}{2}}} s \int_0^{\frac{L^2}{2s}} d\zeta e^{-\zeta} \mathcal{I}_\alpha^{(1)}(\zeta) \right], \quad (7.2.80)$$

where we introduced the UV cut-off ϵ to regulate the small s behaviour of the integral. The resulting integrals are quite cumbersome but their computation is straightforward, and for $d = 4$ we find

$$S_A^{R=0} = \frac{L^2}{24\epsilon^2} - \frac{(1-\alpha)\alpha}{6} \log\left(\frac{L}{\epsilon}\right) + \mathcal{O}(1). \quad (7.2.81)$$

With the singular modes of φ we find instead

$$S_A^{R=0} = \frac{L^2}{24\epsilon^2} - \frac{(1-\alpha)\alpha - 2\zeta\alpha - 2\tilde{\zeta}(1-\alpha)}{6} \log\left(\frac{L}{\epsilon}\right) + \mathcal{O}(1), \quad (7.2.82)$$

which precisely cancels eq. (7.2.74). Thus, in the theory of a free complex scalar the contribution of the monodromy defect to the universal part of the EE vanishes in $d = 4$. This is in agreement with the relation (7.2.69) proven in [50], and it confirms our findings in eqs. (7.2.54) and (7.2.47).

When $d = 6$, we can use our computations of $a_\Sigma^{(4d)}$ and $d_2^{(4d)}$ to make a prediction for the defect contribution to the universal part of the EE of half-space orthogonal to the defect. From eq. (6.2.45), we find that for monodromy defects in free scalar field theories¹⁰

$$S_A^{\text{def}}|_{\log \frac{L}{\epsilon}} = - \left[\frac{\alpha^2}{360} (1-\alpha)^2 + \frac{\alpha^3 \zeta}{90} + \frac{\tilde{\zeta}}{90} (1-\alpha)^3 \right]. \quad (7.2.83)$$

7.3 Free fermion

In this section, we compute h , a_I , and $c_{\mathcal{DD}}$ for monodromy defects in a theory of free Dirac fermions in arbitrary dimension $d \geq 3$. As in the case of the free scalars, we will eventually specialise to $d = 4$ and $d = 6$ in order to connect the results to the defect Weyl anomaly coefficients. Lastly, we will compute defect EE as a check on $a_\Sigma^{(2d)}$ and $d_2^{(2d)}$ in $d = 4$.

Our starting point is the background geometry described in eq. (7.1.1) on which we introduce frame fields e^M with components $e^M = e^M_\mu dx^\mu$ for $M = 0, \dots, d-1$ such that

$$e^0 = dt, \quad e^1 = d\rho, \quad e^2 = \rho d\theta, \quad e^\beta = dx_{\parallel}^{\beta-2}, \quad (7.3.84)$$

where $\beta = 3, \dots, d-1$.

On this background, we place a single free Dirac fermion ψ , which in d dimensions has $2^{\lfloor \frac{d}{2} \rfloor}$ components. Turning on a background gauge field A for the vector $U(1)_V$ symmetry eq. (2.5.43a), the Dirac action can then be written as

$$I_{\text{fermion}} = -i \int d^d x |e| \psi^\dagger \gamma^0 \nabla \psi, \quad (7.3.85)$$

where we denote the Dirac operator in the presence of a background gauge field A_μ as $\nabla = \gamma^\mu (D_\mu - iA_\mu)$. Here, $D_\mu = \partial_\mu + \Omega_\mu$ with $\Omega_\mu = \frac{1}{8} \omega_\mu^{MN} [\gamma_M, \gamma_N]$ and ω_μ^{MN} being

¹⁰We are grateful to J. S. Dowker for alerting us to a typo in an earlier version of ref. [1], where a variant of this computation originally appeared.

the spin-connection. We denote the γ -matrices in curvilinear coordinates by $\gamma_\mu = e^M{}_\mu \gamma_M$, which obey the Clifford algebra $\gamma_\mu \gamma_\nu + \gamma_\nu \gamma_\mu = +2g_{\mu\nu}$. Finally, we define the Dirac conjugate $\bar{\psi} \equiv i\psi^\dagger \gamma^0$.

7.3.1 Mode expansion and propagator

The fermion propagator can be computed by employing the same methods as in section 7.2 for the free scalar. We refer to appendix C.3 for a more detailed discussion. In a suitable Clifford algebra basis, the Dirac equation can be solved by a spinor with $2^{\lfloor \frac{d}{2} \rfloor - 1}$ components proportional to $J_{\pm(n-\alpha)}$ and the other $2^{\lfloor \frac{d}{2} \rfloor - 1}$ components proportional to $J_{\pm(n+1-\alpha)}$ with $n \in \mathbb{Z}$. Note that for $n \neq 0$ with $0 < \alpha < 1$, one choice of sign results in a spinor with all components either regular or all divergent as $\rho \rightarrow 0$. For the divergent solutions at least one of the components diverges as $\mathcal{O}(\rho^{-1})$ or worse, which makes them physically inadmissible.

For $n = 0$, both (\pm) solutions are admissible provided that $\alpha \neq 0, 1$. In this case, half of the components are regular whereas the other half have divergent behaviour between $\mathcal{O}(\rho^{-1})$ and $\mathcal{O}(1)$. This tamer behaviour makes both solutions acceptable. Generally, one can introduce a parameter $\zeta \in [0, 1]$ which interpolates between these two solutions, and study the theory's correlation functions as a function of ζ .

In order to write down the fermion mode expansion, we adopt complex coordinates in the directions normal to the defect $z = \rho e^{i\theta}$ and $\bar{z} = \rho e^{-i\theta}$. We then perform a gauge transformation $A \rightarrow A - \alpha d\theta$ in order to remove the background gauge field A from correlation functions at the expense of introducing an extra factor of $e^{-i\alpha\theta}$ in the fermion mode expansion. The mode expansion in this gauge can be written as

$$\psi = \psi_{-\alpha} \left(\frac{z}{\rho} \right)^{-\alpha + \frac{1}{2}} + \psi_\alpha \left(\frac{\bar{z}}{\rho} \right)^{\alpha - \frac{1}{2}} + \sum_{n=1}^{\infty} \psi_{n-\alpha} \left(\frac{z}{\rho} \right)^{n-\alpha + \frac{1}{2}} + \sum_{n=1}^{\infty} \psi_{n+\alpha} \left(\frac{\bar{z}}{\rho} \right)^{n+\alpha - \frac{1}{2}}, \quad (7.3.86)$$

where

$$\psi_{n\pm\alpha} = \sum_{s=1}^{2^{\lfloor \frac{d}{2} \rfloor - 1}} \int_{-\infty}^{\infty} d^{d-3} \vec{k}_\parallel \int_0^\infty dk_\rho \left(\tilde{f}(k) a_{\mp n}^s(k) u_{\mp n, k}^s + \tilde{f}^*(k) b_{\mp n}^{s\dagger}(k) v_{\mp n, k}^s \right), \quad (7.3.87)$$

and

$$\tilde{f}(k) = \frac{e^{-i\omega t + i\vec{k}_\parallel \cdot \vec{x}_\parallel}}{(\sqrt{2\pi})^{d-2}} \sqrt{\frac{k_\rho}{2^{\lfloor \frac{d}{2} \rfloor} \omega}}. \quad (7.3.88)$$

At $n = 0$, there are two solutions $\psi_{-\alpha}$ and ψ_{α} with $\xi \in [0, 1]$ interpolating between them:

$$\psi_{-\alpha} = \sqrt{1 - \xi} \sum_{s=1}^{2^{\lfloor \frac{d}{2} \rfloor - 1}} \int_{-\infty}^{\infty} \mathbf{d}^{d-3} \vec{k}_{\parallel} \int_0^{\infty} dk_{\rho} \left(\tilde{f}(k) a_0^{(+s)}(k) u_{0,k}^{(+s)} + \tilde{f}^*(k) b_0^{(+s)\dagger}(k) v_{0,k}^{(+s)} \right), \quad (7.3.89a)$$

$$\psi_{\alpha} = \sqrt{\xi} \sum_{s=1}^{2^{\lfloor \frac{d}{2} \rfloor - 1}} \int_{-\infty}^{\infty} \mathbf{d}^{d-3} \vec{k}_{\parallel} \int_0^{\infty} dk_{\rho} \left(\tilde{f}(k) a_0^{(-s)}(k) u_{0,k}^{(-s)} + \tilde{f}^*(k) b_0^{(-s)\dagger}(k) v_{0,k}^{(-s)} \right). \quad (7.3.89b)$$

In the above equations, $u_{\mp n,k}^s$ and $v_{\mp n,k}^s$ for $n \geq 1$ are spinors whose components involve Bessel functions $J_{n \pm \alpha}(k_{\rho} \rho)$ and $J_{n \mp (1-\alpha)}(k_{\rho} \rho)$ and, in the frame we are using, are purely functions of ρ . For $n = 0$, the spinors $u_{0,k}^{(\pm)s}$ and $v_{0,k}^{(\pm)s}$ have components $J_{\mp \alpha}(k_{\rho} \rho)$ and $J_{\pm (1-\alpha)}(k_{\rho} \rho)$. See appendix C.3 for more details. Explicit solutions for the spinors in $d = 4$ are given in eqs. (C.3.33) and (C.3.34). Demanding that the defect corresponds to the infinite limit of a physical solenoid singles out either $\xi = 0$ or $\xi = 1$, depending on the sign of the flux α [324].

In order to compute the propagator, one can canonically quantise the mode expansions. However, this is cumbersome in general dimensions, and we will not present this method here. Instead, we will make use of the scalar propagator eq. (7.2.31) to directly achieve the same result. It is well-known that in the absence of a monodromy, one can write the fermion propagator $G_{\text{F}}(x, x') = -\langle \bar{\psi}(x') \psi(x) \rangle$ in terms of the scalar propagator $G_{\text{S}}(x, x') = \langle \varphi^{\dagger}(x) \varphi(x') \rangle$. Schematically, $G_{\text{F}}(x, x') = -\mathcal{D} G_{\text{S}}(x, x')$, where $\mathcal{D} \equiv \gamma^{\mu} D_{\mu}$ is explicitly with respect to the unprimed coordinates.

In the presence of a monodromy, the relation between G_{F} and G_{S} is modified as follows. Let $P_{\pm} = \frac{1}{2}(\mathbb{1} \pm i\gamma_1 \gamma_2)$, where $\mathbb{1}$ is the $2^{\lfloor \frac{d}{2} \rfloor} \times 2^{\lfloor \frac{d}{2} \rfloor}$ dimensional identity matrix. Then the fermion propagator in the presence of a monodromy defect takes the form¹¹

$$G_{\text{F},\alpha,\xi}(x, x') = -\mathcal{D} \left(P_{-} e^{i(\theta-\theta')/2} G_{\text{S},\alpha,1-\xi,0}(x, x') + P_{+} e^{-i(\theta-\theta')/2} G_{\text{S},\alpha,0,\xi}(x, x') \right), \quad (7.3.90)$$

where $G_{\text{S},\alpha,\xi,\tilde{\xi}}(x, x')$ is the scalar propagator with singular modes as defined in eq. (7.2.26). The factors of $e^{\pm i(\theta-\theta')/2}$ are due to working in the rotating frame eq. (7.3.84) and ensure that the modes in the scalar Green's functions combine correctly into modes of the spinor Green's function. Notice that for any $\xi \in [0, 1]$, one always needs a singular mode in at least one of the two scalar Green's functions because both $n = 0$ modes of the fermion are singular.

¹¹This is similar to the approach taken in [167]. We thank Christopher Herzog for pointing that out to us, and suggesting to use such a relation.

In computing h , a_J , and $c_{\mathcal{D}\mathcal{D}}$ we will only need to compute particular derivatives of G_S evaluated in either the coincident or defect limits, and so we will not display G_F in full detail. Notice that in writing eq. (7.3.90) in terms of eq. (7.2.26) we have implicitly performed a Wick rotation to Euclidean signature $t \rightarrow -i\tau$.

7.3.2 Correlation functions and central charges

Equipped with the general form of the propagator in eq. (7.3.90), we now compute the one-point functions of the stress tensor $T_{\mu\nu}$ and the $U(1)_V$ current J_μ , as well as the two-point function of the displacement operator \mathcal{D}_i .

7.3.2.1 One-point function of $T_{\mu\nu}$

We commence with an analysis of the components of the stress tensor one-point function from which we will extract h in general $d \geq 3$. Specialising to $d = 4$ and $d = 6$, we will thus obtain the defect Weyl anomaly coefficients $d_2^{(2d)}$ and $d_2^{(4d)}$, respectively.

In Euclidean signature, ψ and $\bar{\psi}$ are independent, and the action can be taken to be

$$I_{\text{fermion}}^E = \int d^d x e \bar{\psi} \not{\nabla} \psi. \quad (7.3.91)$$

The classical stress tensor can be computed by varying eq. (7.3.91) with respect to the frame fields e^M_μ as in eq. (2.4.33). The result is

$$T_{\mu\nu} = \frac{1}{2} \bar{\psi} \gamma_{(\mu} \overset{\leftrightarrow}{\nabla}_{\nu)} \psi, \quad (7.3.92)$$

where the parenthesis denotes symmetrisation over the indices, and

$$\bar{\psi} \gamma_\mu \overset{\leftrightarrow}{\nabla}_\nu \psi = \bar{\psi} \gamma_\mu (\partial_\nu + \Omega_\nu - iA_\nu) \psi - (\partial_\nu \bar{\psi}) \gamma_\mu \psi + \bar{\psi} (\Omega_\nu - iA_\nu) \gamma_\mu \psi. \quad (7.3.93)$$

The one-point function of the stress tensor can then be written in terms of the fermion propagator $G_{F,\alpha,\xi}$ as follows:

$$\langle T_{\mu\nu}(x) \rangle = -\frac{1}{2} \lim_{x' \rightarrow x} \text{Tr} \left[\left(\gamma_{(\mu} \partial_{\nu)} - \gamma_{(\mu} \partial'_{\nu)} + \gamma_{(\mu} \Omega_{\nu)} + \Omega_{(\mu} \gamma_{\nu)} \right) G_{F,\alpha,\xi}(x, x') \right], \quad (7.3.94)$$

where ∂'_ν denotes the derivative with respect to primed coordinates, and A has been gauged away.

In order to compute h , it will suffice to analyse a single non-vanishing component of $\langle T_{\mu\nu} \rangle$ with others following from the tensor structures dictated by the remaining

conformal symmetry. To that end, let us consider

$$\langle T_{\tau\tau} \rangle = -\frac{1}{2} \lim_{x' \rightarrow x} \text{Tr} [\gamma^0 (\partial_\tau - \partial_{\tau'}) G_{F,\alpha,\xi}(x, x')]. \quad (7.3.95)$$

To evaluate $\langle T_{\tau\tau} \rangle$, we need to substitute eq. (7.3.90) and compute the coincident limit of various combinations of derivatives acting on the scalar propagator. Each term contains at least one derivative of G_ζ with respect to τ or τ' . Using the integral representation given by eq. (7.2.31), it is easy to see that all the terms with a single derivative with respect to τ or τ' vanish in the coincident limit $x \rightarrow x'$ due to the appearance of η in the integrand. The only terms that survive are

$$\langle T_{\tau\tau} \rangle = \frac{1}{2} \sum_{\zeta=\pm} \text{Tr}(\gamma^0 P_\zeta \gamma^0) (\partial_\tau^2 - \partial_{\tau'} \partial_\tau) G_\zeta, \quad (7.3.96)$$

where we defined

$$G_\zeta \equiv \begin{cases} \lim_{x' \rightarrow x} G_{S,\alpha,0,\xi}(x, x'), & \zeta = + \\ \lim_{x' \rightarrow x} G_{S,\alpha,1-\xi,0}(x, x'), & \zeta = - . \end{cases} \quad (7.3.97)$$

Evaluating the traces using standard γ -matrix identities and utilising the fact that $\partial_{\tau'} \partial_\tau G_\pm = -\partial_\tau^2 G_\pm$, one finds that

$$\langle T_{\tau\tau} \rangle = 2^{\lfloor \frac{d}{2} \rfloor - 1} \partial_\tau^2 (G_+ + G_-). \quad (7.3.98)$$

All that remains is to compute the $\partial_\tau^2 G_\zeta$, which can be done straightforwardly using the integral representation of the scalar propagator eq. (7.2.31). Using the same scheme as in section 7.2, one finds

$$\begin{aligned} \partial_\tau^2 G_+ &= -\frac{1}{2(2\pi)^{d/2} \rho^d} \int_0^\infty d\zeta e^{-\zeta} \zeta^{\frac{d}{2}-1} (\mathcal{I}_\alpha^{(1)}(\zeta) + \zeta (I_{-1+\alpha}(\zeta) - I_{1-\alpha}(\zeta))) \\ &= \frac{(2d\zeta - 2\alpha - d) \Gamma\left(\frac{d}{2} - \alpha\right) \Gamma\left(\frac{d}{2} + \alpha\right) \sin(\pi\alpha)}{2^{d+1} \pi^{\frac{1}{2}(d+1)} d \Gamma\left(\frac{d+1}{2}\right)} \frac{1}{\rho^d}. \end{aligned} \quad (7.3.99)$$

Computing $\partial_\tau^2 G_-$ follows similarly,

$$\partial_\tau^2 G_- = \frac{(2\alpha - 2d\zeta + d - 2) \Gamma\left(\frac{d}{2} - \alpha + 1\right) \Gamma\left(\frac{d}{2} + \alpha - 1\right) \sin(\pi\alpha)}{2^{d+1} \pi^{\frac{1}{2}(d+1)} d \Gamma\left(\frac{d+1}{2}\right)} \frac{1}{\rho^d}. \quad (7.3.100)$$

Combining $\partial_\tau^2 G_+ + \partial_\tau^2 G_-$, we thus arrive at¹²

$$\langle T_{\tau\tau} \rangle = - \frac{((1-2\alpha)d\xi + \alpha(2\alpha+d-2))\Gamma\left(\frac{d}{2}-\alpha\right)\Gamma\left(\frac{d}{2}+\alpha-1\right)\sin(\pi\alpha)}{2^{d+1-\lfloor\frac{d}{2}\rfloor}\pi^{\frac{1}{2}(d+1)}d\Gamma\left(\frac{d+1}{2}\right)} \frac{1}{\rho^d}. \quad (7.3.101)$$

Using eq. (3.1.13), we find

$$h = \frac{((1-2\alpha)d\xi + \alpha(2\alpha+d-2))\Gamma\left(\frac{d}{2}-\alpha\right)\Gamma\left(\frac{d}{2}+\alpha-1\right)\sin(\pi\alpha)}{2^{d+1-\lfloor\frac{d}{2}\rfloor}\pi^{\frac{1}{2}(d+1)}d\Gamma\left(\frac{d+1}{2}\right)}. \quad (7.3.102)$$

It is clear from the functional form that $h \geq 0$ for any value of $\alpha \in [0, 1]$ and $\xi \in [0, 1]$ in $d \geq 3$, and $h = 0$ for all $\xi \in [0, 1]$ at $\alpha = 0$ and $\alpha = 1$. Setting $d = 4$ and $d = 6$ to extract $d_2^{(2d)}$ and $d_2^{(4d)}$, respectively, we find using eqs. (3.4.41) and (6.2.39)

$$d_2^{(2d)} = -3\alpha(1-\alpha)(\alpha(1+\alpha) + 2\xi(1-2\alpha)), \quad (7.3.103)$$

$$d_2^{(4d)} = -\frac{\alpha(1-\alpha^2)(2-\alpha)}{18}(\alpha(\alpha+2) + 3(1-2\alpha)\xi). \quad (7.3.104)$$

Note that $d_2^{(2d)}$ and $d_2^{(4d)}$ are negative, which is expected if the ANEC holds in the presence of a $p = 2$ and $p = 4$ defect, respectively [50].

7.3.2.2 One-point function of J_θ

In this subsection, we will analyse the current one-point function in order to extract a_J in general $d \geq 3$ and then compute $a_\Sigma^{(2d)}$ and $a_\Sigma^{(4d)}$ when $d = 4$ and $d = 6$ by integrating a_J . From the form of the $U(1)_V$ current

$$J^\mu(x) = -i\bar{\psi}\gamma^\mu\psi(x), \quad (7.3.105)$$

and the fermion propagator in eq. (7.3.90), we can express $\langle J_\theta \rangle$ as

$$\langle J_\theta \rangle = i \lim_{\theta \rightarrow \theta'} \sum_{\zeta=\pm} \left(\text{Tr}[\gamma^\mu P_\zeta \gamma_\theta] \partial_\mu (e^{-i\zeta(\theta-\theta')/2} G_\zeta) + \text{Tr}[\gamma^\theta \Omega_\theta P_\zeta \gamma_\theta] G_\zeta \right), \quad (7.3.106)$$

where ∂_μ is again with respect to the unprimed coordinates. All other components of $\langle J_\mu \rangle$ will turn out to vanish, so we do not display them here.

To evaluate eq. (7.3.106), we need to compute the coincident limit ($\eta \rightarrow 1$) of the scalar propagator G_S and its first derivatives. This limit has already been computed for G_+ in section 7.2 and is given by the sum of eqs. (7.2.34) and (7.2.36). For convenience we

¹²The stress tensor one-point function for $\xi = 0$ was previously computed in [331].

reproduce the result here:

$$\begin{aligned} G_+ &= \frac{1}{2(2\pi)^{d/2}\rho^{d-2}} \int_0^\infty d\zeta e^{-\zeta} \zeta^{\frac{d}{2}-2} (\mathcal{I}_\alpha^{(1)}(\zeta) + \zeta(I_{-1+\alpha}(\zeta) - I_{1-\alpha}(\zeta))) \\ &= \frac{(2\alpha + (d-2)(2\zeta - 1))\Gamma\left(\frac{d}{2} - \alpha - 1\right)\Gamma\left(\frac{d}{2} + \alpha - 1\right)\sin(\pi\alpha)}{2^d \pi^{\frac{1}{2}(d+1)}(d-2)\Gamma\left(\frac{d-1}{2}\right)} \frac{1}{\rho^{d-2}}. \end{aligned} \quad (7.3.107)$$

The limit G_- is again computed in the same manner as G_+ with $\alpha \rightarrow 1 - \alpha$ and $\zeta \rightarrow 1 - \zeta$ in the singular mode, which gives

$$G_- = \frac{(2\alpha - 2(d-2)\zeta + d - 2)\Gamma\left(\frac{d}{2} - \alpha - 1\right)\Gamma\left(\frac{d}{2} + \alpha - 1\right)\sin(\pi\alpha)}{2^d \pi^{\frac{1}{2}(d+1)}(d-2)\Gamma\left(\frac{d-1}{2}\right)} \frac{1}{\rho^{d-2}}. \quad (7.3.108)$$

We also need the coincident limit of first derivatives of the scalar propagator. Due to the appearance of η in the integral representation of the propagator in eq. (7.2.31), first derivatives along the defect vanish in the coincident limit. Derivatives along the transverse directions, however, are non-trivial. The ρ -derivative produces the same integral as G_\pm up to a factor of $-(d-2)/(2\rho)$.

The θ -derivative of G_+ produces a new integral, which has also been computed in section 7.2. It is proportional to eq. (7.2.49). With the singular mode we find

$$\begin{aligned} \partial_\theta G_+ &= \frac{i}{2(2\pi)^{d/2}\rho^{d-2}} \int_0^\infty d\zeta e^{-\zeta} \zeta^{\frac{d}{2}-2} \left[\mathcal{I}_\alpha^{(2)}(\zeta) - \zeta(1-\alpha)(I_{-1+\alpha}(\zeta) - I_{1-\alpha}(\zeta)) \right] \\ &= \frac{i((2\alpha - 1)(2\alpha + d - 4) - 4(\alpha - 1)(d - 1)\zeta)\Gamma\left(\frac{d}{2} - \alpha\right)\Gamma\left(\frac{d}{2} + \alpha - 2\right)\sin(\pi\alpha)}{2^{d+2}\pi^{\frac{1}{2}(d+1)}\Gamma\left(\frac{d+1}{2}\right)} \frac{1}{\rho^{d-2}}. \end{aligned} \quad (7.3.109)$$

Finally, we also have

$$\partial_\theta G_- = \frac{i(4\alpha(d-1)\zeta - (2\alpha + 1)(2\alpha + d - 2))\Gamma\left(\frac{d}{2} - \alpha - 1\right)\Gamma\left(\frac{d}{2} + \alpha - 1\right)\sin(\pi\alpha)}{2^{d+2}\pi^{\frac{1}{2}(d+1)}\Gamma\left(\frac{d+1}{2}\right)} \frac{1}{\rho^{d-2}}. \quad (7.3.110)$$

With these results we return to evaluating eq. (7.3.106). The γ -matrix traces can be performed using standard Clifford algebra identities. Recalling that derivatives of G_\pm along the defect vanish in the coincident limit, we find

$$\langle J_\theta \rangle = 2^{\lfloor \frac{d}{2} \rfloor - 1} \left(\rho \partial_\rho (G_+ - G_- - i \partial_\theta (G_+ + G_-)) \right). \quad (7.3.111)$$

Now using eqs. (7.3.107) to (7.3.110), the one-point function of the $U(1)_V$ current evaluates to

$$\langle J_\theta \rangle = - \frac{(2(1-\alpha) - d + 2\zeta(d-1)) \Gamma\left(\frac{d}{2} - \alpha\right) \Gamma\left(\frac{d}{2} + \alpha - 1\right) \sin(\pi\alpha)}{2^{d+1-\lfloor \frac{d}{2} \rfloor} \pi^{\frac{1}{2}(d+1)} \Gamma\left(\frac{d+1}{2}\right)} \frac{1}{\rho^{d-2}}. \quad (7.3.112)$$

Via eq. (7.1.4), we can read off a_J for the fermion monodromy defect directly from eq. (7.3.112). Note that a_J does not have a definite sign. For all $\alpha \in [0, 1]$, $a_J > 0$ when $\zeta = 0$ whereas $a_J < 0$ for $\zeta = 1$. Moreover, $a_J \rightarrow -a_J$ when $\alpha \rightarrow 1 - \alpha$ and $\zeta \rightarrow 1 - \zeta$, which implies that $a_J = 0$ when $\alpha = \zeta = \frac{1}{2}$, as expected.

Since derivatives along the defect vanish in the coincident limit, $\langle J_a \rangle = 0$. The only other non-trivial component to check is $\langle J_\rho \rangle$ which also evaluates to zero.

At this point, we set $d = 4$ and $d = 6$, use eqs. (7.1.10) and (7.1.11) and integrate over the flux α to obtain the A-type defect central charges

$$a_\Sigma^{(2d)} = \alpha^2(2 - \alpha^2 - 2\zeta(3 - 2\alpha)) + \zeta, \quad (7.3.113)$$

$$a_\Sigma^{(4d)} = \frac{\alpha^2}{360}(2\alpha^4 - 15\alpha^2 + 24) + \frac{(1 - 2\alpha)}{360}(6\alpha^4 - 12\alpha^3 - 16\alpha^2 + 22\alpha + 11)\zeta, \quad (7.3.114)$$

where we assumed that ζ is independent of α . To fix the integration constant $c(\zeta)$, we assumed that it is linear in ζ , and required that $a_\Sigma^{(2d)} = a_\Sigma^{(4d)} = 0$ when $\alpha = \zeta = 0$ and when $\alpha = \zeta = 1$. This sets $c(\zeta) = \zeta$ when $d = 4$, and $c(\zeta) = -\frac{11}{360}\zeta$ when $d = 6$.

In computing the defect EE when $d = 4$ in section 7.3.3, we will independently check $c(\zeta) = \zeta$ from the result for $d_2^{(2d)}$ above. Note that non-vanishing of the central charge at $\alpha \rightarrow 0, 1$ suggests the existence of a decoupled sector of defect fermionic modes similar to the edge fermions in the (integer) quantum Hall effect. In fact we don't expect these fermions to be chiral for a monodromy generated by $U(1)_V$ and thus the situation is more similar to the quantum spin Hall effect [332], where a pair of fermions with opposite chirality emerges at the edge.

7.3.2.3 Two-point function of \mathcal{D}_i

In this subsection, we compute the displacement operator two-point function in general $d \geq 3$ and use its normalisation $c_{\mathcal{D}\mathcal{D}}$ in $d = 4$ and $d = 6$ to extract $d_1^{(2d)}$ and $d_1^{(4d)}$, respectively. Working with the complex coordinates z, \bar{z} adopted above, the frame fields become

$$e^M_z = \frac{e^{-i\theta}}{2\rho}(\rho e^M_\rho - i e^M_\theta), \quad e^M_{\bar{z}} = \frac{e^{i\theta}}{2\rho}(\rho e^M_\rho + i e^M_\theta), \quad (7.3.115)$$

and we can thus write

$$\gamma_z = \frac{\bar{z}}{\rho} \gamma_1 P_-, \quad \gamma_{\bar{z}} = \frac{z}{\rho} \gamma_1 P_+, \quad (7.3.116)$$

with P_{\pm} defined above eq. (7.3.90).

The form of the displacement operator can be found by the same arguments as in section 7.2. Using the mode expansion in eqs. (7.3.86)–(7.3.89), we make the ansatz

$$D_z = c_1 [\bar{\psi}_{1+\alpha} \gamma_1 P_- \psi_{-\alpha}] + c_2 [\bar{\psi}_{\alpha} \gamma_1 P_- \psi_{1-\alpha}], \quad (7.3.117a)$$

$$D_{\bar{z}} = c_3 [\bar{\psi}_{-\alpha} \gamma_1 P_+ \psi_{1+\alpha}] + c_4 [\bar{\psi}_{1-\alpha} \gamma_1 P_+ \psi_{\alpha}], \quad (7.3.117b)$$

where the coefficients $c_{1,\dots,4}$ are arbitrary complex numbers and the square brackets denote the defect operator defined by taking the defect limit $\rho \rightarrow 0$. We can fix the coefficients by checking the Ward identity

$$\int_{-\infty}^{\infty} d^{d-2} x'_{\parallel} \langle \bar{\psi} \gamma_{\bar{z}} \psi(0, z, \bar{z}) D_z(x'_{\parallel}) \rangle = -\partial_z \langle \bar{\psi} \gamma_{\bar{z}} \psi(0, z, \bar{z}) \rangle = -\partial_z \left(\frac{1}{2\bar{z}} \langle J_{\theta} \rangle \right). \quad (7.3.118)$$

The correlator on the left-hand side can be written as

$$\begin{aligned} \langle \bar{\psi} \gamma_{\bar{z}} \psi(z, \bar{z}, 0) D_z(x'_{\parallel}) \rangle &= -c_1 \text{Tr} \left[G_{F,\alpha}^{-\alpha}(x', x) \gamma_1 P_+ G_{F,\alpha}^{1+\alpha}(x, x') \gamma_1 P_- \right] \\ &\quad - c_2 \text{Tr} \left[G_{F,\alpha}^{1-\alpha}(x', x) \gamma_1 P_+ G_{F,\alpha}^{\alpha}(x, x') \gamma_1 P_- \right], \end{aligned} \quad (7.3.119)$$

where $x = \{0, z, \bar{z}\}$, $x' = \{x'_{\parallel}, 0, 0\}$, and $G_{F,\alpha}^{\nu}$ denotes the two-point function of the defect operators labeled by ν , i.e. the Wick contraction of $\hat{\psi}_{\nu}$ and $\hat{\bar{\psi}}_{\nu}$. The two-point function can be evaluated explicitly after performing the traces over γ -matrices. By then taking the result for $\langle \bar{\psi} \gamma_{\bar{z}} \psi(0, z, \bar{z}) D_z(x'_{\parallel}) \rangle$ and comparing to the right-hand side of eq. (7.3.118), which can be easily computed from eq. (7.3.112), $c_{1,2}$ are fixed uniquely. A similar analysis can be performed for $D_{\bar{z}}$ such that eqs. (7.3.117a) and (7.3.117b) become

$$D_z = 2\pi\alpha [\bar{\psi}_{1+\alpha} \gamma_1 P_- \psi_{-\alpha}] - 2\pi(1-\alpha) [\bar{\psi}_{\alpha} \gamma_1 P_- \psi_{1-\alpha}], \quad (7.3.120a)$$

$$D_{\bar{z}} = -2\pi\alpha [\bar{\psi}_{-\alpha} \gamma_1 P_+ \psi_{1+\alpha}] + 2\pi(1-\alpha) [\bar{\psi}_{1-\alpha} \gamma_1 P_+ \psi_{\alpha}]. \quad (7.3.120b)$$

Having found D_z and $D_{\bar{z}}$ in the presence of singular modes with $\xi \neq 0$, we can now proceed with computing their two-point function, which takes the form

$$\begin{aligned} \langle D_{\bar{z}}(x_{\parallel}) D_z(0) \rangle &= 4\pi^2 \alpha^2 (1-\xi) \text{Tr} \left[G_{F,\alpha}^{-\alpha}(0, x_{\parallel}) \gamma_1 P_+ G_{F,\alpha}^{1+\alpha}(x_{\parallel}, 0) \gamma_1 P_- \right] \\ &\quad + 4\pi^2 (1-\alpha)^2 \xi \text{Tr} \left[G_{F,\alpha}^{1-\alpha}(0, x_{\parallel}) \gamma_1 P_+ G_{F,\alpha}^{\alpha}(x_{\parallel}, 0) \gamma_1 P_- \right]. \end{aligned} \quad (7.3.121)$$

The γ -matrix traces can again be performed easily with Clifford algebra identities, and one is left with derivatives of the scalar propagator along the defect. Taking the defect

limit, we find

$$\langle \mathcal{D}_{\bar{z}}(x_{\parallel}) \mathcal{D}_z(0) \rangle = \frac{((1-2\alpha)d\xi + \alpha(2\alpha + d - 2))\Gamma\left(\frac{d}{2} - \alpha\right)\Gamma\left(\frac{d}{2} + \alpha - 1\right)\sin(\pi\alpha)}{2^{2-\lfloor \frac{d}{2} \rfloor} \pi^{d-1}} \frac{1}{|x_{\parallel}|^{2d-2}}, \quad (7.3.122)$$

where $c_{\mathcal{D}\mathcal{D}}$ can be read off using eq. (7.2.63). Setting $p = d - 2$, one can see that $c_{\mathcal{D}\mathcal{D}}$ and h computed in eqs. (7.3.122) and (7.3.101), respectively, obey the conjectured relation (5.5.15).

Finally to compute $d_1^{(2d)}$ and $d_1^{(4d)}$, we set $d = 4$ and $d = 6$, respectively, which gives

$$d_1^{(2d)} = 3(1-\alpha)\alpha(\alpha(1+\alpha) + 2\xi(1-2\alpha)), \quad (7.3.123)$$

$$d_1^{(4d)} = -\frac{2}{9}\alpha(1-\alpha^2)(2-\alpha)(\alpha(2+\alpha) + 3(1-2\alpha)\xi), \quad (7.3.124)$$

after using eqs. (3.4.40) and (6.2.20). Note that $d_1^{(2d)} \geq 0$ and $d_1^{(4d)} \leq 0$, as expected by unitarity.

7.3.3 Entanglement entropy

In this subsection, we will compute the EE for the free fermion in $d = 4$ in the presence of a monodromy defect following the same methods used in section 7.2.3. In fact, most of the results for the scalar EE can be directly brought to bear. That is, since $\nabla^2 = \nabla^2$ on \mathbb{R}^4 , the complex scalar and fermion heat kernels are directly related by

$$K_{\mathbb{F}}(s; x, x'; \alpha) = \frac{1}{2}K_{\mathbb{S}}(s; x, x'; \alpha) \mathbb{1}_4, \quad (7.3.125)$$

where the factor of 1/2 arises because we are considering a complex scalar. Thus, we will proceed with the computation by noting the relevant places where the approach for the free fermion differs slightly from the free scalar.

We start by partitioning the background into a region A and its complement \bar{A} . We take A to be the half-space orthogonal to the defect with the entangling surface ∂A at $\tau = x^1 = 0$. We will adopt polar coordinates in the (τ, x^1) -plane as $\tau = r \cos \phi$ and $x^1 = r \sin \phi$. Rotations around the entangling surface are generated by $U(\phi) = \exp(\frac{1}{2}\gamma_0\gamma_3\phi)$. In these new polar coordinates the fermionic heat kernel takes the form $K_{\mathbb{F}} = \frac{1}{2}U(\phi)K_{\mathbb{S}}$. Note that now the heat kernel is anti-periodic around the entangling surface i.e. $K_{\mathbb{F}}(s; x(\phi + 2\pi), x'; \alpha) = -K_{\mathbb{F}}(s; x(\phi), x'; \alpha)$. Placing the system on the cone, the asymptotic expansion of the fermion heat kernel is modified as compared to the asymptotic expansion of the scalar heat kernel due to this anti-periodicity. The heat kernel for the Dirac fermion in the presence of the conical

singularity has been found in [333] (see also [334]) and it reads

$$K_{F,n}(s; x, x'; \alpha) = K_F(s; x, x'; \alpha) + i \int_{\Gamma} \frac{d\omega}{8\pi n} \csc \frac{\omega - \Delta\phi}{2n} U(\omega) K_S(s; x(\omega), x'; \alpha), \quad (7.3.126)$$

where $\Delta\phi \equiv \phi' - \phi$. The contour Γ is the same as in the scalar heat kernel as discussed below eq. (4.3.27).

In order to proceed, we will need to compute the trace

$$\begin{aligned} \text{Tr} K_{F,n}(s; x, x'; \alpha) &= \frac{L^2}{16\pi^2 s} \int_0^{\frac{L^2}{2s}} d\zeta \sum_m e^{-\zeta} I_{|m-\alpha|}(\zeta) \int_0^{2\pi n} d\phi \text{Tr} U(\phi) \\ &+ \frac{i}{32\pi} \int_{\Gamma} d\omega \frac{\text{Tr} U(\omega)}{\sin \frac{\omega}{2n} \sin^2 \frac{\omega}{2}} \int_0^{\frac{L^2}{2s}} d\zeta \sum_m e^{-\zeta} I_{|m-\alpha|}(\zeta). \end{aligned} \quad (7.3.127)$$

From the form of $U(\omega)$ above, $\text{Tr} U(\omega) = 4 \cos\left(\frac{\omega}{2}\right)$. The contour integral then evaluates to

$$\frac{i}{8\pi} \int_{\Gamma} d\omega \cos\left(\frac{\omega}{2}\right) \csc \frac{\omega}{2n} \csc^2 \frac{\omega}{2} = \frac{n^2 - 1}{12n}. \quad (7.3.128)$$

Plugging this into eq. (7.3.127), we thus need to compute

$$\text{Tr} K_{F,n}(s; x, x'; \alpha) = \left(\frac{L^2 \sin(n\pi)}{2\pi^2 s} + \frac{n^2 - 1}{12n} \right) \int_0^{\frac{L^2}{2s}} d\zeta \sum_m e^{-\zeta} I_{|m-\alpha|}(\zeta). \quad (7.3.129)$$

All of these sums and integrals were already encountered in eq. (7.2.80), and so the rest of the computation of the fermion EE mirrors exactly the scalar computation.

From eq. (7.3.90), we see that the contribution of a single Dirac fermion with monodromy α to the defect EE contains terms coming from the regular modes and the two divergent $n = 0$ modes coupled with $(1 - \zeta)$ and ζ . The result is

$$S_A^{\text{def}} = \dots + \frac{\alpha^2 + (1 - 2\alpha)\zeta}{6} \log \frac{L}{\epsilon} + \mathcal{O}(1), \quad (7.3.130)$$

where \dots contain the non-universal terms. From eqs. (7.3.103) and (7.3.113), we find $(a_{\Sigma}^{(2d)} + d_2^{(2d)}/3) = \alpha^2 + (1 - 2\alpha)\zeta$. This is precisely 6 times the coefficient of the log-term in eq. (7.3.130), again in agreement with eq. (7.2.69). Note that the defect EE did not rely on any integration in parameter space and so confirms that the constant of integration $c(\zeta) = \zeta$ in eq. (7.3.113).

When $d = 6$, we can use our results in eq. (7.3.114) and (7.3.104) to make a prediction for the EE via eq. (6.2.45). Indeed, we find for a monodromy defect in a theory of free

Dirac fermions in $d = 6$,

$$S_A^{\text{def}} \Big|_{\log \frac{L}{\epsilon}} = - \left[\frac{\alpha^2}{90} (16 - 5\alpha^2) + \frac{\tilde{\zeta}}{90} (20\alpha^3 - 30\alpha^2 - 12\alpha + 11) \right]. \quad (7.3.131)$$

7.4 Defect RG flows

The singular modes encountered in sections 7.2 and 7.3 allow one to consider deformations by relevant defect operators, triggering a defect RG flow. We study these flows for the scalar and fermion in turn, and provide evidence for the existence of an IR fixed point which we characterise.

7.4.1 Scalar monodromy flows

Let us begin with the monodromy defect in the free scalar theory introduced in section 7.2. As discussed there, only two singular modes are allowed to appear in the φ defect OPE: $\hat{\mathcal{O}}_{-\alpha}^-$ and $\hat{\mathcal{O}}_{1-\alpha}^-$. Here, we consider the case where only the operator $\hat{\mathcal{O}}_{-\alpha}^-$ is present (i.e. $\tilde{\zeta} = 0$ and $\zeta \neq 0$), and we show that the IR fixed point corresponds to the DCFT with $\tilde{\zeta} = \zeta = 0$. The other case will be completely analogous, and the IR fixed point is again the DCFT with $\tilde{\zeta} = \zeta = 0$. Switching on both ζ and $\tilde{\zeta}$ would not make any conceptual difference in this derivation.

Using the singular mode $\hat{\mathcal{O}}_{-\alpha}^-(x_{\parallel})$ we can construct the relevant quadratic deformation¹³

$$\lambda \int d^{d-2}x_{\parallel} \hat{\mathcal{O}}_{-\alpha}^-(x_{\parallel}) \hat{\mathcal{O}}_{-\alpha}^+(x_{\parallel}). \quad (7.4.132)$$

Here, λ is a relevant parameter with mass dimension 2α . In terms of a dimensionless coupling $\bar{\lambda}$ and an UV energy scale Λ , $\lambda = \bar{\lambda}\Lambda^{2\alpha}$. Notice that this deformation is present only for $\zeta \neq 0$. We would like to analyse the IR fixed point of the defect RG flow triggered by this deformation. Thus, we compute the correlator

$$\langle \varphi(x) \varphi^\dagger(x') \rangle_{\lambda} \equiv \frac{\left\langle \varphi(x) \varphi^\dagger(x') e^{-\lambda \int d^{d-2}y_{\parallel} \hat{\mathcal{O}}_{-\alpha}^-(y_{\parallel}) \hat{\mathcal{O}}_{-\alpha}^+(y_{\parallel})} \right\rangle}{\left\langle e^{-\lambda \int d^{d-2}y_{\parallel} \hat{\mathcal{O}}_{-\alpha}^-(y_{\parallel}) \hat{\mathcal{O}}_{-\alpha}^+(y_{\parallel})} \right\rangle}, \quad (7.4.133)$$

where without loss of generality we set $x = \{x_{\parallel}, \rho, \theta\}$ and by normal rotational and defect translational symmetries $x' = \{0, \rho', 0\}$. Expanding the exponential, performing

¹³Note that there exist other more general relevant deformations which are not quadratic. We will comment more on these operators in the discussion section 8.4.

the Wick contractions and the combinatorics we get

$$\begin{aligned} \langle \varphi(x) \varphi^\dagger(x') \rangle_\lambda &= \langle \varphi(x) \varphi^\dagger(x') \rangle \\ &+ \sum_{n=1}^{\infty} (-\lambda)^n \int \prod_{i=1}^n d^{d-2} y_{i,\parallel} \frac{\langle \varphi(x) \hat{\mathcal{O}}_{-\alpha}^{+-}(y_{1,\parallel}) \rangle \langle \varphi^\dagger(x') \hat{\mathcal{O}}_{-\alpha}^-(y_{n,\parallel}) \rangle}{\prod_{j=1}^{n-1} |y_{j,\parallel} - y_{j+1,\parallel}|^{d-2-2\alpha}}, \end{aligned} \quad (7.4.134)$$

where the denominator comes from the defect propagator $\langle \hat{\mathcal{O}}_{-\alpha}^-(y_{k,\parallel}) \hat{\mathcal{O}}_{-\alpha}^{+-}(y_{k+1,\parallel}) \rangle$ in eq. (7.2.29), the propagator $\langle \varphi(x) \varphi^\dagger(x') \rangle$ is eq. (7.2.26) evaluated at $\tilde{\zeta} = 0$, and the bulk-to-defect propagator is

$$\langle \varphi(x) \hat{\mathcal{O}}_{-\alpha}^{+-}(y_{1,\parallel}) \rangle = \frac{(c_{-\alpha}^-)^{1/2} e^{i\alpha\theta}}{\rho^\alpha (\rho^2 + (x_{\parallel} - y_{1,\parallel})^2)^{\frac{d}{2}-1-\alpha}}, \quad (7.4.135)$$

with $c_{-\alpha}^-$ given in eq. (7.2.28a).

In order to resum eq. (7.4.134), it is useful to Fourier transform to momentum space in the directions along the defect. Consider the following Fourier representation

$$\frac{1}{(\rho^2 + x_{\parallel}^2)^{\frac{d}{2}-1-\alpha}} = \int \frac{d^{d-2} k_{\parallel}}{(2\pi)^{d-2}} f(k\rho) k^{-2\alpha} e^{ik_{\parallel} \cdot x_{\parallel}}, \quad (7.4.136)$$

where we slightly abuse notation by writing $k \equiv |k_{\parallel}| = \sqrt{\delta^{ab} k_a k_b}$ to avoid any further cluttering of equations, and the function $f(k\rho)$ is given by

$$f(k\rho) = k^{2\alpha} \int d^{d-2} x_{\parallel} \frac{e^{-ik_{\parallel} \cdot x_{\parallel}}}{(\rho^2 + x_{\parallel}^2)^{\frac{d}{2}-1-\alpha}} = \frac{2\pi^{\frac{d}{2}-1}}{\Gamma(\frac{d}{2} - 1 - \alpha)} (2k\rho)^\alpha K_\alpha(k\rho), \quad (7.4.137)$$

with $K_\nu(\zeta)$ denoting the modified Bessel function of the second kind. Inserting this into eq. (7.4.134) we get

$$\begin{aligned} \langle \varphi(x) \varphi^\dagger(x') \rangle_\lambda &= \langle \varphi(x) \varphi^\dagger(x') \rangle + \\ &\frac{c_{-\alpha}^- e^{i\alpha\theta}}{\rho^\alpha \rho'^\alpha} \sum_{n=1}^{\infty} (-\lambda)^n \int \prod_{i=1}^n d^{d-2} x_{i,\parallel} \prod_{j=1}^{n+1} \frac{d^{d-2} k_{j,\parallel} k_j^{-2\alpha}}{(2\pi)^{d-2}} f(k_1\rho) f(0)^{n-1} f(k_{n+1}\rho') e^{i \sum_l k_{l,\parallel} \cdot (x_{l-1,\parallel} - x_{l,\parallel})}, \end{aligned} \quad (7.4.138)$$

where it is understood that $x_{0,\parallel} \equiv x_{\parallel}$ and $x_{n+1,\parallel} = 0$. The integration over the n positions $x_{i,\parallel}$ gives n delta functions which we use to perform n momentum integrations. Finally, we perform the sum over n leading to

$$\langle \varphi \varphi^\dagger \rangle_\lambda = \langle \varphi \varphi^\dagger \rangle - \int \frac{d^{d-2} k_{\parallel}}{(2\pi)^{d-2}} e^{ik_{\parallel} \cdot x_{\parallel}} \frac{\lambda k^{-2\alpha}}{1 + \lambda f(0) k^{-2\alpha}} c_{-\alpha}^- \frac{f(k\rho)}{(k\rho)^\alpha} \frac{f(k\rho')}{(k\rho')^\alpha} e^{i\alpha\theta}, \quad (7.4.139)$$

where for brevity we have suppressed the coordinate dependence in the correlation functions and

$$f(0) = \frac{4^\alpha \pi^{\frac{d}{2}-1} \Gamma(\alpha)}{\Gamma(\frac{d}{2} - 1 - \alpha)}. \quad (7.4.140)$$

The integral in eq. (7.4.139) must be cut off to include only momenta below the UV scale Λ . To probe the IR, we expand the integrand for momenta $k \ll \Lambda$ and keep only the leading term,

$$\langle \varphi \varphi^\dagger \rangle_{\text{IR}} = \langle \varphi \varphi^\dagger \rangle - \zeta \frac{e^{i\alpha\theta} \sin \pi\alpha}{\pi^2} \int \frac{d^{d-2} k_{\parallel}}{(2\pi)^{d-2}} e^{ik_{\parallel} \cdot x_{\parallel}} K_\alpha(k\rho) K_\alpha(k\rho'). \quad (7.4.141)$$

The integral can be performed and the final result is

$$\langle \varphi \varphi^\dagger \rangle_{\text{IR}} = \langle \varphi \varphi^\dagger \rangle - \zeta \frac{\Gamma\left(\frac{d}{2} - 1 - \alpha\right)}{4\pi^{d/2} \Gamma(1 - \alpha)} F_{\hat{\Delta}^-, -\alpha}(\eta, \theta) + \zeta \frac{\Gamma\left(\frac{d}{2} - 1 + \alpha\right)}{4\pi^{d/2} \Gamma(1 + \alpha)} F_{\hat{\Delta}^+, -\alpha}(\eta, \theta) \quad (7.4.142)$$

with the defect blocks defined in eq. (7.2.25).¹⁴ The two-point function thus exhibits conformal behaviour at large distances. Had we kept the subleading terms in the expansion of eq. (7.4.139), we would have obtained corrections that are suppressed by an additional factor of $(\rho\Lambda)^{-2\alpha}$ at large distances. Comparing this result with the propagator eq. (7.2.26) and the coefficients eq. (7.2.28a), one easily sees that the last two terms on the right-hand side of eq. (7.4.142) precisely cancel the implicit ζ dependence of the first term, leaving only the $F_{\hat{\Delta}^+, -\alpha}$ block with the coefficient expected for a $\zeta = 0$ monodromy defect. In particular, starting with a $\zeta = 1$ defect in the UV, the second term on the right-hand side removes the block corresponding to $\hat{\mathcal{O}}_{-\alpha}^-$ while the last term adds in a new block for $\hat{\mathcal{O}}_{-\alpha}^+$. This suggests that starting with any value of ζ in the UV, the RG flow triggered by the relevant deformation in eq. (7.4.132) leads to the $\zeta = 0$ defect in the IR.

The arguments presented above were rather heuristic as they do not involve a thorough RG analysis. We will present further evidence for our claimed IR structure of the defect shortly. Let us first briefly consider the implications of such a defect RG flow in $d = 4$. Starting in the UV with arbitrary $\zeta \in [0, 1]$ and comparing to the IR with $\zeta = 0$, one can see that $a_{\Sigma}^{(2d)}$, as given in eq. (7.2.54), satisfies $a_{\Sigma, \text{UV}}^{(2d)} \geq a_{\Sigma, \text{IR}}^{(2d)}$ for any starting value of ζ . The inequality is saturated only for the trivial case of $\zeta = 0$ in the UV. Thus, this flow obeys the defect c-theorem of ref. [55]. Similarly, looking at the behaviour of $a_{\Sigma}^{(4d)}$ in eq. (7.2.55) when $d = 6$ under this flow, we see that $a_{\Sigma, \text{UV}}^{(4d)} \geq a_{\Sigma, \text{IR}}^{(4d)}$ for all values of $\zeta \in [0, 1]$, consistent with the defect c-theorem of ref. [57]. In arbitrary d , the RG flows for monodromy defects in free scalar CFTs can be analogously studied on the boundary $\partial\mathbb{H}^{d-1}$ of $\mathbb{H}^{d-1} \times S^1$ as in [322] where a general defect c-theorem [156] was verified.

¹⁴Since the modified Bessel function K_α falls off exponentially at large arguments, one makes only an exponentially small mistake by extending the integral beyond the cut-off to infinity.

Having passed the checks of various c-theorems across dimensions, we present as further evidence numerical results for the variation of the one-point function $\Delta \langle |\varphi|^2 \rangle \equiv \langle |\varphi|^2 \rangle_\lambda - \langle |\varphi|^2 \rangle_{\lambda=0}$ induced by the relevant quadratic perturbation. This requires the coincident limit of the propagator eq. (7.4.139). For simplicity, let us restrict our attention to $d = 4$, where

$$\Delta \langle |\varphi|^2 \rangle = -\frac{2^{-1+2\alpha}}{\pi\Gamma(1-\alpha)^2} \frac{\xi}{\rho^2} \int_0^{+\infty} d\zeta \frac{\zeta \rho^{2\alpha} \lambda}{\zeta^{2\alpha} + \rho^{2\alpha} \lambda f(0)} K_\alpha(\zeta) K_\alpha(\zeta). \quad (7.4.143)$$

We notice that the deformation correctly goes to zero at short distances, $\rho \rightarrow 0$, and it saturates to a constant value in the IR, $\rho \gg 1/\Lambda$, or $\rho\lambda^{\frac{1}{2\alpha}} \gg 1$. In the IR limit, the integral can be solved analytically to give

$$\Delta \langle |\varphi|^2 \rangle \xrightarrow{\text{IR}} -\frac{\alpha\xi}{4\pi^2\rho^2}, \quad (7.4.144)$$

which is exactly the difference between the one-point functions in eq. (7.2.39) with the values at $\xi = 0$ and ξ .

For generic values of $\rho\lambda^{\frac{1}{2\alpha}}$ the integral must be solved numerically. In figure 7.2 we show the behaviour of

$$\rho^2 \langle |\varphi|^2 \rangle_\xi - \rho^2 \langle |\varphi|^2 \rangle_{\xi=0} = \rho^2 \Delta \langle |\varphi|^2 \rangle + \frac{\alpha\xi}{4\pi^2} \quad (7.4.145)$$

for different values of ξ . In the UV regime $\rho\lambda^{\frac{1}{2\alpha}} \ll 1$ the curves depend on ξ but they all reduce to zero in the IR limit $\rho\lambda^{\frac{1}{2\alpha}} \gg 1$. This is again consistent with having an IR fixed point corresponding to $\xi = 0$.

Another perspective on the defect RG flow is provided by studying the two-point function of defect operators. Since the relevant deformation is quadratic in $\hat{\mathcal{O}}_{-\alpha}^-$, Wick's theorem and orthogonality imply that only correlation functions involving $\hat{\mathcal{O}}_{-\alpha}^-$ can be non-trivially affected. Consider the two-point function of $\hat{\mathcal{O}}_{-\alpha}^-$. A similar computation as above gives

$$\begin{aligned} \langle \hat{\mathcal{O}}_{-\alpha}^-(x_\parallel) \hat{\mathcal{O}}_{-\alpha}^+(x'_\parallel) \rangle_\lambda &= \langle \hat{\mathcal{O}}_{-\alpha}^-(x_\parallel) \hat{\mathcal{O}}_{-\alpha}^+(x'_\parallel) \rangle \\ &\quad - \lambda f^2(0) \int \frac{d^{d-2}k_\parallel}{(2\pi)^{d-2}} \frac{k^{-4\alpha}}{1 + \lambda f(0)k^{-2\alpha}} e^{ik_\parallel \cdot (x_\parallel - x'_\parallel)}. \end{aligned} \quad (7.4.146)$$

Expanding the integrand for $k \ll \Lambda$, one finds

$$\langle \hat{\mathcal{O}}_{-\alpha}^-(x_\parallel) \hat{\mathcal{O}}_{-\alpha}^+(x'_\parallel) \rangle_\lambda \propto \frac{1}{\lambda^2} \frac{1}{|x_\parallel - x'_\parallel|^{d-2+2\alpha}} \quad (7.4.147)$$

to leading order, where the proportionality factor is a strictly positive function of α for values in the allowed range. The higher order terms are suppressed by additional factors of $(|x_\parallel - x'_\parallel|\Lambda)^{-2\alpha}$. Thus, the two-point function at large distances again

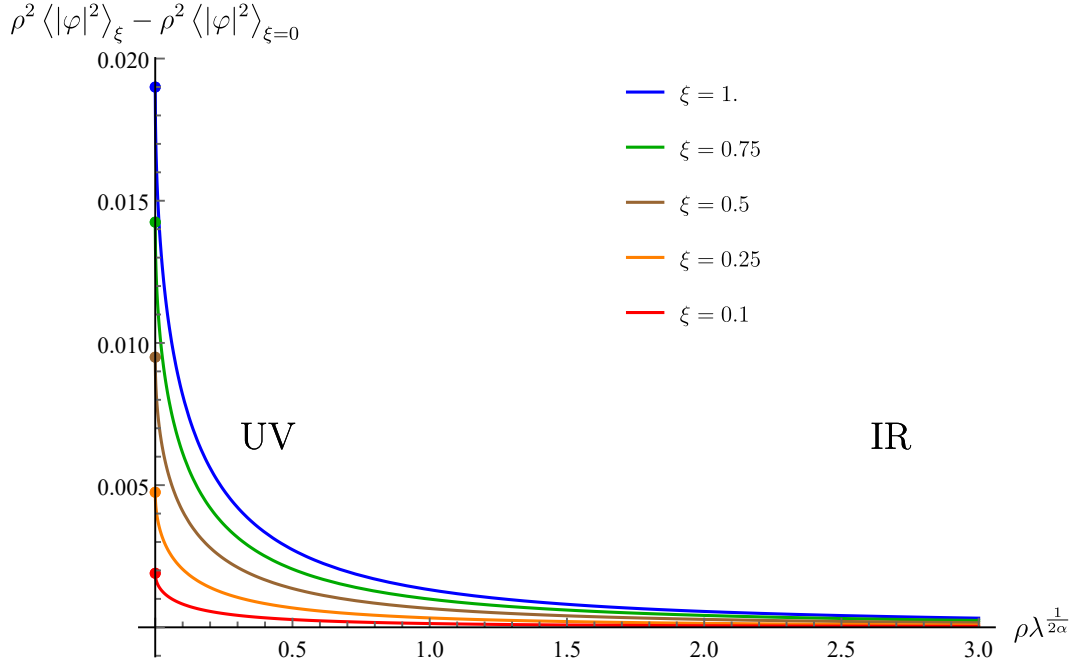


FIGURE 7.2: The quantity $\rho^2 \langle |\varphi|^2 \rangle_\xi - \rho^2 \langle |\varphi|^2 \rangle_{\xi=0}$ as a function of the dimensionless quantity $\rho \lambda^{\frac{1}{2\alpha}}$ for $d = 4$, $\alpha = 0.75$, and different values of ξ . While in the UV the quantity depends on ξ , in the IR limit all the curves go to zero.

exhibits conformal behaviour, however, the defect operator's scaling dimension changes from $\hat{\Delta}_{-\alpha}^-$ in the UV to $\hat{\Delta}_{-\alpha}^+$ in the IR. This suggests that $\hat{\mathcal{O}}_{-\alpha}^-$ acquires a large anomalous dimension, effectively turning into $\hat{\mathcal{O}}_{-\alpha}^+$ at large distances.¹⁵

One can check this expectation in the regime where $\alpha \ll 1$ and $\bar{\lambda} \ll 1$ using conformal perturbation theory. The leading order beta function can be obtained by the standard methods used in bulk CFTs (see e.g. refs. [35, 335])

$$\beta_{\bar{\lambda}} = \Lambda \frac{\partial \bar{\lambda}}{\partial \Lambda} = -2\alpha \bar{\lambda} + \frac{\pi^{\frac{d}{2}-1}}{\Gamma\left(\frac{d}{2}-1\right)} C_{\mathcal{O}_\lambda \mathcal{O}_\lambda}^{\mathcal{O}_\lambda} \bar{\lambda}^2 + \mathcal{O}(\lambda^3, \alpha^2), \quad (7.4.148)$$

where $C_{\mathcal{O}_\lambda \mathcal{O}_\lambda}^{\mathcal{O}_\lambda}$ is the OPE coefficient of the composite operator $\mathcal{O}_\lambda = \hat{\mathcal{O}}_{-\alpha}^- \hat{\mathcal{O}}_{-\alpha}^-$ with itself. We can find this OPE coefficient by using the Wick contractions of $\hat{\mathcal{O}}_{-\alpha}^-$ inside

¹⁵Ref. [5] observed very similar behaviour for boundary RG flows in free BCFTs. The BCFTs studied there include an ordinary massless free scalar field ϕ with Neumann boundary conditions $\partial_\perp \phi|_\partial = 0$. Here, ∂_\perp is a derivative along the direction normal to the boundary, and $|_\partial$ denotes the restriction of an operator to the boundary. This BCFT allows for a boundary relevant quadratic deformation $c \int_\partial \phi^2$, where $c = \bar{c}\Lambda$ is a relevant coupling and \bar{c} is dimensionless. The two-point function $\langle \phi(0, x_\parallel) \phi(0, x'_\parallel) \rangle$ at large separations $|x_\parallel - x'_\parallel| \Lambda \gg 1$ is again conformal to leading order, scaling like $c^{-2} |x_\parallel - x'_\parallel|^{-d}$. The boundary scalar $\phi|_\partial$, which has scaling dimension $\Delta = \frac{d-2}{2}$ in the UV, behaves as if it had $\Delta = \frac{d}{2}$ at large distances. This is precisely the scaling dimension of $\partial_\perp \phi|_\partial$, which was set to zero by the boundary conditions in the UV. This is consistent with the IR fixed point being described by a free massless scalar with Dirichlet boundary conditions. Under the boundary RG flow, $\phi|_\partial$ is removed from the spectrum while $\partial_\perp \phi|_\partial$ is added in the IR.

\mathcal{O}_λ , which gives $C_{\mathcal{O}_\lambda \mathcal{O}_\lambda}^{\mathcal{O}_\lambda} = 2$. Inserting this value for the OPE coefficient gives the perturbative beta function

$$\beta_{\bar{\lambda}} = -2\alpha\bar{\lambda} + 2\frac{\pi^{\frac{d}{2}-1}}{\Gamma\left(\frac{d}{2}-1\right)}\bar{\lambda}^2 + \mathcal{O}(\bar{\lambda}^3, \alpha^2). \quad (7.4.149)$$

This beta function admits a fixed point

$$\bar{\lambda}^* = \alpha\frac{\Gamma\left(\frac{d}{2}-1\right)}{\pi^{\frac{d}{2}-1}} + \mathcal{O}(\alpha^2). \quad (7.4.150)$$

Since $C_{\mathcal{O}_\lambda \mathcal{O}_\lambda}^{\mathcal{O}_\lambda} > 0$, the location of the fixed point only receives corrections at $\mathcal{O}(\alpha^2)$ from the $\mathcal{O}(\bar{\lambda}^{\geq 3})$ terms of the beta function. We expect this fixed point to persist for the entire permissible range of α . A full all-orders computation of the beta function, however, lies beyond the scope of this thesis. Such a computation together with a full RG analysis is essential to rigorously establish the existence of an IR fixed point. We leave this important computation for future investigation.

Using the first non-trivial contribution to the beta function eq. (7.4.149), one obtains the anomalous dimension of \mathcal{O}_λ ,

$$\gamma_\lambda^* = 2\gamma_{\hat{\mathcal{O}}_{-\alpha}^-}^* = \left. \frac{\partial \beta_{\bar{\lambda}}}{\partial \bar{\lambda}} \right|_{\bar{\lambda}=\bar{\lambda}^*} = +2\alpha, \quad (7.4.151)$$

where the anomalous dimension is defined as the deviation from the $\alpha = 0$ point. Thus, the scaling dimension of $\hat{\mathcal{O}}_{-\alpha}^-$ becomes that of $\hat{\mathcal{O}}_{-\alpha}^+$ at the fixed point $\bar{\lambda}^*$. This is effectively equivalent to the operator $\hat{\mathcal{O}}_{-\alpha}^-$ not existing at the IR fixed point. Note that these results were derived in conformal perturbation theory to leading order in α , yet our discussion around eq. (7.4.142) suggests that the beta function and anomalous dimension are exact. This one-loop exactness is reminiscent of SUSY theories.

7.4.2 Fermion monodromy flows

In this subsection, we consider the defect RG flow on a monodromy defect in a theory of free Dirac fermions. In this case, we can construct two separate defect operators:

$\hat{\mathcal{O}}_{-\alpha} \equiv \hat{\psi}_{-\alpha} \hat{\psi}_{-\alpha}$ with dimension $\hat{\Delta} = d - 1 - 2\alpha$ and $\hat{\mathcal{O}}_\alpha \equiv \hat{\psi}_\alpha \hat{\psi}_\alpha$ of dimension $\hat{\Delta} = d - 3 + 2\alpha$. Here, $\hat{\psi}_{-\alpha} \equiv \lim_{\rho \rightarrow 0} \psi_\alpha \rho^\alpha / \sqrt{\zeta}$ and $\hat{\psi}_\alpha \equiv \lim_{\rho \rightarrow 0} \psi_\alpha \rho^{1-\alpha} / \sqrt{1-\zeta}$ are the defect operators associated to the divergent components of the modes $\psi_{-\alpha}$ and ψ_α defined in eq. (7.3.89). The operator $\hat{\mathcal{O}}_{-\alpha}$ is relevant when $\alpha > 1/2$, while $\hat{\mathcal{O}}_\alpha$ is relevant for $\alpha < 1/2$, and both are marginal at $\alpha = 1/2$.

The goal is then to show that, for $\alpha > 1/2$, $\hat{\mathcal{O}}_{-\alpha}$ triggers an RG flow toward a defect theory with $\zeta = 1$, while, for $\alpha < 1/2$, $\hat{\mathcal{O}}_\alpha$ triggers a flow to $\zeta = 0$. In the following we will focus on $1/2 < \alpha < 1$ and $0 < \zeta < 1$, and consider a flow triggered by $\hat{\mathcal{O}}_{-\alpha}$. We

repeat some of the analysis performed above for the RG flow in the scalar theory to obtain the corresponding deformed propagator. Finally, we will argue that at large distances the fermion propagator corresponds to $\xi = 1$. The other case follows completely analogously.

To study the desired defect RG flow, we need to compute

$$G_{\text{F},\alpha,\xi}^{(\lambda)}(x, x') \equiv \langle \psi(x) \bar{\psi}(x') \rangle_\lambda = \frac{\langle \psi(x) \bar{\psi}(x') e^{\lambda \int \text{d}^{d-2} x_\parallel \hat{\psi}_{-\alpha} \hat{\psi}_{-\alpha}} \rangle}{\langle e^{\lambda \int \text{d}^{d-2} x_\parallel \hat{\psi}_{-\alpha} \hat{\psi}_{-\alpha}} \rangle}, \quad (7.4.152)$$

where again without loss of generality we take $x = \{x_\parallel, \rho, \theta\}$ and by symmetry transformations set $x' = \{0, \rho', 0\}$. Ultimately, we want to obtain the variation of the propagator $\Delta G_{\text{F}}^{(\lambda)}(x, x') \equiv G_{\text{F},\alpha,\xi}^{(\lambda)}(x, x') - G_{\text{F},\alpha,\xi}^{(0)}(x, x')$. By following the same steps as in the scalar case, we find

$$\begin{aligned} G_{\text{F},\alpha,\xi}^{(\lambda)}(x, x') &= \langle \psi(x) \bar{\psi}(x') \rangle + \sum_{n=1}^{\infty} \lambda^n \int \prod_{i=1}^n \text{d}^{d-2} x_{i,\parallel} \langle \psi(x) \hat{\psi}_{-\alpha}(x_{1,\parallel}) \rangle \times \\ &\times \prod_{k=1}^{n-1} \langle \hat{\psi}_{-\alpha}(x_{k,\parallel}) \hat{\psi}_{-\alpha}(x_{k+1,\parallel}) \rangle \langle \hat{\psi}_{-\alpha}(x_{n,\parallel}) \bar{\psi}(x') \rangle. \end{aligned} \quad (7.4.153)$$

As in the previous section, we need both the defect-defect propagator and the bulk-defect propagator. These can be found by taking the defect limit of the fermion propagator eq. (7.3.90). First of all, we observe that a mode of the scalar propagator labelled by ν may be written in the following form

$$G_{\text{S}}^{(\nu)}(x, x') = \int \frac{\text{d}^{d-2} k_\parallel}{(2\pi)^{d-1}} e^{ik_\parallel \cdot x_\parallel} K_\nu(k\rho) I_\nu(k\rho'), \quad \rho > \rho' > 0, \quad (7.4.154)$$

and the normalisation for the $m = 0$ and $m = 1$ modes adopted in eq. (7.2.21) is understood. The above integral follows straightforwardly from performing the k_ρ -integral in equation eq. (C.2.22).

The defect-defect propagator can be found by first taking the coincident limit in the orthogonal directions and then extracting the singular term proportional to $\rho^{-2\alpha}$ in the defect limit. Taking this ordered pair of limits gives

$$\langle \hat{\psi}_{-\alpha}(x_\parallel) \hat{\psi}_{-\alpha}(0) \rangle = -\frac{2^{2\alpha-1} \Gamma(\alpha)}{2\pi \Gamma(1-\alpha)} \int \frac{\text{d}^{d-2} k_\parallel}{(2\pi)^{d-2}} e^{ik_\parallel \cdot x_\parallel} k^{-2\alpha} i k_a \gamma^a P_- . \quad (7.4.155)$$

The bulk-defect propagator can be similarly obtained by extracting the term in the propagator eq. (7.3.90) which diverges as $\rho'^{-\alpha}$ in the $\rho' \rightarrow 0$ limit. The result is

$$\begin{aligned} \langle \psi(x) \hat{\psi}_{-\alpha}(0) \rangle &= \frac{2^\alpha \sqrt{1-\zeta}}{2\pi\Gamma(1-\alpha)} \int \frac{d^{d-2}k_{\parallel}}{(2\pi)^{d-2}} e^{ik_{\parallel} \cdot x_{\parallel}} e^{i(\frac{1}{2}-\alpha)\theta} k^{-\alpha} \times \\ &\times \left\{ [ik_a \gamma^a K_{-\alpha}(k\rho) P_-] + kK_{1-\alpha}(k\rho) \gamma^1 (P_+ - P_-) \right\}. \end{aligned} \quad (7.4.156)$$

By plugging eqs. (7.4.155) and (7.4.156) into eq. (7.4.153), and following the same steps as in the scalar case, we find

$$\begin{aligned} \Delta G_F^{(\lambda)}(x, x') &= -\frac{2^{2\alpha}(1-\zeta)}{4\pi^2\Gamma(1-\alpha)^2} \lambda \int \frac{d^{d-2}k_{\parallel}}{(2\pi)^{d-2}} e^{ik_{\parallel} \cdot x_{\parallel}} e^{i(\frac{1}{2}-\alpha)\theta_1} \frac{k^{-2\alpha}}{1 + C^2 k^{2-4\alpha} \lambda^2} \times \\ &\times \left([ik_a \gamma^a K_{-\alpha}(k\rho) P_-] - kK_{1-\alpha}(k\rho) \gamma^1 P_- \right) (1 - Ck^{-2\alpha} \lambda ik_a \gamma^a) \times \\ &\times \left([-ik_a \gamma^a K_{-\alpha}(k\rho') P_-] - kK_{1-\alpha}(k\rho') \gamma^1 P_+ \right), \end{aligned} \quad (7.4.157)$$

where $C \equiv 2^{2\alpha-1}\Gamma(\alpha)/(2\pi\Gamma(1-\alpha))$. The contribution of eq. (7.4.157) to the fermion propagator corresponds to a non-conformal defect where the scale invariance of the defect is broken by the dimensionful coupling λ .

We will now provide some evidence that the IR fixed point corresponds to $\zeta = 1$. A complete justification of this claim involves a full computation of the beta function, which is beyond the scope of this thesis. Instead, we will show that to leading order at large distances the propagator corresponds to a conformal monodromy defect with $\zeta = 1$. Namely, we need to prove that

$$\Delta G_F^{\text{IR}}(x, x') = G_{F,\alpha,1}(x, x') - G_{F,\alpha,\zeta}(x, x'), \quad (7.4.158)$$

where the left-hand side is defined by expanding the integrand of eq. (7.4.157) for $k \ll \Lambda$ to leading order. Indeed, the left-hand side reads

$$\begin{aligned} \Delta G_F^{\text{IR}}(x, x') &= \frac{(1-\zeta) \sin \pi\alpha}{\pi^2} \int \frac{d^{d-2}k_{\parallel}}{(2\pi)^{d-2}} e^{ik_{\parallel} \cdot x_{\parallel}} e^{i(\frac{1}{2}-\alpha)\theta} \times \\ &\times \left\{ [ik_a \gamma^a K_{-\alpha}(k\rho) K_{-\alpha}(k\rho') - kK_{1-\alpha}(k\rho) K_{-\alpha}(k\rho') \gamma^1] P_- \right. \\ &\quad \left. - [ik_a \gamma^a K_{1-\alpha}(k\rho) K_{1-\alpha}(k\rho') - kK_{-\alpha}(k\rho) K_{1-\alpha}(k\rho') \gamma^1] P_+ \right\}. \end{aligned} \quad (7.4.159)$$

At this point, it is straightforward to check that eq. (7.4.158) holds by computing the difference $G_{F,\alpha,1} - G_{F,\alpha,\zeta}$ directly from eq. (7.3.90). In the difference, only the modes

$n = 0, 1$ contribute and we are left with

$$G_{F,\alpha,1}(x, x') - G_{F,\alpha,\zeta}(x, x') = \frac{\sin \pi\alpha(1 - \zeta)}{\pi^2} \mathcal{D} \left\{ \int \frac{d^{d-2}k_{\parallel}}{(2\pi)^{d-2}} e^{ik_{\parallel}x_{\parallel}} e^{i(\frac{1}{2}-\alpha)\theta} \times \right. \\ \left. \times [K_{1-\alpha}(k\rho)K_{1-\alpha}(k\rho')P_+ - K_{\alpha}(k\rho)K_{\alpha}(k\rho')P_-] \right\}, \quad (7.4.160)$$

which gives exactly eq. (7.4.159) after performing the derivative \mathcal{D} , thus proving eq. (7.4.158).

As a consistency check, we compute the change in the expectation value of the current $\langle J_{\theta} \rangle$ from the propagator eq. (7.4.157) at a generic value of λ

$$\Delta \langle J^{\theta}(\rho) \rangle = -\frac{i}{\rho} \lim_{\epsilon \rightarrow 0} \text{Tr} \left[\Delta G_{F,\alpha,\zeta}^{(\lambda)}(\rho + \epsilon, \rho) \gamma^2 \right], \quad (7.4.161)$$

where all other coordinate dependence in $\Delta G_{F,\alpha,\zeta}^{(\lambda)}(x, x')$ is suppressed as we set all but ρ to 0. As in the case of computing $\Delta \langle |\varphi|^2 \rangle$ for the scalar RG flow above, we restrict our attention to $d = 4$ where most of the contributions vanish, and we are left to compute the following integral

$$\Delta \langle J^{\theta}(\rho) \rangle = \frac{2^{2\alpha+1}(1 - \zeta)}{4\pi^3\Gamma^2(1 - \alpha)} \frac{C}{\rho^4} \int_0^{+\infty} d\zeta \frac{\zeta^{4-4\alpha}}{\rho^{2-4\alpha}\lambda^{-2} + \zeta^{2-4\alpha}C^2} K_{-\alpha}(\zeta)K_{1-\alpha}(\zeta), \quad (7.4.162)$$

whose IR limit $\rho\lambda^{\frac{1}{2\alpha-1}} \rightarrow +\infty$ gives

$$\Delta \langle J^{\theta}(\rho) \rangle = \frac{(1 - \zeta)(1 - \alpha)\alpha}{\pi^2} \frac{1}{\rho^4}. \quad (7.4.163)$$

As expected, this is exactly the difference $\Delta a_J \equiv a_J(\zeta = 1) - a_J(\zeta)$. Here, a_J is the coefficient of the one-point function of the current found in eq. (7.3.112), which in $d = 4$ reduces to $a_J = (\alpha - 1)\alpha(\alpha - 3\zeta + 1)/(3\pi^2)$.

For generic values of $\rho\lambda^{\frac{1}{2\alpha-1}}$ we need to solve the integral numerically. In figure 7.3 we show the quantity

$$\rho^4 \langle J^{\theta} \rangle_{\zeta} - \rho^4 \langle J^{\theta} \rangle_{\zeta=1} = \rho^4 \Delta \langle J^{\theta} \rangle - \frac{(1 - \zeta)(1 - \alpha)\alpha}{\pi^2} \quad (7.4.164)$$

as a function of $\rho\lambda^{\frac{1}{2\alpha-1}}$ for different values of ζ . In the UV regime $\rho\lambda^{\frac{1}{2\alpha-1}} \rightarrow 0$ the curves depend on ζ while they all go to zero in the IR limit $\rho\lambda^{\frac{1}{2\alpha-1}} \rightarrow +\infty$, suggesting that the IR of all those cases corresponds to $\zeta = 1$.

Let us briefly take note of how $a_{\Sigma}^{(2d)}$ and $a_{\Sigma}^{(4d)}$ behave under defect RG flows. From eqs. (7.3.113) and (7.3.114), we find that for any UV value $\zeta \neq 1$ the A-type defect central charges satisfy $a_{\Sigma,UV}^{(2d)} > a_{\Sigma,IR}^{(2d)}$ and $a_{\Sigma,UV}^{(4d)} > a_{\Sigma,IR}^{(4d)}$, where in both cases the IR has

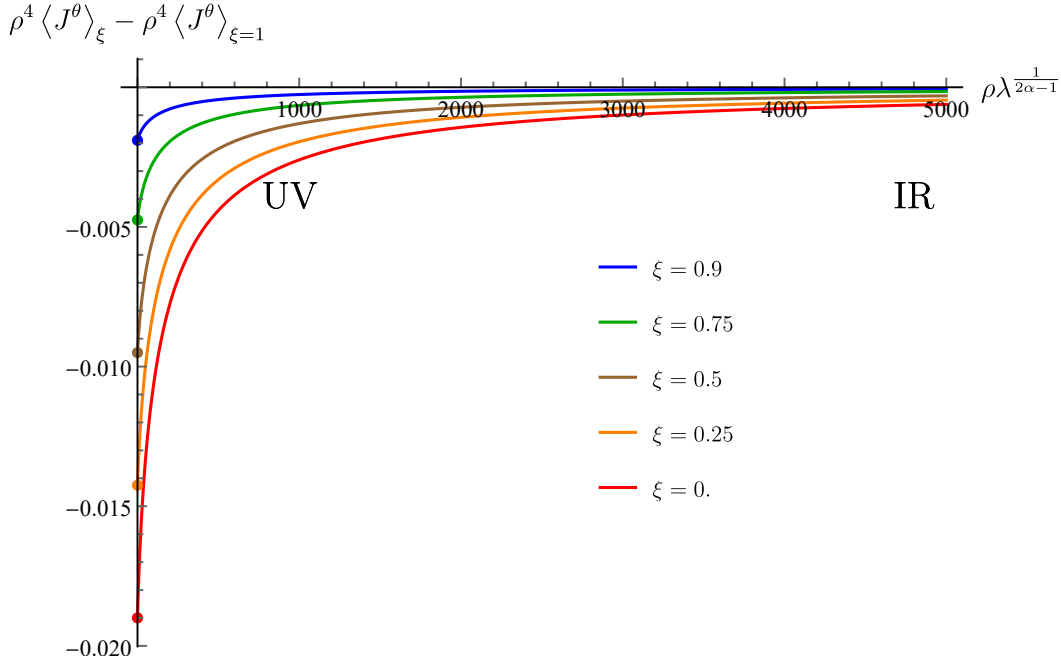


FIGURE 7.3: The quantity $\rho^4 \langle J^\theta \rangle_\xi - \rho^4 \langle J^\theta \rangle_{\xi=1}$ as a function of $\rho \lambda^{\frac{1}{2\alpha-1}}$ for $d = 4$, $\alpha = 0.75$, and different values of ξ . While in the UV the quantity depends on ξ , in the IR limit all the curves go to zero.

$\xi = 1$. Thus the defect c-theorems of refs. [55,57] are obeyed. Further, when $0 < \alpha < 1/2$, the relevant operator $\hat{\mathcal{O}}_\alpha$ drives the flow. Following the same computations as above, one finds a conformal defect with $\xi = 0$ at the IR fixed point. Again for any UV value of $\xi \neq 0$ flowing to $\xi = 0$, the defect RG flow obeys the defect c-theorems.

We conclude this section with a comment on the limit $\alpha \rightarrow 1/2$, where both relevant deformations $\hat{\mathcal{O}}_{-\alpha}$ and $\hat{\mathcal{O}}_\alpha$ become marginal. The marginal case can be studied directly starting from eq. (7.4.157) for the deformation by $\hat{\mathcal{O}}_{-1/2}$. The result is a well-defined propagator without any scale, for *any* value of λ . By a direct computation, it is not difficult to check that for $\alpha = 1/2$, the perturbation does not affect the one-point function of the stress-tensor leading to the same value of h for any value of λ , while the A-type defect central charge is obviously invariant since the defect deformation is marginal. In addition, we observe that the coefficients h in eq. (7.3.102), $a_\Sigma^{(\text{dim})}$ in eqs. (7.3.113) and (7.3.114), and $c_{\mathcal{D}\mathcal{D}}$ in eq. (7.3.122) are in fact independent of ξ precisely at $\alpha = 1/2$. A similar discussion applies to the deformation by $\hat{\mathcal{O}}_{1/2}$.

7.5 Discussion

In this chapter, we presented an extensive study of the behaviour of monodromy defects in d -dimensional free CFTs. In particular, we studied a monodromy defect in

the theories of a complex free scalar and a free Dirac fermion. By utilising the analytic methods available in free field theories, we computed various important correlation functions of the stress tensor, conserved $U(1)$ currents, and the displacement operator. When $d = 4$ and $d = 6$, these correlation functions are related to the Weyl anomaly coefficients of a $p = 2$ and $p = 4$ DCFT, respectively, which we then extracted. Further, we leveraged heat kernel methods to compute the universal part of the defect EE in $d = 4$. In doing so, we provided an explicit check on the A-type and one of the B-type defect central charges.

By considering the mode expansions of the ambient fields in the presence of the defect, we showed that certain modes are allowed which are mildly singular at the location of the defect. For the scalar, these are parametrised by $\zeta, \tilde{\zeta} \in [0, 1]$ whereas the fermion just allows for a single parameter $\zeta \in [0, 1]$. By matching the mode expansions with the defect OPE, we identified the singular modes with certain defect operators that had previously been discussed in refs. [155, 288, 322]. ζ (and $\tilde{\zeta}$) descend to parameters whose existence in the defect OPE had been argued for from an abstract DCFT point of view. The correlation functions that we computed are functions of the monodromy parameter $\alpha \in (0, 1)$, and ζ (and $\tilde{\zeta}$). Intriguingly, the A-type defect central charges $a_{\Sigma}^{(2d)}$ and $a_{\Sigma}^{(4d)}$ depend on ζ (and $\tilde{\zeta}$), suggesting that they cannot be associated with defect marginal couplings. Rather, they may be related to a combination of defect relevant or bulk marginal parameters [168, 169].

Beyond characterising defects through their central charges, we also investigated their behaviour under defect RG flows. In particular, the defect operators corresponding to the mildly singular modes can be used to build relevant quadratic deformations that trigger defect RG flows. In the case of scalar monodromy defects, we presented evidence that no matter what the values of ζ and $\tilde{\zeta}$ are in the UV, the IR fixed point of the defect flow is always a DCFT with $\zeta = \tilde{\zeta} = 0$. Thus, the IR theory only retains the regular modes.

For the case of monodromy defects in the free fermion CFT, the IR values of ζ depend on $\alpha \in (0, 1)$. In the fermionic theory, there are always two paired singular modes $\psi_{-\alpha}$ and ψ_{α} characterised by a $\mathcal{O}(\rho^{-\alpha})$ and $\mathcal{O}(\rho^{\alpha-1})$ behaviour as $\rho \rightarrow 0$ respectively. When $0 < \alpha < \frac{1}{2}$, the flow to the putative IR fixed point takes $\zeta \rightarrow 0$, i.e. the mode ψ_{α} disappears from the spectrum, whereas for $\frac{1}{2} < \alpha < 1$, the theory flows to a DCFT with $\zeta = 1$, i.e. the one without $\psi_{-\alpha}$. Similarly to the scalar case, the IR theory always retains the least singular mode. Both scalar and fermion defect RG flows obey the c-theorems of refs. [55, 57].

If the flux is set to $\alpha = \frac{1}{2}$, the fermionic defect allows for two exactly marginal deformations. This is a rather interesting feature as non-trivial conformal manifolds without SUSY are not common. We leave a more extensive study of this manifold for future work.

Although in this work we only considered quadratic relevant deformations, this is not the only possibility. For instance, in the scalar theory it is possible to construct more general operators of the type $(\hat{\mathcal{O}}_{-\alpha}^- \hat{\mathcal{O}}_{-\alpha}^{+-})^n$ where $n \geq 1$ is an integer. A straightforward dimensional counting shows that these operators are relevant provided $\alpha > \frac{(n-1)(d-2)}{(2n)}$. Thus, we find non-quadratic relevant deformations if $2 < d < 6$. Interestingly, when $d = 3$ or $d = 4$ one can always restrict the range of α such that the operator is relevant for *any* $n > 1$. In the fermionic case instead we find non-quadratic relevant deformations only if $2 < d < 4$. This kind of operators may provide a dynamical mechanism for having non-trivial interacting fixed points with $\xi \neq 0, 1$. We leave a systematic study of such flows to future work.

Chapter 8

Central Charges of 2d Superconformal Defects

This chapter is based on ref. [3], which I co-authored. In chapter 6, we derived universal results about defect central charges of a large class of defects. In chapter 7, we then computed correlation functions and defect central charges in non-trivial examples. We used our results from chapter 6 and exact techniques available in free field CFTs. In this chapter, we are interested in interacting CFTs, for which defect central charges are hard to compute. Prior to our work in ref. [3], they had only been computed in holographic CFTs [50, 71–73, 295, 336–344], which *a priori* are only valid at large N .

In this chapter, we will develop exact methods for the computation of defect central charges, without any limits or approximations. To make the problem tractable, we impose SUSY in addition to conformal symmetry, which provides us with tools to compute certain observables exactly. In particular, we will make use of SUSY localisation which was reviewed in section 5.2. This allows us to compute partition functions on backgrounds of the type S^d and $S^1 \times S^{d-1}$. We will then argue how to extract defect central charges from these partition functions. Since our methods don't rely on any approximations, our answers are exact and non-perturbative. Along the way, we illustrate our methods with numerous examples.

In section 8.1, we review key facts about certain 2d superconformal defects of SCFTs, which were introduced in section 5.5. In section 8.2 we demonstrate that the A-type central charge of a $p = \text{even}$ dimensional defect can be obtained from the localised partition function on S^d , with the defect wrapping an equatorial S^p .¹ In section 8.3 we argue that a linear combination of B-type central charges can be extracted from localised partition functions on $S_R^1 \times S^{d-1}$ with the defect wrapping $S_R^1 \times S^{p-1}$, where

¹My main contribution was to demonstrate how the A-type defect central charge can be extracted, and its explicit computation in many examples.

R is the radius of the circle. When $p = 2$, we can identify the defect central charge obtained this way. Whenever our results overlap with computations in holographic CFTs, we find exact agreement with our results, demonstrating that the holographic computations are not merely large- N approximations. In section 8.4 we conclude with a summary, and discuss possible directions for future research. In appendix D.1, we collect some technical results that we will need along the way.

8.1 Review: 2d superconformal defects

8.1.1 2d Levi type- \mathbb{L} defects

In section 3.2, we presented a broad partitioning of defects as order- or disorder-type. The latter are constructed by prescribing boundary, or singularity conditions, on ambient fields. In section 5.5, we briefly introduced a SUSY example of a disorder-type defect in 4d $\mathcal{N} = 4$ SYM theory, which was constructed by refs. [293, 345], and is often called a Gukov-Witten defect.

Consider $\mathcal{N} = 4$ SYM theory on $\mathcal{M}_4 = \mathbb{R}^4$ with coordinates $\{x^\mu\}$ ($\mu = 1, \dots, 4$), and a $\frac{1}{2}$ -BPS surface operator supported on $\Sigma_2 = \mathbb{R}^2$ with coordinates $\{x^1, x^2\}$. Let us write the coordinates on the normal bundle $N\Sigma = \mathbb{C}$ as $x^3 + ix^4 = z = \rho e^{i\theta}$. To define the surface defect, one needs to prescribe a singularity in the normal component of the gauge field A and one of the complex scalars in the adjoint $\mathcal{N} = 2$ hypermultiplet φ . In preserving 2d $\mathcal{N} = (4, 4)$ SUSY along Σ_2 , A and φ have to satisfy a set of simple BPS conditions that take the form of Hitchin's equations (after a GL twist) [17, 293, 346]. The leading singular behaviour of the BPS solutions that additionally preserve defect conformal symmetry is given by

$$A \rightarrow \alpha d\theta, \quad \varphi \rightarrow \frac{1}{2z}(\beta + i\gamma) \quad (8.1.1)$$

for constants (α, β, γ) . Relaxing the constraint that the defect preserves conformal symmetry would allow for non-trivial dependence on the radial coordinate ρ .² Note that this defect is very similar to the monodromy defect studied in chapter 7, however, for the Gukov-Witten defect, the gauge field is dynamical.

If the ambient 4d theory has only $\mathcal{N} = 2$ SUSY rather than $\mathcal{N} = 4$, one constructs a $\frac{1}{2}$ -BPS surface defect by prescribing a singularity in the 4d gauge field only. In these cases the BPS conditions do not allow for a singularity in any scalar fields, so no analogue of β or γ exists—those are special to $\mathcal{N} = 4$ SYM theory.

²Due to the simple pole in φ , such a defect is often called “tame”. By allowing for a higher-order singularities, one can construct “wild” surface operators [347], which we will not consider here.

The data (α, β, γ) describing the $\frac{1}{2}$ -BPS defect are valued in the Cartan subalgebra \mathfrak{t} corresponding to the maximal torus \mathbb{T} of the gauge group G . Thus, quantisation of the 2d-4d system requires the preserved gauge symmetry consistent with solving the BPS equations to be a subgroup of G containing \mathbb{T} , called the *Levi subgroup* $\mathbb{L} \subset G$. There are a number of ways to construct \mathbb{L} , and choosing a particular $\mathbb{L} \subset G$ is part of defining the defect. For this reason we refer to these defects as Levi type- \mathbb{L} defects here. Unless otherwise specified, we will only consider $G = U(N)$ or $SU(N)$ and Levi subgroups of the form $\mathbb{L} = S \left[\prod_{i=1}^{n+1} U(N_i) \right]$ with the constraint that $\sum_{i=1}^{n+1} N_i = N$.

There are two types of 2d Levi type- \mathbb{L} defects commonly encountered in the literature that are given special names and will be considered below. For gauge group $G = SU(N)$, if $\mathbb{L} = S[U(N-1) \times U(1)]$ then the surface defect is called *simple*, and if $\mathbb{L} = \mathbb{T} = U(1)^{N-1}$ then the surface defect is called *full*.

Lastly, in addition to \mathbb{L} and (α, β, γ) , one can turn on a quantum 2d theta angle parameter, η , along the defect for each $U(1)$ factor in \mathbb{T} . The importance of η can be seen in studying the behaviour of Levi type- \mathbb{L} defects under dualities. Under electromagnetic duality, α and η are exchanged, and so for a generic 2d $\mathcal{N} = (4, 4)$ superconformal defect in 4d $\mathcal{N} = 4$ SYM theory, specifying $(\mathbb{L}; \alpha, \beta, \gamma, \eta)$ completely describes the defect. The parameters (β, γ) are together valued in the \mathbb{L} -invariant part of \mathfrak{t} , while α is valued in the \mathbb{L} -invariant part of \mathbb{T} and η is valued in the ${}^L\mathbb{L}$ -invariant part of the maximal torus ${}^L\mathbb{T}$ of the Langlands dual ${}^L G$ of G . All of the parameters grouped together transform in the part of $(\mathbb{T} \times \mathfrak{t}^2 \times {}^L\mathbb{T})$ invariant under the Weyl group of \mathbb{L} [293, 345].

Unless otherwise stated, the Levi type- \mathbb{L} surface defect examples considered below will have $\beta = \gamma = 0$. This is particularly relevant for the computation of SCIs for $\mathcal{N} \geq (2, 2)$ defects. The parameter $\beta + i\gamma$ being non-zero is generally incompatible with the necessary symmetries for computing the defect index. In particular, non-zero β and/or γ breaks rotational symmetry in the plane normal to Σ_2 .

Having set the basis to describe Levi type- \mathbb{L} defects, it is useful to understand the physical meaning of the parameters $(\alpha, \beta, \gamma, \eta)$. 2d $\mathcal{N} = (4, 4)$ superconformal defects defined by eq. (8.1.1) are elements of the moduli space of singular solutions to Hitchin's equations, \mathcal{M}_H . As mentioned, the η parameter is a 2d theta angle, but the other "classical" parameters (α, β, γ) encode geometric information about \mathcal{M}_H . \mathcal{M}_H is constructed by a hyper-Kähler quotient [348], and as such there are both complex structure — one of three labelled I, J, K — and Kähler parameters that describe the local geometry. By making a choice of which parameters go into the solution for φ in eq. (8.1.1), we are in effect picking a complex structure, while the parameter controlling the singular behaviour of the 4d gauge field A is the Kähler parameter. In ref. [293], the combination $\beta + i\gamma$ was identified with complex structure I , and in this complex structure α was the Kähler parameter. Cyclicly permuting the roles of the

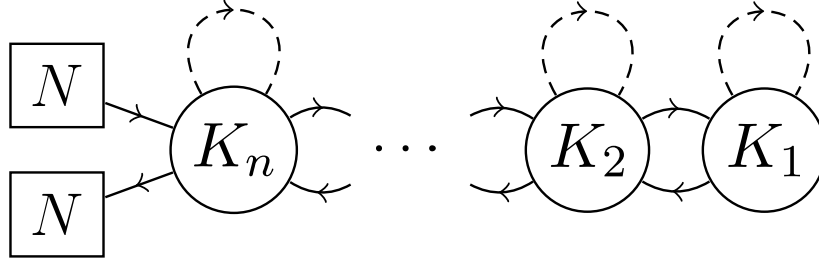


FIGURE 8.1: Linear quiver diagram corresponding to a 2d $\mathcal{N} = (2,2)$ GLSM. Its field content consists of $U(K_i)$ 2d vector multiplets for $i = 1, \dots, n$, N fundamental ϕ_n^{fund} and N anti-fundamental $\tilde{\phi}_n^{\text{anti-fund}}$ chiral multiplets coupled to the $U(K_n)$ vector, one chiral multiplet $\phi_{i(i+1)}^{\text{bif}}$ in the bifundamental representation of $(\mathbf{K}_i, \bar{\mathbf{K}}_{i+1})$, and one chiral multiplet $\phi_{(i+1)i}^{\text{bif}}$ in the bifundamental representation $(\bar{\mathbf{K}}_i, \mathbf{K}_{i+1})$ for each $1 \leq i \leq n-1$. Additionally, depending on the particular details of the 2d $\mathcal{N} = (2,2)$ gauge theory, there can be one adjoint chiral X_i of $U(K_i)$ for each node. This quiver diagram can be used to construct a surface operator whenever the 4d $\mathcal{N} = 2$ gauge theory has at least an $S[U(N) \times U(N)]$ flavour or gauge symmetry group.

parameters, one may identify $\gamma + i\alpha$ and $\alpha + i\beta$ with complex structures J and K with Kähler parameters β and γ , respectively.

8.1.2 2d defects from 2d QFTs

An order-type defect is engineered by adding DOF on the support of the defect, and coupling them to the ambient fields. We will consider cases where the latter are a GLSM or a NLSM, which we introduced in section 5.1. The 4d and 2d DOF can be coupled in various ways, e.g. by superpotential couplings and/or by gauging a shared symmetry group [293, 298, 345, 349, 350].

In the present chapter we consider 4d SCFTs that enjoy at least $\mathcal{N} \geq 2$ SUSY. To engineer a $\frac{1}{2}$ -BPS surface defect, consider the GLSM with $\mathcal{N} \geq (2,2)$ SUSY and gauge group G_{2d} described by the quiver in figure 8.1. The i^{th} circular node denotes a 2d gauge multiplet with gauge group $U(K_i)$, the directed edges connecting the i^{th} and $(i+1)^{\text{th}}$ node represent chiral multiplets in the bifundamental representation $(\mathbf{K}_i, \bar{\mathbf{K}}_{i+1})$ or $(\bar{\mathbf{K}}_i, \mathbf{K}_{i+1})$ of $U(K_i) \times U(K_{i+1})$ — depending on the direction of the arrow. We collectively denote the fields in the bifundamental by $\phi_{i(i+1)}^{\text{bif}}$ and $\phi_{(i+1)i}^{\text{bif}}$, respectively. The dashed directed edges starting and ending on the same node are adjoint chiral multiplets X_i . In what follows our quivers will always have the bifundamental fields, but may or may not have the adjoint chirals, depending on the type of defect we wish to study. For each gauge node, we may also turn on an FI parameter and a 2d theta angle for its $U(1)$ factor. The square nodes on the left indicate the number of flavours of the (anti-)fundamental chiral multiplets under the $U(K_n)$ gauge group. We denote these fundamental and anti-fundamental chiral multiplets by ϕ_n^{fund} and $\tilde{\phi}_n^{\text{anti-fund}}$, respectively.

The fields in a chiral multiplet can be given a real (twisted) mass in a SUSY preserving way, see e.g. ref. [207]. If we set the masses of all matter fields to zero, and provided that the FI parameters do not run, such a GLSM may flow to an interacting IR fixed point [351]. To the best of our knowledge, it is unknown whether an IR fixed point exists for a given such GLSM. However, whenever it does exist, the 2d SCFT has central charge $c^{(2d)}$ given by

$$\frac{c^{(2d)}}{3} = \sum_{\mathcal{R}} (1 - q_{\mathcal{R}}) \dim \mathcal{R} - \dim G_{2d}, \quad (8.1.2)$$

where \mathcal{R} are the 2d fields' representations of G_{2d} and $q_{\mathcal{R}}$ are their R-charges. The representation data and $\dim G_{2d}$ can be expressed in terms of the ranks of the gauge groups, K_i . We will compute several explicit examples in section 8.2, but important illustrative examples are the GLSMs engineering $\frac{1}{2}$ -BPS surface defects in $\mathcal{N} = 4$ $SU(N)$ SYM. In this case $c^{(2d)}$ can be written more usefully in terms of the difference of adjacent ranks, $N_i = K_i - K_{i-1}$, with $K_0 \equiv 0$ and $K_{n+1} \equiv N$. In particular, for an $\mathcal{N} = (4, 4)$ GLSM,

$$\frac{c^{(2d)}}{3} = N^2 - \sum_{i=1}^{n+1} N_i^2, \quad (8.1.3)$$

a result that we will find again in several different ways in the following.

To obtain a $\frac{1}{2}$ -BPS superconformal defect, one couples the ambient theory to a GLSM, and flows to the IR fixed point, if it exists. Typically, the VEVs of the 4d fields enter as (twisted) mass parameters in the 2d partition function [350, 352, 353]. A planar $\frac{1}{2}$ -BPS superconformal defect then breaks the 4d SCA to a subalgebra:

$$\begin{aligned} \mathfrak{su}(2, 2|2) &\rightarrow \mathfrak{su}(1, 1|1) \oplus \mathfrak{su}(1, 1|1) \oplus \mathfrak{u}(1) \text{ for an } \mathcal{N} = 2 \text{ SCFT, or for an } \mathcal{N} = 4 \text{ SCFT,} \\ \mathfrak{psu}(2, 2|4) &\rightarrow \mathfrak{psu}(1, 1|2) \oplus \mathfrak{psu}(1, 1|2) \oplus \mathfrak{u}(1). \end{aligned}$$

An alternative description of a $\frac{1}{2}$ -BPS surface defect can be obtained by coupling a 2d NLSM to the ambient field theory [45, 293, 345, 349]. The NLSM description is obtained from the GLSM above by a defect RG flow: at a generic point on the Higgs branch of the moduli space the gauge group is Higgsed, and the 2d vector multiplets become massive. As the relevant gauge coupling in the GLSM becomes parametrically large, the massive modes decouple and one obtains the NLSM as an effective theory. The Higgs branch of the GLSM maps to the target space of the NLSM.

As mentioned in section 3.2, under certain conditions order- and disorder-type defects are equivalent. One may suspect that integrating out the 2d DOF produces the delta-function singularities in the 4d fields on the support of the defect. Indeed, this does turn out to be the case for a $\frac{1}{2}$ -BPS surface defect in 4d $\mathcal{N} = 4$ SYM theory with gauge group G [293, 345, 349]. In order to obtain a Levi type- \mathbb{L} defect from coupling a GLSM to the ambient theory, the GLSM needs to have $\mathcal{N} = (4, 4)$ SUSY, and global

symmetry G . Moreover, the Levi subgroup \mathbb{L} is captured by the gauge symmetry in the linear quiver: Consider the linear quiver of figure 8.1 whose gauge group $U(K_1) \times \dots \times U(K_n)$ is such that $K_i > K_{i-1}$ for all $i = 2, \dots, n$. Then, the Levi subgroup is $\mathbb{L} = S[\prod_{i=1}^{n+1} U(N_i)]$ where $N_i = K_i - K_{i-1}$ with $K_0 \equiv 0$ and $K_{n+1} \equiv N$. The parameters $(\alpha, \beta, \gamma, \eta)$ are encoded in the GLSM as follows. The linear combination $\alpha_k + i\eta_k$ (for $k = 1, \dots, n+1$) in the Levi type- \mathbb{L} defect corresponds to the complexified FI parameters of the GLSM, and the complex structure moduli $\beta_k + i\gamma_k$ characterise the 2d superpotentials.

In the NLSM description, the requirement of $\mathcal{N} = (4, 4)$ SUSY and global symmetry G translate to requiring the target space to be hyper-Kähler and to admit a G -action. In terms of the NLSM description, (α, β, γ) are encoded in the moduli of the target space, whereas η is associated with a 2-form B-field on moduli space whose periods give η_k . For the NLSM to engineer a Levi type- \mathbb{L} defect, the target space must be $T^*(G/\mathbb{L})$, which agrees with the moduli space \mathcal{M}_H of the defect [349]. The complex dimension of the target space is

$$\dim_{\mathbb{C}} T^*(G/\mathbb{L}) = N^2 - \sum_{i=1}^{n+1} N_i^2, \quad (8.1.4)$$

which holds for general values of the parameters $(\alpha, \beta, \gamma, \eta)$. Note that the complex dimension of the target space agrees with $c^{(2d)}/3$ of the IR fixed point of the associated $\mathcal{N} = (4, 4)$ GLSM in eq. (8.1.3).³

In the case of an ambient $\mathcal{N} = 2$ gauge theory there is a similar but weaker statement. A 4d $\mathcal{N} = 2$ theory coupled to a 2d GLSM with $\mathcal{N} = (2, 2)$ SUSY, or NLSM whose target space admits a Kähler structure, is IR dual to the $\mathcal{N} = 2$ theory with prescribed singularities in the gauge field on the support of the defect [354].

8.1.3 2d defects in theories of class \mathcal{S}

A large class of $\mathcal{N} = 2$ SCFTs are the so-called *class \mathcal{S}* theories of ref. [217], which were introduced in section 5.3. The starting point is the 6d $\mathcal{N} = (2, 0)$ SCFT of type A_{N-1} on a product manifold $\mathcal{M}_4 \times \mathcal{C}_{g,n}$ where \mathcal{M}_4 is a four-manifold and $\mathcal{C}_{g,n}$ is a genus- g Riemann surface with n punctures. A puncture corresponds to a co-dimension two defect of the 6d $\mathcal{N} = (2, 0)$ SCFT inserted at a point on the Riemann surface and wrapping all of 4d space. Each defect carries additional data which determine the behaviour of the 6d fields near it. In order to preserve SUSY, one needs to mix part of the R-symmetry with some of the Lorentz generators. This is called a partial topological twist, or a SUSY twist. See e.g. ref. [355] for a review in the present

³The factor of $\frac{1}{3}$ comes from the well-known fact that each pair of a real 2d boson and a fermion contributes $\frac{3}{2}$ to $c^{(2d)}$.

context. In the compactification to the 4d theory, the co-dimension two defects give rise to hypermultiplets with some flavour symmetry depending on the type of puncture. E.g. a *simple* puncture encodes a $U(1)$ flavour symmetry whereas a *full* puncture gives an $SU(N)$ flavour symmetry.⁴

As a result of the SUSY twist, the corresponding partition function is independent of the size of both \mathcal{M}_4 and $\mathcal{C}_{g,n}$ (though still dependent on their shape). Thus, one can shrink either \mathcal{M}_4 or $\mathcal{C}_{g,n}$ to zero without affecting the value of the partition function on $\mathcal{M}_4 \times \mathcal{C}_{g,n}$. Taking the area of $\mathcal{C}_{g,n}$ to zero produces a 4d $\mathcal{N} = 2$ SCFT labelled by $\mathcal{C}_{g,n}$. These theories have a moduli space of vacua (along which conformal symmetry is spontaneously broken). The SW curve is identified with an N -sheeted cover of $\mathcal{C}_{g,n} \supset T^*\mathcal{C}_{g,n}$. Class \mathcal{S} theories include a large variety of $\mathcal{N} = 2$ SCFTs of varying complexity, however, we will only discuss the theory of N^2 free hypermultiplets (from the compactification on $\mathcal{C}_{0,3}$ with two full punctures and a simple one), $SU(N)$ SQCD with $2N$ flavours (from $\mathcal{C}_{0,4}$ with two full punctures and two simple ones) and $\mathcal{N} = 4$ SYM theory (from $\mathcal{C}_{1,0}$). These theories all have Lagrangian descriptions. Thus, when $\mathcal{M}_4 = S^4$, the partition function can be computed exactly via SUSY localisation [23], which we reviewed in section 5.2. However, the class \mathcal{S} construction allows for more general SCFTs which are inherently strongly coupled and non-Lagrangian. E.g. by allowing for more general punctures [356–358], one finds the theories of ref. [359] and many previously unknown SCFTs.

Alternatively, compactifying on \mathcal{M}_4 gives rise to a non-SUSY 2d CFT on $\mathcal{C}_{g,n}$. When the 6d SCFT is labelled by $\mathfrak{g}_{6d} = A_{N-1}$, the resulting 2d CFT on $\mathcal{C}_{g,n}$ is A_{N-1} Toda theory. When $N = 2$, this is just the Liouville CFT [319]. However, when $N > 2$, Toda theory has $N - 2$ holomorphic higher spin currents in addition to the stress tensor, enlarging the Virasoro algebra to a \mathcal{W}_N algebra [360]. The Alday-Gaiotto-Tachikawa (AGT) correspondence is the statement that the S^4 partition function of the class \mathcal{S} theory is equivalent to a Toda correlator on $\mathcal{C}_{g,n}$ [319, 360].

Class \mathcal{S} theories admit defect operators which descend naturally from the co-dimension four and two defects of the parent 6d $\mathcal{N} = (2, 0)$ theory, which are described by representations and nilpotent orbits of $\mathfrak{g}_{6d} = A_{N-1}$, respectively. The co-dimension four, or Wilson surface, defects localised at a point on $\mathcal{C}_{g,n}$ were discussed in detail in ref. [298] and refined in ref. [350]. In the 4d SCFT, they descend to a surface defect described by the n -node quiver GLSM of figure 8.1 with $K_i < K_{i+1}$, an adjoint chiral multiplet on every node except the n^{th} one, and non-vanishing complexified FI parameter only for the n^{th} node, which corresponds to the position of the defect on $\mathcal{C}_{g,n}$. The information encoded in the quiver can be summarised by a

⁴Note that these flavour symmetry groups arise from a partition of N , which is why the same terminology as for the Levi type- \mathbb{L} defect is used. In the 6d $A_{N-1} = \mathfrak{su}(N)$ SCFT, a (tame) simple puncture corresponds to fields acquiring a pole with residue determined by the partition $[1, N - 1]$, preserving a $U(1)$ symmetry. A full puncture corresponds to a pole with residue determined by $[1^N]$, which preserves the full $SU(N)$ symmetry. See e.g. ref. [355] for a pedagogical discussion.

Young tableau of width n which labels a representation of A_{N-1} . The length of the j^{th} column is the difference in the ranks of the j^{th} and $(j-1)^{\text{th}}$ node, i.e. $K_j - K_{j-1}$. Furthermore, the authors of refs. [298, 350] show that in the AGT correspondence to Toda theory on $\mathcal{C}_{g,n}$, this surface defect corresponds to the insertion of a degenerate Toda primary labelled by the Young tableau, and whose position on $\mathcal{C}_{g,n}$ is specified by the FI parameter of the n^{th} node.

In addition to the co-dimension two defects wrapping \mathcal{M}_4 giving rise to the punctures of $\mathcal{C}_{g,n}$, one can introduce co-dimension two defects wrapping $\mathcal{C}_{g,n}$ and a 2d surface in \mathcal{M}_4 . These defects were studied in refs. [361, 362]. Since the defect wraps $\mathcal{C}_{g,n}$, it alters the dictionary of AGT. Indeed, the surface defect in a 4d $\mathcal{N} = 2$ SCFT was found to be described by a Wess-Zumino-Novikov-Witten (WZNW) model on $\mathcal{C}_{g,n}$, rather than Toda theory.

In the 4d SCFT, the authors of ref. [293, 345, 354] proposed a duality between the 2d defects that arising from the co-dimension two and four defects of the parent 6d SCFT. More specifically, the duality is a particular type of integral transform between the partition functions of the Toda and WZNW theories living on $\mathcal{C}_{g,n}$ in the two cases. We will not need any details of this duality except that, like any duality, it is a mapping between physical observables of the two cases. Of importance to us is the fact that under the duality the metric on \mathcal{M}_4 and the submanifold Σ_2 are invariant, and the stress tensor maps to itself. As a result, the Weyl anomaly is invariant under the duality, and hence the defect central charges are also. We will see that this is indeed the case in our examples below.

8.1.4 Holographic results

As reviewed in chapter 4, the defect contribution to the EE of a spherical region centred on a 2d conformal defect in a higher-dimensional CFT includes a logarithmic term with a universal coefficient given by a linear combination of $a_{\Sigma}^{(2d)}$ and $d_2^{(2d)}$, see eq. (4.5.45). Furthermore, as discussed in chapter 3, $d_2^{(2d)}$ determines the stress tensor's one-point function eq. (3.1.13) in the presence of the defect. By calculating this EE and the stress tensor one-point function holographically, calculations of $a_{\Sigma}^{(2d)}$ and $d_2^{(2d)}$ have been performed for Levi type- \mathbb{L} defects in 4d $\mathcal{N} = 4$ $SU(N)$ SYM [50, 363, 364] and for $p = 2$ defects in the 6d $\mathcal{N} = (2, 0)$ A_{N-1} SCFT [50, 73, 193, 363]. One of our goals is to reproduce these results using purely field theory means, so let us review them in detail.

For the Levi type- \mathbb{L} surface defect in 4d $\mathcal{N} = 4$ $SU(N)$ SYM theory, the holographic results for $a_{\Sigma}^{(2d)}$ and $d_2^{(2d)}$ are

$$a_{\Sigma}^{(2d)} = 3(N^2 - \sum_{i=1}^{n+1} N_i^2), \quad (8.1.5a)$$

$$d_2^{(2d)} = -3(N^2 - \sum_{i=1}^{n+1} N_i^2) - \frac{24\pi^2 N}{\lambda} \sum_{i=1}^{n+1} N_i |\beta_i^2 + \gamma_i^2|, \quad (8.1.5b)$$

where λ is the 't Hooft coupling of $\mathcal{N} = 4$ SYM theory, $\lambda = Ng_{\text{YM}}^2$.

As discussed in section 5.5, ref. [288] proved that $d_2^{(2d)} = -d_1^{(2d)}$ if transverse rotations are preserved, so in fact the holographic calculations provide all three defect central charges when $\beta = \gamma = 0$. As also mentioned in section 5.5, these defects preserve enough SUSY that $a_\Sigma^{(2d)}$ cannot depend on defect or ambient marginal couplings, while $d_1^{(2d)}$ and $d_2^{(2d)}$ can. The $a_\Sigma^{(2d)}$ in eq. (8.1.5a) indeed does not depend on defect or ambient marginal couplings, and in fact depends only on the choice of Levi subgroup \mathbb{L} . On the other hand, $d_2^{(2d)}$ manifestly depends on the ambient marginal parameters β_i and γ_i . It also appears to depend on the ambient marginal coupling λ , however this is a choice of convention, since this dependence can be absorbed into a redefinition of the scalar φ in eq. (8.1.1) [293], or equivalently of β_i and γ_i .

In fact, this must be possible because of S-duality. Under S-duality, $N/\lambda \rightarrow \lambda/N$, so naïvely $d_2^{(2d)}$ appear to change under S-duality. However, as mentioned at the end of the previous sub-section, Weyl anomaly coefficients are invariant under any duality that leaves the metric on \mathcal{M}_4 and the submanifold Σ_2 invariant, and maps the stress tensor to itself. This includes the S-duality of 4d $\mathcal{N} = 4$ SYM theory. Indeed, after accounting for the S-duality transformations of β_i and γ_i [293], the combination of N , λ , β_i , and γ_i in eq. (8.1.5b) is invariant under the S-duality of $\mathcal{N} = 4$ SYM theory.

Our first result is simply the observation that $a_\Sigma^{(2d)}$ from eq. (8.1.5a) agrees exactly with $c^{(2d)}$ of the GLSM in eq. (8.1.3) that engineers a 2d Levi type- \mathbb{L} defect, and thus also with the complex dimension of the target space of the NLSM construction, eq. (8.1.4). Moreover, the expression in eq. (8.1.4) was conjectured to hold for arbitrary values of the parameters $(\alpha, \beta, \gamma, \eta)$, which strongly suggests that we can uniquely identify $\frac{c^{(2d)}}{3} = \dim_{\mathbb{C}} X$ with $\frac{a_\Sigma^{(2d)}}{3}$ and not $-\frac{d_2^{(2d)}}{3}$ or $\frac{d_1^{(2d)}}{3}$, since the latter depend on β_i and γ_i .⁵

For the Wilson surface defects in the 6d $\mathcal{N} = (2, 0)$ A_{N-1} SCFT, we will be able to clearly distinguish $a_\Sigma^{(2d)}$ from $-d_2^{(2d)}$ since in that case generically $a_\Sigma^{(2d)} \neq -d_2^{(2d)}$. A Wilson surface defect is labelled by a Young tableau corresponding to a representation of $\mathfrak{su}(N)$ with highest weight ω . The holographic results for $a_\Sigma^{(2d)}$ and $d_2^{(2d)}$ for a Wilson surface are [50, 73, 193, 363]

$$a_\Sigma^{(2d)} = 24(\rho, \omega) + 3(\omega, \omega), \quad (8.1.6a)$$

$$d_2^{(2d)} = -24(\rho, \omega) - 6(\omega, \omega), \quad (8.1.6b)$$

⁵Strictly speaking, we do not know if $d_1^{(2d)}$ depends on β_i and γ_i but it is expected to generically depend on marginal parameters. As we will see, the discussion in the following sections strongly supports the identification of $c^{(2d)}$ with $a_\Sigma^{(2d)}$.

where ρ is the Weyl vector of $\mathfrak{su}(N)$ and (\cdot, \cdot) denotes the inner product on the dual space of the Cartan subalgebra given by the inverse of the Killing form. Clearly in these cases $a_{\Sigma}^{(2d)} + d_2^{(2d)} = -3(\omega, \omega)$, so that generically $a_{\Sigma}^{(2d)} \neq -d_2^{(2d)}$. In section 8.3 we will extract a defect central charge from the SUSY partition function of the 6d $\mathcal{N} = (2, 0)$ A_{N-1} SCFT on $S_R^1 \times S^5$ with a Wilson surface along $S_R^1 \times S^1$, where R is the radius of the circle. Since $a_{\Sigma}^{(2d)} \neq -d_2^{(2d)}$, we can unambiguously say that the defect central charge we obtain is $\propto d_2^{(2d)}$. However, in this case ref. [288] provided compelling evidence, though not a rigorous proof, that $d_2^{(2d)} = -d_1^{(2d)}$, so the defect central charge we obtain could in fact be a linear combination of $d_2^{(2d)}$ and $d_1^{(2d)}$.

8.2 Partition function on S^4

In this section, we extract defect central charges from partition functions of $\mathcal{N} \geq 2$ SCFTs on $\mathcal{M}_4 = S^4$ with $\frac{1}{2}$ -BPS superconformal defects along an equatorial $\Sigma_2 = S^2$. The full integrated Weyl anomaly, including the defect contribution eq. (3.4.38), takes the following form

$$\begin{aligned} \delta_{\omega} \log Z = & -\frac{1}{16\pi^2} \int_{\mathcal{M}_4} d^4x \sqrt{g} (a_{\mathcal{M}}^{(4d)} E_4 - c^{(4d)} W_{\mu\nu\rho\sigma} W^{\mu\nu\rho\sigma}) \delta\omega \\ & + \frac{1}{24\pi} \int_{\Sigma_2} d^2\sigma \sqrt{\bar{g}} \left(a_{\Sigma}^{(2d)} \bar{E}_2 + d_1^{(2d)} \mathring{\Pi}_{ab}^{\mu} \mathring{\Pi}_{\mu}^{ab} + d_2^{(2d)} W_{ab}{}^{ab} \right. \\ & \left. + \epsilon^{ab} n_{ij} (\tilde{d}_1^{(2d)} (R^{\perp})^{ij}{}_{ab} + \tilde{d}_2^{(2d)} \mathring{\Pi}_{ac}^i \mathring{\Pi}_b^j{}^c) \right) \delta\omega, \end{aligned} \quad (8.2.7)$$

where E_4 and \bar{E}_2 are the Euler densities for \mathcal{M}_4 and Σ_2 , respectively, and $a_{\mathcal{M}}^{(4d)}$ and $c^{(4d)}$ are the central charges of the 4d CFT. As explained in section 3.4, when $\mathcal{M}_4 = S^4$ and the defect wraps an equatorial $\Sigma_2 = S^2$, all the B-type terms above vanish. Thus, the full integrated Weyl anomaly reduces to a linear combination of the A-type anomaly coefficients $a_{\mathcal{M}}^{(4d)}$ and $a_{\Sigma}^{(2d)}$,

$$\delta_{\omega} \log Z = -4a_{\mathcal{M}}^{(4d)} + \frac{a_{\Sigma}^{(2d)}}{3}. \quad (8.2.8)$$

In other words, under a global Weyl rescaling $\delta g_{\mu\nu} = 2g_{\mu\nu}$ of $\mathcal{M}_4 = S^4$, $Z \rightarrow \exp((-4a_{\mathcal{M}}^{(4d)} + a_{\Sigma}^{(2d)}/3) \delta\omega) Z$. Hence, we may extract the linear combination of central charges in eq. (8.2.8) from the transformation of the partition function Z under a global Weyl re-scaling, and if we know $a_{\mathcal{M}}^{(4d)}$ for the 4d CFT, then we can identify $a_{\Sigma}^{(2d)}$.

If the DCFT preserves enough SUSY, one can use existing results for Z computed via SUSY localisation [22, 23] to extract novel results for $a_{\Sigma}^{(2d)}$. As reviewed in section 5.2, SUSY localisation is performed on the Ω -background, $\mathbb{R}_{\epsilon_1, \epsilon_2}^4$, or by putting the theory on an S_b^4 deformed by the ratio of equivariant parameters $\epsilon_2/\epsilon_1 \equiv b^2$. The dimensionless parameter b determines how the sphere is “squashed,” which we

denote as S_b^4 . Viewed as a hypersurface in \mathbb{R}^5 , S_b^4 is defined by

$$x_0^2 + (r\epsilon_1)^2 (x_1^2 + x_2^2) + (r\epsilon_2)^2 (x_3^2 + x_4^2) = r^2, \quad (8.2.9)$$

where $\{x_i\}$ with $i = 0, \dots, 4$ are the Euclidean coordinates on \mathbb{R}^5 , and r is the equatorial radius. Note that the mass dimensions of $\epsilon_{1,2}$ are 1, which we denote by $[\epsilon_{1,2}] = 1$. In section 5.2, we took the round sphere limit $r\epsilon_1 = r\epsilon_2 = 1$ but since in the literature results are stated for generic $\epsilon_{1,2}$, we introduce them here. The deformation parameters $\epsilon_{1,2}$ break the isometry group of the 4-sphere to $U(1) \times U(1)$. An $\mathcal{N} = 2$ theory on this background preserves an $\mathfrak{su}(1|1) \subset \mathfrak{osp}(2|4)$ SUSY subalgebra of the round S^4 .

The localised partition function of a 4d $\mathcal{N} \geq 2$ gauge theory without a defect factorises into three contributions [23]: a classical part Z_{class} , a 1-loop part $Z_{1\text{-loop}}$, and an instanton part Z_{inst} . Each of these is parametrised by the VEV of the adjoint scalar $\langle \Phi \rangle = a$ which is valued in the Cartan subalgebra $\mathfrak{t} \subset \mathfrak{g}$. The full partition function is obtained by integrating with respect to a over \mathfrak{h} , as in eq. (5.2.3).

We implement global Weyl re-scalings by taking $r\epsilon_1 = r\epsilon_2 = 1$ and then re-scaling $r \rightarrow \lambda r$, in which case the 4d Weyl anomaly implies $Z_{S^4} \rightarrow \lambda^{-4a_{\mathcal{M}}^{(4d)}} Z_{S^4}$. The only contributions to $a_{\mathcal{M}}^{(4d)}$ come from the integration measure da and $Z_{1\text{-loop}}$, since the other factors are Weyl-invariant. More specifically, $Z_{1\text{-loop}}$ is a product of one-loop determinants of Laplacians for fields of different spins. Each such one-loop determinant is an infinite product of eigenvalues that diverges, and needs to be regulated. We use zeta-function regularisation, which was introduced in section 4.3. Crudely speaking, it results in the replacement of each infinite product with special functions, usually combinations of (higher) Gamma functions, as illustrated in appendix D.1. From that point of view, the ‘‘quantum’’ contribution to the Weyl anomaly of Z_{S^4} comes from the ‘‘anomalous’’ scaling properties of these special functions, while the ‘‘classical’’ contribution comes from da . We provide more details of this in appendix D.1, and we will see explicit examples below.

Now consider a surface defect wrapping $\Sigma_2 = S_{\epsilon_1}^2 \subset S_b^4$ located at $x_3 = x_4 = 0$ in \mathbb{R}^5 such that it preserves the $U(1) \times U(1)$ isometry. Its embedding into \mathbb{R}^5 is

$$x_0^2 + (r\epsilon_1)^2 (x_1^2 + x_2^2) = r^2. \quad (8.2.10)$$

A 2d $\mathcal{N} = (2, 2)$ theory on Σ_2 preserves the same $\mathfrak{su}(1|1) \subset \mathfrak{osp}(2|2)$ SUSY subalgebra as above. Thus one can introduce couplings between the 2d $\mathcal{N} = (2, 2)$ theory and the ambient 4d $\mathcal{N} = 2$ theory on Σ_2 without breaking any further SUSY. To do so, we can introduce superpotential couplings on Σ_2 to couple the 2d and 4d matter multiplets and/or by gauge a global symmetry on Σ_2 and identify it with an ambient 4d global/gauge symmetry [298, 350].

Some of the examples of 2d superconformal defects considered below are constructed from 2d $\mathcal{N} = (2, 2)$ GLSMs in the UV before flowing to the putative IR superconformal fixed point. As reviewed in section 5.2, the S^2 partition function of a purely 2d GLSM, Z_{S^2} , can also be computed through SUSY localisation, and is most conveniently done on the Coulomb branch of the moduli space [206, 207]. The field configurations on the locus are parametrised by a charge-quantised 2d gauge flux $\mathfrak{m} = \frac{1}{2\pi} \int F$ on $S^2_{\epsilon_1}$ and the VEV of a real vector multiplet scalar σ . The localised partition function is the integral over σ and sum over \mathfrak{m} of three contributions, a classical piece Z_{class} , and two one-loop determinants, $Z_{1\text{-loop}}^{\text{gauge}}$ and $Z_{1\text{-loop}}^{\text{matter}}$, as in eq. (5.2.4), which we restate here for convenience:

$$Z_{S^2} = \frac{1}{|\mathcal{W}_{\mathfrak{g}_{2d}}|} \sum_{\mathfrak{m} \in \mathfrak{t}_{2d}^{\mathbb{Z}}} \int_{\mathfrak{t}_{2d}} d\sigma Z_{\text{class}} Z_{1\text{-loop}}^{\text{gauge}} Z_{1\text{-loop}}^{\text{matter}}, \quad (8.2.11)$$

Note that the kinetic term of σ in the vector multiplet action is normalised such that $[\sigma] = 1$. We emphasise that the localised partition function is independent of the 2d Yang-Mills coupling, and only depends on the S^2 (or $S^2_{\epsilon_1}$) through its equatorial radius.

We will again implement a global Weyl re-scaling by re-scaling $r \rightarrow \lambda r$, in which case the 2d Weyl anomaly implies $Z_{S^2} \rightarrow \lambda^{c(2d)/3} Z_{S^2}$. Similarly to Z_{S^4} , the quantum contribution to the 2d Weyl anomaly comes from zeta-function regularisation of the infinite products in $Z_{1\text{-loop}}^{\text{gauge}} Z_{1\text{-loop}}^{\text{matter}}$, while the classical contribution comes from $d\sigma$. We will also see explicit examples in the following.

Our aim in this section is to extract $a_{\Sigma}^{(2d)}$ from the Weyl anomaly of the localised partition function of 2d-4d coupled systems. For such systems many SUSY localised partition functions have been computed, but we will focus on cases where the 4d ambient theory is conformal, e.g. N^2 free massless hypermultiplets, $\mathcal{N} = 4$ $SU(N)$ SYM theory, and $\mathcal{N} = 2$ $SU(N)$ SQCD with $2N$ flavours, with $\frac{1}{2}$ -BPS $\mathcal{N} = (2, 2)$ surface operators (enhanced to $\mathcal{N} = (4, 4)$ for $\mathcal{N} = 4$ SYM).

8.2.1 Free massless hypermultiplets with a generic surface defect

To start, we consider the theory of N^2 free massless hypermultiplets on S^4_b . This theory enjoys global $USp(2N^2)$ flavour symmetry. Now, to this ambient theory we couple the 2d GLSM in Fig. 8.1, including adjoint chirals for all nodes, which we put on $\Sigma_2 = S^2_{\epsilon_1}$. The GLSM enjoys the an $SU(N) \times SU(N)$ symmetry which acts on the (anti-)fundamental chirals, whereas the bifundamental and adjoint chirals enjoy a $U(1)$ symmetry. We couple the ambient free hypers to the GLSM via cubic and quintic superpotential couplings that identify the shared 2d-4d flavour symmetry $SU(N) \times SU(N) \times U(1) \subset USp(2N^2)$.

Absent an ambient 4d vector multiplet to couple to the GLSM, the saddle points of the 2d-4d theory are parametrised by independent contributions from decoupled 2d and 4d loci, and so the SUSY localised partition function of this theory factorises [298, 350]

$$Z_{\Sigma_2 \hookrightarrow S_b^4} = Z_{S_b^4}^{\text{free}} Z_{\Sigma_2}. \quad (8.2.12)$$

We denote Z_{Σ_2} as the partition function of the GLSM on $S_{\epsilon_1}^2$, and

$$Z_{S_b^4}^{\text{free}} = \left(Y \left(\frac{\epsilon_1 + \epsilon_2}{2} \middle| \epsilon_1, \epsilon_2 \right) \right)^{-N^2} \quad (8.2.13)$$

is the partition function of the N^2 free massless hypers in zeta-function regularisation. The Upsilon function is defined as

$$Y(z|a, b) \equiv \frac{1}{\Gamma_2(z|a, b) \Gamma_2(a + b - z|a, b)}, \quad (8.2.14)$$

where $\Gamma_2(z|a, b)$ is the double Gamma function. For more details about these special functions, see appendix D.1. However, the only information we currently need about the Upsilon function is its behaviour under re-scaling of its arguments, eq. (D.1.17),

$$Y \left(\frac{z}{r} \middle| \frac{a}{r}, \frac{b}{r} \right) = r^{-2\zeta_2(0; z|a, b)} Y(z|a, b), \quad (8.2.15)$$

where $\zeta_2(t; z|a, b)$ is the Barnes double zeta-function defined in eq. (D.1.1).

Since the 2d-4d partition function factorises, it is sufficient to just consider the scaling of Z_{Σ_2} in order to compute $a_{\Sigma}^{(2d)}$. Hence, $a_{\Sigma}^{(2d)}$ is identified with $c^{(2d)}$.

However, to be clear, we hasten to add that this $c^{(2d)}$ is not (necessarily) the central charge of a 2d CFT, because the 2d stress tensor of our defect DOF is not necessarily conserved, due to the coupling to the ambient 4d fields. This implies various differences from a 2d CFT: no lower bound on our $a_{\Sigma}^{(2d)} = c^{(2d)}$ is currently known, the usual 2d c-theorem does not necessarily apply (although the defect c-theorem of ref. [55] does), and so on. In practical terms, however, the upshot is that we still compute $c^{(2d)}$ from eq. (8.1.2), which in particular requires identifying the representations and R-charges of the 2d fields.

It is illustrative to re-derive eq. (8.1.2) by studying the scaling behaviour of the three contributions to eq. (8.2.11) separately. We do so following ref. [351]. The strategy will be to write the localised partition function in terms of the dimensionless combination $r\sigma$. The scalar VEV σ parametrises the BPS locus, and thus the localised path integral becomes a finite-dimensional integral over the Cartan subalgebra \mathfrak{t}_{2d} of the 2d gauge algebra \mathfrak{g}_{2d} with measure $\int_{\mathfrak{t}_{2d}} d\sigma = r^{-\text{rank } G_{2d}} \int_{\mathfrak{t}_{2d}} d(r\sigma)$. In the last step we wrote the integral over the BPS locus in terms of the dimensionless combination $r\sigma$, which is just a dummy variable in the integration. This gave us a factor of $r^{-\text{rank } G_{2d}}$ in units of the

UV cut-off. As a result, the measure contributes a scaling weight of $-\text{rank } G_{2d}$ under $r \rightarrow \lambda r$.

If G_{2d} has n $U(1)$ factors, the classical part of the localised partition function takes the form

$$Z_{\text{class}} = \prod_{j=1}^n z_j^{\text{Tr}_j(i r \sigma + \frac{\mathfrak{m}}{2})} \bar{z}_j^{\text{Tr}_j(i r \sigma - \frac{\mathfrak{m}}{2})}, \quad (8.2.16)$$

where $z_j \equiv e^{-2\pi\tilde{\zeta}_j + i\theta_j}$, $\tilde{\zeta}_j$ are FI parameters, θ_j are theta-angles, and Tr_j denotes a projection to the j^{th} $U(1)$ factor [351]. Clearly, the behaviour of eq. (8.2.16) under Weyl re-scaling is trivial.

The 1-loop contribution coming from the gauge sector takes the form

$$Z_{1\text{-loop}}^{\text{gauge}} = e^{2\pi i \rho_{2d}(\mathfrak{m})} \prod_{\alpha \in \Delta^+} \left[\frac{1}{r^2} \left(\frac{\alpha(\mathfrak{m})^2}{4} + \alpha(r\sigma)^2 \right) \right], \quad (8.2.17)$$

where Δ^+ is the set of positive roots and ρ_{2d} is the Weyl vector of \mathfrak{g}_{2d} , the Lie algebra associated to G_{2d} . Collecting the overall factors of r , and using that $|\Delta^+| = \frac{1}{2}(\dim G_{2d} - \text{rank } G_{2d})$, we see that under Weyl re-scalings eq. (8.2.17) transforms with weight $-\dim G_{2d} + \text{rank } G_{2d}$.

After zeta-function regularisation, the 1-loop partition function of the matter sector — composed of massless chiral multiplets in the \mathcal{R} representation of G_{2d} — becomes

$$Z_{1\text{-loop}}^{\text{matter}} = \prod_{\mathcal{R}} \prod_{\{h_{\mathcal{R}}\}} \frac{\Gamma\left(\frac{q_{\mathcal{R}}}{2} - i h_{\mathcal{R}}(r\sigma) - \frac{h_{\mathcal{R}}(\mathfrak{m})}{2}\right)}{\Gamma\left(1 - \frac{q_{\mathcal{R}}}{2} + i h_{\mathcal{R}}(r\sigma) - \frac{h_{\mathcal{R}}(\mathfrak{m})}{2}\right)} r^{1 - q_{\mathcal{R}} + 2i h_{\mathcal{R}}(r\sigma)}, \quad (8.2.18)$$

where $q_{\mathcal{R}}$ is the 2d R-charge of the multiplet, and $\{h_{\mathcal{R}}\}$ denotes the set of weights of \mathcal{R} . Counting the factors of r that appear in eq. (8.2.18), we see that $Z_{1\text{-loop}}^{\text{matter}}$ transforms with weight $\sum_{\mathcal{R}} (1 - q_{\mathcal{R}}) \dim \mathcal{R}$ under Weyl re-scaling. For semi-simple \mathfrak{g}_{2d} , the remaining $\sum_{\mathcal{R}} \sum_{\{h_{\mathcal{R}}\}} 2i h_{\mathcal{R}}(r\sigma)$ reduces to a sum over the charges under the $U(1)$ factors of G_{2d} , and gives rise to the renormalisation of the complexified FI parameters. If the sum does not vanish, one can tune it to zero by the addition of appropriate auxiliary DOF such that the FI parameters do not run.⁶

Combining the weights from the gauge sector, the matter sector, and the measure, one finds that the partition function is scale invariant up to an overall factor of $r^{c^{(2d)}/3}$, where $c^{(2d)}$ is given in eq. (8.1.2). This factor is identified with the central charge of the 2d SCFT at the fixed point. Hence, $a_{\Sigma}^{(2d)} = c^{(2d)}$ in the round sphere limit $\epsilon_1 = \epsilon_2 = \frac{1}{r}$, as argued above.

⁶Supposing $\sum_{\mathcal{R}} \sum_{\{h_{\mathcal{R}}\}} 2i h_{\mathcal{R}}(r\sigma)$ does not vanish immediately, one may add a massive spectator chiral multiplet with 2d R-charge $q = 0$ that precisely cancels that term. By taking their masses to be large and integrating out the spectator chiral multiplets, one recovers the original theory without the sum over $U(1)$ charges [207].

Even though the 4d theory is very simple, considering the case of N^2 free massless hypers with a surface defect illustrates the important point that the non-trivial contribution to the central charge comes from the scaling of the 1-loop partition function. The simplicity of the above example stems from the factorisation in eq. (8.2.12), which immediately led to identifying $a_{\Sigma}^{(2d)} = c^{(2d)}$.

For a more generic 2d-4d system, one might suspect that matter charged under both 2d and 4d gauge groups would spoil the factorisation of $Z_{\Sigma_2 \rightarrow S^4}$ and possibly alter $a_{\Sigma}^{(2d)}$. However, that is not the case if the system enjoys enough SUSY. It is now understood that a $\frac{1}{2}$ -BPS surface defect engineered in a generic 4d $\mathcal{N} = 2$ gauge theory by gauging symmetries [353] or through Higgsing [352] mixes ambient and defect DOF in only two ways. Firstly, any 4d adjoint hypermultiplet scalars frozen at their VEVs enter as twisted mass parameters in Z_{Σ} , while keeping its functional form unchanged. Secondly, any coupling of 2d and 4d DOF leads to an extra factor in the partition function that is entirely non-perturbative: it arises from the interactions of instantons and vortices, and has no scale-dependence. The 1-loop part of the partition function receives no modifications. Hence, central charges extracted from Weyl re-scalings of the partition function are unchanged. In other words, we expect $a_{\Sigma}^{(2d)} = c^{(2d)}$ to be the case always. Indeed, we will see examples of this below.

Let us point out that the scaling behaviour of the partition function can often be obtained in a more straightforward, yet ad hoc way by using three facts: only the 1-loop partition function (and the measure of the integration over the VEV of the adjoint scalar) contributes, factors of $\frac{1}{r}$ arise in the evaluation of 1-loop determinants, and special functions are the result of zeta-function regularisation. This is important because often the dependence on the scale r is left implicit. If one was given the partition function Z_{Σ} without any scale factors, one could still deduce the scaling behaviour by re-instating the correct r -dependence, dealing with special functions appropriately and accounting for the measure. For example, if one encounters the Euler Gamma-function $\Gamma\left(\frac{q_{\mathcal{R}}}{2} - ih_{\mathcal{R}}(\sigma) - \frac{h_{\mathcal{R}}(\mathfrak{m})}{2}\right)$, one first needs to insert appropriate factors of r to make its argument dimensionless, i.e. $\sigma \rightarrow r\sigma$. The natural function that appears in the zeta-function regularisation of the matter sector 1-loop partition function is the Barnes single Gamma-function $\Gamma_1(z|a, b)$ defined in eq. (D.1.2). To obtain the scaling behaviour one should interpret the Euler Gamma-function as $\Gamma_1\left(\frac{1}{r}\left(\frac{q_{\mathcal{R}}}{2} - ih_{\mathcal{R}}(r\sigma) - \frac{h_{\mathcal{R}}(\mathfrak{m})}{2}\right)\middle|\frac{1}{r}\right)$. Using the properties

$$\Gamma_1\left(\frac{z}{r}\middle|\frac{1}{r}\right) = r^{\frac{1}{2}-z} \Gamma_1(z|1), \quad \Gamma_1(z|1) = \frac{1}{\sqrt{2\pi}} \Gamma(z), \quad (8.2.19)$$

one correctly recovers the partition function Z_{Σ} with appropriate scale factors. We refer to appendix D.1 for more details and definitions of these special functions.

8.2.2 Examples of defects coupled to free massless hypermultiplets

Having determined $a_{\Sigma}^{(2d)} = c^{(2d)}$ for superconformal surface defects coupled to 4d free massless hypers, we can now consider some specific defect models. All that needs to be done to compute $a_{\Sigma}^{(2d)}$ is to determine the 2d R-charges $q_{\mathcal{R}}$ of the matter fields.

Due to the $\mathfrak{su}(1|1)$ -invariant coupling between the 2d $\mathcal{N} = (2, 2)$ GLSM and the hypermultiplets, the 2d R-symmetry generators are linear combinations of the $U(1)_N$ generator of rotations in the normal bundle to Σ_2 and $U(1)_R \subset SU(2)_R$ of the ambient R-symmetry [350]. The coefficients determining the exact 2d R-symmetry depend on \mathfrak{b} . The 2d R-charges of the 4d hypermultiplet scalars restricted to Σ_2 can be found in terms of their 4d charges under $U(1)_N \times U(1)_R$. Requiring that the 2d-4d superpotentials have 2d R-charge $q = 2$ together with constraints from the identified flavour symmetry then fixes the R-charges of the 2d fields and sets their twisted masses to zero.

The precise superpotential terms depend on the particular quiver diagram, and were found in refs. [298, 350]. In particular, they depend on whether the j^{th} node has an adjoint chiral X_j . If it does, we define $\eta_j \equiv +1$, and if it does not, $\eta_j \equiv -1$. Further let us define $\varepsilon_i \equiv \prod_{j=i}^n \eta_j$. One finds that the hypermultiplet scalars restricted to Σ_2 have 2d R-charge $q^{\text{hyper}} = 1 + \mathfrak{b}^2$, the fundamental and anti-fundamental chirals have $q_n^{\text{fund}} + q_n^{\text{anti-fund}} = 1 - \mathfrak{b}^2$, the adjoint chirals have

$$q_{X_j} = \begin{cases} 2 + 2\mathfrak{b}^2 & \text{if } \varepsilon_{j+1} = \varepsilon_j = -1 \\ -2\mathfrak{b}^2 & \text{if } \varepsilon_{j+1} = \varepsilon_j = +1, \end{cases} \quad (8.2.20)$$

and the bifundamentals have R-charges

$$q_{j(j-1)}^{\text{bif}} + q_{(j-1)j}^{\text{bif}} = \begin{cases} -2\mathfrak{b}^2 & \text{if } \varepsilon_j = -1 \\ 2 + 2\mathfrak{b}^2 & \text{if } \varepsilon_j = +1, \end{cases} \quad (8.2.21)$$

where we have a total of n nodes and $\varepsilon_{n+1} \equiv +1$. Notice that in a 2d SCFT, with a conserved stress tensor, unitarity and the BPS bound require positive R-charges. In contrast, our 2d defect fields do not have a conserved 2d stress tensor, and so can have negative R-charges.

Example 1: $\mathcal{N} = (2, 2)$ SQCD. As a first example consider $\mathcal{N} = (2, 2)$ SQCD with gauge group $G_{2d} = U(K)$ and N fundamental and N anti-fundamental chiral multiplets coupled to N^2 ambient free massless hypers. Note that $q_n^{\text{fund}} + q_n^{\text{anti-fund}} = 0$ in the round sphere limit $\mathfrak{b} = 1$. Thus, using eq. (8.1.2) we find

$$\frac{a_{\Sigma}^{(2d)}}{3} = 2NK - K^2 = K(2N - K). \quad (8.2.22)$$

Example 2: $\mathcal{N} = (2, 2)$ SQCDA. We now add an adjoint chiral to the previous example, where $q_X = -2$ in the limit $\mathfrak{b} = 1$. Using eq. (8.1.2), this “extra” field thus contributes an additional $(1 - q_X)\dim \mathcal{R} = 3K^2$ to the value of $a_\Sigma^{(2d)}$ of the previous example,

$$\frac{a_\Sigma^{(2d)}}{3} = 2NK - K^2 + 3K^2 = 2K(N + K). \quad (8.2.23)$$

These two examples clearly obey the c-theorem of ref. [55]. If we start in the UV with SQCDA, with $a_\Sigma^{(2d)}$ in eq. (8.2.23), and deform the theory by a mass term for the adjoint chiral, then in the IR we will find SQCD [298], with $a_\Sigma^{(2d)}$ in eq. (8.2.22). In this case, $a_{\Sigma,UV}^{(2d)} - a_{\Sigma,IR}^{(2d)} = 9K^2 \geq 0$.

Example 3: $\mathcal{N} = (2, 2)$ quiver with n adjoint chirals. We can also consider more general quiver gauge theories. For example, consider the n -node quiver depicted in figure 8.1 with gauge group $G_{2d} = U(K_1) \times \dots \times U(K_n)$, N fundamental and N anti-fundamental chirals of $U(K_n)$ and adjoint chirals on each node, coupled to N^2 free hypers. Using $q_{X_j} = -2$, $q_{j(j-1)}^{\text{bif}} + q_{(j-1)j}^{\text{bif}} = 4$ and $q_n^{\text{fund}} + q_n^{\text{anti-fund}} = 0$, and eq. (8.1.2) we find after a bit of algebra that

$$\frac{a_\Sigma^{(2d)}}{3} = 2 \sum_{i=1}^n (K_i - K_{i-1})K_i + 2K_n N, \quad (8.2.24)$$

where we have defined $K_0 \equiv 0$.

Example 4: $\mathcal{N} = (2, 2)$ quiver with $(n - 1)$ adjoint chirals. Consider the same quiver as the previous example, but with adjoint chirals on all nodes but the n^{th} one. When the FI parameters of all nodes vanish except for possibly the n^{th} one, this defect has a 6d origin. As discussed in section 8.1.3, it descends from a Wilson surface defect in the 6d A_{N-1} $\mathcal{N} = (2, 0)$ SCFT at a point on $\mathcal{C}_{0,3}$. In this case, $q_{X_j} = 4$, $q_{j(j-1)}^{\text{bif}} + q_{(j-1)j}^{\text{bif}} = -2$, and $q_n^{\text{fund}} + q_n^{\text{anti-fund}} = 0$, so that

$$\frac{a_\Sigma^{(2d)}}{3} = -4 \sum_{i=1}^n (K_i - K_{i-1})K_i + 2K_n N + 3K_n^2. \quad (8.2.25)$$

These two examples also obey the defect c-theorem of ref. [55]. If we start in the UV with an $\mathcal{N} = (2, 2)$ quiver with n adjoint chirals, with $a_\Sigma^{(2d)}$ in eq. (8.2.24) and deform by a mass term for the n^{th} adjoint chiral, then in the IR we will find an $\mathcal{N} = (2, 2)$ quiver with $n - 1$ adjoint chirals [298], with $a_\Sigma^{(2d)}$ in eq. (8.2.25). We thus have

$$\frac{a_{\Sigma,UV}^{(2d)}}{3} - \frac{a_{\Sigma,IR}^{(2d)}}{3} = -3K_n^2 + 6 \sum_{i=1}^n (K_i - K_{i-1})K_i = 3 \sum_{i=1}^n (K_i - K_{i-1})^2, \quad (8.2.26)$$

where the final equality holds because $K_0 \equiv 0$. Clearly in this case $a_{\Sigma,UV}^{(2d)} - a_{\Sigma,IR}^{(2d)} \geq 0$, and so the defect c-theorem is satisfied.

To our knowledge all four of the examples above, and indeed the general statement $a_{\Sigma}^{(2d)} = c^{(2d)}$, are novel results for $a_{\Sigma}^{(2d)}$ of 2d superconformal defects. Notice that in all of our examples $a_{\Sigma}^{(2d)} \geq 0$: for eqs. (8.2.22), (8.2.23), and (8.2.24) this is manifest, while for eq. (8.2.25) this can be checked straightforwardly, e.g. by considering limiting cases.

8.2.3 $\mathcal{N} = 4$ SYM with a generic surface defect

To construct a $\frac{1}{2}$ -BPS superconformal surface defect in $\mathcal{N} = 4$ SYM theory, one can couple a 2d $\mathcal{N} = (4, 4)$ GLSM to the ambient theory [349]. $\mathcal{N} = (4, 4)$ SUSY requires the i^{th} node in figure 8.1 to have an adjoint chiral multiplet X_i for all i . The $\mathcal{N} = (2, 2)$ adjoint chiral recombines with the $\mathcal{N} = (2, 2)$ vector multiplet into an $\mathcal{N} = (4, 4)$ vector multiplet. Similarly, the bifundamentals $\phi_{i(i+1)}^{\text{bif}}$ and $\phi_{(i+1)i}^{\text{bif}}$ regroup into bifundamental hypers, and the N (anti-)fundamental chirals ϕ_n^{fund} and $\tilde{\phi}_n^{\text{anti-fund}}$ recombine into N fundamental hypermultiplets. The N hypers enjoy $SU(N)$ flavour symmetry such that the GLSM can be coupled to 4d $\mathcal{N} = 4$ $SU(N)$ SYM theory by gauging the 2d flavour group. As argued in the previous subsection, $a_{\Sigma}^{(2d)} = c^{(2d)}$ as there is no perturbative 2d-4d contribution to the partition function. We may thus calculate $a_{\Sigma}^{(2d)}$ through yet another counting exercise.⁷

Assuming the GLSM flows to an IR fixed point, the central charge of the 2d SCFT is given by eq. (8.1.2). To determine the 2d R-charges, one considers the allowed superpotential terms which schematically look like $W = \phi X \tilde{\phi}$ in $\mathcal{N} = (2, 2)$ language. The R-charge assignments are easily deduced by looking at the $U(1)_R$ action on the mesons built from fundamental chirals, which combine into non-compact scalars at the IR fixed point. The exact low-energy $U(1)_R$ symmetry cannot act as a rotation on the mesons due to chiral factorisation of the R-symmetry in a CFT. This gives the assignment that matter sector chiral multiplets in the (anti-)fundamental and bifundamental representations have $q = 0$, while the adjoint chiral multiplets carry $q = 2$, such that the superpotential has R-charge $q = 2$. Thus, eq. (8.1.2) gives

$$\frac{a_{\Sigma}^{(2d)}}{3} = \frac{c^{(2d)}}{3} = 2 \sum_{i=1}^n K_i (K_{i+1} - K_i) = N^2 - \sum_{i=1}^{n+1} N_i^2, \quad (8.2.27)$$

as quoted in eq. (8.1.3), which is in agreement with the complex dimension of the moduli space of the Levi type- \mathbb{L} defect in eq. (8.1.4), and with the holographic result in eq. (8.1.5a), thus proving that the latter is not merely the large- N limiting value.

⁷We thank B. Le Floch for pointing this out to us, and for discussions directly related to this computation.

8.2.4 $\mathcal{N} = 4$ SYM with a full Levi defect

A useful check of the previous result eq. (8.2.27) can be performed in special cases. In refs. [365,366], the authors consider $\mathcal{N} = 2^*$ SYM with gauge group $G = SU(N)$, i.e. the field content of $\mathcal{N} = 4$ SYM theory but with a mass deformation for the adjoint hypermultiplet which breaks $\mathcal{N} = 4$ to $\mathcal{N} = 2$. In this theory, refs. [365,366] placed a full surface defect ($\mathbb{L} = \mathbb{T}$) engineered by putting the theory on the orbifold $\mathbb{C} \times \mathbb{C}/\mathbb{Z}_N$.⁸ By taking the mass of the 4d adjoint hyper to zero, the $\mathcal{N} = 2^*$ SUSY enhances to $\mathcal{N} = 4$.

Let us now compute $a_\Sigma^{(2d)}$ for this system. The non-trivial contribution comes from the 1-loop partition function,

$$Z_{1\text{-loop}}^{\mathcal{N}=4}[1^N] = \prod_{\substack{i,j=1 \\ i \neq j}}^N \frac{Y\left(a_i - a_j + \left\lceil \frac{j-i}{N} \right\rceil \epsilon_2 \mid \epsilon_1, \epsilon_2\right)}{Y\left(a_i - a_j + \frac{\epsilon_1 + \epsilon_2}{2} + \left\lceil \frac{j-i}{N} \right\rceil \epsilon_2 \mid \epsilon_1, \epsilon_2\right)}, \quad (8.2.28)$$

where a_i are the components of the VEV of the 4d adjoint scalar $\langle \Phi \rangle = \text{diag}(a_1, \dots, a_N)$, and $\lceil x \rceil$ denotes the ceiling of x .

The arguments of the Upsilon-functions in eq. (8.2.28) have mass dimension one. To make the overall scale factor explicit, we should factor out $\frac{1}{r}$ from their arguments. Define the dimensionless quantities $\tilde{\epsilon}_{1,2} \equiv r\epsilon_{1,2}$ and $Q \equiv \tilde{\epsilon}_1 + \tilde{\epsilon}_2$. Under a re-scaling, the Upsilon-function transforms according to eq. (8.2.15), which means eq. (8.2.28) becomes

$$Z_{1\text{-loop}}^{\mathcal{N}=4}[1^N] = \prod_{\substack{i,j=1 \\ i \neq j}}^N \frac{Y(x_{ij} \mid \tilde{\epsilon}_1, \tilde{\epsilon}_2)}{Y(x_{ij} + Q/2 \mid \tilde{\epsilon}_1, \tilde{\epsilon}_2)} r^{\kappa_{ij}}, \quad (8.2.29)$$

where

$$\begin{aligned} x_{ij} &= r \left(a_i - a_j + \left\lceil \frac{j-i}{N} \right\rceil \epsilon_2 \right), \\ \kappa_{ij} &= -2 \zeta_2(0; x_{ij} \mid \tilde{\epsilon}_1, \tilde{\epsilon}_2) + 2 \zeta_2(0; x_{ij} + Q/2 \mid \tilde{\epsilon}_1, \tilde{\epsilon}_2), \end{aligned} \quad (8.2.30)$$

and $\zeta_2(t; z \mid a, b)$ is the Barnes double zeta-function defined in eq. (D.1.1). Using eq. (D.1.3) and taking $\mathfrak{b} \rightarrow 1$, one finds

$$\sum_{\substack{i,j=1 \\ i \neq j}}^N \kappa_{ij} = \sum_{\substack{i,j=1 \\ i \neq j}}^N (2x_{ij} - 1) = 2 \frac{N^2 - N}{2} - (N^2 - N) = 0. \quad (8.2.31)$$

⁸Ref. [365] observed that the instanton moduli space of a 4d $\mathcal{N} = 2$ gauge theory with full surface defect matches the instanton moduli space without the defect but with the theory on the orbifold $\mathbb{C} \times \mathbb{C}/\mathbb{Z}_N$. This allows one to compute the instanton partition function of the coupled 2d-4d system by instead working on the orbifold. It was then conjectured in ref. [366] that this equivalence should hold more generally for the full partition function. Indeed, ref. [366] computes the 1-loop determinants on the orbifold and goes on to check that the partition function obtained in this way correctly encodes the coupled 2d-4d and 2d DOF.

In other words, the 1-loop determinant in the presence of the full Levi defect is scale-invariant. Hence, by eq. (8.2.8),

$$-4a_{\mathcal{M}}^{(4d)} + \frac{a_{\Sigma}^{(2d)}}{3} = -(N-1). \quad (8.2.32)$$

The right-hand side is the contribution of the measure in eq. (5.2.3). Indeed, expressing the $(N-1)$ dimensional integral over the Cartan subalgebra in terms of the dimensionless combination ra produces an overall factor of $r^{-(N-1)}$, giving rise to the right-hand side.

The central charge $a_{\mathcal{M}}^{(4d)}$ for $\mathcal{N} = 4$ $SU(N)$ SYM theory is well-known, $4a_{\mathcal{M}}^{(4d)} = N^2 - 1$, and so we find

$$\frac{a_{\Sigma}^{(2d)}}{3} = N^2 - N, \quad (8.2.33)$$

which agrees with eq. (8.2.27) in this special case, as advertised.

This agreement may seem surprising, given the different 6d origins of this surface defect and the defects that lead to eq. (8.2.27). This full surface defect comes from the compactification on a torus of the 6d $\mathcal{N} = (2, 0)$ theory with a co-dimension two defect [365, 366]. On the other hand, the surface defects that lead to eq. (8.2.27), namely the GLSM quivers reviewed in section 8.1, come from a co-dimension four defect in the 6d theory, i.e. a Wilson surface defect localised at a point on the torus. In these two descriptions $a_{\Sigma}^{(2d)}$ agrees because of the duality of refs. [293, 345, 354, 367], mentioned in section 8.1, which leaves invariant the S^4 , the $\Sigma_2 = S^2$ wrapped by the defect, and the stress tensor, and hence leaves invariant $a_{\Sigma}^{(2d)}$. Of course, also crucial is the fact that $a_{\Sigma}^{(2d)}$ depends only on the Levi subgroup of each defect: if $a_{\Sigma}^{(2d)}$ depended on more detailed information, then the equivalence would not be possible.

8.2.5 $\mathcal{N} = 2$ SQCD with $2N$ flavours and a full Levi defect

Another simple, yet non-trivial example of a class \mathcal{S} theory is massless $\mathcal{N} = 2$ SQCD with $2N$ flavours. A full surface defect in this theory is considered in ref. [366].

The 1-loop determinant with a full surface defect is

$$\begin{aligned} Z_{1\text{-loop}}^{\text{SQCD}}[1^N] & \quad (8.2.34) \\ &= \frac{\prod_{\alpha \in \Delta^+} Y(\alpha(a) + \epsilon_2 | \epsilon_1, \epsilon_2) Y(-\alpha(a) | \epsilon_1, \epsilon_2)}{\prod_{i,j=1}^N Y\left(h_i(a) + \frac{\epsilon_1 + \epsilon_2}{2} + \left\lfloor \frac{N-i-j+1}{N} \right\rfloor \epsilon_2 | \epsilon_1, \epsilon_2\right) Y\left(-h_i(a) + \frac{\epsilon_1 + \epsilon_2}{2} + \left\lfloor \frac{i-j}{N} \right\rfloor \epsilon_2 | \epsilon_1, \epsilon_2\right)}, \end{aligned}$$

where h_i are the weights of the fundamental representation of $SU(N)$.

Following the same strategy as above, we factor out $\frac{1}{r}$ to write the arguments of the special functions in terms of dimensionless quantities $\tilde{\epsilon}_{1,2}$. Let us consider the

numerator first. The scaling behaviour of the Upsilon-functions in eq. (8.2.15) in the $b \rightarrow 1$ limit gives a scaling weight of the numerator of the form

$$-\frac{(N^2 - N)}{3} - 4\rho(ra) - \sum_{\alpha \in \Delta} (\alpha(ra))^2, \quad (8.2.35)$$

where ρ is the Weyl vector, and Δ is the set of all (positive and negative) roots. The denominator contributes a factor

$$\frac{2}{3}N^2 - N + 4\rho(ra) + 2N \sum_{i=1}^N (h_i(ra))^2 \quad (8.2.36)$$

to the overall scaling weight. A vanishing beta function implies (see e.g. ref. [23])

$$\sum_{\alpha \in \Delta} (\alpha(a))^2 = 2N \sum_{i=1}^N (h_i(a))^2. \quad (8.2.37)$$

Hence, upon summing the contributions of the numerator and denominator one finds that all terms that depend on the VEV a cancel, giving an overall scaling weight for eq. (8.2.34) of the form

$$\frac{1}{3}N^2 - \frac{2}{3}N. \quad (8.2.38)$$

Finally, to account for $a_{\mathcal{M}}^{(4d)}$, we normalise by the partition function without the defect:

$$Z_{1\text{-loop}}^{\text{SQCD}} = \frac{\prod_{\alpha \in \Delta^+} Y(\alpha(a)|\epsilon_1, \epsilon_2) Y(-\alpha(a)|\epsilon_1, \epsilon_2)}{\prod_{i,j=1}^N Y(h_i(a) + \frac{\epsilon_1 + \epsilon_2}{2}|\epsilon_1, \epsilon_2) Y(-h_i(a) + \frac{\epsilon_1 + \epsilon_2}{2}|\epsilon_1, \epsilon_2)}, \quad (8.2.39)$$

which scales with weight

$$-\frac{7}{6}N^2 + \frac{5}{6}N, \quad (8.2.40)$$

where we have again used eq. (8.2.37). Subtracting eq. (8.2.40) from eq. (8.2.38), and since the measure contributions cancel, we find that $a_{\Sigma}^{(2d)}$ for a full Levi type- \mathbb{L} defect in $\mathcal{N} = 2$ conformal SQCD is given by

$$\frac{a_{\Sigma}^{(2d)}}{3} = \frac{3}{2}(N^2 - N). \quad (8.2.41)$$

8.3 SUSY partition function on $S^1 \times S^{d-1}$

In section 5.3, we considered the partition function Z of a SCFT on $\mathcal{M}_d = S_R^1 \times S^{d-1}$ and argued that it is identified with the SCI [224], up to a normalisation factor. Here S_R^1 is the temporal circle with radius R around which the fermions have periodic boundary conditions. In this section we will first argue for the appearance of the central charge $d_2^{(2d)}$ in Z in the presence of a 2d superconformal defect wrapping $\Sigma_2 = S_R^1 \times S^1$. After setting the general framework in section 8.3.1, we will examine a

model where $d_2^{(2d)}$ has been calculated holographically [50]: the Wilson surface operator in the 6d $\mathcal{N} = (2, 0)$ A_{N-1} SCFT (section 8.3.2). We will see that upon deformation of Z by these specific 2d defects the exponent in the normalisation, i.e. the SCE [227, 229, 230], changes by a factor proportional to $d_2^{(2d)}$.

The logic of the construction that computed $d_2^{(2d)}$ in this example is straightforward to extend to superconformal defects of arbitrary co-dimension. In the final part of this section, we will propose the form of a B-type anomaly coefficient (or possibly a linear combination thereof) of a $\frac{1}{2}$ -BPS co-dimension two defect wrapping $S_R^1 \times S^3$ in the 6d $\mathcal{N} = (2, 0)$ A_{N-1} SCFT, our eq. (8.3.60) below. However, we have not been able to identify which of the 22 parity-even B-type defect central charges in eq. (6.1.1) we computed.

8.3.1 Anomalies and SUSY Casimir energy

In this subsection we argue that the change of the SCE due to a defect on Σ_2 is proportional to $d_2^{(2d)}$. To begin, consider the partition function of a SCFT, $Z(R, \mu_j)$, on $\mathcal{M}_d = S_R^1 \times S^{d-1}$ for even d , where μ_j are chemical potentials for superconformal Cartan generators that commute with the supercharge used to define the index, \mathcal{I} , as in eq. (5.3.8). The main argument in refs. [227–229] is that by utilising SUSY localisation to compute $Z(R, \mu_j)$, one finds a general form proportional to the SCI. The proportionality factor defines the SCE, E_c . The understanding here is that, as an object counting protected operators starting from the identity operator, \mathcal{I} is an ascending polynomial in non-negative powers of fugacities, q_j , starting at one, i.e.

$$\mathcal{I} = 1 + q_j^\# + \dots, \text{ with } \# > 0.$$

In the presence of a defect preserving the supercharge used to define the index, \mathcal{I} will generically pick up negative powers in an expansion in q , which will need to be compensated in order to maintain the normalisation that the index begins counting with the identity operator [290, 368]. That is, the SCI in the presence of a surface defect is still counting states, in a similar sense as in the ambient theory, but now including defect states in radial quantisation around the defect.

As reviewed in section 5.4 around eq. (5.4.11), the SCE in a SCFT has been conjectured to be given by the equivariant integration of the anomaly polynomial [229]. To our knowledge this conjecture has not been rigorously proven, however, there is compelling evidence for its validity.

Now, we would like to outline how we conjecture a p -dimensional defect wrapping $\Sigma_p \hookrightarrow \mathcal{M}_d$ modifies E_c . One line of reasoning starts from eq. (5.4.11), and requires that we make two assumptions from the start: (i) the deformed anomaly polynomial

factorises into ambient and defect localised contributions

$$\mathcal{A}_{d+2}(\Sigma \hookrightarrow \mathcal{M}_d) \rightarrow \mathcal{A}_{d+2}(\mathcal{M}_d) + \delta_{\Sigma_p}^{(q)} \mathcal{A}_{p+2}(\Sigma_p), \quad (8.3.42)$$

(ii) there is a sufficient amount of superconformal symmetry preserved by the defect such that the defect Weyl anomaly sits in a multiplet with other global defect localised anomalies, e.g. defect chiral anomalies. In addition to finding a general proof of E_c being given by $\int \mathcal{A}_{d+2}(\mathcal{M})$, proving the validity of these assumptions is the focus of on-going work.

If both assumptions (i) and (ii) hold, then the result of the equivariant integration of $\mathcal{A}_{p+2}(\Sigma_p)$ is related to the integrated defect Weyl anomaly for even p . That is, the anomaly coefficients that can appear in $\int \mathcal{A}_{p+2}(\Sigma)$ are controlled by coefficients appearing in the non-vanishing contributions to the integrated defect Weyl anomaly.

When $p = 2$, it is immediately clear from the form of the defect Weyl anomaly eq. (3.4.38) that the A-type term will not contribute: the Euler characters of $\Sigma_2 = S_R^1 \times S^1$ and its squashings vanish. However, the integrated B-type contributions coming from \mathbb{H}^2 and $W_{ab}{}^{ab}$ do not necessarily vanish on a squashed sphere. Moreover, for our 2d superconformal defects $d_2^{(2d)} = -d_1^{(2d)}$ has been proven in $d = 4$ and conjectured in other $d > 4$ [288]. Thus, if assumptions (i) and (ii) hold, then the change in E_c due to the presence of a superconformal defect wrapping Σ_2 must be proportional to $d_2^{(2d)}$ when $d = 4$, at least for a parity-preserving defect. Supported by evidence in the following subsections, we conjecture that it is proportional to $d_2^{(2d)}$ in other d as well.

Finally, while not directly related to anomalies, a different line of reasoning also suggests the appearance of $d_2^{(2d)}$ in the SCE. From the point of view of constructing VOAs from 4d SCFTs [256, 257] and 6d SCFTs [258], the Schur limit of the SUSY partition function of an $\mathcal{N} \geq 2$ SCFT on $S^1 \times S^3$ or $\mathcal{N} = (2, 0)$ SCFT on $S^1 \times S^5$ is the character of the vacuum module of the VOA, see e.g. ref. [369]. As shown in ref. [290], the 4d SCI in the presence of a superconformal surface defect inserted normal to the VOA plane instead computes in the Schur limit the character of some non-vacuum module. As mentioned in section 5.5, the dimension of the defect identity in the module is given by $d_2^{(2d)}$ [288]. This is precisely the statement that introducing the defect shifts E_c by a term $\propto d_2^{(2d)}$.

8.3.2 6d SUSY Casimir energy

In this subsection, we consider the partition function of the 6d $\mathcal{N} = (2, 0)$ A_{N-1} SCFT on the squashed $S_R^1 \times S^5$ in the presence of 2d or 4d superconformal defects.⁹ The 2d

⁹The metric on the squashed $S_R^1 \times S^5$ can be found in, e.g. appendix B in ref. [311]. Our calculations, however, will not require specific details about the ambient geometry.

defect (co-dimension four), i.e. a Wilson surface operator, is placed along $\Sigma_2 = S^1_R \times S^1$. The 4d defect (co-dimension two), is placed along $S^1_R \times S^3$. Ref. [311] carried out a systematic study of the twisted partition function of this 6d SCFT with both types of defects. Using the results of ref. [311] and our arguments from section 8.3.1, we will calculate central charges for both types of defects. For the Wilson surfaces, we will unambiguously find $d_2^{(2d)}$ in the SCE. For the 4d defects, however, we cannot say exactly which central charge(s) we are computing. Our result serves as a prediction for such putative central charge(s).

Let us briefly review the 6d $\mathcal{N} = (2, 0)$ SCI and its unrefined limit. Let ϵ_i be the squashing parameters of the S^5 . In contrast to section 8.2, we will take the squashing parameters $\epsilon_{1,2,3}$ to be dimensionless, i.e. they come with appropriate factors of the equatorial radius of the S^5 , which we take to be the identity in this section. The bosonic part of the SCA of the theory is $\mathfrak{so}(6, 2) \oplus \mathfrak{usp}(4)_R \subset \mathfrak{osp}(8^*|4)$ with Cartan generators $(E, R_1, R_2, h_1, h_2, h_3)$. The generators h_i rotate the planes $\mathbb{R}_{\epsilon_i}^2 \subset \mathbb{R}^6$ into which the squashed S^5 is embedded. Among the SUSY generators $Q_{h_1 h_2 h_3}^{R_1 R_2}$, where the indices are all $\pm \frac{1}{2}$, the privileged supercharge used to construct the index is $Q \equiv Q_{-+ -}$. The states contributing to the SCI obey the shortening condition in saturating the bound

$$E \geq 2(R_1 + R_2) + h_1 + h_2 + h_3. \quad (8.3.43)$$

Assuming saturation of eq. (8.3.43), the index can be expressed as

$$\mathcal{I} = \text{Tr}_{\mathcal{H}_Q} (-1)^F p^{R_1 - R_2} \prod_{i=1}^3 q_i^{h_i + \frac{R_1 + R_2}{2}}, \quad (8.3.44)$$

where \mathcal{H}_Q is the subspace of the Hilbert space annihilated by Q and Q^\dagger . The fugacities are $q_i \equiv e^{-R\epsilon_i}$ and $p \equiv e^{-R\mu}$, where μ is the chemical potential for the R-symmetry generator $R_1 - R_2$. The unrefined limit of \mathcal{I} is defined by $\mu \rightarrow \frac{1}{2}(\epsilon_1 + \epsilon_2 - \epsilon_3)$. In this limit, an additional supercharge $Q' \equiv Q_{++ -}$ commutes with the Cartan generators, and so the unrefined index collapses to

$$\mathcal{I}_{\text{unref}} = \text{Tr}_{\mathcal{H}_{Q, Q'}} (-1)^F q^{E - R_1} s^{h_1 + R_2}, \quad (8.3.45)$$

where $q \equiv q_3$ and $s \equiv q_1/q_2$. Note the privileged status of rotations in the plane $\mathbb{R}_{\epsilon_3}^2$, which is identified with the VOA plane of the 6d theory [258]. The index $\mathcal{I}_{\text{unref}}$ is then interpreted as the character of the vacuum module of the VOA, and the SCE is identified with the central charge of the VOA, $c_{\text{VOA}}^{(2d)}$, up to a factor [229].

Famously, the 6d $\mathcal{N} = (2, 0)$ A_{N-1} SCFT does not have a known Lagrangian description. However, its circle reduction on S^1_R gives 5d $\mathcal{N} = 2$ $SU(N)$ SYM theory with coupling $g_{\text{YM}}^2 = 2\pi R$. It is a long-standing conjecture that the full path integral of 5d $\mathcal{N} = 2$ SYM theory captures the full 6d $\mathcal{N} = (2, 0)$ theory, where instanton particles

are identified with Kaluza-Klein modes of the 6d theory on the circle [370–372]. Using this conjecture, the authors of refs. [373, 374] argue that both the perturbative and non-perturbative contributions to the localised partition function of $\mathcal{N} = 2$ SYM theory on the squashed S^5 are sufficient to count the states contributing to the 6d index. The co-dimension four and two defects wrapping S^1_R in 6d reduce to Wilson lines or certain 3d defects in the 5d SYM theory on the squashed S^5 . Ref. [311] argues that the localised partition functions with these defects are sufficient to compute the deformations of the SCI. Although this is far from a proven fact about the dimensional reduction to 5d, we will adopt the same working assumption. The fact that for Wilson surfaces we will recover precisely the holographic result for $d_2^{(2d)}$ provides some evidence for this assumption.

In the absence of defects, the localised partition function of the 5d $U(N)$ $\mathcal{N} = 2$ SYM theory on a squashed S^5 takes the form

$$Z_{S^5} = \int \frac{d^{N-1}a}{N!} i^{N-1} e^{\frac{2\pi^2}{\epsilon_1 \epsilon_2 \epsilon_3} \text{Tr} a^2} Z_1 Z_2 Z_3, \quad (8.3.46)$$

where Z_1 is the Nekrasov partition function [22, 375] on $S^1_1 \times \mathbb{R}^4_{\epsilon_2, \epsilon_3}$, with Z_2 and Z_3 obtained from Z_1 by cyclic permutation of the labels $\{1, 2, 3\}$, and a is a constant adjoint-valued scalar parametrising the BPS locus.

Without any defects, the localised partition function of the 6d $\mathcal{N} = (2, 0)$ A_{N-1} theory in the unrefined limit computes, in the VOA, the character of the vacuum module of the \mathcal{W}_N algebra. Defining $2\pi i \tau = -R\epsilon_3$ so that $q = e^{2\pi i \tau}$, and defining $\epsilon_1 \epsilon_2 = 1$ and $\mathfrak{b}^2 = \epsilon_1 / \epsilon_2$, the partition function sees contributions in the unrefined limit from the three fixed points on the S^1_i of the form [311, 374, 376]

$$Z_1 = \prod_{e \in \Delta^+} 2 \sin \frac{\pi}{\mathfrak{b}}(e, a), \quad Z_2 = \prod_{e \in \Delta^+} 2 \sin \mathfrak{b} \pi(e, a), \quad Z_3 = \eta(-\tau^{-1})^{1-N}, \quad (8.3.47)$$

where $\eta(\cdot)$ is the Dedekind η function. Let $Q = \rho(\mathfrak{b} + \mathfrak{b}^{-1})$ with ρ being the Weyl vector of $\mathfrak{su}(N)$, and let $\mathcal{W}_{\mathfrak{g}}$ be the Weyl group of $\mathfrak{g} = A_{N-1}$. After integrating over a , eq. (8.3.46) becomes

$$Z_{S^5} = \frac{q^{-\frac{1}{2}(Q, Q)}}{\eta(\tau)^{N-1}} \sum_{\sigma \in \mathcal{W}_{\mathfrak{g}}} \varepsilon(\sigma) q^{-(\sigma(\rho), \rho) + (\rho, \rho)}, \quad (8.3.48)$$

where $\varepsilon(\sigma) = (-1)^{\ell(\sigma)}$ and $\ell(\sigma)$ is the length of the Weyl group element σ . See e.g. eq. (3.4) of ref. [311]. The exponent of the prefactor is related to the central charge $c_{\text{VOA}}^{(2d)}$ of the VOA as $q^{-\frac{c_{\text{VOA}}^{(2d)}}{24}}$. Recalling that $\eta(\tau) \propto q^{1/24}$, we thus have

$$c_{\text{VOA}}^{(2d)} = (N-1) + 12(Q, Q) = (N-1) + N(N^2 - 1)(\mathfrak{b} + \mathfrak{b}^{-1})^2, \quad (8.3.49)$$

where we identify $c_{\text{VOA}}^{(2d)}/24$ as the 6d SCE of the unrefined SCI [229].

8.3.2.1 2d defects

Adding a surface operator wrapping $S_R^1 \times S_1^1$ deforms the index to compute the character of a degenerate module of the associated \mathcal{W}_N -algebra in the VOA plane. The reduction to 5d yields a Wilson loop operator on S_1^1 carrying an irreducible representation of $\mathfrak{su}(N)$ with highest weight ω_1 . The fixed point contributions on S_1^1 are modified from those in eq. (8.3.47). In ref. [311] they were found to be (see their section 3.2 for more details)

$$Z_1 = \prod_{e \in \Delta^+} 2 \sin \frac{\pi}{\mathfrak{b}}(e, a) \text{Tr}_{\omega_1} e^{\frac{2\pi i a}{\mathfrak{b}}}, \quad (8.3.50)$$

where Tr_ω is a trace over the representation specified by ω . Z_2 and Z_3 remain unchanged compared to eq. (8.3.47). Note that we could have just as well inserted the Wilson loop on S_2^1 . However, since the plane $\mathbb{R}_{e_3}^2$ is designated as the VOA plane, the Wilson loop cannot wrap S_3^1 and also preserve the necessary nilpotent charge needed to define the VOA.¹⁰ Plugging Z_1 from eq. (8.3.50) into the partition function and integrating over a gives [311]

$$Z_{S^5}^{\omega_1} = q^{-C_{\omega_1}/24} \sum_{\sigma \in \mathcal{W}(\mathfrak{g})} \varepsilon(\sigma) e^{-(\sigma(\rho), \rho + \omega_1) + (\rho, \rho + \omega_1)}, \quad (8.3.51)$$

where the new ‘‘central charge’’ is

$$C_{\omega_1} = (N - 1) + 12(Q + \mathfrak{b}^{-1}\omega_1, Q + \mathfrak{b}^{-1}\omega_1). \quad (8.3.52)$$

To isolate the defect contribution to the partition function, we divide eq. (8.3.51) by the ambient theory result in eq. (8.3.48), which gives the change in the central charge,

$$C_{\omega_1} - c_{\text{VOA}}^{(2d)} = \frac{24}{\mathfrak{b}}(Q, \omega_1) + \frac{12}{\mathfrak{b}^2}(\omega_1, \omega_1). \quad (8.3.53)$$

To compare to the holographic result for a Wilson surface in section 8.1, we take $\mathfrak{b} \rightarrow 1$, so that $Q = \rho(\mathfrak{b} + \mathfrak{b}^{-1}) \rightarrow 2\rho$, and use $d_2^{(2d)} = -24(\rho, \omega_1) - 6(\omega_1, \omega_1)$ from eq. (8.1.6b), such that

$$C_{\omega_1} - c_{\text{VOA}}^{(2d)} = 48(\rho, \omega_1) + 12(\omega_1, \omega_1) = -2d_2^{(2d)}. \quad (8.3.54)$$

We have thus shown that a single defect changes the normalisation factor from $q^{-c_{\text{VOA}}^{(2d)}/24}$ to $q^{-C_{\omega_1}/24}$, or recalling that $q = e^{2\pi i \tau} = e^{-R\epsilon_3}$, the defect shifts the SCE from

¹⁰It is also true for 2d $\mathcal{N} = (4, 4)$ defects in 4d $\mathcal{N} = 4$ SYM theory that the surface operators must be inserted orthogonal to the chiral algebra plane. Note, though, that a 2d chiral (e.g. $\mathcal{N} = (0, 8)$ or $(0, 4)$) superconformal defect could be inserted along the chiral algebra plane while preserving the nilpotent supercharge used to define the VOA. We thank W. Peelaers for pointing this out.

$E_c = -\frac{c_{\text{VOA}}^{(2d)}}{24} \epsilon_3$ to $E_c = -\frac{c_{\omega_1}}{24} \epsilon_3$. Our result eq. (8.3.54) then shows that the change in E_c is $\propto d_2^{(2d)}$, as advertised.

Crucially, for a Wilson surface in the 6d $\mathcal{N} = (2, 0)$ theory at large N we can distinguish $-d_2^{(2d)}$ and $a_{\Sigma}^{(2d)}$, namely $a_{\Sigma}^{(2d)} + d_2^{(2d)} = -3(\omega_1, \omega_1)$. The comparison thus leaves no doubt: $d_2^{(2d)}$ controls the defect contribution to the SCE. The calculation here involved no approximations, relying only on SUSY and the assumptions about the reduction on S_R^1 mentioned above. Our result eq. (8.3.54) thus provides strong evidence that the holographic result for $d_2^{(2d)}$ in eq. (8.1.6b) is in fact exact, and not just the leading large- N limiting value.

In the above discussion, we contented ourselves with the study of a single Wilson surface on $S_R^1 \times S^1$. A more general BPS configuration involving *two* non-intersecting Wilson surfaces on $S_R^1 \times S^5$ was studied in ref. [3], upon which this chapter is based. The second Wilson surface is taken to wrap $S_R^1 \times S_2^1$, which also preserves the necessary nilpotent supercharge needed to define the VOA. Ref. [311] computed the localised partition function of the compactification on S_R^1 in the presence of both defects. Inclusion of the second defect leads to a modification of eq. (8.3.53) [3]. Interestingly, the result is not merely the sum of $d_2^{(2d)}$ for each of the two defects but it involves a cross term which depends on the inner product (ω_1, ω_2) , where ω_2 is the highest weight of the representation labelling the second Wilson surface. We speculate that this cross term arises from the interaction energy between the two loops on $S_R^1 \times S^5$.

8.3.2.2 4d defects

In the 6d $\mathcal{N} = (2, 0)$ A_{N-1} SCFT, there is another class of superconformal defects that one could construct: 4d defects. The authors of ref. [311] also constructed the index for these 4d defects, using arguments similar to the 2d case.

Co-dimension two operators in 6d $\mathcal{N} = (2, 0)$ A_{N-1} SCFTs, in particular, are labelled by nilpotent orbits of A_{N-1} , or equivalently, by homomorphisms $\varrho : \mathfrak{su}(2) \rightarrow A_{N-1}$. In the unrefined limit they correspond to a deformation of the VOA by the insertion of a semi-degenerate operator labelled by a partition of N , i.e. $[N_1, \dots, N_{n+1}]$ where $\sum_{i=1}^{n+1} N_i = N$. That is, 4d superconformal operators preserve the Levi subalgebra $\mathfrak{l} = \mathfrak{s} \left[\bigoplus_{i=1}^{n+1} \mathfrak{u}(N_i) \right]$.

In the reduction along S_R^1 , which the co-dimension two defect wraps, it has an equivalent description as a prescribed singularity in the gauge field of the resulting 5d $\mathcal{N} = 2$ SYM theory. Given a Levi subalgebra \mathfrak{l} , the monodromy parameters are $\vec{m} = \bigoplus_{i=1}^{n+1} \vec{m}_i$ with each \vec{m}_i being a rank N_i vector whose components are all identically m_i , and the Weyl vector of \mathfrak{l} is $\rho_{\mathfrak{l}} = \bigoplus_{i=1}^{n+1} \rho_{N_i}$ with each ρ_{N_i} being the Weyl vector of

$\mathfrak{su}(N_i)$. The BPS locus is parametrised by the adjoint scalar VEV a and $\sigma \in \mathcal{W}_{\mathfrak{g}}/\mathcal{W}_{\mathfrak{l}}$ — where $\mathcal{W}_{\mathfrak{g}}$ and $\mathcal{W}_{\mathfrak{l}}$ are the Weyl groups of $\mathfrak{g} = A_{N-1}$ and \mathfrak{l} , respectively — which also labels a permutation of the monodromies, i.e. different inequivalent choices of embeddings of \mathfrak{l} in A_{N-1} .

To compute the index in the presence of the defect, we need to use the form of the localised partition function in eq. (8.3.46) supplemented by the classical action from the monodromies given by $e^{-2\pi i(\sigma(\vec{m}), a)}$ and the Nekrasov partition functions corresponding to the particular ϱ and choice of σ

$$Z_1^{\varrho, \sigma} = \prod_{i=1}^{n+1} \prod_{e \in \Delta_i^+} 2 \sin \frac{\pi}{\mathfrak{b}}(e, \sigma(a)), \quad Z_2^{\varrho, \sigma} = \prod_{i=1}^{n+1} \prod_{e \in \Delta_i^+} 2 \sin \pi \mathfrak{b}(e, \sigma(a)), \quad (8.3.55)$$

where Δ_i^+ is the space of positives roots of the i^{th} summand of \mathfrak{l} and as above $Z_3 = \eta(-\tau^{-1})^{1-N}$. See section 3.3 of ref. [311] for further details. Summing over all σ and integrating over the locus parametrised by a gives

$$Z_{S^5}^{\varrho} = q^{-C_{\varrho}/24} \sum_{\sigma} \varepsilon(\sigma) q^{-(\sigma(\rho_{\mathfrak{l}}) - \rho_{\mathfrak{l}}, \rho_{\mathfrak{l}})}. \quad (8.3.56)$$

Dividing $Z_{S^5}^{\varrho}$ by the ambient theory partition function changes the normalisation factor to $q^{-(C_{\varrho} - c_{\text{VOA}}^{(2d)})/24}$, where

$$C_{\varrho} - c_{\text{VOA}}^{(2d)} = -24(Q, \mu_{\varrho}) + 12(\mu_{\varrho}, \mu_{\varrho}), \quad (8.3.57)$$

and

$$\mu_{\varrho} = Q + \vec{m} - (\mathfrak{b} + \mathfrak{b}^{-1})\rho_{\mathfrak{l}}. \quad (8.3.58)$$

Using $Q = \rho(\mathfrak{b} + \mathfrak{b}^{-1})$ and $(\vec{m}, \rho_{\mathfrak{l}}) = 0$, we find

$$C_{\varrho} - c_{\text{VOA}}^{(2d)} = 12(\mathfrak{b} + \mathfrak{b}^{-1})^2 [(\rho_{\mathfrak{l}}, \rho_{\mathfrak{l}}) - (\rho, \rho)] + 12(\vec{m}, \vec{m}). \quad (8.3.59)$$

We can easily compute $(\rho_{\mathfrak{l}}, \rho_{\mathfrak{l}}) = \frac{1}{12}(\sum_{i=1}^{n+1}(N_i^3 - N_i))$ by considering each individual $\mathfrak{su}(N_i)$ summand in \mathfrak{l} . In the limit $\mathfrak{b} \rightarrow 1$ we thus find

$$C_{\varrho} - c_{\text{VOA}}^{(2d)} = -4 \left(N^3 - \sum_{i=1}^{n+1} N_i^3 - 3(\vec{m}, \vec{m}) \right). \quad (8.3.60)$$

As mentioned above, we do not know which B-type defect central charge(s) in eq. (6.1.1) we have computed. For now, eq. (8.3.60) serves as a prediction for 4d superconformal defects in the 6d $\mathcal{N} = (2, 0)$ A_{N-1} SCFT.

Our result in eq. (8.3.60) bears a resemblance, modulo overall sign and powers of N and N_i , to $d_2^{(2d)}$ for the $\mathcal{N} = (4, 4)$ Levi type- \mathbb{L} surface operator in 4d $\mathcal{N} = 4$ SYM theory in eq. (8.1.5b). Given the connection between the two constructions via

dimensional reduction, this superficial resemblance is perhaps not surprising. Beyond the scope of the current work, but the focus of on-going investigation, is finding the behaviour of the defect Weyl anomaly of the 4d Levi type- \mathbb{L} defect in 6d under dimensional reduction to a 2d Levi type- \mathbb{L} defect in 4d $\mathcal{N} \geq 2$ SCFTs.

8.4 Discussion

In this chapter, we illustrated techniques for computing the central charges $a_{\Sigma}^{(2d)}$ and $d_2^{(2d)}$ of 2d superconformal defects in SCFTs. Our methods rely only on a sufficient amount of SUSY, and involve no approximations. In particular, we used existing results for SUSY localisation and SCIs to extract new results for $a_{\Sigma}^{(2d)}$ and $d_2^{(2d)}$.

Whenever our results overlapped with existing holographic results, they agreed perfectly, proving that the latter were not merely large- N or strong-coupling limits, but were in fact exact.

Our results pave the way for many fruitful generalisations. Obviously, a variety of other existing results for SUSY partition functions on S^d and $S^1 \times S^{d-1}$ could be mined for further novel results for $a_{\Sigma}^{(2d)}$ and $d_2^{(2d)}$. This includes twist field defects relevant for calculations of SUSY Rényi entropy [377–379], where information theoretic constraints may imply bounds on the defect’s central charges [380]. Additionally, to our knowledge a variety of 2d superconformal defects have yet to be described using any of the SUSY methods we have discussed. A prominent example is chiral defects, such as defects with 2d $\mathcal{N} = (0, 4)$ SUSY. Chiral defects break parity, producing parity-odd terms in the trace anomaly. These in turn define the two parity-odd central charges $\tilde{d}_1^{(2d)}$ and $\tilde{d}_2^{(2d)}$ in eq. (8.2.7). In principle, these could be calculated using the methods we have described. Furthermore, as deformations of the SCI, 2d $\mathcal{N} = (0, 4)$ defects can preserve the nilpotent supercharge used in the cohomological construction of VOAs from 4d SCFTs [256], and so their central charges may appear in the vacuum character of a deformed VOA.

Other approaches to computing SUSY partition functions on S^d and $S^1 \times S^{d-1}$ could also be developed along similar lines as useful tools to extract defect central charges in novel systems. Examples include geometric engineering [381, 382], or computing a 5d SUSY partition function on $S^1 \times S^4$ with a 3d SUSY defect along $S^1 \times S^2$ [383] and then reducing on the common S^1 to obtain a 4d SUSY partition function on S^4 with a 2d defect along $S^2 \hookrightarrow S^4$ [45]. More importantly, studying how the defect trace anomalies and associated central charges behave under dimensional reduction could provide a new window into how defect physics changes under RG flows across dimensions [384].

All the above methods could also be straightforwardly generalised to defects of other dimensions. For example, in 4d SCFTs various $\frac{1}{2}$ -BPS interfaces and domain walls

have been studied using holography [385–387], SUSY localisation [388], and other methods [219]. In these cases the interface contribution to the trace anomaly defines two central charges, $b_1^{(3d)}$ and $b_2^{(3d)}$ in eq. (3.4.45), that could in principle be calculated from existing results. In 5d and 6d SCFTs, higher-dimensional defects are possible, such as the 4d defect in the 6d $\mathcal{N} = (2, 0)$ A_{N-1} theory that we discussed at the end of section 8.3. However, it is unclear what (linear combination) of central charges the SUSY methods could compute. Finding the precise relation between the defect contribution to the SCE and defect anomalies across dimensions is an important question that we are eager to settle in future work.

Chapter 9

Concluding Remarks

In this thesis, we studied conformal defects through their contributions to the Weyl anomaly. The coefficients of each term, the defect central charges, encode valuable physical information about the defect. They enter in various physical observables, and have a host of interesting properties. Importantly, some defect central charges must decrease under defect RG flows by certain monotonicity theorems. These give rise to a notion of irreversibility along defect RG flows and provide order in the space of admissible defects. This makes them crucial for characterising and classifying defects and perhaps QFTs more generally.

Our emphasis in this work was on exact methods to study defects via their central charges. We derived novel universal results, applied existing exact methods to compute defect central charges, and developed new non-perturbative tools. In doing so, we made use of a wide range of concepts, including DCFT methods, information theory, and SUSY. Although not reviewed explicitly in this work, much of the inspiration was drawn from string and M-theory. In particular, string theory arguments imply the existence of SCFTs in dimensions $d = 5$ and $d = 6$ for which no conventional Lagrangian formulation can exist. These theories are inherently strongly coupled and the local operator spectrum of these SCFTs is shrouded in mystery. However, string theory suggests that these SCFTs admit defects of various defect dimensions p .

Motivated by the co-dimension two defects of the 6d $\mathcal{N} = 2$ SCFTs, we studied $p = 4$ defects in chapter 6. Our main result was the full form of the defect Weyl anomaly for any co-dimension, including parity-breaking terms, in eq. (6.1.1). In addition to the Euler density, it consists of 22 parity-even terms which are allowed for any co-dimension. The number of parity-breaking terms is dependent on the co-dimension. Importantly, we showed how some of the defect central charges appear in correlation functions of universal DCFT operators. They include the displacement operator two-point function, and the stress tensor one-point function in flat space

when $d \geq 6$ and curved space when $d = 5$. Through their appearance in correlation functions, we are able to derive bounds on these defect central charges stemming from unitarity and the ANEC. Further, we argued that the defect's contribution to the universal part of EE of a spherical region centred on the defect depends on two of its central charges.

In chapter 7, we studied monodromy defects in the theories of a free complex scalar and a free Dirac fermion. Monodromy defects are simple, yet non-trivial, co-dimension two defects which one can introduce whenever the theory has a global symmetry. Using existing techniques available in free field theories, we were able to compute various correlation functions exactly. We then showed that we can extract some of the defect central charges when $d = 4$ and $d = 6$. In the latter case we applied many of our results of chapter 6. As a check of our results in $d = 4$, we computed the EE using heat kernel methods. In our analysis of monodromy defects, we observed that the defect OPE contains special defect local operators with low scaling dimensions. Using these operators, we constructed quadratic relevant deformations, triggering an RG flow. Our results are consistent with the defect c-theorems of refs. [55, 57]. Interestingly, we observed that for special values of the monodromy parameter in the free fermion CFT, there exist exactly marginal defect operators, signalling the existence of a non-SUSY defect conformal manifold.

Finally in chapter 8, we studied a set of conformal defects in interacting CFTs. To make the problem tractable, we imposed superconformal invariance. We then devised new non-perturbative methods to compute defect central charges, which rely on SUSY localisation. In particular, using the fact that A-type central charges appear in sphere partition functions, we explained how the exact value of the A-type defect central charge can be extracted from the localised partition function of a defect wrapping an equatorial $S^p \hookrightarrow S^d$, with $p = 2\mathbb{Z}$. We illustrated our methods in numerous examples of $p = 2$ defects in 4d SCFTs. We then argued that a linear combination of B-type defect central charges appears in the SCE, a part of the localised partition function on $S_R^1 \times S^{d-1}$, with the defect wrapping $S_R^1 \times S^{p-1}$. For the co-dimension four defects of the 6d $\mathcal{N} = (2, 0)$ A_{N-1} SCFT, we were able to identify the precise defect central charge computed in this way. Our methods are broadly applicable to a large class of superconformal defects across dimensions, and open up many new possibilities for characterising and classifying defects, boundaries, and CFTs with various p and d .

Many of the possible immediate extensions of our results and further directions were discussed at the end of chapters 6, 7, and 8. Here we conclude with a few general remarks related to our main motivation of classifying, or mapping out the space of QFTs, which led us to defects in the first place.

As argued in chapter 1, the detailed study of defect Weyl anomalies is an important step towards this goal. Since conformal defects occupy a privileged position in the

space of admissible defects, they are a natural starting point for the exploration of defects and their role in QFT. This makes our result of the 4d defect Weyl anomaly in chapter 6 so essential. It provides us with previously unknown parameters that characterise a large class of defects, from which others may be reached by appropriate deformations. Moreover, we initiated the detailed study of these parameters, deriving novel universal results. Indeed, determining how these parameters appear in correlation functions is a key step in identifying and deriving monotonicity theorems, which provide order in the space of defects. As shown for some of these coefficients of the 4d defect Weyl anomaly, physical principles can impose further bounds on them. It is tempting to speculate that identifying all such constraints would carve out the space of physically admissible conformal defects.

Our computations of defect central charges in numerous examples in chapters 7 and 8 are just as important. Examples often reveal patterns which may in fact be general features. These properties may be amenable to a rigorous proof. Conversely, examples can rule out the possibility of certain bounds or monotonicity theorems for some central charges. As such, our computations provide crucial data points to explore the space of defects in QFT. Moreover, given a pair of examples of defects in a CFT, existing monotonicity theorems reveal whether they can possibly be connected by a defect RG flow from one to the other, providing a relative hierarchy between them.

For defects in interacting CFTs, performing exact computations of these quantities is typically challenging. This underscores the importance of the methods for interacting SCFTs developed and outlined in chapter 8. To our knowledge, these methods allowed us to perform the first exact computations of examples of defect central charges in interacting theories. Previously, only holographic results at large N were known whereas our computations do not involve any approximations and are non-perturbative. Moreover, for theories with a holographic dual, our methods give results that contain implicit statements about quantum gravity. Indeed, by virtue of being exact in N , they must encode quantum gravitational effects on anti-de Sitter spacetimes in the dual frame.

One particular example of such a theory is the 6d $\mathcal{N} = (2, 0)$ SCFT, which describes the low energy limit of branes in M-theory. From a purely field theoretic perspective, however, the absence of a Lagrangian in the interacting case makes it prohibitively difficult to study using conventional QFT methods. Since co-dimension two and four defects are some of the few superconformal operators known to exist in this theory, it is essential to characterise them. Our computations in chapter 8 for the co-dimension four defects provide new pieces of data and additional constraints on this SCFT. The theory's co-dimension two defects have proven harder to investigate. Our results for the Weyl anomaly of 4d conformal defects discussed in chapter 6 provide another angle on these defects. Indeed, one now has concrete parameters at one's disposal that

are computable in principle. Pinning down this exotic theory will presumably reveal general features about strongly coupled QFTs.

As mentioned in section 8.4, understanding defect RG flows across dimensions constitutes an integral part of mapping out the space of defects. The theories of class \mathcal{S} are an ideal starting point to study these flows. As discussed in chapter 8, they are a rich yet highly constrained set of 4d SCFTs which arise from (twisted) compactification of the 6d $\mathcal{N} = (2,0)$ SCFT on a Riemann surface. These compactifications can be enriched with defects: a defect in the 6d theory extending along some of the non-compact directions descends to a defect in class \mathcal{S} . By allowing defects to (partially or fully) wrap the Riemann surface, one can further engineer defects in 4d with a different dimension than their parent defect. Our methods of chapter 8 will be vital for understanding these types of flows, and, in particular, how the central charges of the parent defect determine the central charges of the compactified defect.

Still closer to our objective of classifying QFTs through the defects that they admit, one could imagine using our methods to study RG interfaces. Starting with a CFT, say, on flat space, one can integrate a relevant deformation over half of space. This triggers an RG flow on one half whereas the other half stays unaffected. If the endpoint in the IR is another CFT, this flow engineers a conformal interface between two CFTs connected by an RG flow. A classification of conformal interfaces would then reveal which ordinary bulk CFTs may be connected by an RG flow. If the endpoint of the flow on half-space is gapped, this engineers a conformal boundary condition for the theory on the other side. A classification of conformal boundary conditions would then reveal the gapped vacua that a CFT may admit. In either case, the resulting DCFT or BCFT is likely to be much simpler to study than the corresponding bulk flows because CFT methods are available. Restricting ourselves further to SUSY-preserving flows, our methods developed in chapter 8 can be directly brought to bear.

In this thesis, we imposed highly restrictive spacetime symmetries for tractability. One may wonder to what extent global symmetries can help with the classification problem of QFTs and their admissible defects. Recently, the traditional notions of global symmetry were extended to include various generalisations that lead to a paradigm shift. Rather than characterising symmetry through the presence of conserved currents and charges, ordinary global symmetries from a modern point of view are associated with topological co-dimension one defects, called symmetry defects, which have a group-like fusion product. Their action on charged local operators realises the symmetry in the QFT. One advantage of this approach is that it provides a natural language to discuss discrete symmetries. Moreover, this new description can be generalised in a number of ways: Firstly, one can relax the assumption that the symmetry defects are co-dimension one, and consider topological defects of higher co-dimension [154]. These encode so-called higher-form symmetries. Secondly, one may further relax the assumption of a group-like fusion law to a more

general fusion ring, giving rise to the notion of non-invertible symmetries [234,389]. In both cases, the objects charged under these symmetries are $p \geq 0$ defects that need not be topological.

These generalisations of symmetry may seem exotic at first but they have been demonstrated to appear in many QFTs of various spacetime dimensions. E.g. higher-form symmetries appear in $d = 4$ gauge theory, including theories as simple as pure Maxwell and YM theory [154]. Non-invertible symmetries, which were originally observed in low-dimensional examples, have recently been identified in many ordinary QFTs in $d = 4$ [390–393]. This makes it rather surprising that they have eluded our attention for more than half a century.

From this modern point of view, local and extended charged operators are treated on the same footing. The study of defects has been central to the discovery of these new symmetries, and may perhaps lead to further generalisations of symmetry. Conversely, these symmetries may suggest a way towards a classification of admissible defects in QFT. E.g. line defects and flavour Wilson lines in class \mathcal{S} theories have recently been shown to fall into equivalence classes of certain categorical generalisations of symmetry, called 2-group symmetries [236,394]. Whether similar classification schemes exist for higher-dimensional defects in SCFTs remains to be seen.

As with ordinary symmetries, these generalisations of symmetry constrain a given QFT in various ways, e.g. through an analogue of 't Hooft anomaly matching along RG flows or through selection rules on correlation functions. Remarkably, the study of higher-form symmetries has led to some progress on the YM mass gap problem. By analysing a mixed anomaly between a higher-form symmetry and an ordinary discrete symmetry in YM theory, ref. [395] showed that at theta angle $\theta = \pi$ YM theory cannot be trivially gapped. Moreover, 't Hooft anomaly matching for 2-group symmetries allowed ref. [396] to prove that in 6d SCFTs the A-type central charge $a_{\mathcal{M}}^{(6d)} > 0$ provided the theory has a vacuum manifold parametrised by VEVs of scalars in the gauge multiplet. Non-invertible symmetries have been explored to a lesser extent. A systematic analysis of their constraints on QFTs will undoubtedly lead to a better understanding of what QFT is.

In view of these recent developments involving symmetries, it is tempting to speculate that QFT may be due for a reformulation in a perhaps more algebraic language. Such a reformulation should naturally allow for the description of strongly coupled physics, and treat local and extended operators on an equal footing. Ideally, it should suggest new computational strategies in strongly coupled QFTs but that may be too much to wish for. SCFTs would be the ideal theoretical laboratories to explore such ideas. On the one hand, they exhibit some of the interesting features of strongly

coupled physics observed in nature. On the other hand, the vast amount of symmetry makes their analysis tractable.

Ultimately, however, one wants to move away from (super)conformal symmetry. In fact, many physical systems that can be probed in a real laboratory are not even Lorentz-invariant. An interesting class of lattice spin models considered in the condensed matter literature describes fractons. These models are characterised by a large and robust ground state degeneracy, and their massive excitations, i.e. the fractons, have restricted mobility. See e.g. ref. [397] for a review. The continuum limit of these lattice models gives rise to exotic QFTs breaking Lorentz invariance. Fractonic excitations are modelled by defects in these QFTs.

A peculiar feature of these models is that they can be shown to exhibit yet another type of symmetry, called subsystem symmetry, whose symmetry defects are not topological but conserved in time [398]. They are called subsystem symmetries because their symmetry defects can only be supported on certain submanifolds. Remarkably, some low energy observables receive contributions from large momenta, giving rise to a mixing of UV and IR DOF [399]. These models violate the Wilsonian paradigm, and call into question what is meant by QFT. A reformulation of QFT should also encapsulate these phenomena.

In recent years, there has been significant interest in condensed matter systems that have topological order, a gapped phase of matter characterised by a protected ground state degeneracy and dependent on the topology of space. Such matter has been suggested as a medium for fault-tolerant quantum computation [400]. See e.g. ref. [401] for a review. Curiously, topological order does not fit the ordinary Landau paradigm which states that phases of matter are classified by spontaneously broken global symmetries. The discussion in the previous paragraphs suggests an enlarged Landau paradigm that incorporates generalisations of symmetry. Importantly, defects play the role of order parameters classifying phases in which higher-dimensional objects condense. Whether all phases of matter can be described in this way remains to be seen.

Boundaries can have interesting dynamics and transport properties in condensed matter systems. These include systems with topological order, e.g. (integer and fractional) quantum Hall states have gapless boundary excitations [402], but are not limited to them. One system that has received considerable interest in recent years is graphene, a $(2 + 1)$ d sheet of carbon atoms whose bonds form a (bipartite) hexagonal lattice. Different boundary conditions can be introduced by cutting the sheet at an angle [403]. In the continuum, graphene is described by free fermions. Ref. [404] showed that one of the possible boundary conditions corresponds to a BCFT. Since BCFTs are partially characterised by their boundary central charges, strips of graphene could be studied with techniques similar to the ones discussed in this thesis. If

boundary central charges can be related to transport coefficients, one would perhaps be able to measure them in a laboratory. This would allow one to experimentally verify or falsify theoretical bounds, and may lead to the discovery of new ones. Moreover, ref. [404] showed that graphene has a boundary condition that is scale but not conformally invariant. It would be interesting to explore the constraints of scale invariance alone on boundaries and defects in QFT.

We intend to explore many of these directions in future research.

Part III

Appendices

Appendix A

Chapter 3

A.1 Isolating the anomaly: $p = 2$ conformal defect in a $d = 4$ CFT

In this appendix we illustrate the algorithm discussed in sections 2.5 and 3.4 with a simple example: the case of a $p = 2$ defect in a $d = 4$ ambient CFT. We will reproduce the known result of refs. [50,71,72,97,98,158–160], stated in eq. (3.4.38). The structure of this section follows that of the supplemental Mathematica notebook available from ref. [1], and we use notation that mirrors the notation in the notebook. Readers interested in reproducing our results for $p = 4$ defects may wish to consult this appendix first, as a warm-up exercise, before diving into our notebook.

Step 1: We begin by finding a basis of terms for the defect Weyl anomaly. The terms need to be scalars built out of the metric $g_{\mu\nu}$, the pullback e_a^μ , the Weyl variation parameter $\delta\omega$, and two derivatives. There are 10 of them.

It is convenient to separate the terms into three categories. The first one involves scalars with a non-trivial Weyl transformation. There are three such terms:

$$\mathcal{B}_1 = \bar{R}, \quad \mathcal{B}_2 = R, \quad \mathcal{B}_3 = \Pi^i \Pi_i. \quad (\text{A.1.1})$$

The second category involves scalars that are trivially Weyl invariant. There are four linearly-independent such terms:

$$\tilde{\mathcal{B}}_1 = \mathring{\Pi}_{ab}^i \mathring{\Pi}_i^{ab}, \quad \tilde{\mathcal{B}}_2 = \bar{g}^{ac} \bar{g}^{bd} W_{abcd}, \quad \tilde{\mathcal{B}}_3 = (R^\perp)^{ij}{}_{ab}, \quad \tilde{\mathcal{B}}_4 = n_{ij} \epsilon^{ab} \mathring{\Pi}_{ac}^i \mathring{\Pi}_b^{jc}. \quad (\text{A.1.2})$$

Finally, we list terms with derivatives acting on the variation parameter. There are three of them:

$$\mathcal{D}_1 = \Pi^i D_i \delta\omega, \quad \mathcal{D}_2 = N^{ij} D_i D_j \delta\omega, \quad \mathcal{D}_3 = n_{ij} \Pi^i D^j \delta\omega. \quad (\text{A.1.3})$$

In general, these will all appear in the anomaly as

$$\delta\omega \mathcal{W}^{(1)} = \int_{\Sigma_2} \sqrt{\bar{g}} \left(\sum_{i=1}^3 \mathfrak{b}_i \mathcal{B}_i \delta\omega + \sum_{i=1}^4 \tilde{\mathfrak{b}}_i \tilde{\mathcal{B}}_i \delta\omega + \sum_{i=1}^3 \mathfrak{d}_i \mathcal{D}_i \right). \quad (\text{A.1.4})$$

A few comments are in order. In constructing this basis, and making sure that it is not over-complete, we have used a number of geometric relations. Since the Weyl tensor $W_{\mu\nu\rho\sigma}$ is a linear combination of Riemann tensor, Ricci tensor and Ricci scalar, we are free to disregard any terms built out of $R_{\mu\nu\rho\sigma}$. Similarly, we have traded in a Π_{ab}^μ for its traceless part $\hat{\Pi}_{ab}^\mu$ and its trace Π^μ . Moreover, any term containing two copies of either ϵ^{ab} or n^{ij} can be re-written without any epsilon symbols using $\epsilon_{ab} \epsilon^{cd} = \delta_a^c \delta_b^d - \delta_b^c \delta_a^d$, and similarly $n_{ij} n^{kl} = N_i^k N_j^\ell - N_j^k N_i^\ell$. Further, we only consider quantities that do not need to be extended into the bulk. An example is $N^{ij} D_i \Pi_j$, which crucially depends on how Π_j is extended into the ambient geometry. Since there is no canonical way to do so, we do not consider such terms here. In general, we don't expect such terms be part of the physical Weyl anomaly. In the present 2d case, WZ consistency eliminates them. One may have also expected the following terms:

$$\begin{aligned} \mathcal{C}_1 &= \bar{g}^{ab} R_{ab}, & \mathcal{C}_2 &= N^{ij} R_{ij}, & \mathcal{C}_3 &= N^{ik} N^{j\ell} W_{ijkl}, & \mathcal{C}_4 &= \bar{g}^{ab} N^{ij} W_{aibj}, \\ \mathcal{C}_5 &= R_{ijab}^\perp n^{ij} \epsilon^{ab}, & \mathcal{C}_6 &= E_\mu^a \bar{D}_a \Pi^\mu, & \mathcal{C}_7 &= E_\mu^b \bar{D}^a \hat{\Pi}_{ab}^\mu, \end{aligned} \quad (\text{A.1.5})$$

where R^\perp is the normal bundle curvature, i.e. the curvature associated with the connection induced from D that maps normal vectors to normal vectors by parallelly transporting them along the submanifold. However, these are not linearly independent. Firstly, $\mathcal{C}_1 = \mathcal{B}_2 - \mathcal{C}_2$. We can use this relation to eliminate \mathcal{C}_1 . Now, \mathcal{C}_2 appears in the twice contracted Gauss eq. (3.3.32c). Trading the Riemann tensor for the Weyl tensor, it reads

$$3\mathcal{C}_2 = -\mathcal{B}_1 + \mathcal{B}_2 - \tilde{\mathcal{B}}_1 + \tilde{\mathcal{B}}_2 + \frac{3}{4} \tilde{\mathcal{B}}_3. \quad (\text{A.1.6})$$

Thus we can use it to eliminate \mathcal{C}_2 . Furthermore, the fact that the trace of any two indices of $W_{\mu\nu\rho\sigma}$ with the ambient metric $g_{\mu\nu}$ vanishes implies that $\mathcal{C}_3 = -\mathcal{C}_4 = \tilde{\mathcal{B}}_2$. \mathcal{C}_5 can be removed by the Ricci identity eq. (3.3.34). Finally, $\mathcal{C}_6 = -\mathcal{B}_3$ using $E_\mu^a \Pi^\mu = 0$ and the definition of Π , and similarly $\mathcal{C}_7 = -\tilde{\mathcal{B}}_1$. This leaves us with the terms in eqs. (A.1.1), (A.1.2) and (A.1.3).

Step 2: WZ consistency reduces the number of terms to 7. To compute $[\delta_1, \delta_2] \mathcal{W}^{(1)}$ we take a second Weyl variation of the above basis. We anti-symmetrise in the

variation parameters, $\delta\omega_1$ and $\delta\omega_2$, which generates linear combinations of the following terms

$$\begin{aligned} \mathcal{D}_1^{\text{WZ}} &= \delta\omega_2 \Pi^i D_i \delta\omega_1 - (1 \leftrightarrow 2), & \mathcal{D}_2^{\text{WZ}} &= \delta\omega_2 N^{ij} D_i D_j \delta\omega_1 - (1 \leftrightarrow 2), \\ \mathcal{D}_3^{\text{WZ}} &= \delta\omega_2 n_{ij} \Pi^i D^j \delta\omega_1 - (1 \leftrightarrow 2), & \mathcal{D}_4^{\text{WZ}} &= n^{ij} D_j \delta\omega_2 D_i \delta\omega_1 - (1 \leftrightarrow 2). \end{aligned} \quad (\text{A.1.7})$$

The second Weyl variations are

$$\begin{aligned} (\sqrt{\bar{g}})^{-1} \delta_1 (\sqrt{\bar{g}} \mathcal{B}_1 \delta\omega_2) - (1 \leftrightarrow 2) &= 0, \\ (\sqrt{\bar{g}})^{-1} \delta_1 (\sqrt{\bar{g}} \mathcal{B}_2 \delta\omega_2) - (1 \leftrightarrow 2) &= 4 \left(\mathcal{D}_1^{\text{WZ}} - \mathcal{D}_2^{\text{WZ}} \right), \\ (\sqrt{\bar{g}})^{-1} \delta_1 (\sqrt{\bar{g}} \mathcal{B}_3 \delta\omega_2) - (1 \leftrightarrow 2) &= -4 \mathcal{D}_1^{\text{WZ}}, \\ (\sqrt{\bar{g}})^{-1} \delta_1 (\sqrt{\bar{g}} \tilde{\mathcal{B}}_1 \delta\omega_2) - (1 \leftrightarrow 2) &= 0, \\ (\sqrt{\bar{g}})^{-1} \delta_1 (\sqrt{\bar{g}} \tilde{\mathcal{B}}_2 \delta\omega_2) - (1 \leftrightarrow 2) &= 0, \\ (\sqrt{\bar{g}})^{-1} \delta_1 (\sqrt{\bar{g}} \tilde{\mathcal{B}}_3 \delta\omega_2) - (1 \leftrightarrow 2) &= 0, \\ (\sqrt{\bar{g}})^{-1} \delta_1 (\sqrt{\bar{g}} \tilde{\mathcal{B}}_4 \delta\omega_2) - (1 \leftrightarrow 2) &= 0, \\ (\sqrt{\bar{\gamma}})^{-1} \delta_1 (\sqrt{\bar{g}} \mathcal{D}_1^\partial \delta\omega_2) - (1 \leftrightarrow 2) &= 0, \\ (\sqrt{\bar{g}})^{-1} \delta_1 (\sqrt{\bar{g}} \mathcal{D}_2^\partial \delta\omega_2) - (1 \leftrightarrow 2) &= 0, \\ (\sqrt{\bar{g}})^{-1} \delta_1 (\sqrt{\bar{g}} \mathcal{D}_3^\partial \delta\omega_2) - (1 \leftrightarrow 2) &= -4 \mathcal{D}_4^{\text{WZ}}, \end{aligned} \quad (\text{A.1.8})$$

where $(1 \leftrightarrow 2)$ only exchanges the subscripts on the Weyl variation parameters, and \mathcal{D}_i^∂ denotes the operator version of \mathcal{D}_i in eq. (A.1.3) with the variation parameter $\delta\omega$ omitted. In the above we have dropped total derivatives along the submanifold $\bar{D}(\dots)$ since the above terms appear in $[\delta_1, \delta_2] \mathcal{W}$ under an integral.

Solving WZ consistency reduces to a simple problem in linear algebra. Let $(\underline{\mathcal{B}}^{\text{WZ}})^T = (\mathcal{B}_1, \dots, \mathcal{B}_3, \tilde{\mathcal{B}}_1, \dots, \tilde{\mathcal{B}}_4, \mathcal{D}_1^\partial, \dots, \mathcal{D}_3^\partial)$ and $(\underline{\mathcal{D}}^{\text{WZ}})^T = (\mathcal{D}_1^{\text{WZ}}, \dots, \mathcal{D}_4^{\text{WZ}})$. Let M^{WZ} be the 10×4 matrix that implements the transformation,

$$\left(M^{\text{WZ}} \right)^T = \begin{pmatrix} 0 & 4 & -4 & 0 & 0 & 0 & 0 & 0 & 0 & 0 \\ 0 & -4 & 0 & 0 & 0 & 0 & 0 & 0 & 0 & 0 \\ 0 & 0 & 0 & 0 & 0 & 0 & 0 & 0 & 0 & 0 \\ 0 & 0 & 0 & 0 & 0 & 0 & 0 & 0 & 0 & -4 \end{pmatrix}, \quad (\text{A.1.9})$$

i.e. $\mathcal{S}^2 \underline{\mathcal{B}}^{\text{WZ}} = M^{\text{WZ}} \underline{\mathcal{D}}^{\text{WZ}}$, where the operator \mathcal{S}^2 acts like

$\mathcal{S}^2 A = (\sqrt{\bar{g}})^{-1} \delta_1 (\sqrt{\bar{g}} A \delta\omega_2) - (1 \leftrightarrow 2)$ for some A . The (right) null space of $(M^{\text{WZ}})^T$ is the general solution to the condition $[\delta_1, \delta_2] \mathcal{W}^{(1)} = 0$. In this example, the solutions are particularly simple: they just correspond to $\mathcal{B}_1 \delta\omega$, $\tilde{\mathcal{B}}_1 \delta\omega$, $\tilde{\mathcal{B}}_2 \delta\omega$, $\tilde{\mathcal{B}}_3 \delta\omega$, $\tilde{\mathcal{B}}_4 \delta\omega$, \mathcal{D}_1 and \mathcal{D}_2 , each added with an arbitrary coefficient in the anomaly polynomial, i.e.

$$\delta_\omega \mathcal{W}^{(2)} = \int_{\Sigma_2} \sqrt{\bar{g}} \left(\mathfrak{b}_1 \mathcal{B}_1 \delta\omega + \sum_{i=1}^4 \tilde{\mathfrak{b}}_i \tilde{\mathcal{B}}_i \delta\omega + \sum_{i=1}^2 \mathfrak{d}_i \mathcal{D}_i \right). \quad (\text{A.1.10})$$

The other coefficients must vanish, i.e. $b_2 = b_3 = d_3 = 0$.

More generally, the solutions to WZ consistency may involve a linear combination of terms with fixed relative coefficients, i.e. WZ consistency forces the coefficients of some terms to be determined by one another up to a single overall number. Each such linear combination would appear in $\delta_\omega \mathcal{W}$ with this unfixed coefficient. For example, for a $p = 4$ defect, WZ consistency fixes the relative coefficients appearing in eqs. (6.1.2) and (6.1.3) up to a single overall coefficient for each of them, $d_1^{(4d)}$ and $d_2^{(4d)}$, respectively.

One sometimes also finds linear combinations of \mathcal{D} 's at this stage. Indeed, this is the case for a $p = 4$ defect. As we explain in appendix B.1, however, they are typically not genuine solutions of WZ consistency, but can be made inconsistent by addition of local counterterms.

Step 3: Finally, we introduce local counterterms in \mathcal{W} . By adjusting their coefficients we can set to zero some of the remaining coefficients in eq. (A.1.10). We find 5 scheme-independent terms in the anomaly which cannot be removed by such counterterms.

Let \mathcal{W}_{CT} be the counterterm action. We cannot add any of the \mathcal{D} 's as counterterms because \mathcal{W}_{CT} does not involve the variation parameter $\delta\omega$. In principle, we could introduce the $\tilde{\mathcal{B}}$'s. However, they are Weyl invariant and, therefore, cannot remove any terms from the anomaly. We are thus left with the \mathcal{B} 's. The counterterm action reads

$$\mathcal{W}_{CT} = \int_{\Sigma_2} \sqrt{\bar{g}} \left(\sum_{i=1}^3 c_i \mathcal{B}_i \right). \quad (\text{A.1.11})$$

The first Weyl variation of these terms is

$$\begin{aligned} (\sqrt{\bar{g}})^{-1} \delta \left(\sqrt{\bar{g}} \mathcal{B}_1 \right) &= 0, \\ (\sqrt{\bar{g}})^{-1} \delta \left(\sqrt{\bar{g}} \mathcal{B}_2 \right) &= 4 (\mathcal{D}_1 - \mathcal{D}_2) \delta\omega, \\ (\sqrt{\bar{g}})^{-1} \delta \left(\sqrt{\bar{g}} \mathcal{B}_3 \right) &= -4 \mathcal{D}_1 \delta\omega, \end{aligned} \quad (\text{A.1.12})$$

where we have again dropped total derivatives $\bar{D}(\dots)$.

Determining the terms in the anomaly that cannot be removed by local counterterms reduces again to a linear algebra problem. Let $\underline{\mathcal{B}} = (\mathcal{B}_1, \dots, \mathcal{B}_3)^T$ and $\underline{\mathcal{D}} = (\mathcal{D}_1, \dots, \mathcal{D}_3)^T$. We introduce the 3×3 matrix M ,

$$M = \begin{pmatrix} 0 & 4 & -4 \\ 0 & -4 & 0 \\ 0 & 0 & 0 \end{pmatrix}, \quad (\text{A.1.13})$$

which implements the first Weyl variation with appropriate factors of \sqrt{g} , i.e. $S\mathcal{B} = M\mathcal{D}$, where S acts like $SA = (\sqrt{g})^{-1}\delta(\sqrt{g}A)$. The terms that cannot be removed by local counterterms are given by the (right) null space of M . Generally, a null vector is a linear combination of \mathcal{D} 's, and one must choose a scheme in which one of the terms in that linear combination cannot be set to zero.

In the present case, however, the null space is just the span of \mathcal{D}_3 . Therefore, all but \mathcal{D}_3 can be removed unambiguously by adjusting the values of the coefficients c_i . In particular,

$$\delta_\omega \mathcal{W} = \delta_\omega \mathcal{W}^{(2)} + \delta_\omega \mathcal{W}_{CT} \quad (\text{A.1.14})$$

with arbitrary $c_1, c_2 = \frac{1}{4}\mathfrak{d}_2$, and $c_3 = \frac{1}{4}(\mathfrak{d}_1 + \mathfrak{d}_2)$ sets the coefficients of \mathcal{D}_1 and \mathcal{D}_2 to zero. Since WZ consistency requires that the coefficient of \mathcal{D}_3 vanishes, the scheme-independent part of the anomaly is therefore

$$\delta_\omega \mathcal{W} = \int_{\Sigma_2} \sqrt{g} (\mathfrak{b}_1 \mathcal{B}_1 + \tilde{\mathfrak{b}}_1 \tilde{\mathcal{B}}_1 + \tilde{\mathfrak{b}}_2 \tilde{\mathcal{B}}_2 + \tilde{\mathfrak{b}}_3 \tilde{\mathcal{B}}_3 + \tilde{\mathfrak{b}}_4 \tilde{\mathcal{B}}_4) \delta\omega. \quad (\text{A.1.15})$$

After appropriately relabelling the coefficients, we find eq. (3.4.38) with $q = 2$.

Appendix B

Chapter 6

B.1 4d defect Weyl anomaly basis

In this appendix, we present some details of the algorithm discussed in sections 2.5 and 3.4 applied to the case of a $p = 4$ conformal defect. For the complete workings we refer to our supplemental Mathematica notebook available from ref. [1].

B.1.1 Arbitrary co-dimension

We begin with the part of the anomaly that is admissible in any co-dimension $q \geq 2$. The $q = 1$ case is a simple adaptation of the $q \geq 2$ case.

Step 1: First, we determine the basis of terms. There are 36 scalars that transform non-trivially under Weyl transformations, and that do not have any derivatives acting on $\delta\omega$. They are

$$\begin{aligned}
 \mathcal{B}_1 &= R^2, & \mathcal{B}_2 &= R_{ab}R^{ab}, & \mathcal{B}_3 &= (N^{ij}R_{ij})^2, \\
 \mathcal{B}_4 &= W_{ab}{}^{ab}N^{ij}R_{ij}, & \mathcal{B}_5 &= RW_{ab}{}^{ab}, & \mathcal{B}_6 &= RN^{ij}R_{ij}, \\
 \mathcal{B}_7 &= R_{ab}W_c{}^{acb}, & \mathcal{B}_8 &= R_{ij}W^{iaj}{}_a, & \mathcal{B}_9 &= R_{ij}R^{ij}, \\
 \mathcal{B}_{10} &= R\Pi^i\Pi_i, & \mathcal{B}_{11} &= W_{ab}{}^{ab}\Pi^i\Pi_i, & \mathcal{B}_{12} &= N^{jk}R_{jk}\Pi^i\Pi_i, \\
 \mathcal{B}_{13} &= R\overset{\circ}{\Pi}_{ab}{}^i\overset{\circ}{\Pi}_i{}^{ab}, & \mathcal{B}_{14} &= N^{jk}R_{jk}\overset{\circ}{\Pi}_{ab}{}^i\overset{\circ}{\Pi}_i{}^{ab}, & \mathcal{B}_{15} &= R_{ij}\Pi^i\Pi^j, \\
 \mathcal{B}_{16} &= R_{ij}\overset{\circ}{\Pi}_{ab}{}^i\overset{\circ}{\Pi}{}^{abj}, & \mathcal{B}_{17} &= R^{ab}\overset{\circ}{\Pi}_{ab}{}^i\Pi_i, & \mathcal{B}_{18} &= R_a{}^b\overset{\circ}{\Pi}_b{}^c\overset{\circ}{\Pi}_{ic}{}^a, \\
 \mathcal{B}_{19} &= W^a{}_i{}^b{}_j\overset{\circ}{\Pi}_{ab}{}^i\Pi^j, & \mathcal{B}_{20} &= W^{acb}{}_c\overset{\circ}{\Pi}_{ab}{}^i\Pi_i, & \mathcal{B}_{21} &= W_{iaj}{}^a\Pi^i\Pi^j, \\
 \mathcal{B}_{22} &= W_{ic}{}^{ac}\overline{D}^b\overset{\circ}{\Pi}_{ab}{}^i, & \mathcal{B}_{23} &= W_{ic}{}^{ac}\overline{D}_a\Pi^i, & \mathcal{B}_{24} &= \Pi^i D_i R, \\
 \mathcal{B}_{25} &= \overset{\circ}{\Pi}{}^{abi}D_i W_{acb}{}^c, & \mathcal{B}_{26} &= \Pi^i D_i W_{ab}{}^{ab}, & \mathcal{B}_{27} &= D^i D_i R,
 \end{aligned} \tag{B.1.1}$$

$$\begin{aligned}
\mathcal{B}_{28} &= D^i D_i W_{ab}{}^{ab}, & \mathcal{B}_{29} &= \Pi^i \text{Tr} \hat{\Pi}_i \hat{\Pi}^j \hat{\Pi}_j, & \mathcal{B}_{30} &= \Pi^i \Pi_i \text{Tr} \hat{\Pi}^j \hat{\Pi}_j, \\
\mathcal{B}_{31} &= \Pi^i \Pi^j \text{Tr} \hat{\Pi}_i \hat{\Pi}_j, & \mathcal{B}_{32} &= (\Pi^i \Pi_i)^2, & \mathcal{B}_{33} &= \bar{D}_a \hat{\Pi}_i{}^{ab} \bar{D}_b \Pi^i, \\
\mathcal{B}_{34} &= \bar{D}_a \Pi_i \bar{D}^a \Pi^i, & \mathcal{B}_{35} &= \bar{D}_a \hat{\Pi}_{bc}{}^i \bar{D}^a \Pi_i{}^{bc}, & \mathcal{B}_{36} &= \bar{D}^b \hat{\Pi}_{ba}{}^i \bar{D}^c \Pi_c{}^i,
\end{aligned}$$

where $\bar{D}_a \hat{\Pi}_i{}^{ab} \bar{D}_b \Pi^i = N_{\mu\nu} \bar{D}_a \hat{\Pi}{}^{ab\mu} \bar{D}_b \Pi^\nu$, and similarly for the other terms of the form $(\bar{D}\Pi)^2$. There are 24 trivial Weyl invariants without derivatives on $\delta\omega$:

$$\begin{aligned}
\tilde{\mathcal{B}}_1 &= W_{abcd} W^{abcd}, & \tilde{\mathcal{B}}_2 &= (W_{ab}{}^{ab})^2, & \tilde{\mathcal{B}}_3 &= W_{abcd} W^{ab}{}_{ef} \epsilon^{cdef}, \\
\tilde{\mathcal{B}}_4 &= W_{ijcd} W^{ij}{}_{ef} \epsilon^{cdef}, & \tilde{\mathcal{B}}_5 &= W_{iajb} W^{iajb}, & \tilde{\mathcal{B}}_6 &= W_{abi}{}^b W^{aci}{}_c, \\
\tilde{\mathcal{B}}_7 &= W_{ijkl} W^{ijkl}, & \tilde{\mathcal{B}}_8 &= W_{aijk} W^{aijk}, & \tilde{\mathcal{B}}_9 &= W_{abjk} W^{abjk}, \\
\tilde{\mathcal{B}}_{10} &= W_{acb}{}^c W^{adb}{}_d, & \tilde{\mathcal{B}}_{11} &= W_{iaj}{}^a W^{ibj}{}_b, & \tilde{\mathcal{B}}_{12} &= W_{ab}{}^{ab} \hat{\Pi}_{cd}{}^i \hat{\Pi}_i{}^{cd}, \\
\tilde{\mathcal{B}}_{13} &= W_a{}^b{}_{ij} \hat{\Pi}_b{}^i \hat{\Pi}_c{}^j \hat{\Pi}_c{}^a, & \tilde{\mathcal{B}}_{14} &= W_{aibj} \hat{\Pi}{}^{ibc} \hat{\Pi}_c{}^j \hat{\Pi}_a{}^i, & \tilde{\mathcal{B}}_{15} &= W^{abcd} \hat{\Pi}_{ac}{}^i \hat{\Pi}_{bd}{}^i, \quad (\text{B.1.2}) \\
\tilde{\mathcal{B}}_{16} &= W_{ab}{}^a{}_d \hat{\Pi}_f{}^b \hat{\Pi}_i{}^d \hat{\Pi}_i{}^f, & \tilde{\mathcal{B}}_{17} &= W_{icj}{}^c \hat{\Pi}_a{}^i \hat{\Pi}_b{}^j \hat{\Pi}_a{}^i, & \tilde{\mathcal{B}}_{18} &= W^{abcd} \hat{\Pi}_a{}^e \hat{\Pi}_b{}^f \hat{\Pi}_c{}^i \epsilon_{def}, \\
\tilde{\mathcal{B}}_{19} &= \text{Tr} \hat{\Pi}^i \hat{\Pi}_i \hat{\Pi}^j \hat{\Pi}_j, & \tilde{\mathcal{B}}_{20} &= \text{Tr} \hat{\Pi}^i \hat{\Pi}^j \hat{\Pi}_i \hat{\Pi}_j, & \tilde{\mathcal{B}}_{21} &= \text{Tr} \hat{\Pi}^i \hat{\Pi}_i \text{Tr} \hat{\Pi}^j \hat{\Pi}_j, \\
\tilde{\mathcal{B}}_{22} &= \text{Tr} \hat{\Pi}^i \hat{\Pi}^j \text{Tr} \hat{\Pi}_i \hat{\Pi}_j, & \tilde{\mathcal{B}}_{23} &= \hat{\Pi}_a{}^e \hat{\Pi}_{be}{}^j \hat{\Pi}_c{}^f \hat{\Pi}_{df}{}^i \epsilon^{abcd}, & \tilde{\mathcal{B}}_{24} &= W_{ijcd} \hat{\Pi}_e{}^b \hat{\Pi}_f{}^j \epsilon^{cdef}.
\end{aligned}$$

Finally, there are 41 terms with derivatives acting on $\delta\omega$

$$\begin{aligned}
\mathcal{D}_1 &= W_{ic}{}^{ac} \hat{\Pi}_{ab}{}^i \bar{D}^b \delta\omega, & \mathcal{D}_2 &= W_{ic}{}^{ac} \Pi^i \bar{D}_a \delta\omega, & \mathcal{D}_3 &= \hat{\Pi}_{ab}{}^i R^{ab} D_i \delta\omega, \\
\mathcal{D}_4 &= \Pi^i R D_i \delta\omega, & \mathcal{D}_5 &= \Pi^i N^{jk} R_{jk} D_i \delta\omega, & \mathcal{D}_6 &= \hat{\Pi}{}^{abi} W_{acb}{}^c D_i \delta\omega, \\
\mathcal{D}_7 &= \hat{\Pi}{}^{abi} W_{iajb} D^j \delta\omega, & \mathcal{D}_8 &= \Pi^i W_{ab}{}^{ab} D_i \delta\omega, & \mathcal{D}_9 &= \Pi^i R_i{}^j D_j \delta\omega, \\
\mathcal{D}_{10} &= \Pi^i W_{iaj}{}^a D^j \delta\omega, & \mathcal{D}_{11} &= R \bar{\square} \delta\omega, & \mathcal{D}_{12} &= N^{ij} R_{ij} \bar{\square} \delta\omega, \\
\mathcal{D}_{13} &= W_{acb}{}^c \bar{D}^a \bar{D}^b \delta\omega, & \mathcal{D}_{14} &= D^i R D_i \delta\omega, & \mathcal{D}_{15} &= R D^i D_i \delta\omega, \\
\mathcal{D}_{16} &= N^{ij} R_{ij} D^k D_k \delta\omega, & \mathcal{D}_{17} &= W_{ab}{}^{ab} \bar{\square} \delta\omega, & \mathcal{D}_{18} &= W_{ab}{}^{ab} D^i D_i \delta\omega, \\
\mathcal{D}_{19} &= D^i W_{ab}{}^{ab} D_i \delta\omega, & \mathcal{D}_{20} &= W_{aci}{}^c \bar{D}^a D^i \delta\omega, & \mathcal{D}_{21} &= W_{icj}{}^c D^i D^j \delta\omega, \\
\mathcal{D}_{22} &= R^{ij} D_i D_j \delta\omega, & \mathcal{D}_{23} &= \text{Tr} \hat{\Pi}^i \hat{\Pi}_i \hat{\Pi}^j D_j \delta\omega, & \mathcal{D}_{24} &= \Pi^j \text{Tr} \hat{\Pi}^i \hat{\Pi}_i D_j \delta\omega, \quad (\text{B.1.3}) \\
\mathcal{D}_{25} &= \Pi^i \text{Tr} \hat{\Pi}_i \hat{\Pi}^j D_j \delta\omega, & \mathcal{D}_{26} &= \Pi^i \Pi_i \Pi^j D_j \delta\omega, & \mathcal{D}_{27} &= \hat{\Pi}_i{}^{ab} \bar{D}_a \Pi^i \bar{D}_b \delta\omega, \\
\mathcal{D}_{28} &= \hat{\Pi}_i{}^{ab} \Pi^i \bar{D}_a \bar{D}_b \delta\omega, & \mathcal{D}_{29} &= \Pi_i \bar{D}_a \Pi^i \bar{D}^a \delta\omega, & \mathcal{D}_{30} &= \hat{\Pi}_{ab}{}^i \hat{\Pi}_i{}^{ab} \bar{\square} \delta\omega, \\
\mathcal{D}_{31} &= \hat{\Pi}_i{}^{ab} \bar{D}^c \hat{\Pi}_{cb}{}^i \bar{D}_a \delta\omega, & \mathcal{D}_{32} &= \hat{\Pi}_i{}^{ac} \hat{\Pi}_c{}^b \bar{D}_a \bar{D}_b \delta\omega, & \mathcal{D}_{33} &= \text{Tr} \hat{\Pi}^i \hat{\Pi}^j D_i D_j \delta\omega, \\
\mathcal{D}_{34} &= \text{Tr} \hat{\Pi}^i \hat{\Pi}_i D^j D_j \delta\omega, & \mathcal{D}_{35} &= \Pi^i \Pi^j D_i D_j \delta\omega, & \mathcal{D}_{36} &= \Pi^i \Pi_i D^j D_j \delta\omega, \\
\mathcal{D}_{37} &= \Pi^i D_i D^j D_j \delta\omega, & \mathcal{D}_{38} &= \Pi^i \bar{\square} D_i \delta\omega, & \mathcal{D}_{39} &= \hat{\Pi}_{ab}{}^i \bar{D}^a \bar{D}^b D_i \delta\omega, \\
\mathcal{D}_{40} &= (D_i D^i)^2 \delta\omega, & \mathcal{D}_{41} &= \hat{\Pi}_{bf}{}^i \bar{D}_c \hat{\Pi}_{d^f}{}^i \epsilon^{abcd} \bar{D}_a \delta\omega.
\end{aligned}$$

In total, our basis is 101-dimensional. For $q = 1$ the basis is over-complete because some terms that are distinct in $q \geq 2$ may reduce to the same term in $q = 1$. Moreover some terms vanish identically when $q = 1$.

Step 2: Next, we find solutions to WZ consistency. Computing a second Weyl variation produces terms of the form $\mathcal{D}_i^{\text{WZ}} = \delta\omega_2 \mathcal{D}_i^\partial \delta\omega_1 - (1 \leftrightarrow 2)$ for $i = 1, \dots, 41$, where \mathcal{D}_i^∂ corresponds to the operator version of \mathcal{D}_i in eq. (B.1.3) with the variation parameter $\delta\omega$ omitted. In addition, there are the following terms

$$\begin{aligned} \mathcal{D}_{42}^{\text{WZ}} &= W_{aci}{}^c \bar{D}^a \delta\omega_1 D^i \delta\omega_2 - (1 \leftrightarrow 2), & \mathcal{D}_{43}^{\text{WZ}} &= \Pi^i D_i \delta\omega_1 \bar{\square} \delta\omega_2 - (1 \leftrightarrow 2), \\ \mathcal{D}_{44}^{\text{WZ}} &= \Pi^i \bar{D}_a D_i \delta\omega_1 \bar{D}^a \delta\omega_2 - (1 \leftrightarrow 2), & \mathcal{D}_{45}^{\text{WZ}} &= \overset{\circ}{\Pi}_{ab}^i D_i \delta\omega_1 \bar{D}^a \bar{D}^b \delta\omega_2 - (1 \leftrightarrow 2), \\ \mathcal{D}_{46}^{\text{WZ}} &= \overset{\circ}{\Pi}_{ab}^i \bar{D}^a D_i \delta\omega_1 \bar{D}^b \delta\omega_2 - (1 \leftrightarrow 2), & \mathcal{D}_{47}^{\text{WZ}} &= \Pi^i D_i \delta\omega_1 D^j D_j \delta\omega_2 - (1 \leftrightarrow 2), \\ \mathcal{D}_{48}^{\text{WZ}} &= \Pi^i D_j D_i \delta\omega_1 D^j \delta\omega_2 - (1 \leftrightarrow 2), & \mathcal{D}_{49}^{\text{WZ}} &= \bar{\square} \delta\omega_1 D^i D_i \delta\omega_2 - (1 \leftrightarrow 2), \\ \mathcal{D}_{50}^{\text{WZ}} &= D^i D_i \delta\omega_1 D^j D_j \delta\omega_2 - (1 \leftrightarrow 2), & \mathcal{D}_{51}^{\text{WZ}} &= D^i \delta\omega_1 D_i D^j D_j \delta\omega_2 - (1 \leftrightarrow 2). \end{aligned} \quad (\text{B.1.4})$$

The 24 $\tilde{\mathcal{B}}$'s trivially solve WZ consistency. In addition, one also finds four non-trivial linear combinations of \mathcal{B} 's. Three of them correspond to $\bar{E}_4, \mathcal{J}_1, \mathcal{J}_2$. The final one can be written as a linear combination of other invariants and $W_{iabc} W^{iabc}$. In eq. (6.1.1), we redefine our basis to include $W_{iabc} W^{iabc}$ instead of this extra conformal invariant.

Step 3: We also find 33 linear combinations of \mathcal{D} 's that naively solve WZ consistency. However, 32 of them can be rendered WZ inconsistent by a choice of scheme. One can introduce counterterms that remove at least one of the constituent terms of the linear combination such that the remainder is inconsistent. The anomaly, however, must be WZ consistent in any scheme. Thus, we must insist that the overall coefficients of these 32 linear combinations of \mathcal{D} 's must be zero in any scheme. Therefore, they are absent in the anomaly. The one remaining linear combination of \mathcal{D} 's, which just consists of the single term \mathcal{D}_{41} in eq. (B.1.3), is unaffected by local counterterms. It is related to the term in eq. (6.1.1) whose coefficient is $\tilde{d}_3^{(4d)}$. As we comment in the main body, it is a genuine anomaly coefficient.

This leaves us with 23 parity-even contributions to the trace anomaly. One of them is A-type and the remaining 22 are B-type. There are 6 terms that are parity-odd along the defect that are admissible in any co-dimension q , although 3 of them vanish identically when $q = 1$.

B.1.2 Parity-odd terms in the normal bundle when $q = 2$

In addition to the terms that are parity-odd along the defect, there are terms that break parity in the normal bundle. First, consider the co-dimension $q = 2$ case.

Step 1: The extra parity-odd terms in the normal bundle are

$$\mathcal{B}_1^{(6)} = R_i{}^j n_{jk} \Pi^i \Pi^k, \quad \mathcal{B}_2^{(6)} = R_i{}^j n_{jk} \overset{\circ}{\Pi}_{ab}^i \overset{\circ}{\Pi}{}^{abk}, \quad \mathcal{B}_3^{(6)} = R^{ab} \Pi^i \overset{\circ}{\Pi}_{ab}^j n_{ij},$$

$$\begin{aligned}
\mathcal{B}_4^{(6)} &= W_{aibj} \mathring{\Pi}^{abi} \Pi_k n^{jk}, & \mathcal{B}_5^{(6)} &= W_{aibj} \mathring{\Pi}_k^{ab} \Pi^i n^{jk}, & \mathcal{B}_6^{(6)} &= W_{ic}{}^{ac} n^{ij} \bar{D}^b \mathring{\Pi}_{abj}, \\
\mathcal{B}_7^{(6)} &= W_{ic}{}^{ac} n^{ij} \bar{D}_a \Pi_j, & \mathcal{B}_8^{(6)} &= \Pi_i n^{ij} D_j R, & \mathcal{B}_9^{(6)} &= \mathring{\Pi}^{abi} n_{ij} D^j W_{acb}{}^c, \\
\mathcal{B}_{10}^{(6)} &= \Pi^i n^{kj} D_j R_{ki}, & \mathcal{B}_{11}^{(6)} &= \Pi^i n_{ij} \text{Tr} \mathring{\Pi}^k \mathring{\Pi}_k \mathring{\Pi}^j, & \mathcal{B}_{12}^{(6)} &= \Pi^i \Pi^j n_{jk} \text{Tr} \mathring{\Pi}^k \mathring{\Pi}_i, \\
\mathcal{B}_{13}^{(6)} &= n_{ij} \bar{D}^a \Pi^i \bar{D}^b \mathring{\Pi}_{ab}^j,
\end{aligned} \tag{B.1.5}$$

and

$$\tilde{\mathcal{B}}_1^{(6)} = W_{ajbk} \mathring{\Pi}_i^{ac} \mathring{\Pi}_c{}^{bj} n^{ik}, \tag{B.1.6}$$

as well as

$$\begin{aligned}
\mathcal{D}_1^{(6)} &= W_{ic}{}^{ac} \mathring{\Pi}_{abj} n^{ij} \bar{D}^b, & \mathcal{D}_2^{(6)} &= W_{ic}{}^{ac} \Pi_j n^{ij} \bar{D}_a, & \mathcal{D}_3^{(6)} &= \mathring{\Pi}_{abj} R^{ab} n^{ij} D_i, \\
\mathcal{D}_4^{(6)} &= \Pi_i n^{ij} R D_j, & \mathcal{D}_5^{(6)} &= \mathring{\Pi}_k^{ab} n^{ik} W_{iajb} D^j, & \mathcal{D}_6^{(6)} &= \mathring{\Pi}^{abi} W_{iajb} n^{jk} D_k, \\
\mathcal{D}_7^{(6)} &= \Pi_k n^{ki} W_{iaj}{}^a D^j, & \mathcal{D}_8^{(6)} &= \Pi^i R_{ik} n^{jk} D_j, & \mathcal{D}_9^{(6)} &= n^{ki} \Pi_k R_i{}^j D_j, \\
\mathcal{D}_{10}^{(6)} &= n^{ij} D_i R D_j, & \mathcal{D}_{11}^{(6)} &= W_{aci}{}^c n^{ij} \bar{D}^a D_j, & \mathcal{D}_{12}^{(6)} &= R^{ij} n_{jk} D^k D_i, \\
\mathcal{D}_{13}^{(6)} &= n^{ij} D_j R_{ia} \bar{D}^a, & \mathcal{D}_{14}^{(6)} &= n^{jk} D_k R_{ij} D^i, & \mathcal{D}_{15}^{(6)} &= \text{Tr} \mathring{\Pi}^i \mathring{\Pi}_i \mathring{\Pi}^j n_{jk} D^k, \\
\mathcal{D}_{16}^{(6)} &= n_{jk} \Pi^j \text{Tr} \mathring{\Pi}^i \mathring{\Pi}_i D^k, & \mathcal{D}_{17}^{(6)} &= n_{jk} \Pi^i \text{Tr} \mathring{\Pi}_i \mathring{\Pi}^j D^k, & \mathcal{D}_{18}^{(6)} &= n_{jk} \Pi^i \Pi_i \Pi^j D^k, \\
\mathcal{D}_{19}^{(6)} &= n_{ij} \bar{D}^a \Pi^i \mathring{\Pi}_{ab}^j \bar{D}^b, & \mathcal{D}_{20}^{(6)} &= n_{ij} \Pi^i \mathring{\Pi}_{ab}^j \bar{D}^a \bar{D}^b, & \mathcal{D}_{21}^{(6)} &= n_{ij} \Pi^i \bar{D}_a \Pi^j \bar{D}^a, \\
\mathcal{D}_{22}^{(6)} &= n_{ij} \mathring{\Pi}_{ab}^i \bar{D}_c \mathring{\Pi}^{cbj} \bar{D}^a, & \mathcal{D}_{23}^{(6)} &= \text{Tr} \mathring{\Pi}^i \mathring{\Pi}^j n_{jk} D^k D_i, & \mathcal{D}_{24}^{(6)} &= \Pi^i \Pi^j n_{jk} D^k D_i, \\
\mathcal{D}_{25}^{(6)} &= n_{ik} \Pi^i D^k D^j D_j, & \mathcal{D}_{26}^{(6)} &= n_{ik} \Pi^i \bar{\square} D^k, & \mathcal{D}_{27}^{(6)} &= n_{ik} \mathring{\Pi}_{ab}^i \bar{D}^a \bar{D}^b D^k.
\end{aligned} \tag{B.1.7}$$

Note that the identity $n_{ij} n^{kl} = N_i^k N_j^\ell - N_j^k N_i^\ell$ is very restrictive in combination with various symmetry properties of tensors, and it sets to zero many candidate terms.

Step 2: In addition to $\mathcal{D}_i^{(6),\text{WZ}} = \delta\omega_2 \mathcal{D}_i^{(6),\partial} \delta\omega_1 - (1 \leftrightarrow 2)$ for $i = 1, \dots, 27$, the following terms are generated when computing a second Weyl variation:

$$\begin{aligned}
\mathcal{D}_{28}^{(6),\text{WZ}} &= W_{aibj} n^{ij} \bar{D}^a \delta\omega_1 \bar{D}^b \delta\omega_2 - (1 \leftrightarrow 2), & \mathcal{D}_{29}^{(6),\text{WZ}} &= W_{ai}{}^{aj} n_{kj} D^k \delta\omega_1 D^i \delta\omega_2 - (1 \leftrightarrow 2), \\
\mathcal{D}_{30}^{(6),\text{WZ}} &= W_{ac}{}^{aj} n_{ij} D^i \delta\omega_1 \bar{D}^c \delta\omega_2 - (1 \leftrightarrow 2), & \mathcal{D}_{31}^{(6),\text{WZ}} &= R n_{ij} D^i \delta\omega_1 D^j \delta\omega_2 - (1 \leftrightarrow 2), \\
\mathcal{D}_{32}^{(6),\text{WZ}} &= R_{ij} n^{kj} D^i \delta\omega_1 D_k \delta\omega_2 - (1 \leftrightarrow 2), & \mathcal{D}_{33}^{(6),\text{WZ}} &= \mathring{\Pi}_{cd}^j \mathring{\Pi}^{cdk} n_{ij} D_k \delta\omega_1 D^i \delta\omega_2 - (1 \leftrightarrow 2), \\
\mathcal{D}_{34}^{(6),\text{WZ}} &= \Pi^i \Pi^j n_{jk} D_i \delta\omega_1 D^k \delta\omega_2 - (1 \leftrightarrow 2), & \mathcal{D}_{35}^{(6),\text{WZ}} &= \mathring{\Pi}_a{}^{cj} \mathring{\Pi}_{cb}^i n_{ij} \bar{D}^a \delta\omega_2 \bar{D}^b \delta\omega_1 - (1 \leftrightarrow 2), \\
\mathcal{D}_{36}^{(6),\text{WZ}} &= \mathring{\Pi}_{ab}^j n_{ij} \bar{D}^b D^i \delta\omega_1 \bar{D}^a \delta\omega_2 - (1 \leftrightarrow 2), & \mathcal{D}_{37}^{(6),\text{WZ}} &= \mathring{\Pi}^{cdi} n_{ki} D^k \delta\omega_2 \bar{D}_d \bar{D}_c \delta\omega_1 - (1 \leftrightarrow 2), \\
\mathcal{D}_{38}^{(6),\text{WZ}} &= \Pi^i n_{ij} D^j \delta\omega_2 D^k D_k \delta\omega_1 - (1 \leftrightarrow 2), & \mathcal{D}_{39}^{(6),\text{WZ}} &= \Pi^i n_{ij} D^j \delta\omega_2 \bar{\square} \delta\omega_1 - (1 \leftrightarrow 2), \\
\mathcal{D}_{40}^{(6),\text{WZ}} &= \Pi^i n^{jk} D_k D_i \delta\omega_1 D_j \delta\omega_2 - (1 \leftrightarrow 2), & \mathcal{D}_{41}^{(6),\text{WZ}} &= \Pi^i n_{ij} \bar{D}^a D^j \delta\omega_2 \bar{D}_a \delta\omega_1 - (1 \leftrightarrow 2), \\
\mathcal{D}_{42}^{(6),\text{WZ}} &= n^{ij} D_j D^k D_k \delta\omega_1 D_i \delta\omega_2 - (1 \leftrightarrow 2), & \mathcal{D}_{43}^{(6),\text{WZ}} &= n_{ij} D^i \delta\omega_2 \bar{\square} D^j \delta\omega_1 - (1 \leftrightarrow 2), \\
\mathcal{D}_{44}^{(6),\text{WZ}} &= n^{ij} D_i D_k \delta\omega_1 D_j D^k \delta\omega_2 - (1 \leftrightarrow 2).
\end{aligned} \tag{B.1.8}$$

There are no solutions of WZ consistency involving \mathcal{B} 's. Only $\tilde{\mathcal{B}}_1^{(6)}$ and linear combinations of \mathcal{D} 's (naively) solve WZ consistency.

Step 3: All of the linear combinations of \mathcal{D} 's are scheme-dependent. There is only one genuine scheme-independent solution to WZ consistency that is parity-odd in the normal bundle: the trivial Weyl invariant $\tilde{\mathcal{B}}_1^{(6)}$ which appears in eq. (6.1.8).

B.1.3 Parity-odd terms in the normal bundle when $q = 4$

The co-dimension $q = 4$ case is more restrictive. The only new terms that one can write down are trivial Weyl invariants:

$$\begin{aligned}
 \tilde{\mathcal{B}}_1^{(8)} &= \epsilon^{abcd} n^{ijkl} W_{abij} W_{cdkl}, & \tilde{\mathcal{B}}_2^{(8)} &= n^{ijkl} W_{aibj} W_{k^\circ{}^\ell}, \\
 \tilde{\mathcal{B}}_3^{(8)} &= n^{ijkl} W_{piqj} W_{k^\circ{}^\ell}, & \tilde{\mathcal{B}}_4^{(8)} &= n^{ijkl} W_{aipj} W_{k^\circ{}^\ell}, \\
 \tilde{\mathcal{B}}_5^{(8)} &= n_{ijkl} \epsilon_{abcd} W^{abij} \mathring{\Pi}_f^{ck} \mathring{\Pi}^{fd\ell}, & \tilde{\mathcal{B}}_6^{(8)} &= n_{ijkl} W^{abij} \mathring{\Pi}_{ac}^k \mathring{\Pi}_b^{cl}.
 \end{aligned} \tag{B.1.9}$$

These trivially solve WZ consistency and cannot be removed by counterterms. They appear in eq. (6.1.9).

Appendix C

Chapter 7

C.1 Spherical defects

In this section we outline the derivation of eq. (7.1.10) for a spherical defect in \mathbb{R}^d . Our strategy will be to apply a conformal transformation on flat space \mathbb{R}^d that maps the support of the defect from the sphere S^{d-2} of radius R to the plane \mathbb{R}^{d-2} . This relates the spherical defect to the flat defect for which $J \cdot A = \alpha J^\theta$.

More concretely, let X^μ with $\mu = 1, \dots, d$ be coordinates in flat space. We take the support of the defect to lie on $X^\mu X^\nu \delta_{\mu\nu} = R^2$ and $X^2 = 0$. The following transformation maps the sphere to the flat defect

$$X^1 = R \frac{4x^\mu x^\mu - R^2}{R^2 + 4x^\mu x^\mu + 4R x^1}, \quad X^k = 4R^2 \frac{x^k}{R^2 + 4x^\mu x^\mu + 4R x^1}, \quad (\text{C.1.1})$$

with inverse

$$x^1 = \frac{R}{2} \frac{R^2 - X^\mu X^\mu}{(R - X^1)^2 + X^k X^k}, \quad x^k = R^2 \frac{X^k}{(R - X^1)^2 + X^k X^k}, \quad (\text{C.1.2})$$

where $k = 2, \dots, d$, and x^1 and x^2 are the transverse directions to the defect in the new coordinates. Under this transformation, the Jacobian factor is

$$\frac{\partial x^\mu}{\partial X^\nu} = \Omega(X) \times (\text{rotation})^\mu{}_\nu, \quad \Omega(X) = \frac{R^2}{[(R - X^1)^2 + X^k X^k]}, \quad (\text{C.1.3})$$

where we won't need the rotation part. In order to show eq. (7.1.10), we need to compute the integral on the right-hand side of eq. (7.1.7) when the defect is spherical. Namely, we need to evaluate the following integral

$$I_J \equiv \int d^d X \langle J^\mu(X) \rangle_{\text{spherical}} f_\mu(X), \quad (\text{C.1.4})$$

where the shape function $f_\mu(X)$, whose precise form we do not need, is the one of a spherical defect. Under the conformal transformation,

$$\langle J^\mu(X) \rangle_{\text{spherical}} f_\mu(X) = \langle J^\mu(x(X)) \rangle_{\text{flat}} f_\mu(x(X)) \Omega^d(X), \quad (\text{C.1.5})$$

where we used that $\Delta_J = d - 1$ and $\Delta_A = 1$. Finally, we are left with the following integral

$$I_J = a_J \int d^d X \left[\frac{2R}{\sqrt{(R^2 - X^\mu X^\mu)^2 + 4R^2(X^2)^2}} \right]^d. \quad (\text{C.1.6})$$

To perform the integration, it is convenient to employ spherical coordinates. We choose

$$X^2 = r \cos \phi_1, \quad X^1 = r \sin \phi_1 \cos \phi_2, \quad \dots \quad X^d = r \sin \phi_1 \sin \phi_2 \dots \cos \phi_{d-1}, \quad (\text{C.1.7})$$

which gives

$$\begin{aligned} I_J &= a_J \text{vol}(S^{d-2}) \int_0^{+\infty} dr \int_0^\pi d\phi_1 r^{d-1} \sin^{d-2} \phi_1 \left[\frac{2R}{\sqrt{(R^2 - r^2)^2 + 4R^2 r^2 \cos^2 \phi_1}} \right]^d \\ &= \frac{2^d \sqrt{\pi} \Gamma\left(\frac{d-1}{2}\right)}{\Gamma\left(\frac{d}{2}\right)} \text{vol}(S^{d-2}) a_J \int_0^{+\infty} dr R^d \frac{r^{d-1}}{(R^2 + r^2) |R^2 - r^2|^{d-1}}. \end{aligned} \quad (\text{C.1.8})$$

The integral over r converges in the range $0 < d < 2$ while is divergent for $d \geq 2$. We will adopt dimensional regularisation to obtain the value in our range of interest $d \geq 2$. Performing the integral is straightforward and we obtain

$$I_J = a_J \frac{2\pi^{\frac{d}{2}+1}}{\Gamma\left(\frac{d}{2}\right) \sin\left(\frac{\pi}{2}d\right)}. \quad (\text{C.1.9})$$

We note that the above result is well-defined for any value of $d > 0$ with $d \neq \text{even}$, while when d is an even number the expression has a simple pole. This pole is expected since the free energy acquires an additional divergence due to the trace anomaly. In our case this corresponds to the derivative with respect to α of the A-type defect anomaly. We can extract the coefficient of the divergence by replacing $d \rightarrow d - \varepsilon$ where now d is assumed to be a positive even integer and $0 < \varepsilon \ll 1$. Thus we find,

$$I_J = -(-1)^{d/2} a_J \frac{4\pi^{d/2}}{\Gamma\left(\frac{d}{2}\right)} \frac{1}{\varepsilon} + \mathcal{O}(\varepsilon), \quad d = \text{even}. \quad (\text{C.1.10})$$

The pole in the dimensional regularisation maps to a logarithmic divergence when the integral eq. (C.1.8) is regularised by a UV cut-off ε , i.e. $1/\varepsilon \rightarrow \log(R/\varepsilon)$. More precisely, the integral diverges at the location of the defect $r = R$, and we must divide

the integration region as follows $r \in (0, R - \epsilon) \cup (R + \epsilon, +\infty)$, where ϵ is a UV cut-off. Thus,

$$-\frac{d}{d\alpha} \log Z[\alpha] = \begin{cases} a_J \frac{2\pi^{\frac{d}{2}+1}}{\Gamma\left(\frac{d}{2}\right) \sin\left(\frac{\pi}{2}d\right)} & d \neq \text{even}, \\ -(-1)^{d/2} a_J \frac{4\pi^{d/2}}{\Gamma\left(\frac{d}{2}\right)} \log\left(\frac{R}{\epsilon}\right) & d = \text{even}. \end{cases} \quad (\text{C.1.11})$$

This straightforwardly gives the results in eqs. (7.1.8), and (7.1.9).¹

C.2 Scalar propagator

Below we study the mode expansion and the propagator of a scalar field in the presence of a non-trivial monodromy in Lorentzian signature $(-, +, \dots, +)$. In the Minkowski space-time with metric eq. (7.1.1), the EOM for φ reads

$$\frac{1}{\rho} \partial_\rho (\rho \partial_\rho \varphi) + \left[-\partial_t^2 + \frac{1}{\rho^2} (\partial_\theta - i\alpha)^2 + D_\parallel^2 \right] \varphi = 0, \quad (\text{C.2.12})$$

where D_\parallel^2 is the spatial part of the Laplacian in the direction parallel to the flux α . To find the general solution to the EOM, we use the cylindrical symmetry of the problem and write the ansatz

$$\varphi = e^{-i\omega t} e^{i\vec{k}_\parallel \cdot \vec{x}_\parallel} e^{in\theta} h(\rho). \quad (\text{C.2.13})$$

Plugging eq. (C.2.13) into eq. (C.2.12), we obtain an equation for $h(\rho)$

$$\rho^2 h'' + \rho h' + \left[(\omega^2 - \vec{k}_\parallel^2) \rho^2 - (m - \alpha)^2 \right] h = 0, \quad (\text{C.2.14})$$

whose solutions are the Bessel functions

$$h = J_{\pm(n-\alpha)}(k_\rho \rho), \quad k_\rho = \sqrt{\omega^2 - \vec{k}_\parallel^2}. \quad (\text{C.2.15})$$

While the large ρ behaviour of the functions J_β is physically reasonable for any β , their behaviour near $\rho = 0$ needs to be discussed carefully. Expanding the Bessel function near zero, one finds

$$J_\beta(\zeta) = \zeta^\beta \left(\frac{2^{-\beta}}{\Gamma(\beta+1)} - \frac{2^{-\beta-2}\zeta^2}{(\beta+1)\Gamma(\beta+1)} + \mathcal{O}(\zeta^3) \right). \quad (\text{C.2.16})$$

¹In principle one might worry about other α -dependent terms contributing to the partition function. Indeed in the presence of a bulk trace anomaly one gets a logarithmically divergent term proportional to $\int F \wedge \star F$, where F is the curvature of background gauge field eq. (7.1.6). This term, however, is quadratic in delta functions and hence doesn't contribute.

Depending on β , the function may be divergent as $\zeta \rightarrow 0$.

If one asks for regularity of the scalar field in the limit $\rho \rightarrow 0$, one must require the order of the Bessel function to be non-negative, i.e. $\pm(n - \alpha) \geq 0$. This leads to the following solution

$$\begin{aligned} \varphi = \sum_{n=-\infty}^{\infty} \int dk_{\rho} \int d^{d-3}\vec{k}_{\parallel} \left[\tilde{a}_n(k) e^{in\theta} J_{|n-\alpha|}(k_{\rho}\rho) e^{-i\omega t + i\vec{k}_{\parallel} \cdot \vec{x}_{\parallel}} \right. \\ \left. + \tilde{b}_n^*(k) e^{-in\theta} J_{|n+\alpha|}(k_{\rho}\rho) e^{i\omega t - i\vec{k}_{\parallel} \cdot \vec{x}_{\parallel}} \right], \end{aligned} \quad (\text{C.2.17})$$

where $\tilde{a}_n(k)$ and $\tilde{b}_n(k)$ are undetermined functions of $k = (\vec{k}_{\parallel}, k_{\rho})$. This choice of boundary conditions has been argued to correspond to a monodromy defect engineered by an infinitely thin and infinitely long solenoid carrying a magnetic flux α [323–325].

To quantise the theory, we impose the canonical equal-time commutation relation $[\varphi(t, x), \dot{\varphi}^{\dagger}(t, x')] = i\delta^{(d-1)}(x - x')$. After the quantisation, the coefficients $\tilde{a}_n(k)$ and $\tilde{b}_n(k)$ become operators, which are proportional to the canonical creation and annihilation operators $a_n(k)$ and $b_n(k)$ which satisfy²

$$[a_n(k), a_{n'}^{\dagger}(k')] = [b_n(k), b_{n'}^{\dagger}(k')] = \delta^{(d-3)}(\vec{k}_{\parallel} - \vec{k}'_{\parallel}) \delta(k_{\rho} - k'_{\rho}) \delta_{n, n'}. \quad (\text{C.2.18})$$

In terms of these, the correctly normalised mode expansion for φ reads

$$\begin{aligned} \varphi = \sum_{n=-\infty}^{\infty} \int dk_{\rho} \int d^{d-3}\vec{k}_{\parallel} \frac{\sqrt{k_{\rho}}}{(\sqrt{2\pi})^{d-2} \sqrt{2\omega}} \left[a_n(k) e^{in\theta} J_{|n-\alpha|}(k_{\rho}\rho) e^{-i\omega t + i\vec{k}_{\parallel} \cdot \vec{x}_{\parallel}} \right. \\ \left. + b_n^{\dagger}(k) e^{-in\theta} J_{|n+\alpha|}(k_{\rho}\rho) e^{i\omega t - i\vec{k}_{\parallel} \cdot \vec{x}_{\parallel}} \right]. \end{aligned} \quad (\text{C.2.19})$$

More generally, we can relax the assumption that the defect corresponds to a solenoid. In this case we just require that the integral of the charge density $Q \sim \int \phi \phi^{\dagger}$ is finite near $\rho \sim 0$, and one can allow for a mild singular behaviour $\varphi \sim \rho^{-1+\epsilon}$ with $\epsilon > 0$. In particular, restricting the range of α to lie in the interval $\alpha \in (0, 1)$, we can allow for the Bessel function $J_{-\alpha}$ (for the $n = 0$ mode) in addition to $J_{+\alpha}$, and $J_{\alpha-1}$ (for $n = 1$) in addition to $J_{1-\alpha}$. In the most general case there will be a specific ladder operator corresponding to each Bessel J , i.e. we will have $a_0^{(-)}, a_0^{(+)}, a_1^{(-)}, a_1^{(+)}$ and analogously for the ladder operators b . The modes with the $+$ sign correspond to the regular modes while the $-$ sign to the mildly divergent ones. The only non-trivial

²We found the following orthogonality property useful: $\int_0^{\infty} d\rho \rho J_{\alpha}(\rho v) J_{\alpha}(\rho u) = \frac{\delta(u-v)}{u}$.

commutators are

$$[a_0^{(\pm)}(k), a_0^{(\pm)\dagger}(k')] = [a_1^{(\pm)}(k), a_1^{(\pm)\dagger}(k')] = \delta^{(d-3)}(\vec{k}_{\parallel} - \vec{k}'_{\parallel}) \delta(k_{\rho} - k'_{\rho}), \quad (\text{C.2.20})$$

and similarly for the b ladder operators. In order to respect the commutation relation $[\varphi(t, x), \dot{\varphi}(t, x')] = i\delta^{(d-1)}(x - x')$, we need to introduce a specific normalisation for the modes $n = 0, 1$ described by two free parameters $\zeta, \tilde{\zeta} \in [0, 1]$ as in eq. (7.2.21). In particular, if we choose $\zeta = 0$, only the regular mode J_{α} will occur, while for $\zeta = 1$ we will have only the singular one. The same happens for the mode $n = 1$ and $\tilde{\zeta}$.

From the mode expansion eq. (C.2.19) and the modification due to the singular mode, it is straightforward to write down eq. (7.2.18).

Massless scalar propagator

From the field solution eq. (C.2.19) we can easily compute the propagator. The Euclidean two-point function can be written as

$$\begin{aligned} G_{S, \alpha, \zeta, \tilde{\zeta}}(x, x') &= \sum_{m=1}^{+\infty} e^{i(m-\alpha)(\theta-\theta')} G_S^{(m-\alpha)}(x, x') + \sum_{m=0}^{+\infty} e^{-i(m+\alpha)(\theta-\theta')} G_S^{(m+\alpha)}(x, x') \\ &+ \zeta e^{-i\alpha(\theta-\theta')} \left[G_S^{(-\alpha)}(x, x') - G_S^{(\alpha)}(x, x') \right] + \tilde{\zeta} e^{i(1-\alpha)(\theta-\theta')} \left[G_S^{(\alpha-1)}(x, x') - G_S^{(1-\alpha)}(x, x') \right], \end{aligned} \quad (\text{C.2.21})$$

where we defined

$$G_S^{(\nu)}(x, x') \equiv \int d^{d-3} \vec{k}_{\parallel} dk_{\rho} dk_{\tau} \frac{k_{\rho}}{(2\pi)^{d-1}} \frac{e^{-ik_{\tau}(\tau-\tau') + i\vec{k}_{\parallel} \cdot (\vec{x}_{\parallel} - \vec{x}'_{\parallel})}}{k_{\rho}^2 + \vec{k}_{\parallel}^2 + k_{\tau}^2} J_{\nu}(k_{\rho} \rho) J_{\nu}(k_{\rho} \rho'). \quad (\text{C.2.22})$$

By employing the identity

$$\frac{1}{\kappa^2} = \int_0^{\infty} ds e^{-\kappa^2 s}, \quad \kappa^2 > 0, \quad (\text{C.2.23})$$

and performing the Gaussian integration over \vec{k}_{\parallel} and k_{τ} , we obtain

$$\begin{aligned} G_S^{(\nu)}(x, x') &= \int_0^{+\infty} ds \int_0^{+\infty} dk_{\rho} \frac{k_{\rho}}{2^{d-1} \pi^{d/2}} \frac{1}{s^{d/2-1}} e^{-\frac{(\vec{x}_{\parallel} - \vec{x}'_{\parallel})^2 + (\tau - \tau')^2}{4s}} e^{-k_{\rho}^2 s} \\ &\times J_{\nu}(k_{\rho} \rho) J_{\nu}(k_{\rho} \rho'). \end{aligned} \quad (\text{C.2.24})$$

Now, we integrate over k_{ρ} by using the identity eq. (C.4.42), which gives

$$G_S^{(\nu)}(x, x') = \frac{1}{2^d \pi^{d/2}} \int_0^{\infty} ds s^{d/2-2} e^{-s(\rho^2 + \rho'^2 + (x_{\parallel} - x'_{\parallel})^2)/4} I_{\nu} \left(\frac{s \rho \rho'}{2} \right). \quad (\text{C.2.25})$$

This is the form of the propagator that we employ in section 7.2.2 to obtain the desired correlation functions. Further, note that the propagator is precisely in the form of eq. (4.3.20) such we can identify the heat kernel as the integrand of eq. (C.2.25) and use it to compute the EE in section 7.2.3. Nonetheless, the integral over s can be performed analytically by noting the following relation

$$I_\alpha(z) = e^{\mp i\alpha\pi/2} J_\alpha \left(z e^{\pm i\pi/2} \right). \quad (\text{C.2.26})$$

Using the identity eq. (C.4.41), the result is

$$\begin{aligned} G_S^{(\nu)}(x, x') &= \frac{\Gamma\left(\frac{d}{2} - 1 + \nu\right)}{4\pi^{d/2}\Gamma(1 + \nu)} \left(\frac{1}{\rho\rho'}\right)^{\frac{d}{2}-1} \left(\frac{\rho\rho'}{\rho^2 + \rho'^2 + (\sigma - \sigma')^2}\right)^{\frac{d}{2}-1+\nu} \\ &\times {}_2F_1\left(\frac{d-2}{4} + \frac{\nu}{2}, \frac{d-2}{4} + \frac{\nu}{2} + \frac{1}{2}; \nu + 1; \frac{4\rho^2\rho'^2}{(\rho^2 + \rho'^2 + (x_\parallel - x'_\parallel)^2)^2}\right). \end{aligned} \quad (\text{C.2.27})$$

It is straightforward to show that this reproduces exactly (up to the θ dependence) the defect blocks (7.2.25) with the coefficients c_s defined in eqs. (7.2.27), (7.2.28a) and (7.2.28b).

C.3 Fermion propagator

In this appendix we provide concrete expressions for the fermion mode expansion in $d = 4$, and explicitly compute the propagator eq. (7.3.90). We will do so by imposing that the components of the Dirac fermion obey the canonical equal-time anti-commutation relations $\{\psi_A(t, x), \psi_B^\dagger(t, x')\} = \delta^{(d-1)}(x - x')\delta_{AB}$, where $A, B = 1, \dots, 4$ are spinor indices.

It will be convenient to use the following Clifford algebra representation

$$\gamma^0 = \begin{pmatrix} i\sigma^3 & 0 \\ 0 & -i\sigma^3 \end{pmatrix}, \quad \gamma^1 = \begin{pmatrix} 0 & i\mathbb{1}_2 \\ -i\mathbb{1}_2 & 0 \end{pmatrix}, \quad \gamma^2 = \begin{pmatrix} -\sigma^2 & 0 \\ 0 & \sigma^2 \end{pmatrix}, \quad \gamma^3 = \begin{pmatrix} \sigma^1 & 0 \\ 0 & -\sigma^1 \end{pmatrix}, \quad (\text{C.3.28})$$

where $\sigma^{1,2,3}$ are the Pauli matrices and $\mathbb{1}_2$ is the 2×2 identity matrix. To solve the Dirac equation, we make the ansatz

$$\psi = e^{-i\omega t} e^{im\theta} e^{ik_\parallel x_\parallel} \begin{pmatrix} \Psi(\rho) \\ \pm\Psi(\rho) \end{pmatrix}, \quad (\text{C.3.29})$$

where Ψ is a two-component spinor with ρ -dependence only, $m \in \mathbb{Z} + \frac{1}{2}$, and $\omega, k_{\parallel} \in \mathbb{R}$.³ The Dirac equation in the basis eq. (C.3.28) reduces to two coupled first-order ordinary differential equations for the components of Ψ

$$-i(\omega \pm k_{\parallel})\Psi_2 + \left(\frac{d}{d\rho} - \frac{\nu}{\rho} \right) \Psi_1 = 0, \quad (\text{C.3.30a})$$

$$-i(\omega \mp k_{\parallel})\Psi_1 + \left(\frac{d}{d\rho} + \frac{\nu+1}{\rho} \right) \Psi_2 = 0, \quad (\text{C.3.30b})$$

where $\nu = m - \alpha - \frac{1}{2}$. These two equations can be combined into Bessel's equations for Ψ_1 and Ψ_2 , and their solutions can be written in terms of Bessel functions of the first kind, J , as follows

$$\Psi = c^1 \begin{pmatrix} J_{\nu}(\rho k_{\rho}) \\ iB_{\pm} J_{\nu+1}(\rho k_{\rho}) \end{pmatrix} + c^2 \begin{pmatrix} J_{-\nu}(\rho k_{\rho}) \\ -iB_{\pm} J_{-(\nu+1)}(\rho k_{\rho}) \end{pmatrix}, \quad (\text{C.3.31})$$

where $k_{\rho} = \sqrt{\omega^2 - k_{\parallel}^2}$, $B_{\pm} \equiv \frac{k_{\rho}}{\omega \pm k_{\parallel}}$, and $c^{1,2}$ are arbitrary integration constants. A field configuration is physically admissible if it is less divergent than ρ^{-1} as we approach the defect at $\rho = 0$. This requires setting either $c^1 = 0$ or $c^2 = 0$ for all $n \equiv m - \frac{1}{2} \in \mathbb{Z} \setminus \{0\}$. In the case of $n = 0$, both solutions are admissible. For the solution with coefficient c^1 , the first component $\Psi_1 \sim \rho^{-\alpha}$ as $\rho \rightarrow 0$, whereas Ψ_2 is regular. For the solution with coefficient c^2 , the second component $\Psi_2 \sim \rho^{-1+\alpha}$, whereas Ψ_1 is regular. Note that both solutions have one component that diverges at the defect. As shown in [324], it is the former that corresponds to an infinitely long and infinitely thin solenoid. The most general solution keeps both modes with a parameter $\zeta \in [0, 1]$ interpolating between them as in eq. (7.3.89).

Taking a linear combination, one obtains the general solution to the Dirac equation

$$\begin{aligned} \psi = & \sum_{n=-\infty}^{\infty} ' \sum_{s=1}^2 \int_{-\infty}^{\infty} \frac{dk_{\parallel}}{2\pi} \int_0^{\infty} dk_{\rho} \sqrt{\frac{k_{\rho}}{4\omega}} e^{-i\omega t} e^{+ik_{\parallel}x_{\parallel}} e^{+in\theta} e^{i\theta/2} a_n^s(k) u_{n,k}^s \\ & + \sum_{n=-\infty}^{\infty} ' \sum_{s=1}^2 \int_{-\infty}^{\infty} \frac{dk_{\parallel}}{2\pi} \int_0^{\infty} dk_{\rho} \sqrt{\frac{k_{\rho}}{4\omega}} e^{+i\omega t} e^{-ik_{\parallel}x_{\parallel}} e^{+in\theta} e^{i\theta/2} b_n^{s*}(k) v_{n,k}^s, \end{aligned} \quad (\text{C.3.32})$$

where now ω is understood to be a function of $k = (k_{\parallel}, k_{\rho})$. The spinors are

$$u_{n,k}^1 = \begin{pmatrix} C_+ J_{\zeta_n(n-\alpha)}(\rho k_{\rho}) \\ i\zeta_n C_- J_{\zeta_n(n+1-\alpha)}(\rho k_{\rho}) \\ C_+ J_{\zeta_n(n-\alpha)}(\rho k_{\rho}) \\ i\zeta_n C_- J_{\zeta_n(n+1-\alpha)}(\rho k_{\rho}) \end{pmatrix}, \quad u_{n,k}^2 = \begin{pmatrix} C_- J_{\zeta_n(n-\alpha)}(\rho k_{\rho}) \\ i\zeta_n C_+ J_{\zeta_n(n+1-\alpha)}(\rho k_{\rho}) \\ -C_- J_{\zeta_n(n-\alpha)}(\rho k_{\rho}) \\ -i\zeta_n C_+ J_{\zeta_n(n+1-\alpha)}(\rho k_{\rho}) \end{pmatrix}, \quad (\text{C.3.33})$$

³In this subsection only we will use x_{\parallel} to denote the single spatial coordinate along the defect in $d = 4$ (rather than \vec{x}_{\parallel}). Similarly, the momentum along x_{\parallel} will be denoted by k_{\parallel} (rather than \vec{k}).

and

$$v_{n,k}^1 = \begin{pmatrix} C_+ J_{\zeta_n(n-\alpha)}(\rho k_\rho) \\ -i\zeta_n C_- J_{\zeta_n(n+1-\alpha)}(\rho k_\rho) \\ C_+ J_{\zeta_n(n-\alpha)}(\rho k_\rho) \\ -i\zeta_n C_- J_{\zeta_n(n+1-\alpha)}(\rho k_\rho) \end{pmatrix}, \quad v_{n,k}^2 = \begin{pmatrix} C_- J_{\zeta_n(n-\alpha)}(\rho k_\rho) \\ -i\zeta_n C_+ J_{\zeta_n(n+1-\alpha)}(\rho k_\rho) \\ -C_- J_{\zeta_n(n-\alpha)}(\rho k_\rho) \\ i\zeta_n C_+ J_{\zeta_n(n+1-\alpha)}(\rho k_\rho) \end{pmatrix}, \quad (\text{C.3.34})$$

where $C_\pm \equiv \sqrt{\omega \pm k_\parallel}$. In the above, $\zeta_n = +1$ for $n \geq 1$ and $\zeta_n = -1$ for $n \leq -1$, and \sum' is an instruction to sum over both $n = 0$ modes. More concretely, denote the spinors with $\zeta_0 = \pm 1$ by $u_{0,k}^{(\pm)s}$ and $v_{0,k}^{(\pm)s}$, and the ladder operators by $a_0^{(\pm)s}(k)$ and $b_0^{(\pm)s*}(k)$. As in the scalar case, one can introduce a parameter $\xi \in [0, 1]$ which interpolates between the two $n = 0$ modes. Then \sum' means: sum the $\zeta_0 = +1$ mode with an extra overall factor of $\sqrt{1 - \xi}$, and the $\zeta_0 = -1$ mode with an extra factor of $\sqrt{\xi}$. Promoting $a_n^{1,2}(k)$ and $b_n^{1,2}(k)$ to operators whose non-zero anti-commutators are

$$\left\{ a_n^s(k), a_{n'}^{s'\dagger}(k') \right\} = \left\{ b_n^s(k), b_{n'}^{s'\dagger}(k') \right\} = \delta(k_\parallel - k'_\parallel) \delta(k_\rho - k'_\rho) \delta_{nn'} \delta^{ss'}, \quad (\text{C.3.35})$$

the components of the Dirac spinor then obey the canonical equal time commutation relations.

Using the explicit mode expansions, the fermion propagator

$$G_{F,\alpha,\xi}(x, x')_{AB} = \begin{cases} \langle \psi_A(t, x_\parallel, \rho, \theta) \bar{\psi}_B(t', x'_\parallel, \rho', \theta') \rangle & \text{if } t > t', \\ -\langle \bar{\psi}_B(t', x'_\parallel, \rho', \theta') \psi_A(t, x_\parallel, \rho, \theta) \rangle & \text{if } t' > t, \end{cases} \quad (\text{C.3.36})$$

can be straightforwardly computed. Assuming $t > t'$,

$$G_{F,\alpha,\xi}(x, x')_{AB} = i \sum_n' \int \frac{dk_\parallel}{2\pi} \int \frac{dk_\rho}{2\pi} \frac{k_\rho}{4\omega} e^{-i\omega(t-t')} e^{ik_\parallel(x_\parallel - x'_\parallel)} e^{in(\theta - \theta')} e^{i(\theta - \theta')/2} \left((u_{n,k}^1)_A (u_{n,k}^{1\dagger})_B \gamma^0 + (u_{n,k}^2)_A (u_{n,k}^{2\dagger})_B \right), \quad (\text{C.3.37})$$

and similarly for $t < t'$. Using the scalar mode expansion. It is straightforward to verify that

$$G_{F,\alpha,\xi}(x, x')_{AB} = -\gamma^\mu (\partial_\mu + \Omega_\mu - iA_\mu) \left(P_- \sum_n'' \mathcal{I}_{\zeta_n(n-\alpha)} e^{in(\theta - \theta')} + P_+ \sum_n'' \mathcal{I}_{\zeta_n(n+1-\alpha)} e^{in(\theta - \theta')} \right), \quad (\text{C.3.38})$$

where

$$\mathcal{I}_v = \int \frac{dk_\parallel}{2\pi} \int \frac{dk_\rho}{2\pi} \frac{k_\rho}{2\omega} J_v(\rho k_\rho) J_v(\rho' k_\rho) e^{-i\omega(t-t')} e^{ik_\parallel(x_\parallel - x'_\parallel)} e^{i(\theta - \theta')/2}, \quad (\text{C.3.39})$$

and \sum'' is an instruction to sum over both $n = 0$ modes, one with $\zeta_0 = +1$ and an

extra overall factor of $1 - \xi$, and the other with $\zeta_0 = -1$ and an extra factor of ξ . Comparing with eq. (C.2.21), one identifies

$$\sum_n'' \mathcal{I}_{\zeta_n(n-\alpha)} e^{in(\theta-\theta')} = e^{i(\theta-\theta')/2} G_{S,\alpha,1-\xi,0}(x, x'), \quad (\text{C.3.40a})$$

$$\sum_n'' \mathcal{I}_{\zeta_n(n+1-\alpha)} e^{in(\theta-\theta')} = e^{-i(\theta-\theta')/2} G_{S,\alpha,0,\xi}(x, x'), \quad (\text{C.3.40b})$$

which gives precisely eq. (7.3.90) after applying the gauge transformation eq. (7.1.3).

C.4 Useful formulae

In this appendix, we collect identities that were used in the main body of the text. The following integral identity involving a single Bessel- J function

$$\int_0^\infty ds s^{\lambda-1} e^{-ps} J_\alpha(as) = \left(\frac{a}{2p}\right)^\alpha \frac{\Gamma(\lambda+\alpha)}{p^\lambda \Gamma(\alpha+1)} {}_2F_1\left(\frac{\lambda+\alpha}{2}, \frac{\lambda+\alpha+1}{2}; \alpha+1; -\frac{a^2}{p^2}\right), \quad (\text{C.4.41})$$

which is valid for $\text{Re}(\alpha + \lambda) > 0$ and $\text{Re}(p \pm ia) > 0$ was used in the evaluation of the scalar propagator. In the same computation, we also encountered integrals involving products of $J_\alpha(as)$, which required the following integral identity

$$\int_0^\infty ds s e^{-p^2 s^2} J_\alpha(as) J_\alpha(bs) = \frac{1}{2p^2} e^{-\frac{a^2+b^2}{4p^2}} I_\alpha\left(\frac{ab}{2p}\right), \quad (\text{C.4.42})$$

where $I_\alpha(s) = e^{i\pi\alpha/2} J_\alpha(is)$ is the modified Bessel function of the first kind.

Finally, we used the following identities involving sums of Bessel functions:

$$\sum_{k=0} I_{k+\nu}(z) = \frac{1}{2(1-\nu)} \left(e^z \int_0^z dt e^{-t} I_{\nu-1}(t) - z(I_{\nu-1}(z) + I_\nu(z)) \right), \quad (\text{C.4.43})$$

and

$$\sum_{k=1}^\infty (k+\nu) I_{k+\nu}(z) = \frac{z}{2} (I_{\nu+1}(z) + I_\nu(z)). \quad (\text{C.4.44})$$

Appendix D

Chapter 8

D.1 Special functions and zeta-function regularisation

In this appendix, we give a quick overview of the special functions appearing in chapter 8 and explain how they arise from zeta-function regularisation of infinite products. For more details on some of these functions we refer to refs. [405,406].

By meromorphic continuation to the complex s -plane the Barnes multiple-zeta function $\zeta_N(t; z|a_1, \dots, a_N)$ and the multiple Gamma-function are defined

$$\zeta_N(t; z|a_1, \dots, a_N) \equiv \sum_{n_1, \dots, n_N \geq 0} (z + n_1 a_1 + \dots + n_N a_N)^{-t}, \quad (\text{D.1.1})$$

$$\Gamma_N(z|a_1, \dots, a_N) \equiv \exp(\partial_t \zeta_N(t; z|a_1, \dots, a_N)|_{t=0}). \quad (\text{D.1.2})$$

The cases of particular interest to us are $N = 1, 2$, which include the single $\zeta_1(t; z|a)$ and double zeta-function $\zeta_2(t; z|a, b)$. In particular, we will need their values at $s = 0$

$$\begin{aligned} \zeta_1(0; z|a) &= \frac{1}{2} - \frac{z}{a}, \\ \zeta_2(0; z|a, b) &= \frac{1}{4} + \frac{1}{12} \left(\frac{a}{b} + \frac{b}{a} \right) - \frac{z}{2} \left(\frac{1}{a} + \frac{1}{b} \right) + \frac{z^2}{2ab}. \end{aligned} \quad (\text{D.1.3})$$

From the definition above, the single Gamma-function $\Gamma_1(z|a)$ is related to the ordinary Euler Gamma-function $\Gamma(z)$ via

$$\Gamma_1(z|a^{-1}) = \frac{a^{\frac{1}{2}-az}}{\sqrt{2\pi}} \Gamma(az). \quad (\text{D.1.4})$$

Further, the double Gamma-function is used in defining the special function

$$Y(z|a, b) \equiv \frac{1}{\Gamma_2(z|a, b) \Gamma_2(a + b - z|a, b)}, \quad (\text{D.1.5})$$

which frequently appears in Liouville/Toda theory. This Upsilon-function obeys

$$Y(z + b|a, b) = \gamma_1(z|a)Y(z|a, b), \quad (\text{D.1.6})$$

where

$$\gamma_1(z|a) \equiv \frac{\Gamma_1(z|a)}{\Gamma_1(a - z|a)}, \quad (\text{D.1.7})$$

and a similar relation for the shift $Y(z + a|a, b)$ replacing $a \rightarrow b$. This can be recast in the more familiar form

$$Y(z + b|a, b) = a^{2z/a-1} \gamma(z/a)Y(z|a, b), \quad (\text{D.1.8})$$

where

$$\gamma(z) \equiv \frac{\Gamma(z)}{\Gamma(1 - z)}. \quad (\text{D.1.9})$$

The special functions above appear in the evaluation of 1-loop determinants in section 8.2. One usually encounters infinite products that diverge and require regularisation. As explained in section 4.3, zeta-function regularisation instructs us to replace a diverging product

$$\prod_{k=0}^{\infty} \lambda_k \rightarrow \exp(-\partial_t \mathfrak{Z}(t)|_{t=0}), \quad (\text{D.1.10})$$

where $\mathfrak{Z}(t)$ is the associated zeta-function defined as the meromorphic continuation to the complex t -plane of the series

$$\sum_{k=0}^{\infty} \lambda_k^{-t}. \quad (\text{D.1.11})$$

For divergent products of the form

$$\prod_{k=0}^{\infty} \left(\frac{k}{r} + z \right), \quad (\text{D.1.12})$$

the associated zeta function is $\zeta_1(t; z|r^{-1})$, and hence zeta-function regularisation gives

$$\prod_{k=0}^{\infty} \left(\frac{k}{r} + z \right) \rightarrow \frac{1}{\Gamma_1(z|r^{-1})} = \frac{\sqrt{2\pi} r^{rz-\frac{1}{2}}}{\Gamma(rz)}. \quad (\text{D.1.13})$$

Most importantly for our analysis, we need to understand the behaviour of the multiple Gamma-function appearing in 1-loop determinants under a constant Weyl rescaling. Generically,

$$\Gamma_N \left(\frac{z}{r} \middle| \frac{a_1}{r}, \dots, \frac{a_N}{r} \right) = r^{\zeta_N(0|z|a_1, \dots, a_N)} \Gamma_N(z|a_1, \dots, a_N). \quad (\text{D.1.14})$$

For $N = 1$ this reduces to

$$\Gamma_1 \left(\frac{z}{r} \middle| \frac{a}{r} \right) = r^{\frac{1}{2} - \frac{z}{a}} \Gamma_1(z|a), \quad (\text{D.1.15})$$

such that

$$\gamma_1 \left(\frac{z}{r} \middle| \frac{a}{r} \right) = r^{1 - \frac{2z}{a}} \gamma_1(z|a). \quad (\text{D.1.16})$$

For $N = 2$ one finds

$$\Upsilon \left(\frac{z}{r} \middle| \frac{a}{r}, \frac{b}{r} \right) = r^{-2\zeta_2(0; z|a, b)} \Upsilon(z|a, b). \quad (\text{D.1.17})$$

References

- [1] A. Chalabi, C. P. Herzog, A. O’Bannon, B. Robinson and J. Sisti, *Weyl anomalies of four dimensional conformal boundaries and defects*, *JHEP* **02** (2022) 166, [2111.14713].
- [2] L. Bianchi, A. Chalabi, V. Procházka, B. Robinson and J. Sisti, *Monodromy defects in free field theories*, *JHEP* **08** (2021) 013, [2104.01220].
- [3] A. Chalabi, A. O’Bannon, B. Robinson and J. Sisti, *Central charges of 2d superconformal defects*, *JHEP* **05** (2020) 095, [2003.02857].
- [4] A. Chalabi, S. P. Kumar, A. O’Bannon, A. Pribytok, R. Rodgers and J. Sisti, *Holographic entanglement entropy of the Coulomb branch*, *JHEP* **04** (2021) 153, [2012.05188].
- [5] A. Chalabi, C. P. Herzog, K. Ray, B. Robinson, J. Sisti and A. Stergiou, *Boundaries in Free Higher Derivative Conformal Field Theories*, 2211.14335.
- [6] E. Fradkin, *Field Theories of Condensed Matter Physics*. Cambridge University Press, 2 ed., 2013, 10.1017/CBO9781139015509.
- [7] E. Witten, *Quantum Field Theory and the Jones Polynomial*, *Commun. Math. Phys.* **121** (1989) 351–399.
- [8] E. Witten, *Supersymmetry and Morse theory*, *J. Diff. Geom.* **17** (1982) 661–692.
- [9] M. F. Atiyah, *Topological quantum field theory*, *Publications Mathématiques de l’IHÉS* **68** (1988) 175–186.
- [10] G. B. Segal, *The Definition of Conformal Field Theory*, pp. 165–171. Springer Netherlands, 1988. 10.1007/978-94-015-7809-7.
- [11] S. K. Donaldson, *An application of gauge theory to four-dimensional topology*, *J. Diff. Geom.* **18** (1983) 279–315.
- [12] A. Floer, *An instanton-invariant for 3-manifolds*, *Communications in Mathematical Physics* **118** (1988) 215–240.
- [13] E. Witten, *Topological Quantum Field Theory*, *Commun. Math. Phys.* **117** (1988) 353.

- [14] E. Witten, *Monopoles and four manifolds*, *Math. Res. Lett.* **1** (1994) 769–796, [hep-th/9411102].
- [15] V. G. Drinfel'd, *Quantum groups*, *Journal of Soviet Mathematics* **41** (1988) 898–915.
- [16] R. E. Borcherds, *Monstrous moonshine and monstrous lie superalgebras*, *Inventiones mathematicae* **109** (1992) 405–444.
- [17] A. Kapustin and E. Witten, *Electric-Magnetic Duality And The Geometric Langlands Program*, *Commun. Num. Theor. Phys.* **1** (2007) 1–236, [hep-th/0604151].
- [18] S. Durr et al., *Ab-Initio Determination of Light Hadron Masses*, *Science* **322** (2008) 1224–1227, [0906.3599].
- [19] N. Seiberg and E. Witten, *Electric - magnetic duality, monopole condensation, and confinement in $N=2$ supersymmetric Yang-Mills theory*, *Nucl. Phys. B* **426** (1994) 19–52, [hep-th/9407087].
- [20] N. Seiberg and E. Witten, *Monopoles, duality and chiral symmetry breaking in $N=2$ supersymmetric QCD*, *Nucl. Phys. B* **431** (1994) 484–550, [hep-th/9408099].
- [21] K. Hori, S. Katz, A. Klemm, R. Pandharipande, R. Thomas, C. Vafa et al., *Mirror symmetry*, vol. 1 of *Clay mathematics monographs*. AMS, Providence, USA, 2003.
- [22] N. A. Nekrasov, *Seiberg-Witten prepotential from instanton counting*, *Adv. Theor. Math. Phys.* **7** (2003) 831–864, [hep-th/0206161].
- [23] V. Pestun, *Localization of gauge theory on a four-sphere and supersymmetric Wilson loops*, *Commun. Math. Phys.* **313** (2012) 71–129, [0712.2824].
- [24] V. Pestun et al., *Localization techniques in quantum field theories*, *J. Phys. A* **50** (2017) 440301, [1608.02952].
- [25] J. L. Cardy, *Operator Content of Two-Dimensional Conformally Invariant Theories*, *Nucl. Phys. B* **270** (1986) 186–204.
- [26] I. Affleck, *Universal Term in the Free Energy at a Critical Point and the Conformal Anomaly*, *Phys. Rev. Lett.* **56** (1986) 746–748.
- [27] C. Holzhey, F. Larsen and F. Wilczek, *Geometric and renormalized entropy in conformal field theory*, *Nucl. Phys.* **B424** (1994) 443–467, [hep-th/9403108].
- [28] P. Calabrese and J. L. Cardy, *Entanglement entropy and quantum field theory*, *J. Stat. Mech.* **0406** (2004) P06002, [hep-th/0405152].
- [29] S. N. Solodukhin, *Entanglement entropy, conformal invariance and extrinsic geometry*, *Phys. Lett. B* **665** (2008) 305–309, [0802.3117].

- [30] D. V. Fursaev, A. Patrushev and S. N. Solodukhin, *Distributional Geometry of Squashed Cones*, *Phys. Rev. D* **88** (2013) 044054, [1306.4000].
- [31] A. B. Zamolodchikov, *Irreversibility of the Flux of the Renormalization Group in a 2D Field Theory*, *JETP Lett.* **43** (1986) 730–732.
- [32] A. Cappelli, D. Friedan and J. I. Latorre, *C-theorem and spectral representation*, *Nucl. Phys.* **B352** (1991) 616–670.
- [33] H. Casini and M. Huerta, *A Finite entanglement entropy and the c-theorem*, *Phys. Lett.* **B600** (2004) 142–150, [hep-th/0405111].
- [34] Z. Komargodski, *The Constraints of Conformal Symmetry on RG Flows*, *JHEP* **07** (2012) 069, [1112.4538].
- [35] J. L. Cardy, *Is There a c-Theorem in Four-Dimensions?*, *Phys. Lett. B* **215** (1988) 749–752.
- [36] H. Osborn, *Derivation of a Four-dimensional c-Theorem*, *Phys. Lett.* **B222** (1989) 97–102.
- [37] I. Jack and H. Osborn, *Analogues for the c Theorem for Four-dimensional Renormalizable Field Theories*, *Nucl. Phys. B* **343** (1990) 647–688.
- [38] H. Osborn, *Weyl consistency conditions and a local renormalization group equation for general renormalizable field theories*, *Nucl. Phys.* **B363** (1991) 486–526.
- [39] Z. Komargodski and A. Schwimmer, *On Renormalization Group Flows in Four Dimensions*, *JHEP* **12** (2011) 099, [1107.3987].
- [40] H. Casini, E. Testé and G. Torroba, *Markov Property of the Conformal Field Theory Vacuum and the a-Theorem*, *Phys. Rev. Lett.* **118** (2017) 261602, [1704.01870].
- [41] K. G. Wilson, *The renormalization group: Critical phenomena and the kondo problem*, *Rev. Mod. Phys.* **47** (Oct, 1975) 773–840.
- [42] M. R. Douglas, *Spaces of Quantum Field Theories*, *J. Phys. Conf. Ser.* **462** (2013) 012011, [1005.2779].
- [43] O. Aharony, N. Seiberg and Y. Tachikawa, *Reading between the lines of four-dimensional gauge theories*, *JHEP* **08** (2013) 115, [1305.0318].
- [44] S. Gukov and A. Kapustin, *Topological Quantum Field Theory, Nonlocal Operators, and Gapped Phases of Gauge Theories*, 1307.4793.
- [45] S. Gukov, *Surface Operators*, in *New Dualities of Supersymmetric Gauge Theories* (J. Teschner, ed.), pp. 223–259. 2016. 1412.7127. DOI.

- [46] N. Andrei et al., *Boundary and Defect CFT: Open Problems and Applications*, *J. Phys. A* **53** (2020) 453002, [1810.05697].
- [47] D. V. Fursaev, *Quantum Entanglement on Boundaries*, *JHEP* **07** (2013) 119, [1305.2334].
- [48] D. V. Fursaev and S. N. Solodukhin, *Anomalies, entropy and boundaries*, *Phys. Rev. D* **93** (2016) 084021, [1601.06418].
- [49] N. Kobayashi, T. Nishioka, Y. Sato and K. Watanabe, *Towards a C-theorem in defect CFT*, *JHEP* **01** (2019) 039, [1810.06995].
- [50] K. Jensen, A. O'Bannon, B. Robinson and R. Rodgers, *From the Weyl Anomaly to Entropy of Two-Dimensional Boundaries and Defects*, *Phys. Rev. Lett.* **122** (2019) 241602, [1812.08745].
- [51] C. P. Herzog, K.-W. Huang and K. Jensen, *Universal Entanglement and Boundary Geometry in Conformal Field Theory*, *JHEP* **01** (2016) 162, [1510.00021].
- [52] C. Herzog, K.-W. Huang and K. Jensen, *Displacement Operators and Constraints on Boundary Central Charges*, *Phys. Rev. Lett.* **120** (2018) 021601, [1709.07431].
- [53] C. P. Herzog and K.-W. Huang, *Boundary Conformal Field Theory and a Boundary Central Charge*, *JHEP* **10** (2017) 189, [1707.06224].
- [54] V. Prochazka, *The Conformal Anomaly in bcFT from Momentum Space Perspective*, *JHEP* **10** (2018) 170, [1804.01974].
- [55] K. Jensen and A. O'Bannon, *Constraint on Defect and Boundary Renormalization Group Flows*, *Phys. Rev. Lett.* **116** (2016) 091601, [1509.02160].
- [56] H. Casini, I. Salazar Landea and G. Torroba, *Irreversibility in quantum field theories with boundaries*, *JHEP* **04** (2019) 166, [1812.08183].
- [57] Y. Wang, *Defect a-Theorem and a-Maximization*, 2101.12648.
- [58] J. J. Heckman and T. Rudelius, *Top Down Approach to 6D SCFTs*, *J. Phys. A* **52** (2019) 093001, [1805.06467].
- [59] J. J. Heckman, D. R. Morrison and C. Vafa, *On the Classification of 6D SCFTs and Generalized ADE Orbifolds*, *JHEP* **05** (2014) 028, [1312.5746].
- [60] D. Gaiotto and A. Tomasiello, *Holography for (1,0) theories in six dimensions*, *JHEP* **12** (2014) 003, [1404.0711].
- [61] M. Del Zotto, J. J. Heckman, A. Tomasiello and C. Vafa, *6d Conformal Matter*, *JHEP* **02** (2015) 054, [1407.6359].

- [62] J. J. Heckman, *More on the Matter of 6D SCFTs*, *Phys. Lett. B* **747** (2015) 73–75, [1408.0006].
- [63] M. Del Zotto, J. J. Heckman, D. R. Morrison and D. S. Park, *6D SCFTs and Gravity*, *JHEP* **06** (2015) 158, [1412.6526].
- [64] J. J. Heckman, D. R. Morrison, T. Rudelius and C. Vafa, *Atomic Classification of 6D SCFTs*, *Fortsch. Phys.* **63** (2015) 468–530, [1502.05405].
- [65] L. Bhardwaj, *Classification of 6d $\mathcal{N} = (1, 0)$ gauge theories*, *JHEP* **11** (2015) 002, [1502.06594].
- [66] P. Liendo, L. Rastelli and B. C. van Rees, *The Bootstrap Program for Boundary CFT_d*, *JHEP* **07** (2013) 113, [1210.4258].
- [67] M. Billó, M. Caselle, D. Gaiotto, F. Gliozzi, M. Meineri and R. Pellegrini, *Line defects in the 3d Ising model*, *JHEP* **07** (2013) 055, [1304.4110].
- [68] D. Gaiotto, D. Mazac and M. F. Paulos, *Bootstrapping the 3d Ising twist defect*, *JHEP* **03** (2014) 100, [1310.5078].
- [69] A. Söderberg, *Anomalous Dimensions in the WF O(N) Model with a Monodromy Line Defect*, *JHEP* **03** (2018) 058, [1706.02414].
- [70] J. M. Maldacena, *The Large N limit of superconformal field theories and supergravity*, *Adv. Theor. Math. Phys.* **2** (1998) 231–252, [hep-th/9711200].
- [71] D. E. Berenstein, R. Corrado, W. Fischler and J. M. Maldacena, *The Operator product expansion for Wilson loops and surfaces in the large N limit*, *Phys. Rev. D* **59** (1999) 105023, [hep-th/9809188].
- [72] C. R. Graham and E. Witten, *Conformal anomaly of submanifold observables in AdS / CFT correspondence*, *Nucl. Phys. B* **546** (1999) 52–64, [hep-th/9901021].
- [73] J. Estes, D. Krym, A. O’Bannon, B. Robinson and R. Rodgers, *Wilson Surface Central Charge from Holographic Entanglement Entropy*, *JHEP* **05** (2019) 032, [1812.00923].
- [74] P. Di Francesco, P. Mathieu and D. Senechal, *Conformal Field Theory*. Graduate Texts in Contemporary Physics. Springer-Verlag, New York, 1997, 10.1007/978-1-4612-2256-9.
- [75] S. Rychkov, *EPFL Lectures on Conformal Field Theory in D ≥ 3 Dimensions*. SpringerBriefs in Physics. 1, 2016, 10.1007/978-3-319-43626-5.
- [76] M. Ammon and J. Erdmenger, *Gauge/gravity duality: Foundations and applications*. No. ISBN: 9781107010345. 2015.

- [77] D. Simmons-Duffin, *The Conformal Bootstrap*, in *Theoretical Advanced Study Institute in Elementary Particle Physics: New Frontiers in Fields and Strings*, pp. 1–74, 2017, 1602.07982, DOI.
- [78] D. Simmons-Duffin, *Phys 229ab Advanced Mathematical Methods: Conformal Field Theory*. 2020.
- [79] H. Osborn, *Lectures on Conformal Field Theories in more than two dimensions*. 2019.
- [80] Z. Komargodski, “Lecture notes.” Available at https://higgs.ph.ed.ac.uk/media/workshop/48/resource/Zohar_Komargodsky_Lectures_0.pdf.
- [81] J. Penedones, *TASI lectures on AdS/CFT*, in *Theoretical Advanced Study Institute in Elementary Particle Physics: New Frontiers in Fields and Strings*, pp. 75–136, 2017, 1608.04948, DOI.
- [82] K. Osterwalder and R. Schrader, *Axioms for euclidean green’s functions*, *Communications in Mathematical Physics* **31** (1973) 83–112.
- [83] P. Kravchuk, J. Qiao and S. Rychkov, *Distributions in CFT. Part II. Minkowski space*, *JHEP* **08** (2021) 094, [2104.02090].
- [84] J. Polchinski, *String theory. Vol. 1: An introduction to the bosonic string*. Cambridge Monographs on Mathematical Physics. Cambridge University Press, 12, 2007, 10.1017/CBO9780511816079.
- [85] D. Pappadopulo, S. Rychkov, J. Espin and R. Rattazzi, *OPE Convergence in Conformal Field Theory*, *Phys. Rev. D* **86** (2012) 105043, [1208.6449].
- [86] D. Poland, S. Rychkov and A. Vichi, *The Conformal Bootstrap: Theory, Numerical Techniques, and Applications*, *Rev. Mod. Phys.* **91** (2019) 015002, [1805.04405].
- [87] T. Hartman, D. Mazac, D. Simmons-Duffin and A. Zhiboedov, *Snowmass White Paper: The Analytic Conformal Bootstrap*, in *2022 Snowmass Summer Study, 2*, 2022, 2202.11012.
- [88] R. Bertlmann, *Anomalies in Quantum Field Theory*. International series of monographs on physics. Clarendon Press, 1996.
- [89] D. Tong, “Gauge theory.” Available at <https://www.damtp.cam.ac.uk/user/tong/gaugetheory/gt.pdf>, 2018.
- [90] D. M. Capper and M. J. Duff, *Trace anomalies in dimensional regularization*, *Nuovo Cim. A* **23** (1974) 173–183.
- [91] S. Deser, M. J. Duff and C. J. Isham, *Nonlocal Conformal Anomalies*, *Nucl. Phys. B* **111** (1976) 45–55.

- [92] T. Nishioka, *Entanglement entropy: holography and renormalization group*, *Rev. Mod. Phys.* **90** (2018) 035007, [1801.10352].
- [93] J. Wess and B. Zumino, *Consequences of anomalous Ward identities*, *Phys. Lett. B* **37** (1971) 95–97.
- [94] M. Probst, *New Supersymmetric Defects in Three and Six Dimensions*, Ph.D. thesis, London, UK, 2021.
- [95] L. Bonora, P. Pasti and M. Bregola, *WEYL COCYCLES*, *Class. Quant. Grav.* **3** (1986) 635.
- [96] S. Deser and A. Schwimmer, *Geometric classification of conformal anomalies in arbitrary dimensions*, *Phys. Lett. B* **309** (1993) 279–284, [hep-th/9302047].
- [97] M. Henningson and K. Skenderis, *Weyl anomaly for Wilson surfaces*, *JHEP* **06** (1999) 012, [hep-th/9905163].
- [98] A. Schwimmer and S. Theisen, *Entanglement Entropy, Trace Anomalies and Holography*, *Nucl. Phys. B* **801** (2008) 1–24, [0802.1017].
- [99] A. Bzowski, P. McFadden and K. Skenderis, *Renormalised 3-point functions of stress tensors and conserved currents in CFT*, *JHEP* **11** (2018) 153, [1711.09105].
- [100] S. Deser, *Conformal anomalies: Recent progress*, *Helv. Phys. Acta* **69** (1996) 570–581, [hep-th/9609138].
- [101] J. Erdmenger and H. Osborn, *Conserved currents and the energy momentum tensor in conformally invariant theories for general dimensions*, *Nucl. Phys. B* **483** (1997) 431–474, [hep-th/9605009].
- [102] A. M. Polyakov, *Quantum Geometry of Bosonic Strings*, *Phys. Lett. B* **103** (1981) 207–210.
- [103] J. Polchinski, *Scale and Conformal Invariance in Quantum Field Theory*, *Nucl. Phys. B* **303** (1988) 226–236.
- [104] Y. Nakayama, *Scale invariance vs conformal invariance*, *Phys. Rept.* **569** (2015) 1–93, [1302.0884].
- [105] V. Riva and J. L. Cardy, *Scale and conformal invariance in field theory: A Physical counterexample*, *Phys. Lett. B* **622** (2005) 339–342, [hep-th/0504197].
- [106] D. Anselmi, D. Z. Freedman, M. T. Grisaru and A. A. Johansen, *Nonperturbative formulas for central functions of supersymmetric gauge theories*, *Nucl. Phys. B* **526** (1998) 543–571, [hep-th/9708042].
- [107] H. Osborn and A. C. Petkou, *Implications of conformal invariance in field theories for general dimensions*, *Annals Phys.* **231** (1994) 311–362, [hep-th/9307010].

- [108] D. M. Hofman and J. Maldacena, *Conformal collider physics: Energy and charge correlations*, *JHEP* **05** (2008) 012, [0803.1467].
- [109] D. M. Hofman, D. Li, D. Meltzer, D. Poland and F. Rejon-Barrera, *A Proof of the Conformal Collider Bounds*, *JHEP* **06** (2016) 111, [1603.03771].
- [110] L. Bonora, S. Giaccari and B. Lima de Souza, *Trace anomalies in chiral theories revisited*, *JHEP* **07** (2014) 117, [1403.2606].
- [111] L. Bonora, A. D. Pereira and B. Lima de Souza, *Regularization of energy-momentum tensor correlators and parity-odd terms*, *JHEP* **06** (2015) 024, [1503.03326].
- [112] L. Bonora and B. Lima de Souza, *Pure contact term correlators in CFT*, *Bled Workshops Phys.* **16** (2015) 22–34, [1511.06635].
- [113] F. Bastianelli and R. Martelli, *On the trace anomaly of a Weyl fermion*, *JHEP* **11** (2016) 178, [1610.02304].
- [114] L. Bonora, M. Cvitan, P. Dominis Prester, A. Duarte Pereira, S. Giaccari and T. Štemberga, *Axial gravity, massless fermions and trace anomalies*, *Eur. Phys. J. C* **77** (2017) 511, [1703.10473].
- [115] Y. Nakayama, *Realization of impossible anomalies*, *Phys. Rev. D* **98** (2018) 085002, [1804.02940].
- [116] L. Bonora, M. Cvitan, P. Dominis Prester, S. Giaccari, M. Paulišić and T. Štemberga, *Axial gravity: a non-perturbative approach to split anomalies*, *Eur. Phys. J. C* **78** (2018) 652, [1807.01249].
- [117] F. Bastianelli and M. Broccoli, *On the trace anomaly of a Weyl fermion in a gauge background*, *Eur. Phys. J. C* **79** (2019) 292, [1808.03489].
- [118] M. B. Fröb and J. Zahn, *Trace anomaly for chiral fermions via Hadamard subtraction*, *JHEP* **10** (2019) 223, [1904.10982].
- [119] L. Bonora and R. Soldati, *On the trace anomaly for Weyl fermions*, 1909.11991.
- [120] F. Bastianelli and M. Broccoli, *Axial gravity and anomalies of fermions*, *Eur. Phys. J. C* **80** (2020) 276, [1911.02271].
- [121] K. Nakagawa and Y. Nakayama, *CP-violating super Weyl anomaly*, *Phys. Rev. D* **101** (2020) 105013, [2002.01128].
- [122] S. Abdallah, S. A. Franchino-Viñas and M. B. Fröb, *Trace anomaly for Weyl fermions using the Breitenlohner-Maison scheme for γ_** , *JHEP* **03** (2021) 271, [2101.11382].

- [123] F. Bastianelli, S. Frolov and A. A. Tseytlin, *Conformal anomaly of (2,0) tensor multiplet in six-dimensions and AdS / CFT correspondence*, *JHEP* **02** (2000) 013, [[hep-th/0001041](#)].
- [124] F. Bastianelli, S. Frolov and A. A. Tseytlin, *Three point correlators of stress tensors in maximally supersymmetric conformal theories in $D = 3$ and $D = 6$* , *Nucl. Phys. B* **578** (2000) 139–152, [[hep-th/9911135](#)].
- [125] H. Elvang, D. Z. Freedman, L.-Y. Hung, M. Kiermaier, R. C. Myers and S. Theisen, *On renormalization group flows and the a-theorem in 6d*, *JHEP* **10** (2012) 011, [[1205.3994](#)].
- [126] B. Grinstein, D. Stone, A. Stergiou and M. Zhong, *Challenge to the a-Theorem in Six Dimensions*, *Phys. Rev. Lett.* **113** (2014) 231602, [[1406.3626](#)].
- [127] J. J. Heckman and T. Rudelius, *Evidence for C-theorems in 6D SCFTs*, *JHEP* **09** (2015) 218, [[1506.06753](#)].
- [128] J. A. Gracey, I. Jack and C. Poole, *The a-function in six dimensions*, *JHEP* **01** (2016) 174, [[1507.02174](#)].
- [129] A. Stergiou, D. Stone and L. G. Vitale, *Constraints on Perturbative RG Flows in Six Dimensions*, *JHEP* **08** (2016) 010, [[1604.01782](#)].
- [130] J. J. Heckman, S. Kundu and H. Y. Zhang, *Effective field theory of 6D SUSY RG Flows*, *Phys. Rev. D* **104** (2021) 085017, [[2103.13395](#)].
- [131] L.-Y. Hung, R. C. Myers and M. Smolkin, *On Holographic Entanglement Entropy and Higher Curvature Gravity*, *JHEP* **04** (2011) 025, [[1101.5813](#)].
- [132] B. R. Safdi, *Exact and Numerical Results on Entanglement Entropy in (5+1)-Dimensional CFT*, *JHEP* **12** (2012) 005, [[1206.5025](#)].
- [133] A. Petkou and K. Skenderis, *A Nonrenormalization theorem for conformal anomalies*, *Nucl. Phys. B* **561** (1999) 100–116, [[hep-th/9906030](#)].
- [134] A. Bzowski, P. McFadden and K. Skenderis, *Scalar 3-point functions in CFT: renormalisation, beta functions and anomalies*, *JHEP* **03** (2016) 066, [[1510.08442](#)].
- [135] A. Bzowski, P. McFadden and K. Skenderis, *Renormalised CFT 3-point functions of scalars, currents and stress tensors*, *JHEP* **11** (2018) 159, [[1805.12100](#)].
- [136] A. Bzowski, P. McFadden and K. Skenderis, *A handbook of holographic 4-point functions*, [2207.02872](#).
- [137] R. C. Myers and A. Sinha, *Seeing a c-theorem with holography*, *Phys. Rev. D* **82** (2010) 046006, [[1006.1263](#)].

- [138] I. R. Klebanov, S. S. Pufu and B. R. Safdi, *F-Theorem without Supersymmetry*, *JHEP* **10** (2011) 038, [1105.4598].
- [139] D. L. Jafferis, I. R. Klebanov, S. S. Pufu and B. R. Safdi, *Towards the F-Theorem: N=2 Field Theories on the Three-Sphere*, *JHEP* **06** (2011) 102, [1103.1181].
- [140] H. Casini and M. Huerta, *On the RG running of the entanglement entropy of a circle*, *Phys. Rev.* **D85** (2012) 125016, [1202.5650].
- [141] S. Giombi and I. R. Klebanov, *Interpolating between a and F*, *JHEP* **03** (2015) 117, [1409.1937].
- [142] J. L. Cardy, *Conformal Invariance and Surface Critical Behavior*, *Nucl. Phys.* **B240** (1984) 514–532.
- [143] J. L. Cardy, *Boundary Conditions, Fusion Rules and the Verlinde Formula*, *Nucl. Phys.* **B324** (1989) 581–596.
- [144] J. L. Cardy and D. C. Lewellen, *Bulk and boundary operators in conformal field theory*, *Phys. Lett. B* **259** (1991) 274–278.
- [145] D. McAvity and H. Osborn, *Energy momentum tensor in conformal field theories near a boundary*, *Nucl. Phys. B* **406** (1993) 655–680, [hep-th/9302068].
- [146] D. M. McAvity and H. Osborn, *Conformal field theories near a boundary in general dimensions*, *Nucl. Phys.* **B455** (1995) 522–576, [cond-mat/9505127].
- [147] M. Billò, V. Gonçalves, E. Lauria and M. Meineri, *Defects in conformal field theory*, *JHEP* **04** (2016) 091, [1601.02883].
- [148] E. Lauria, M. Meineri and E. Trevisani, *Spinning operators and defects in conformal field theory*, *JHEP* **08** (2019) 066, [1807.02522].
- [149] N. B. Agmon and Y. Wang, *Classifying Superconformal Defects in Diverse Dimensions Part I: Superconformal Lines*, 2009.06650.
- [150] E. Lauria, M. Meineri and E. Trevisani, *Radial coordinates for defect CFTs*, *JHEP* **11** (2018) 148, [1712.07668].
- [151] F. Gliozzi, P. Liendo, M. Meineri and A. Rago, *Boundary and Interface CFTs from the Conformal Bootstrap*, *JHEP* **05** (2015) 036, [1502.07217].
- [152] P. Liendo, Y. Linke and V. Schomerus, *A Lorentzian inversion formula for defect CFT*, *JHEP* **08** (2020) 163, [1903.05222].
- [153] A. Kapustin, *Wilson-'t Hooft operators in four-dimensional gauge theories and S-duality*, *Phys. Rev. D* **74** (2006) 025005, [hep-th/0501015].

- [154] D. Gaiotto, A. Kapustin, N. Seiberg and B. Willett, *Generalized Global Symmetries*, *JHEP* **02** (2015) 172, [1412.5148].
- [155] E. Lauria, P. Liendo, B. C. Van Rees and X. Zhao, *Line and surface defects for the free scalar field*, *JHEP* **01** (2021) 060, [2005.02413].
- [156] T. Nishioka and Y. Sato, *Free energy and defect C-theorem in free scalar theory*, 2101.02399.
- [157] C. P. Herzog and A. Shrestha, *Conformal Surface Defects in Maxwell Theory are Trivial*, 2202.09180.
- [158] A. Gustavsson, *On the Weyl anomaly of Wilson surfaces*, *JHEP* **12** (2003) 059, [hep-th/0310037].
- [159] V. Asnin, *Analyticity Properties of Graham-Witten Anomalies*, *Class. Quant. Grav.* **25** (2008) 145013, [0801.1469].
- [160] M. Cvitan, P. Dominis Prester, S. Pallua, I. Smolić and T. Štemberga, *Parity-odd surface anomalies and correlation functions on conical defects*, 1503.06196.
- [161] A. Faraji Astaneh and S. N. Solodukhin, *Boundary conformal invariants and the conformal anomaly in five dimensions*, *Phys. Lett. B* **816** (2021) 136282, [2102.07661].
- [162] A. Lewkowycz and E. Perlmutter, *Universality in the geometric dependence of Rényi entropy*, *JHEP* **01** (2015) 080, [1407.8171].
- [163] L. Bianchi, M. Meineri, R. C. Myers and M. Smolkin, *Rényi entropy and conformal defects*, *JHEP* **07** (2016) 076, [1511.06713].
- [164] T. Faulkner, R. G. Leigh, O. Parrikar and H. Wang, *Modular Hamiltonians for Deformed Half-Spaces and the Averaged Null Energy Condition*, *JHEP* **09** (2016) 038, [1605.08072].
- [165] T. Hartman, S. Kundu and A. Tajdini, *Averaged Null Energy Condition from Causality*, *JHEP* **07** (2017) 066, [1610.05308].
- [166] P. Kravchuk and D. Simmons-Duffin, *Light-ray operators in conformal field theory*, *JHEP* **11** (2018) 102, [1805.00098].
- [167] C. P. Herzog and I. Shamir, *On Marginal Operators in Boundary Conformal Field Theory*, *JHEP* **10** (2019) 088, [1906.11281].
- [168] C. P. Herzog and I. Shamir, *How a-type anomalies can depend on marginal couplings*, *Phys. Rev. Lett.* **124** (2020) 011601, [1907.04952].
- [169] L. Bianchi, *Marginal deformations and defect anomalies*, *Phys. Rev. D* **100** (2019) 126018, [1907.06193].

- [170] M. Nozaki, T. Takayanagi and T. Ugajin, *Central Charges for BCFTs and Holography*, *JHEP* **06** (2012) 066, [1205.1573].
- [171] J. S. Dowker and J. P. Schofield, *Conformal Transformations and the Effective Action in the Presence of Boundaries*, *J. Math. Phys.* **31** (1990) 808.
- [172] D. Fursaev, *Conformal anomalies of CFT's with boundaries*, *JHEP* **12** (2015) 112, [1510.01427].
- [173] S. N. Solodukhin, *Boundary terms of conformal anomaly*, *Phys. Lett. B* **752** (2016) 131–134, [1510.04566].
- [174] J. Melmed, *Conformal Invariance and the Regularized One Loop Effective Action*, *J. Phys. A* **21** (1988) L1131–L1134.
- [175] I. G. Moss, *Boundary Terms in the Heat Kernel Expansion*, *Class. Quant. Grav.* **6** (1989) 759.
- [176] P. Calabrese and J. Cardy, *Entanglement entropy and conformal field theory*, *J. Phys. A* **42** (2009) 504005, [0905.4013].
- [177] H. Casini and M. Huerta, *Lectures on entanglement in quantum field theory*, 2201.13310.
- [178] E. Witten, *APS Medal for Exceptional Achievement in Research: Invited article on entanglement properties of quantum field theory*, *Rev. Mod. Phys.* **90** (2018) 045003, [1803.04993].
- [179] D. Vassilevich, *Heat kernel expansion: User's manual*, *Phys. Rept.* **388** (2003) 279–360, [hep-th/0306138].
- [180] M. Mariño, *Instantons and Large N: An Introduction to Non-Perturbative Methods in Quantum Field Theory*. Cambridge University Press, 9, 2015.
- [181] C. Berthiere and S. N. Solodukhin, *Boundary effects in entanglement entropy*, *Nucl. Phys.* **B910** (2016) 823–841, [1604.07571].
- [182] D. V. Fursaev, *Spectral geometry and one-loop divergences on manifolds with conical singularities*, *Physics Letters B* **334** (1994) 53–60.
- [183] M. Srednicki, *Entropy and area*, *Phys. Rev. Lett.* **71** (1993) 666–669, [hep-th/9303048].
- [184] C. G. Callan, Jr. and F. Wilczek, *On geometric entropy*, *Phys. Lett. B* **333** (1994) 55–61, [hep-th/9401072].
- [185] H. Casini, M. Huerta and R. C. Myers, *Towards a derivation of holographic entanglement entropy*, *JHEP* **05** (2011) 036, [1102.0440].

- [186] I. Affleck and A. W. W. Ludwig, *Universal noninteger 'ground state degeneracy' in critical quantum systems*, *Phys. Rev. Lett.* **67** (1991) 161–164.
- [187] D. Friedan and A. Konechny, *On the boundary entropy of one-dimensional quantum systems at low temperature*, *Phys. Rev. Lett.* **93** (2004) 030402, [[hep-th/0312197](#)].
- [188] H. Casini, I. S. Landea and G. Torroba, *The g-theorem and quantum information theory*, *JHEP* **10** (2016) 140, [[1607.00390](#)].
- [189] I. Affleck and A. W. W. Ludwig, *Exact critical theory of the two impurity Kondo model*, *Phys. Rev. Lett.* **68** (1992) 1046–1049.
- [190] E. Wong and I. Affleck, *Tunneling in quantum wires: A Boundary conformal field theory approach*, *Nucl. Phys. B* **417** (1994) 403–438, [[cond-mat/9311040](#)].
- [191] A. Lewkowycz and J. Maldacena, *Exact results for the entanglement entropy and the energy radiated by a quark*, *JHEP* **05** (2014) 025, [[1312.5682](#)].
- [192] G. Cuomo, Z. Komargodski and A. Raviv-Moshe, *Renormalization Group Flows on Line Defects*, [2108.01117](#).
- [193] R. Rodgers, *Holographic entanglement entropy from probe M-theory branes*, *JHEP* **03** (2019) 092, [[1811.12375](#)].
- [194] D. Gaiotto, *Boundary F-maximization*, [1403.8052](#).
- [195] M. Bertolini, *Lectures on supersymmetry*, .
- [196] P. C. Argyres, “An Introduction to Global Supersymmetry.” Available at <https://homepages.uc.edu/~argyrepc/cu661-gr-SUSY/susy2001.pdf>.
- [197] M. J. Strassler, *An Unorthodox introduction to supersymmetric gauge theory*, in *Theoretical Advanced Study Institute in Elementary Particle Physics (TASI 2001): Strings, Branes and EXTRA Dimensions*, pp. 561–638, 9, 2003, [hep-th/0309149](#), DOI.
- [198] C. Wetterich, *Spinors in euclidean field theory, complex structures and discrete symmetries*, *Nucl. Phys. B* **852** (2011) 174–234, [[1002.3556](#)].
- [199] M. Stone, *Gamma matrices, Majorana fermions, and discrete symmetries in Minkowski and Euclidean signature*, *J. Phys. A* **55** (2022) 205401, [[2009.00518](#)].
- [200] E. Witten, *Phases of N=2 theories in two-dimensions*, *Nucl. Phys. B* **403** (1993) 159–222, [[hep-th/9301042](#)].
- [201] N. Seiberg, *Naturalness versus supersymmetric nonrenormalization theorems*, *Phys. Lett. B* **318** (1993) 469–475, [[hep-ph/9309335](#)].

- [202] V. A. Novikov, M. A. Shifman, A. I. Vainshtein and V. I. Zakharov, *Exact Gell-Mann-Low Function of Supersymmetric Yang-Mills Theories from Instanton Calculus*, *Nucl. Phys. B* **229** (1983) 381–393.
- [203] V. A. Novikov, M. A. Shifman, A. I. Vainshtein and V. I. Zakharov, *The beta function in supersymmetric gauge theories. Instantons versus traditional approach*, *Phys. Lett. B* **166** (1986) 329–333.
- [204] Y. Tachikawa, *N=2 supersymmetric dynamics for pedestrians*. 12, 2013, 10.1007/978-3-319-08822-8.
- [205] S. Cremonesi, *An Introduction to Localisation and Supersymmetry in Curved Space*, *PoS Modave2013* (2013) 002.
- [206] F. Benini and S. Cremonesi, *Partition Functions of $\mathcal{N} = (2, 2)$ Gauge Theories on S^2 and Vortices*, *Commun. Math. Phys.* **334** (2015) 1483–1527, [1206.2356].
- [207] N. Doroud, J. Gomis, B. Le Floch and S. Lee, *Exact Results in D=2 Supersymmetric Gauge Theories*, *JHEP* **05** (2013) 093, [1206.2606].
- [208] L. Eberhardt, *Superconformal symmetry and representations*, *J. Phys. A* **54** (2021) 063002, [2006.13280].
- [209] W. Nahm, *Supersymmetries and their Representations*, *Nucl. Phys. B* **135** (1978) 149.
- [210] E. Witten, *Some comments on string dynamics*, in *STRINGS 95: Future Perspectives in String Theory*, pp. 501–523, 7, 1995, hep-th/9507121.
- [211] A. Strominger, *Open p-branes*, *Phys. Lett.* **B383** (1996) 44–47, [hep-th/9512059].
- [212] N. Seiberg, *Nontrivial fixed points of the renormalization group in six-dimensions*, *Phys. Lett. B* **390** (1997) 169–171, [hep-th/9609161].
- [213] O. Aharony, A. Hanany and B. Kol, *Webs of (p,q) five-branes, five-dimensional field theories and grid diagrams*, *JHEP* **01** (1998) 002, [hep-th/9710116].
- [214] N. Seiberg, *Five-dimensional SUSY field theories, nontrivial fixed points and string dynamics*, *Phys. Lett. B* **388** (1996) 753–760, [hep-th/9608111].
- [215] K. A. Intriligator, D. R. Morrison and N. Seiberg, *Five-dimensional supersymmetric gauge theories and degenerations of Calabi-Yau spaces*, *Nucl. Phys. B* **497** (1997) 56–100, [hep-th/9702198].
- [216] P. Jefferson, S. Katz, H.-C. Kim and C. Vafa, *On Geometric Classification of 5d SCFTs*, *JHEP* **04** (2018) 103, [1801.04036].
- [217] D. Gaiotto, *N=2 dualities*, *JHEP* **08** (2012) 034, [0904.2715].

- [218] O. Aharony, O. Bergman, D. L. Jafferis and J. Maldacena, *N=6 superconformal Chern-Simons-matter theories, M2-branes and their gravity duals*, *JHEP* **10** (2008) 091, [[0806.1218](#)].
- [219] T. Dimofte, D. Gaiotto and S. Gukov, *Gauge Theories Labelled by Three-Manifolds*, *Commun. Math. Phys.* **325** (2014) 367–419, [[1108.4389](#)].
- [220] F. A. Dolan and H. Osborn, *Superconformal symmetry, correlation functions and the operator product expansion*, *Nucl. Phys. B* **629** (2002) 3–73, [[hep-th/0112251](#)].
- [221] F. A. Dolan and H. Osborn, *On short and semi-short representations for four-dimensional superconformal symmetry*, *Annals Phys.* **307** (2003) 41–89, [[hep-th/0209056](#)].
- [222] C. Cordova, T. T. Dumitrescu and K. Intriligator, *Multiplets of Superconformal Symmetry in Diverse Dimensions*, *JHEP* **03** (2019) 163, [[1612.00809](#)].
- [223] C. Romelsberger, *Counting chiral primaries in $N = 1$, $d=4$ superconformal field theories*, *Nucl. Phys. B* **747** (2006) 329–353, [[hep-th/0510060](#)].
- [224] J. Kinney, J. M. Maldacena, S. Minwalla and S. Raju, *An Index for 4 dimensional super conformal theories*, *Commun. Math. Phys.* **275** (2007) 209–254, [[hep-th/0510251](#)].
- [225] J. Bhattacharya, S. Bhattacharyya, S. Minwalla and S. Raju, *Indices for Superconformal Field Theories in 3,5 and 6 Dimensions*, *JHEP* **02** (2008) 064, [[0801.1435](#)].
- [226] E. Witten, *Constraints on Supersymmetry Breaking*, *Nucl. Phys. B* **202** (1982) 253.
- [227] B. Assel, D. Cassani and D. Martelli, *Localization on Hopf surfaces*, *JHEP* **08** (2014) 123, [[1405.5144](#)].
- [228] L. Di Pietro and Z. Komargodski, *Cardy formulae for SUSY theories in $d = 4$ and $d = 6$* , *JHEP* **12** (2014) 031, [[1407.6061](#)].
- [229] N. Bobev, M. Bullimore and H.-C. Kim, *Supersymmetric Casimir Energy and the Anomaly Polynomial*, *JHEP* **09** (2015) 142, [[1507.08553](#)].
- [230] B. Assel, D. Cassani, L. Di Pietro, Z. Komargodski, J. Lorenzen and D. Martelli, *The Casimir Energy in Curved Space and its Supersymmetric Counterpart*, *JHEP* **07** (2015) 043, [[1503.05537](#)].
- [231] X.-G. Wen, *Classifying gauge anomalies through symmetry-protected trivial orders and classifying gravitational anomalies through topological orders*, *Phys. Rev. D* **88** (2013) 045013, [[1303.1803](#)].
- [232] A. Kapustin, *Symmetry Protected Topological Phases, Anomalies, and Cobordisms: Beyond Group Cohomology*, [1403.1467](#).

- [233] A. Kapustin and R. Thorngren, *Anomalies of discrete symmetries in various dimensions and group cohomology*, 1404.3230.
- [234] C.-M. Chang, Y.-H. Lin, S.-H. Shao, Y. Wang and X. Yin, *Topological Defect Lines and Renormalization Group Flows in Two Dimensions*, *JHEP* **01** (2019) 026, [1802.04445].
- [235] C. Córdova, T. T. Dumitrescu and K. Intriligator, *Exploring 2-Group Global Symmetries*, *JHEP* **02** (2019) 184, [1802.04790].
- [236] F. Benini, C. Córdova and P.-S. Hsin, *On 2-Group Global Symmetries and their Anomalies*, *JHEP* **03** (2019) 118, [1803.09336].
- [237] M. Nakahara, *Geometry, topology and physics*. 2003.
- [238] A. Bilal, *Lectures on Anomalies*, 0802.0634.
- [239] N. Boulanger, *General solutions of the Wess-Zumino consistency condition for the Weyl anomalies*, *JHEP* **07** (2007) 069, [0704.2472].
- [240] N. Boulanger, *Algebraic Classification of Weyl Anomalies in Arbitrary Dimensions*, *Phys. Rev. Lett.* **98** (2007) 261302, [0706.0340].
- [241] S. L. Adler, *Axial vector vertex in spinor electrodynamics*, *Phys. Rev.* **177** (1969) 2426–2438.
- [242] J. S. Bell and R. Jackiw, *A PCAC puzzle: $\pi^0 \rightarrow \gamma\gamma$ in the σ model*, *Nuovo Cim. A* **60** (1969) 47–61.
- [243] G. 't Hooft, *Naturalness, chiral symmetry, and spontaneous chiral symmetry breaking*, *NATO Sci. Ser. B* **59** (1980) 135–157.
- [244] F. Benini and N. Bobev, *Exact two-dimensional superconformal R-symmetry and c-extremization*, *Phys. Rev. Lett.* **110** (2013) 061601, [1211.4030].
- [245] F. Benini and N. Bobev, *Two-dimensional SCFTs from wrapped branes and c-extremization*, *JHEP* **06** (2013) 005, [1302.4451].
- [246] E. D'Hoker and D. Z. Freedman, *Supersymmetric gauge theories and the AdS / CFT correspondence*, in *Theoretical Advanced Study Institute in Elementary Particle Physics (TASI 2001): Strings, Branes and EXTRA Dimensions*, pp. 3–158, 1, 2002, hep-th/0201253.
- [247] M. Aghand, G. Arias-Tamargo, A. Mininno, H.-Y. Sun, Z. Sun, Y. Wang et al., *The Hitchhiker's Guide to 4d $\mathcal{N} = 2$ Superconformal Field Theories*, 12, 2021, 2112.14764, DOI.
- [248] M. Beccaria and A. A. Tseytlin, *Conformal anomaly c-coefficients of superconformal 6d theories*, *JHEP* **01** (2016) 001, [1510.02685].

- [249] C. Córdova, T. T. Dumitrescu and K. Intriligator, $\mathcal{N} = (1, 0)$ anomaly multiplet relations in six dimensions, *JHEP* **07** (2020) 065, [1912.13475].
- [250] C. Cordova, T. T. Dumitrescu and X. Yin, Higher Derivative Terms, Toroidal Compactification, and Weyl Anomalies in Six-Dimensional (2,0) Theories, 1505.03850.
- [251] C. Cordova, T. T. Dumitrescu and K. Intriligator, Anomalies, renormalization group flows, and the a -theorem in six-dimensional (1, 0) theories, *JHEP* **10** (2016) 080, [1506.03807].
- [252] K. A. Intriligator and B. Wecht, The Exact superconformal R symmetry maximizes a , *Nucl. Phys. B* **667** (2003) 183–200, [hep-th/0304128].
- [253] A. D. Shapere and Y. Tachikawa, Central charges of $N=2$ superconformal field theories in four dimensions, *JHEP* **09** (2008) 109, [0804.1957].
- [254] D. L. Jafferis, The Exact Superconformal R-Symmetry Extremizes Z , *JHEP* **05** (2012) 159, [1012.3210].
- [255] C. Closset, L. Di Pietro and H. Kim, 't Hooft anomalies and the holomorphy of supersymmetric partition functions, *JHEP* **08** (2019) 035, [1905.05722].
- [256] C. Beem, M. Lemos, P. Liendo, W. Peelaers, L. Rastelli and B. C. van Rees, Infinite Chiral Symmetry in Four Dimensions, *Commun. Math. Phys.* **336** (2015) 1359–1433, [1312.5344].
- [257] C. Beem, W. Peelaers, L. Rastelli and B. C. van Rees, Chiral algebras of class S, *JHEP* **05** (2015) 020, [1408.6522].
- [258] C. Beem, L. Rastelli and B. C. van Rees, \mathcal{W} symmetry in six dimensions, *JHEP* **05** (2015) 017, [1404.1079].
- [259] A. Gadde, L. Rastelli, S. S. Razamat and W. Yan, Gauge Theories and Macdonald Polynomials, *Commun. Math. Phys.* **319** (2013) 147–193, [1110.3740].
- [260] A. Gadde, Lectures on the Superconformal Index, *J. Phys. A* **55** (2022) 063001, [2006.13630].
- [261] M. Lemos, Lectures on chiral algebras of $\mathcal{N} \geq 2$ superconformal field theories, 2006.13892.
- [262] D. Gaiotto and X. Yin, Notes on superconformal Chern-Simons-Matter theories, *JHEP* **08** (2007) 056, [0704.3740].
- [263] N. Drukker, J. Plefka and D. Young, Wilson loops in 3-dimensional $N=6$ supersymmetric Chern-Simons Theory and their string theory duals, *JHEP* **11** (2008) 019, [0809.2787].

- [264] B. Chen and J.-B. Wu, *Supersymmetric Wilson Loops in $N=6$ Super Chern-Simons-matter theory*, *Nucl. Phys. B* **825** (2010) 38–51, [0809.2863].
- [265] S.-J. Rey, T. Suyama and S. Yamaguchi, *Wilson Loops in Superconformal Chern-Simons Theory and Fundamental Strings in Anti-de Sitter Supergravity Dual*, *JHEP* **03** (2009) 127, [0809.3786].
- [266] N. Drukker and D. Trancanelli, *A Supermatrix model for $N=6$ super Chern-Simons-matter theory*, *JHEP* **02** (2010) 058, [0912.3006].
- [267] N. Drukker, M. Tenser and D. Trancanelli, *Notes on hyperloops in $\mathcal{N} = 4$ Chern-Simons-matter theories*, *JHEP* **07** (2021) 159, [2012.07096].
- [268] N. Drukker, Z. Kong, M. Probst, M. Tenser and D. Trancanelli, *Conformal and non-conformal hyperloop deformations of the 1/2 BPS circle*, 2206.07390.
- [269] N. Drukker et al., *Roadmap on Wilson loops in 3d Chern–Simons-matter theories*, *J. Phys. A* **53** (2020) 173001, [1910.00588].
- [270] J. M. Maldacena, *Wilson loops in large N field theories*, *Phys. Rev. Lett.* **80** (1998) 4859–4862, [hep-th/9803002].
- [271] K. Zarembo, *Supersymmetric Wilson loops*, *Nucl. Phys. B* **643** (2002) 157–171, [hep-th/0205160].
- [272] J. Gomis, T. Okuda and D. Trancanelli, *Quantum 't Hooft operators and S -duality in $N=4$ super Yang-Mills*, *Adv. Theor. Math. Phys.* **13** (2009) 1941–1981, [0904.4486].
- [273] D. Correa, J. Henn, J. Maldacena and A. Sever, *An exact formula for the radiation of a moving quark in $N=4$ super Yang Mills*, *JHEP* **06** (2012) 048, [1202.4455].
- [274] B. Fiol, E. Gerchkovitz and Z. Komargodski, *Exact Bremsstrahlung Function in $N = 2$ Superconformal Field Theories*, *Phys. Rev. Lett.* **116** (2016) 081601, [1510.01332].
- [275] D. Gaiotto, G. W. Moore and A. Neitzke, *Framed BPS States*, *Adv. Theor. Math. Phys.* **17** (2013) 241–397, [1006.0146].
- [276] C. Córdova and A. Neitzke, *Line Defects, Tropicalization, and Multi-Centered Quiver Quantum Mechanics*, *JHEP* **09** (2014) 099, [1308.6829].
- [277] C. Cordova, D. Gaiotto and S.-H. Shao, *Infrared Computations of Defect Schur Indices*, *JHEP* **11** (2016) 106, [1606.08429].
- [278] P. Liendo, C. Meneghelli and V. Mitev, *Bootstrapping the half-BPS line defect*, *JHEP* **10** (2018) 077, [1806.01862].
- [279] A. Gimenez-Grau and P. Liendo, *Bootstrapping line defects in $\mathcal{N} = 2$ theories*, *JHEP* **03** (2020) 121, [1907.04345].

- [280] L. Bianchi, G. Bliard, V. Forini, L. Griguolo and D. Seminara, *Analytic bootstrap and Witten diagrams for the ABJM Wilson line as defect CFT₁*, *JHEP* **08** (2020) 143, [2004.07849].
- [281] J. Barrat, P. Liendo, G. Peveri and J. Plefka, *Multipoint correlators on the supersymmetric Wilson line defect CFT*, 2112.10780.
- [282] A. Cavaglià, N. Gromov, J. Julius and M. Preti, *Integrability and conformal bootstrap: One dimensional defect conformal field theory*, *Phys. Rev. D* **105** (2022) L021902, [2107.08510].
- [283] J. Polchinski and J. Sully, *Wilson Loop Renormalization Group Flows*, *JHEP* **10** (2011) 059, [1104.5077].
- [284] M. Beccaria, S. Giombi and A. Tseytlin, *Non-supersymmetric Wilson loop in $\mathcal{N} = 4$ SYM and defect 1d CFT*, *JHEP* **03** (2018) 131, [1712.06874].
- [285] A. Kapustin, B. Willett and I. Yaakov, *Exact Results for Wilson Loops in Superconformal Chern-Simons Theories with Matter*, *JHEP* **03** (2010) 089, [0909.4559].
- [286] L. Bianchi, M. Lemos and M. Meineri, *Line Defects and Radiation in $\mathcal{N} = 2$ Conformal Theories*, *Phys. Rev. Lett.* **121** (2018) 141601, [1805.04111].
- [287] Y. Wang, *Surface Defect, Anomalies and b-Extremization*, 2012.06574.
- [288] L. Bianchi and M. Lemos, *Superconformal surfaces in four dimensions*, *JHEP* **06** (2020) 056, [1911.05082].
- [289] N. Drukker, M. Probst and M. Trépanier, *Defect CFT techniques in the 6d $\mathcal{N} = (2, 0)$ theory*, *JHEP* **03** (2021) 261, [2009.10732].
- [290] C. Cordova, D. Gaiotto and S.-H. Shao, *Surface Defects and Chiral Algebras*, *JHEP* **05** (2017) 140, [1704.01955].
- [291] T. Dimofte, D. Gaiotto and N. M. Paquette, *Dual boundary conditions in 3d SCFT's*, *JHEP* **05** (2018) 060, [1712.07654].
- [292] M. Bullimore, S. Crew and D. Zhang, *Boundaries, Vermas, and Factorisation*, *JHEP* **04** (2021) 263, [2010.09741].
- [293] S. Gukov and E. Witten, *Gauge Theory, Ramification, And The Geometric Langlands Program*, hep-th/0612073.
- [294] J. Gomis and S. Matsuura, *Bubbling surface operators and S-duality*, *JHEP* **06** (2007) 025, [0704.1657].
- [295] N. Drukker, J. Gomis and S. Matsuura, *Probing $\mathcal{N}=4$ SYM With Surface Operators*, *JHEP* **10** (2008) 048, [0805.4199].

- [296] L. F. Alday, D. Gaiotto, S. Gukov, Y. Tachikawa and H. Verlinde, *Loop and surface operators in $N=2$ gauge theory and Liouville modular geometry*, *JHEP* **01** (2010) 113, [0909.0945].
- [297] D. Gaiotto, *Surface Operators in $N = 2$ 4d Gauge Theories*, *JHEP* **11** (2012) 090, [0911.1316].
- [298] J. Gomis and B. Le Floch, *M2-brane surface operators and gauge theory dualities in Toda*, *JHEP* **04** (2016) 183, [1407.1852].
- [299] N. Drukker, I. Shamir and C. Vergu, *Defect multiplets of $\mathcal{N} = 1$ supersymmetry in 4d*, *JHEP* **01** (2018) 034, [1711.03455].
- [300] S. S. Razamat, *Flavored surface defects in 4d $\mathcal{N} = 1$ SCFTs*, *Lett. Math. Phys.* **109** (2019) 1377–1395, [1808.09509].
- [301] N. Drukker, M. Probst and M. Trépanier, *Surface operators in the 6d $N = (2, 0)$ theory*, *J. Phys. A* **53** (2020) 365401, [2003.12372].
- [302] C. P. Herzog, K.-W. Huang, I. Shamir and J. Virrueta, *Superconformal Models for Graphene and Boundary Central Charges*, *JHEP* **09** (2018) 161, [1807.01700].
- [303] D. Gaiotto and E. Witten, *Janus Configurations, Chern-Simons Couplings, And The theta-Angle in $N=4$ Super Yang-Mills Theory*, *JHEP* **06** (2010) 097, [0804.2907].
- [304] D. Gaiotto and E. Witten, *Supersymmetric Boundary Conditions in $N=4$ Super Yang-Mills Theory*, *J. Statist. Phys.* **135** (2009) 789–855, [0804.2902].
- [305] D. Gaiotto and E. Witten, *S-Duality of Boundary Conditions In $N=4$ Super Yang-Mills Theory*, *Adv. Theor. Math. Phys.* **13** (2009) 721–896, [0807.3720].
- [306] M. de Leeuw, C. Kristjansen and K. Zarembo, *One-point Functions in Defect CFT and Integrability*, *JHEP* **08** (2015) 098, [1506.06958].
- [307] T. Gombor and Z. Bajnok, *Boundary states, overlaps, nesting and bootstrapping $AdS/dCFT$* , *JHEP* **10** (2020) 123, [2004.11329].
- [308] S. Komatsu and Y. Wang, *Non-perturbative defect one-point functions in planar $\mathcal{N} = 4$ super-Yang-Mills*, *Nucl. Phys. B* **958** (2020) 115120, [2004.09514].
- [309] C. Kristjansen, D.-L. Vu and K. Zarembo, *Integrable domain walls in ABJM theory*, *JHEP* **02** (2022) 070, [2112.10438].
- [310] O. Chacaltana, J. Distler and Y. Tachikawa, *Nilpotent orbits and codimension-two defects of 6d $N=(2,0)$ theories*, *Int. J. Mod. Phys. A* **28** (2013) 1340006, [1203.2930].
- [311] M. Bullimore and H.-C. Kim, *The Superconformal Index of the $(2,0)$ Theory with Defects*, *JHEP* **05** (2015) 048, [1412.3872].

- [312] A. Faraji Astaneh and S. N. Solodukhin, *Boundary conformal invariants and the conformal anomaly in five dimensions*, *Phys. Lett. B* **816** (2021) 136282, [2102.07661].
- [313] J. M. Martin-Garcia, “xAct, Efficient Tensor Computer Algebra for Mathematica.” <http://www.xact.es>, 2004.
- [314] T. P. Branson and B. Ørsted, *Explicit functional determinants in four dimensions*, *Proceedings of the American Mathematical Society* **113** (1991) 669–682.
- [315] D. Deutsch and P. Candelas, *Boundary effects in quantum field theory*, *Phys. Rev. D* **20** (Dec, 1979) 3063–3080.
- [316] R.-X. Miao and C.-S. Chu, *Universality for Shape Dependence of Casimir Effects from Weyl Anomaly*, *JHEP* **03** (2018) 046, [1706.09652].
- [317] L. Alvarez-Gaume, D. Z. Freedman and S. Mukhi, *The Background Field Method and the Ultraviolet Structure of the Supersymmetric Nonlinear Sigma Model*, *Annals Phys.* **134** (1981) 85.
- [318] A. Faraji Astaneh, C. Berthiere, D. Fursaev and S. N. Solodukhin, *Holographic calculation of entanglement entropy in the presence of boundaries*, *Phys. Rev. D* **95** (2017) 106013, [1703.04186].
- [319] L. F. Alday, D. Gaiotto and Y. Tachikawa, *Liouville Correlation Functions from Four-dimensional Gauge Theories*, *Lett. Math. Phys.* **91** (2010) 167–197, [0906.3219].
- [320] D. Gaiotto and H.-C. Kim, *Surface defects and instanton partition functions*, *JHEP* **10** (2016) 012, [1412.2781].
- [321] M. Gutperle and C. F. Uhlemann, *Surface defects in holographic 5d SCFTs*, *JHEP* **04** (2021) 134, [2012.14547].
- [322] S. Giombi, E. Helfenberger, Z. Ji and H. Khanchandani, *Monodromy Defects from Hyperbolic Space*, 2102.11815.
- [323] Y. Aharonov and D. Bohm, *Significance of electromagnetic potentials in the quantum theory*, *Phys. Rev.* **115** (Aug, 1959) 485–491.
- [324] M. Alford, J. March-Russell and F. Wilczek, *Enhanced baryon number violation due to cosmic strings*, *Nuclear Physics B* **328** (1989) 140–158.
- [325] P. de Sousa Gerbert and R. Jackiw, *Classical and Quantum Scattering on a Spinning Cone*, *Commun. Math. Phys.* **124** (1989) 229.
- [326] J. S. Dowker, *Casimir Effect Around a Cone*, *Phys. Rev. D* **36** (1987) 3095.
- [327] A. Belin, L.-Y. Hung, A. Maloney, S. Matsuura, R. C. Myers and T. Sierens, *Holographic Charged Renyi Entropies*, *JHEP* **12** (2013) 059, [1310.4180].

- [328] C. P. Herzog, *Universal Thermal Corrections to Entanglement Entropy for Conformal Field Theories on Spheres*, *JHEP* **10** (2014) 028, [1407.1358].
- [329] J. Lee, A. Lewkowycz, E. Perlmutter and B. R. Safdi, *Rényi entropy, stationarity, and entanglement of the conformal scalar*, *JHEP* **03** (2015) 075, [1407.7816].
- [330] C. P. Herzog and T. Nishioka, *The Edge of Entanglement: Getting the Boundary Right for Non-Minimally Coupled Scalar Fields*, *JHEP* **12** (2016) 138, [1610.02261].
- [331] J. Dowker, *Vacuum Averages for Arbitrary Spin Around a Cosmic String*, *Phys. Rev. D* **36** (1987) 3742.
- [332] B. A. Bernevig and S.-C. Zhang, *Quantum spin hall effect*, *Phys. Rev. Lett.* **96** (Mar, 2006) 106802.
- [333] R. Bergamin and A. A. Tseytlin, *Heat kernels on cone of AdS_2 and k -wound circular Wilson loop in $AdS_5 \times S^5$ superstring*, *J. Phys. A* **49** (2016) 14LT01, [1510.06894].
- [334] D. Fursaev and D. Vassilevich, *Operators, Geometry and Quanta: Methods of spectral geometry in quantum field theory*. Theoretical and Mathematical Physics. Springer, Berlin, Germany, 2011, 10.1007/978-94-007-0205-9.
- [335] A. M. Polyakov, *Gauge Fields and Strings*, vol. 3. 1987.
- [336] J. Garriga and A. Vilenkin, *Holographic Multiverse*, *JCAP* **0901** (2009) 021, [0809.4257].
- [337] J. Garriga and A. Vilenkin, *Holographic Multiverse and Conformal Invariance*, *JCAP* **0911** (2009) 020, [0905.1509].
- [338] B. Fiol, *Flavor from M5-branes*, *JHEP* **1007** (2010) 046, [1005.2133].
- [339] B. Fiol, *Defect CFTs and Holographic Multiverse*, *JCAP* **1007** (2010) 005, [1004.0618].
- [340] K. Jensen and A. O'Bannon, *Holography, Entanglement Entropy, and Conformal Field Theories with Boundaries or Defects*, *Phys. Rev. D* **88** (2013) 106006, [1309.4523].
- [341] Y. Korovin, *First Order Formalism for the Holographic Duals of Defect CFTs*, *JHEP* **1404** (2014) 152, [1312.0089].
- [342] J. Estes, K. Jensen, A. O'Bannon, E. Tsatis and T. Wrase, *On Holographic Defect Entropy*, *JHEP* **05** (2014) 084, [1403.6475].
- [343] D. Seminara, J. Sisti and E. Tonni, *Corner contributions to holographic entanglement entropy in $AdS_4/BCFT_3$* , *JHEP* **11** (2017) 076, [1708.05080].

- [344] D. Seminara, J. Sisti and E. Tonni, *Holographic entanglement entropy in $AdS_4/BCFT_3$ and the Willmore functional*, *JHEP* **08** (2018) 164, [1805.11551].
- [345] S. Gukov and E. Witten, *Rigid Surface Operators*, *Adv. Theor. Math. Phys.* **14** (2010) 87–178, [0804.1561].
- [346] N. J. Hitchin, *Stable bundles and integrable systems*, *Duke Math. J.* **54** (1987) 91–114.
- [347] E. Witten, *Gauge theory and wild ramification*, 0710.0631.
- [348] N. J. Hitchin, A. Karlhede, U. Lindstrom and M. Rocek, *Hyperkahler Metrics and Supersymmetry*, *Commun. Math. Phys.* **108** (1987) 535.
- [349] A. Gadde and S. Gukov, *2d Index and Surface operators*, *JHEP* **03** (2014) 080, [1305.0266].
- [350] J. Gomis, B. Le Floch, Y. Pan and W. Peelaers, *Intersecting Surface Defects and Two-Dimensional CFT*, *Phys. Rev.* **D96** (2017) 045003, [1610.03501].
- [351] F. Benini and B. Le Floch, *Supersymmetric localization in two dimensions*, *J. Phys.* **A50** (2017) 443003, [1608.02955].
- [352] Y. Pan and W. Peelaers, *Intersecting Surface Defects and Instanton Partition Functions*, *JHEP* **07** (2017) 073, [1612.04839].
- [353] A. Gorsky, B. Le Floch, A. Milekhin and N. Sopenko, *Surface defects and instanton–vortex interaction*, *Nucl. Phys.* **B920** (2017) 122–156, [1702.03330].
- [354] E. Frenkel, S. Gukov and J. Teschner, *Surface Operators and Separation of Variables*, *JHEP* **01** (2016) 179, [1506.07508].
- [355] B. Le Floch, *A slow review of the AGT correspondence*, 2006.14025.
- [356] D. Gaiotto, G. W. Moore and A. Neitzke, *Wall-crossing, Hitchin Systems, and the WKB Approximation*, 0907.3987.
- [357] O. Chacaltana and J. Distler, *Tinkertoys for Gaiotto Duality*, *JHEP* **11** (2010) 099, [1008.5203].
- [358] D. Xie, *General Argyres-Douglas Theory*, *JHEP* **01** (2013) 100, [1204.2270].
- [359] P. C. Argyres and M. R. Douglas, *New phenomena in $SU(3)$ supersymmetric gauge theory*, *Nucl. Phys. B* **448** (1995) 93–126, [hep-th/9505062].
- [360] N. Wyllard, *$A(N-1)$ conformal Toda field theory correlation functions from conformal $N = 2$ $SU(N)$ quiver gauge theories*, *JHEP* **11** (2009) 002, [0907.2189].
- [361] L. F. Alday and Y. Tachikawa, *Affine $SL(2)$ conformal blocks from 4d gauge theories*, *Lett. Math. Phys.* **94** (2010) 87–114, [1005.4469].

- [362] C. Kozcaz, S. Pasquetti, F. Passerini and N. Wyllard, *Affine $sl(N)$ conformal blocks from $N=2$ $SU(N)$ gauge theories*, *JHEP* **01** (2011) 045, [1008.1412].
- [363] S. A. Gentle, M. Gutperle and C. Marasinou, *Entanglement entropy of Wilson surfaces from bubbling geometries in M-theory*, *JHEP* **08** (2015) 019, [1506.00052].
- [364] S. A. Gentle, M. Gutperle and C. Marasinou, *Holographic entanglement entropy of surface defects*, *JHEP* **04** (2016) 067, [1512.04953].
- [365] H. Kanno and Y. Tachikawa, *Instanton counting with a surface operator and the chain-saw quiver*, *JHEP* **06** (2011) 119, [1105.0357].
- [366] S. Nawata, *Givental J-functions, Quantum integrable systems, AGT relation with surface operator*, *Adv. Theor. Math. Phys.* **19** (2015) 1277–1338, [1408.4132].
- [367] S. K. Ashok, M. Billo, E. Dell’Aquila, M. Frau, R. R. John and A. Lerda, *Modular and duality properties of surface operators in $N=2^*$ gauge theories*, *JHEP* **07** (2017) 068, [1702.02833].
- [368] D. Gaiotto, L. Rastelli and S. S. Razamat, *Bootstrapping the superconformal index with surface defects*, *JHEP* **01** (2013) 022, [1207.3577].
- [369] C. Beem and L. Rastelli, *Vertex operator algebras, Higgs branches, and modular differential equations*, *JHEP* **08** (2018) 114, [1707.07679].
- [370] M. Berkooz, M. Rozali and N. Seiberg, *Matrix description of M theory on T^{*4} and T^{*5}* , *Phys. Lett. B* **408** (1997) 105–110, [hep-th/9704089].
- [371] M. R. Douglas, *On $D=5$ super Yang-Mills theory and $(2,0)$ theory*, *JHEP* **02** (2011) 011, [1012.2880].
- [372] N. Lambert, C. Papageorgakis and M. Schmidt-Sommerfeld, *$M5$ -Branes, $D4$ -Branes and Quantum 5D super-Yang-Mills*, *JHEP* **01** (2011) 083, [1012.2882].
- [373] G. Lockhart and C. Vafa, *Superconformal Partition Functions and Non-perturbative Topological Strings*, *JHEP* **10** (2018) 051, [1210.5909].
- [374] H.-C. Kim, J. Kim and S. Kim, *Instantons on the 5-sphere and $M5$ -branes*, 1211.0144.
- [375] N. Nekrasov and A. Okounkov, *Seiberg-Witten theory and random partitions*, *Prog. Math.* **244** (2006) 525–596, [hep-th/0306238].
- [376] H.-C. Kim and S. Kim, *$M5$ -branes from gauge theories on the 5-sphere*, *JHEP* **05** (2013) 144, [1206.6339].
- [377] T. Nishioka and I. Yaakov, *Supersymmetric Renyi Entropy*, *JHEP* **10** (2013) 155, [1306.2958].

- [378] X. Huang and Y. Zhou, $\mathcal{N} = 4$ Super-Yang-Mills on conic space as hologram of STU topological black hole, *JHEP* **02** (2015) 068, [1408.3393].
- [379] S. Yankielowicz and Y. Zhou, Supersymmetric Rényi entropy and Anomalies in 6d (1,0) SCFTs, *JHEP* **04** (2017) 128, [1702.03518].
- [380] Y. Zhou, Information Theoretic Inequalities as Bounds in Superconformal Field Theory, 1607.05401.
- [381] H. Ooguri and C. Vafa, Knot invariants and topological strings, *Nucl. Phys.* **B577** (2000) 419–438, [hep-th/9912123].
- [382] T. Dimofte, S. Gukov and L. Hollands, Vortex Counting and Lagrangian 3-manifolds, *Lett. Math. Phys.* **98** (2011) 225–287, [1006.0977].
- [383] M. Bullimore, H.-C. Kim and P. Koroteev, Defects and Quantum Seiberg-Witten Geometry, *JHEP* **05** (2015) 095, [1412.6081].
- [384] N. Bobev and P. M. Cricigno, Universal RG Flows Across Dimensions and Holography, *JHEP* **12** (2017) 065, [1708.05052].
- [385] O. DeWolfe, D. Z. Freedman and H. Ooguri, Holography and defect conformal field theories, *Phys. Rev.* **D66** (2002) 025009, [hep-th/0111135].
- [386] E. D’Hoker, J. Estes and M. Gutperle, Exact half-BPS Type IIB interface solutions. I. Local solution and supersymmetric Janus, *JHEP* **06** (2007) 021, [0705.0022].
- [387] N. Bobev, K. Pilch and N. P. Warner, Supersymmetric Janus Solutions in Four Dimensions, *JHEP* **06** (2014) 058, [1311.4883].
- [388] N. Drukker, D. Gaiotto and J. Gomis, The Virtue of Defects in 4D Gauge Theories and 2D CFTs, *JHEP* **06** (2011) 025, [1003.1112].
- [389] L. Bhardwaj and Y. Tachikawa, On finite symmetries and their gauging in two dimensions, *JHEP* **03** (2018) 189, [1704.02330].
- [390] J. Kaidi, K. Ohmori and Y. Zheng, Kramers-Wannier-like Duality Defects in (3+1)D Gauge Theories, *Phys. Rev. Lett.* **128** (2022) 111601, [2111.01141].
- [391] Y. Choi, C. Cordova, P.-S. Hsin, H. T. Lam and S.-H. Shao, Noninvertible duality defects in 3+1 dimensions, *Phys. Rev. D* **105** (2022) 125016, [2111.01139].
- [392] L. Bhardwaj, L. Bottini, S. Schafer-Nameki and A. Tiwari, Non-Invertible Higher-Categorical Symmetries, 2204.06564.
- [393] Y. Choi, C. Cordova, P.-S. Hsin, H. T. Lam and S.-H. Shao, Non-invertible Condensation, Duality, and Triality Defects in 3+1 Dimensions, 2204.09025.

- [394] L. Bhardwaj, *2-Group symmetries in class S*, *SciPost Phys.* **12** (2022) 152, [2107.06816].
- [395] D. Gaiotto, A. Kapustin, Z. Komargodski and N. Seiberg, *Theta, Time Reversal, and Temperature*, *JHEP* **05** (2017) 091, [1703.00501].
- [396] C. Cordova, T. T. Dumitrescu and K. Intriligator, *2-Group Global Symmetries and Anomalies in Six-Dimensional Quantum Field Theories*, *JHEP* **04** (2021) 252, [2009.00138].
- [397] R. M. Nandkishore and M. Hermele, *Fractons*, *Ann. Rev. Condensed Matter Phys.* **10** (2019) 295–313, [1803.11196].
- [398] N. Seiberg, *Field Theories With a Vector Global Symmetry*, *SciPost Phys.* **8** (2020) 050, [1909.10544].
- [399] N. Seiberg and S.-H. Shao, *Exotic Symmetries, Duality, and Fractons in 2+1-Dimensional Quantum Field Theory*, *SciPost Phys.* **10** (2021) 027, [2003.10466].
- [400] A. Y. Kitaev, *Fault tolerant quantum computation by anyons*, *Annals Phys.* **303** (2003) 2–30, [quant-ph/9707021].
- [401] C. Nayak, S. H. Simon, A. Stern, M. Freedman and S. Das Sarma, *Non-Abelian anyons and topological quantum computation*, *Rev. Mod. Phys.* **80** (2008) 1083–1159, [0707.1889].
- [402] X.-G. Wen, *Topological orders and edge excitations in FQH states*, *Adv. Phys.* **44** (1995) 405–473, [cond-mat/9506066].
- [403] A. R. Akhmerov and C. W. J. Beenakker, *Boundary conditions for dirac fermions on a terminated honeycomb lattice*, *Phys. Rev. B* **77** (Feb, 2008) 085423.
- [404] S. Biswas and G. W. Semenoff, *Massless Fermions on a half-space: The curious case of 2+1-dimensions*, 2208.06374.
- [405] S. Ruijsenaars, *On barnes' multiple zeta and gamma functions*, *Advances in Mathematics* **156** (2000) 107 – 132.
- [406] M. Spreafico, *On the barnes double zeta and gamma functions*, *Journal of Number Theory* **129** (2009) 2035 – 2063.